

The Synthesis of amido-amine functionalized dendrimers and hyperbranched Polymers, and a comparative study into their use as drug delivery vehicles.



Reyad Elderbag

A dissertation submitted in partial fulfilment of the requirements
for the degree of
Doctor of Philosophy

Supervisor: Dr. Lance J Twyman

Department of chemistry

September 2023

Acknowledgments

Alhamdulillah, I express my heartfelt gratitude and appreciation to the Lord, the Creator, for making my dreams come true. I want to begin by extending my sincerest thanks to my supervisor, Dr. Lance Twyman, for his invaluable guidance, encouragement, and his wealth of advice and constructive feedback, all of which were instrumental in the successful completion of this thesis.

I also want to acknowledge the entire Twyman research group, which provided a supportive and collaborative environment throughout this journey, making us feel like a close-knit family. Special thanks go to Abdelfattah, Abdullatif, Khalid, Naif, Enas, Amal, Chen, Ohoad, Manar, Leema, and Nada, and all the previous Mchem students who contributed to this project.

I want to express my heartfelt gratitude to my family as my last acknowledgment. I'm deeply thankful for your unwavering love and support, which have been instrumental in making all of this possible. I appreciate not only your belief in me but also your patience during the challenging moments, knowing that it couldn't have been easy. I hold all of you dear in my heart, and I am forever thankful for everything you've contributed to my journey.

Abstract

In order to improve the effectiveness of drug treatments and resolve health issues, it is critical to have a variety of efficient drug delivery systems (DDSs). In recent years, researchers and academics have been paying increased attention to dendrimers, for their ability to encapsulate poorly soluble drugs to specific within their hydrophobic structures. With careful design, the hydrophobic interactions can be improved through secondary interactions, between the drug and the dendrimer's internal functionality. The use of dendrimers has been limited by their high cost and lengthy synthetic process. However, these limitations can be offset using a related class of polymer known as a hyperbranched polymer (HBP). These possess similar properties to dendrimers, and can be applied to similar applications, but are less expensive and easier to synthesise. The aim of this thesis is to explore whether or not HBPs could be used as viable alternatives to dendrimers for drug delivery. To study this objectively, systems built up using identical functionality were synthesised. For this work, amido-amine dendrimers and HBPs were prepared and studied.

The first part of this study focused on the first 3 generations of neutral PAMAM dendrimers. Initial studies focused on encapsulation properties using Ibuprofen and a lead anti cancer compound known as F73. The results indicated that the second generation (the G2.5-OH) was the most effective as it provided the optimum internal environment for binding/hosting the guest drug. Concentration experiments indicated that significantly less drug (than expected) could be encapsulated at high dendrimer concentration. Subsequent dynamic light scattering (DLS) experiments identified that the dendrimer formed large, aggregated structures with a diameter of 200 nm at concentrations over 1×10^{-4} M.

The effect of a strong secondary interaction on the level of encapsulation was studied using free base and Zinc-metallated porphyrins. The findings showed that the zinc-metallated porphyrin could be encapsulated 100% better than the corresponding free base porphyrin. The

large increase was due to the ability of the Zinc porphyrin to form a strong coordination bond with the internal amines within the dendrimer.

In the second part of this study, an aromatic hyperbranched polymer (Ar-HBPAMAM-OH) with the same functional group connectivity as the PAMAM dendrimers was synthesised and studied. Encapsulation experiments using Ibuprofen, a Zinc metallated porphyrin and F73, indicated very similar levels of encapsulation to those observed for the dendrimer. The study also analysed the stability and release properties of the drugs in the dendrimer and HBP, and both systems again proved to be very similar. The results show that all drugs were stable within the Ar-HBPAMAM-OH and G2.5-OH PAMAM dendrimer. Additionally, tests on drug release using both systems showed that Ibuprofen and Zn metallated-porphyrin could be released relatively slowly over time, indicating relatively strong interactions between the drugs and the delivery systems. These release results confirm that either of the delivery systems would make a good host for both drugs. However, the same study on F73 indicated a very fast release, suggesting that F73 formed very weak interactions with the host delivery systems. As such, neither delivery system would be an effective drug carriers for F73.

Overall, when comparing HBPs and dendrimers with similar functional group connectivity, we can conclude that both are equally suitable for use as efficient drug delivery systems. Therefore, when deciding which system to use, it may come down to factors such as cost or any therapeutic regulations (that may make it easier/harder for one system to be used).

Abbreviations

Ar-HBPAMAM.....	Aromatic Hyperbranched PAMAM
Ar-HBPAMAM-OH.....	Hydroxyl Aromatic Hyperbranched PAMAM
PAMAM	Poly (amido amine)
ΔA	Delta Absorption
Conc.....	Concentration
DLS.....	Dynamic Light Scattering
DMSO.....	Dimethyl Sulfoxide
D.....	Dendrimer
ES-MS.....	Electrospray Ionisation Mass Spectrometry
G.....	Generation
1H NMR	Proton Nuclear Magnetic Resonance Spectrometry
^{13}C NMR	Carbon-13 Nuclear Magnetic Resonance Spectrometry
GPC	Gel Permeation Chromatography
UV/Vis	Ultraviolet/Visible Spectrometry
TMPP.....	Tetrakis(3,5-dimethoxyphenyl) -porphyrin
THPP	Tetrakis (3,5-dihydroxyphenyl) -porphyrin
ZnTHPP.....	Zinc tetra hydroxy phenylporphyrin
ϵ	Extinction coefficient
PDT	Photodynamic therapy
PS.....	Photosensitizers
MA.....	Methyl acrylate
d.....	Doublet
m.....	Multiplet
s.....	Singlet
t.....	Triplet
q.....	Quartet

Table of Contents

Acknowledgments	i
Abstract	ii
Abbreviations	iv
1. Introduction	9
1.1. Drug delivery system.....	10
1.1.1. Issues with drug delivery.....	11
1.1.2. Nanoparticles for drug delivery	12
1.2. Dendrimer	16
1.2.1. Dendrimers and drug delivery	17
1.2.2. Dendrimer Properties	18
1.3. Synthesising dendrimers.....	22
1.3.1. Divergent synthesis.....	22
1.3.2. Convergent synthesis.....	22
1.4. Therapeutic Applications for Dendrimers.....	24
1.4.1. Dendrimers' therapeutic activities.....	24
1.4.2. Solubilisation	25
1.4.3. Dendrimers in transdermal drug delivery.....	26
1.4.4. Dendrimers in ocular delivery of bioactive.....	26
1.4.5. Dendrimers for pulmonary delivery.....	27
1.4.6. Dendrimers in targeted drug delivery.....	27
1.5. Hyperbranched polymers	29
1.5.1. Synthetic strategies.....	30
1.5.2. Hyperbranched polymers for drug delivery.....	31
2. Aims and objectives	34
3. Synthesis of PAMAM Dendrimer	43
3.1. Overview:.....	44
3.2. Synthesis of PAMAM dendrimer.....	47
3.2.1. Synthesis of half generation (G0.5) PAMAM dendrimers.....	47
3.2.2. Synthesis of complete generation PAMAM dendrimers	49
3.3. Purification of PAMAM dendrimers.....	51
3.4. Characterisation of PAMAM dendrimers.....	54
3.5. Synthesis of hydroxyl-terminated PAMAM dendrimers.....	57
3.6. Characterisation of hydroxyl-terminated PAMAM dendrimers	58
4. Evaluating the drug delivery potential of the hydroxyl terminated PAMAM dendrimers	61

4.1.	Part1: Encapsulation of Ibuprofen in hydroxyl terminated PAMAM dendrimers.	62
4.1.1.	Stability of Ibuprofen within aqueous dendrimer complexes.	71
4.1.2.	Ibuprofen release from G2.5-OH dendrimer.	73
4.2.	Part2: Encapsulation of therapeutic porphyrins in hydroxyl terminated PAMAM dendrimers.....	77
4.2.1.	Syntheses of Tetrakis (3, 5-dihydroxyphenyl)-porphyrin (THPP).....	79
4.2.2.	Tetrakis (3, 5-dihydroxyphenyl)-porphyrin (THPP) encapsulation within hydroxyl dendrimers.....	81
4.2.3.	Synthesis and characterisation of zinc metalated porphyrin (ZnTHPP 14).....	84
4.2.4.	Zn-THPP 14 coordination with PAMAM dendrimers	86
4.2.5.	Stability of ZN-THPP 14 in the dendrimer complexes.....	89
4.2.6.	Zn-THPP 14 release from G2.5-OH dendrimer.....	92
4.3.	Part3: Encapsulation of anticancer drug F37 in hydroxyl terminated PAMAM dendrimers.....	95
4.3.1.	Encapsulation of anticancer drugs in neutral PAMAM-OH dendrimers.....	96
4.3.2.	Stability Study for F73-Polymer Complexes in PAMAM dendrimer	98
4.3.3.	F73 release from G2.5-OH dendrimer.	100
4.4.	Conclusion:.....	102
5.	Synthesis and characterisation of aromatic hyperbranched polymers	103
5.1.	Overview	104
5.2.	Synthesis of Ar-HBPAMAM-OH (intermediate 3 and Monomer 1)	107
5.3.	Characterisation of intermediate 3, and AB2 Monomer1.	107
5.4.	Synthesis of Ar-HBPAMAM-OH (Hyperbranched polymer 4)	110
5.5.	Characterisation of Ar-HBPAMAM-OH (Hyperbranched polymer4).....	111
5.6.	Synthesis and characterisation of hydroxyl-terminated aromatic hyper-branched polymers	113
6.	Chapter: Evaluating the drug delivery potential of the Aromatic hyperbranched PAMAM (Ar-HBPAMAM_OH).....	118
6.1.	Part1: Encapsulation of Ibuprofen in Aromatic hyperbranched PAMAM.	119
6.1.1.	Stability of encapsulated Ibuprofen in Ar-HBPAMAM_OH.....	122
6.1.2.	Ibuprofen release from Ar-HBP.....	124
6.2.	Part2: Encapsulation of Zn-THPP14 in Aromatic hyperbranched PAMAM.....	127
6.2.1.	Stability of Zn-THPP in Ar-HBPAMAM_OH complexes.....	129
6.2.2.	Zn-THPP release from Ar-HBPAMAM-OH	131
6.3.1.	Stability of F73 in Ar-HBPAMAM_OH.....	134
6.3.2.	F73 release from Ar-HBP.....	135
6.4.	Conclusion:.....	138
7.	Comparisons of macromolecules used for drug delivery	139

7.1.	Comparing drug encapsulation efficacies of hydroxyl terminated PAMAM dendrimers and aromatic HB-PAMAM.....	140
7.1.1.	Encapsulation data for the hydroxyl terminated dendrimer and Ar-HBPAMAM-OH based on conventional molar concentrations are shown in Table 30 and compared graphically in Figure 44	142
7.1.2.	Encapsulation data for the hydroxyl terminated dendrimer and Ar-HBPAMAM-OH based on mass/vol concentration equivalent to 0.0001 M are shown in Table 31 and compared graphically in Figure 45.	143
7.1.3.	Comparing the stability of different drugs within dendrimer and Ar-HBPAMAM-OH	145
7.1.4.	The release of Ibuprofen, Zn-THPP, and F73 from G2.5-OH, and Ar-HBPAMAM-OH systems.	148
8.	Conclusion.....	151
	Future Work.....	159
9.	Experimental work	161
9.1.	Chemicals	162
9.2.	NMR Spectroscopy (Nuclear magnetic resonance spectroscopy)	162
9.3.	Mass Spectrometry (MS)	162
9.4.	Ultraviolet-visible spectroscopy (UV-VIS)	162
9.5.	Gel permeation column (GPC)	162
9.6.	Dynamic light scattering (DLS)	163
9.7.	pH analysis	163
9.8.	Fourier Transform Infrared Spectroscopy (FTIR)	163
9.9.	Synthesis of PAMAM dendrimers	163
9.9.1.	General synthesis of half generation PAMAM dendrimers	163
9.9.2.	General synthesis of full generation PAMAM dendrimers	163
9.9.3.	Synthesis of G0.5 PAMAM dendrimer (4 OMe terminal groups)	164
9.9.4.	Synthesis of G1.0 PAMAM dendrimer (4 amine terminal groups)	165
9.9.5.	Synthesis of G1.5 PAMAM dendrimer	166
9.9.6.	Synthesis of PAMAM G2.0 PAMAM dendrimer	167
9.9.7.	Synthesis of PAMAM G 2.5 PAMAM dendrimer	168
9.9.8.	Synthesis of G3.0 PAMAM dendrimer	169
9.9.9.	Synthesis of G 3.5 PAMAM dendrimer	170
9.10.	Synthesis of neutral PAMAM dendrimers.....	172
9.10.1.	General procedure	172
9.10.2.	Synthesis of G0.5-OH PAMAM dendrimer	172
9.10.3.	Synthesis of G1.5-OH PAMAM dendrimer	173
9.10.4.	Synthesis of G2.5-OH PAMAM dendrimer	174

9.10.5.	Synthesis of G3.5-OH PAMAM dendrimer	176
9.11.	Synthesis of aromatic hyperbranched polymers	178
9.11.1.	Synthesis AR-HBP (intermediate 3 and monomer 1).....	179
9.11.2.	Synthesis of Ar-HBP (hyperbranched polymer 4)	180
9.11.3.	Synthesis of an intermediate ester-terminated hyper branched polymer.....	181
9.11.4.	Synthesis of a hydroxyl ester-terminated hyper branched polymer.....	182
9.12.	Solubility and the Beer-Lambert law experiment for Ibuprofen	183
9.13.	Phosphate buffer preparation	183
9.14.	Encapsulation procedures.....	183
9.15.	Preparation of different generations of hydroxyl terminated PAMAM dendrimers with concentrations of (1×10^{-4} M).	184
9.16.	Preparation of G2.5-OH PAMAM dendrimers with different concentrations (1×10^{-6} , 1×10^{-5} , 1×10^{-4} and 1×10^{-3} M).	184
9.17.	Preparation of G2.5-OH PAMAM dendrimers with different concentrations (1×10^{-4} , 2.5×10^{-4} , 5×10^{-4} , 7.5×10^{-4} , and 9×10^{-4} M).....	184
9.18.	Synthesis of 5,10,15,20-tetrakis(3, 5-dimethoxyphenyl) porphyrin (TMPP)	185
9.19.	Synthesis of 5,10,15,20-tetrakis(3, 5-dihydroxy phenyl) porphyrin (THPP)	186
9.20.	Synthesis of Zn-THPP (zinc-porphyrin).....	187
9.21.	Beer-Lambert law for THPP and Zn-THPP	188
9.22.	THPP and Zn-THPP encapsulation in different generations of PAMAM dendrimer.	188
9.23.	Stability of drug-dendrimer complexes	188
9.24.	Zn-THPP 14 release from the G2.5-OH dendrimer and Ar-HBP	189
References		190

Chapter 1

1. Introduction

1.1. Drug delivery system

Drug delivery involves administration of pharmacological compounds to a patient with the aim of achieving a therapeutic effect.¹ Technologies for delivering drugs have developed to a point where they seek to enhance the pharmacokinetic properties of pharmacological compounds, while limiting unwanted adverse impacts and improving outcomes clinically. Thus, delivery methods are increasing in significance in pharmaceuticals, with great potential for future progress in targeting drug delivery, and timed and triggered release of compounds.²

The need has grown for drug delivery systems to develop effectively in line with novel biopharmaceutical components, allowing these to be easily administered, more bioavailable and precisely targeted, with reduced toxicity.

This need has led the worldwide market in technology for drug delivery to grow at a faster rate. The global market for top 10 drug delivery technologies is expected to grow from, with predicted growth from 2009-2015 being from \$43.8 - \$81.5 billion, making an 11% compound yearly growth rate. Research into drug delivery is wide-ranging in scope, including developing new materials and carrier systems to effectively deliver pharmacological compounds. Drugs are frequently delivered at a constant or managed rate, or in a targeted way. From the first development of systems for medical applications, conventional drug administration for different conditions has come to use a range of dosage channels, including in solution, in suspension, in a pill, injection, lotion, paste, cream, ointment, suppository, powder and fast-release capsule, for example. More recently developed systems offer far greater therapeutic possibilities, and these include systems of oral delivery-controlled release, masked taste, quickly dispersed dosages, liposomes, site-specific delivery, transdermal patch systems and aerosol systems.³ In order to treat chronic illnesses, drug delivery systems are crucial. Systems for delivering drugs to a specific location through implantation of a device have been developed, to minimise adverse impacts, and enhance outcomes, at a lower cost of associated health care.⁴

1.1.1. Issues with drug delivery

Drugs can be defined as chemical compounds administered to prevent, treat and diagnose illness, through disturbance of biological processes.⁵ For example, a drug may act upon transporter proteins or enzymes. Side effects are recorded for every drug, and many show toxicity at high dosage, and may even be fatal. Further, drugs may not achieve the aims for which they are administered because of low solubility, being strongly toxic or not being sufficiently bioavailable.⁶ To provide effective treatments in human and animal medicine, pharmaceutical firms need to develop drugs which are precise in targeting the intended treatment area.⁶

Significant studies have been conducted on the subject of drug delivery mechanisms in the last twenty years, primarily due to the constraints posed by the stability and solubility characteristics inherent to various drugs.⁷ To enhance the impact of drugs, it is imperative for the delivery systems to address these limitations. The research has primarily concentrated on achieving consistent levels of drugs within the body, minimizing side effects, expanding the effective range of the drugs, and making advancements in targeting specific tissues or organs.⁸ The primary goal of a drug delivery system is to enhance effectiveness as much as possible. This involves transporting and releasing the medication to the specific intended location. The method of drug delivery can be either active or passive, but its core objective is to minimize unintended accumulation or impact. The ultimate achievement in drug delivery technology is a system that can safeguard the medication, release it precisely where needed, and remain biologically inactive and harmless.⁸ Nevertheless, the current systems have limitations, including restricted accessibility, elevated dosage requirements, the occurrence of the first-pass effect syndrome, intolerance, and vulnerability. These systems cannot be depended upon to produce the intended outcomes consistently and show irregularities in the levels of drugs in the bloodstream. As a consequence, researchers are now exploring novel delivery methods to

overcome these constraints.⁹ A pathway of investigation involves tiny delivery systems at the nanoscale. These systems include liposomes, polymeric micelles, nanogels, nanocapsules, dendrimers, carbon nanotubes, nanocrystals, and solid lipid nanoparticles. This method of delivery possesses the potential to transport small-molecule drugs together with therapeutic large molecules like proteins, peptides, single-strand DNA, and small RNA molecules (siRNA).¹⁰ Moreover, nanomedicines do not display the constraints seen in alternative choices, such as poor distribution in the body and how they are processed, restricted ability to dissolve, issues with resistance to multiple drugs, inability to adequately prevent undesired effects, and the need to determine dosage based on toxicity considerations.¹¹

Nanocarriers offer several notable benefits. These include improving the stability of drugs, enhancing the solubility of substances that do not dissolve easily in water, boosting the distribution and concentration of drugs in the body, releasing their cargo in a controlled manner, and customizing their surface properties to deliver substances precisely to unhealthy cells and tissues.¹² Additionally, these carriers can react to internal and external cues, releasing therapeutic payloads at specific times and locations. When developing nanocarriers, it is essential to consider potential safety issues. These include the materials used to construct the carriers, their dosage or concentration, their dimensions, morphology, electric charge, reactivity, and how easily they dissolve.¹³ It has the potential to decrease the dose-restricting harmful effects of the medication and facilitate the drug in overcoming drug resistance linked to cancer therapy. Both passive and active targeting methods can be employed to enhance the levels of drugs within cancer cells.^{13 14}

1.1.2. Nanoparticles for drug delivery

Nanoparticles encompass tiny particles that exist on a nanoscale, ranging from a single nanometer (nm) to several hundred nanometers. The specific size depends on their application.¹⁵ These particles were established more than a decade ago and have become crucial

in modern medicine due to their favourable properties compared to traditional methods. One significant area where nanoparticles are proving exceptionally useful is in the field of cancer treatment.¹⁵ This is attributed to their ability to penetrate tissues at a molecular level, allowing for effective exposure, diagnosis, and treatment of the disease.¹⁶ Various types of nanocarrier drug delivery systems are available, including liposomes, polymeric micelles, dendrimers, nanospheres, nanocapsules, and nanotubes.¹⁶ Some of these are already on the market, while others are still in the process of development.¹⁷

The commencement of regulated drug discharge is considered the initial phase, as it pioneered the majority of initial medication conveyance mechanisms using oral and transdermal approaches. Nevertheless, this approach had constraints, as it was delicate and did not consistently produce the intended outcome. The inception of nanotechnology dates back more than a century to Michael Faraday 1857, who created nanoscale gold particles. He utilized these gold particles to bind with antibodies, aiming at specific strains of bacteria, a technique known as immune-gold straining. This marked the inception of colloidal gold as a system for delivering drugs.¹⁷

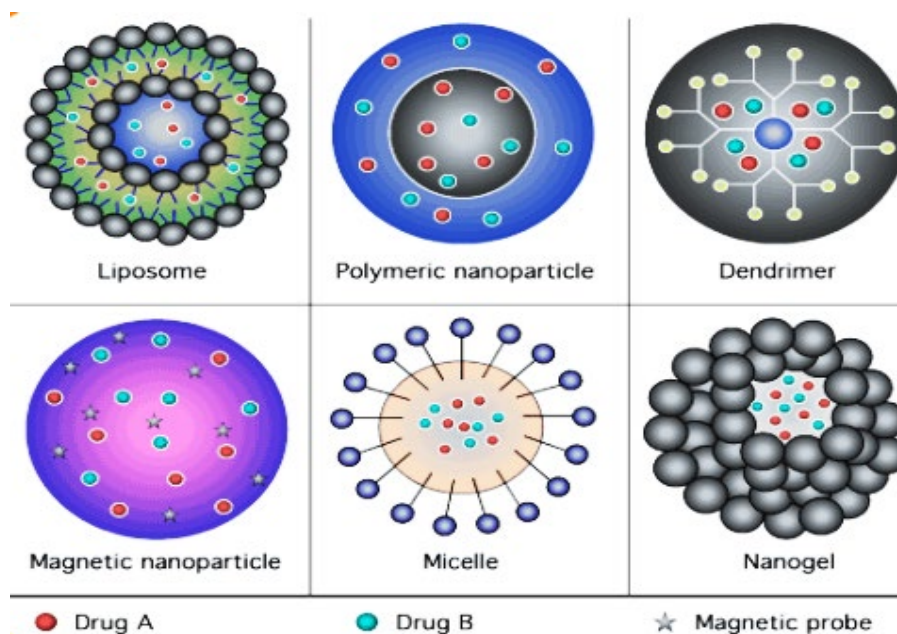


Figure 1: different nanocarriers in medical application.

The primary objectives behind creating nanoparticles for delivering drugs involve gaining command over the size of particles, their surface area, and the controlled release of medically effective substances. These nanoparticles are designed to reach specific cells, ensuring the right amount of drug is delivered at an ideal pace and dosage. This ensures that the medication effectively reaches the affected cells and tissues, achieving the intended outcomes. Although liposomes and polymer micelles were identified in the 1960s, they were not classified as nanoparticles until four decades later.¹⁸ Liposomes possess characteristics useful for transportation purposes, including the ability to reach the desired destination, minimal toxicity, and the capacity to maintain the drugs' intended form. However, they face challenges related to proper storage and limited effectiveness in encapsulation.¹⁹ When exposed to blood components, water-soluble drugs may leak uncontrollably from liposomes.¹⁹ In contrast, polymeric nanoparticles offer notable advantages over liposomes, such as enhanced stability for drugs and proteins, along with commendable properties for controlled release.²⁰ Micelles represent significant strategies for delivering cytotoxic drugs with low solubility, which are employed to achieve controlled drug release. They possess the capability to maintain stability during drug navigation and release processes, yet their stability is compromised in a watery context.²¹ Furthermore, an initial premature drug release can undermine their effectiveness as a nanocarrier, diminishing their reliability.²⁰ Moreover, they possess a substantial surface area despite their compact size, potentially leading to the clumping of particles.²¹ This could result in challenges when managing them in both liquid and dry conditions. Additionally, their dimensions may restrict the amount of drug they can hold and lead to a rapid initial release.²² Further research is required to investigate the constraints of micelles prior to their potential clinical application or introduction into the medical market as nanoparticles.

Polymers have received the greatest attention in research among the substances employed in drug delivery mechanisms. Notably, graft, star, and branched polymer setups show

considerable potential. This is due to their documented reduced toxicity and elevated effectiveness in transfection.²³ Branched polymers have the capability to engage with multiple ligands simultaneously and present chances for both covalent and non-covalent interactions with drugs, all thanks to their multifunctional nature.²⁴ The versatility of branched and dendritic structures also presents novel possibilities for theranostic uses, incorporating both diagnostic and therapeutic functions.²⁴

This study examines how effective PAMAM (polyamnioamide) dendrimers are compared to hyperbranched polymers (HBPs). In both cases, the molecular weights and functionalities can be adjusted to ensure a valid comparison.

Considerable investigation has been conducted regarding the utilization of polymers, particularly graft, star, and branched polymers, which have been explored for their possible applications. These polymers seem to exhibit promising transfection effectiveness with minimal toxicity, as indicated by prior studies.²³

The polymer branches demonstrate the potential for attaching multiple ligands and the ability to interact with drugs through both covalent and non-covalent means due to its versatile nature.²⁴

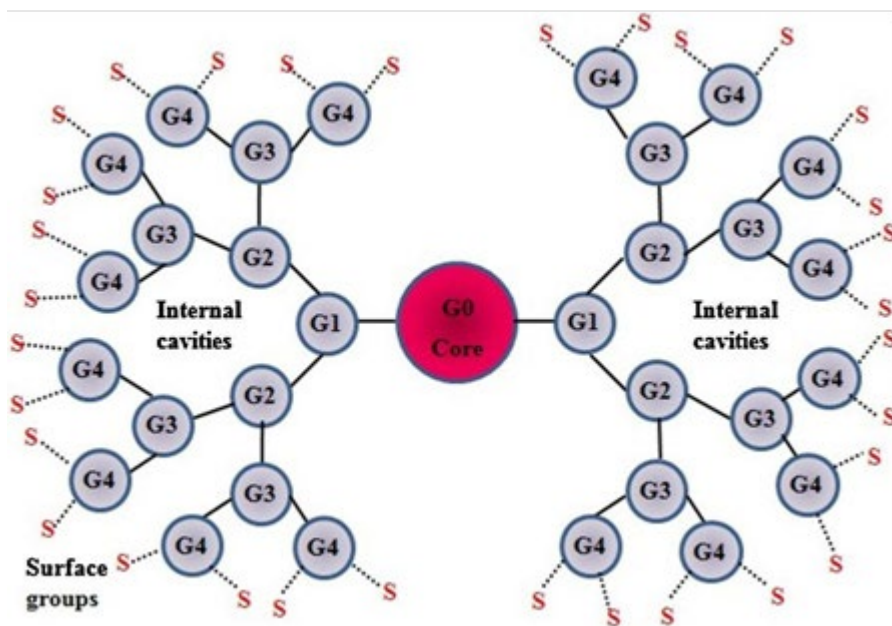
This versatility offers the potential for theragnostic therapy, where the medication can be tailored to match the patient's precise diagnosis and condition. Through the application of chemical modifications to the biopolymers for the purpose of customizing their characteristics, specific attributes can be elicited.²⁵

This study aims to investigate the impact of PAMAM (polyamnioamide) dendrimers in comparison to hyperbranched polymers (HBPs). The manipulation of molecular weights and functionalities will be carried out to thoroughly analyse each factor and make a credible comparison between them.

1.2. Dendrimer

A dendrimer is a monodispersed, hyper-branching, 3D macro-molecule which has a specific molecular weight and allows for host entrapment, with precision in managing how functional groups are placed, as well as form and size.²⁶ Dendrimers bring together properties from polymer materials and small organic molecules, allowing tailoring of chemical/physical characteristics.²⁷

Both dendrons and dendrimers form a novel category of polymer macromolecule, characterised by multiple branches, strongly-defined 3D construction and symmetrical form⁶. These molecules vary between approximately 1 and 10 nanometres, meaning that they can pass numerous bio-barriers²⁸. Structurally, dendrimers are composed from three principle forms, a core/focal point, and dendritic and peripheral terminal units²⁸. Parts of the dendrimer which show similarity with each other are termed as 'dendrons', which are layered in generations. Synthesis of the initial generation layer comes from a core attaching to repeated units to form a single-thickness layer. In contrast, generation two contains two repeat-unit layers, while generation three is three-layered, with layer numbers rising with each generation, with generations growing larger, until the end-groups at the surface of the dendrimer²⁸. Compared to older, linear polymer molecules which contain just 2 end groups for each molecule, dendrimers have multiple functional groups. Dendrimers with more generations show greater structural flexibility and a globular form compared with the flatter low-generation dendrimers²⁹.



Scheme 1 General structure of dendrimer³⁰

1.2.1. Dendrimers and drug delivery

The dendrimer, as a synthetically-produced macromolecule measuring nanometres across, with a globular form and multiple branches, is synthesised through an iterative technique.³¹ While a number of researchers have developed synthetic methodologies and applied this technology across a range of areas, attention is currently focused on making dendrimers more efficient and lowering synthesis costs. In addition, researchers are investigating distinct chemical and physical characteristics for dendrimers, and various possibilities for applying these macromolecules have emerged, while extensive research is needed to clarify unknowns. Dendrimers exhibit mono-dispersal and uniformity of size, as well as allowing their surface and internal space functions to be modified.³² They are also water-soluble, and these and other characteristics offer great potential for application in the delivery of drugs.³²

1.2.2. Dendrimer Properties

1.2.2.1. Monodispersity

Dendrimers, among dendritic polymer classes, are capable of construction to form a clearly-defined structural form, making them different from a linear polymer in that they are monodispersible. This property means that they offer good definition and reproducibility of size which can be scaled.³³ Mass spectroscopy, gel electrophoresis, transmission electron microscopy (TEM) and size exclusion chromatography (SEC) demonstrate dendrimers' monodispersal characteristics in multiple studies.²⁶ The macromolecules are purified at every synthetic stage, leading the resulting dendrimers produced to be almost isomolecular³⁴. It has been demonstrated through mass spectroscopy that applying the divergent method to create PAMAM dendrimers produces macromolecules which are highly monodisperse in early generations (1–5 G). Dendrimer bridging, failure to completely remove ethylene diamine for every generation sequence and other factors can impact monodispersity level.³⁵

1.2.2.2. Nano-size and form

Dendrimers showing uniformity which have good form and size definition have attracted attention for biomedicine due to the fact that they can pass through the cell membrane, in addition to being less likely to be removed by body systems before desired. The ability to manage the architecture of dendrimers closely means that they are prime candidates to form carriers, with systematic increase in dendrimer size and generation numbers being possible, producing dendrimers of between a few nanometres' diameter and tens of nanometres.²⁶ Thus, a dendrimer can be produced which approximates the size and shape of a range of structures occurring in biology, including for instance haemoglobin, which is 5.5 nanometres across, and is approximated by the 5.0 G PAMAM dendrimer³². Synthesis of various dendrimer types has been achieved, using different material for cores, varying branching units and differently

modified surface layers.³⁶ In addition, the size of dendrimers impacts their form in three dimensions, with dendrimers of few generations showing comparative openness and amorphism in structure, while with more generations, the dendrimer becomes more globular and can incorporate molecules of drug. On analysing aggregated dendrimers using X-ray, the results point to a rounder form with more generations, moving away from a linear form as the bigger structure spreads, which may minimise repulsion in segment end groups and convert dendrimer end groups to become neutral or anionic. This can give dendrimers which are less toxic or have no toxicity, as shown in vivo and in vitro. This has been seen with neutral dendrimers such as polyether and polyester, as well as dendrimers with surface engineering such as glycosylated dendrimers and PEGylated dendrimers.³⁵

1.2.2.3. Biocompatibility

Despite toxic properties, dendrimers are viewed as ‘smart carriers’, due to the fact that they can deliver drugs at intracellular level, passing membranes, targeting desired structures and persisting in the circulation for the duration required for therapeutic effects to be seen clinically.³⁶ It is thought that dendrimers have toxic effects because of the end groups they contain at their surface.³⁶ In general, amine-terminated PPI and PAMAM dendrimers show haemolytic properties and toxicity dependent on concentration.³⁷ However, it is possible to avoid toxicity in the cationic dendrimer through partly or completely modifying the peripheral layer using groups with a negative or neutral charge. While terminal amino groups are present in the PPI and PAMAM dendrimer, toxicity patterns differ between the two types of dendrimer. The cationic PAMAM dendrimer becomes more toxic at higher generation numbers, while the cationic PPI dendrimer shows a different toxic pattern.³⁷ Generally, explanations of cytotoxic activity in cationic dendrimers depend on the preferred interaction of the cell membrane’s negative charge and the positive charge at the periphery of the dendrimer, which leads to lysis of the cell.³⁸ However, when cationic end groups are masked or converted to become anionic

or neutral, this reduces and sometimes eliminates dendrimer toxic effects *in vivo* and *in vitro*.³⁸ This has been shown for neutral dendrimers such as polyether and polyester, as well as dendrimers produced through surface engineering including PEGulated and glycosylated dendrimers.³⁹

1.2.2.4. Periphery charge

A dendrimer comprises three primary units in its structure, which are a core, branching units and multiple terminal end groups. The last of these can be positively or negatively charged or neutral, and this is crucial to potential drug delivery applications. The polyvalent characteristic is important when dendrimers are used to carry genes due to the possibility of using cationic dendrimers, including PAMAM, PPI and poly-l-lysine, for complexing DNA, which has a negative charge.⁴⁰ Additionally, positively charged dendrimers are able to interact with organic membranes containing negative charge, meaning that they can be applied to deliver drugs at the intra-cell level.⁴⁰ However, this same polyvalent property means that a dendrimer can be cytotoxic, haemolytic, or toxic in other ways, although this can be countered by modifying the surface of the dendrimer, using for example PEG, carbohydrates or acetate. In light of this, polyvalency can be seen as significant for specific dendrimer characteristics, and is a field which can be explored by researchers in developing dendrimers as drug carriers.³⁸

1.2.2.5. Pharmacokinetics:

Pharmacokinetic properties shown by macromolecules mainly emerge from anatomy and physiology, macromolecule physicochemical characteristics and the way such molecules interact biologically. For intravenously administered drugs, the macromolecule has immediate presence in the circulating blood, and limited diffusion to extravascular regions. The macromolecules in the circulation are later eliminated from the blood and sent to certain tissues/organs for removal through plasma clearance. The ways in which a tissue or organ takes

up a macromolecule is governed by blood circulation to organs, permeability of capillaries, and macromolecule characteristics.⁴¹

Dendrimers have been applied mainly parenterally, with the possibility put forward for dendrimers to be absorbed over epithelial barrier types such as the skin and the intestinal epithelium.⁴² Researchers aim to develop dendrimers for drug delivery in a targeted manner to specific tissue for sufficient therapeutic effectiveness while minimising impacts on cells which are normally-functioning bystanders, in which the free drug may have toxic impacts specific to a given organ. Enhancement of the pharmacokinetic profile has been reported for surface-decorated dendrimers over the undecorated PPI dendrimer.⁴¹

Pharmacokinetic properties have been investigated in tritiated poly-l-lysine dendrimers on intravenous administration.³⁶ High early clearance rates were reported, as well as high and unpredictable initial distribution volume, when amine-terminated 3.0 G and 4.0 G dendrimers were tested.³² Further research made a comparison of peripheral charge's impact on excretion profiles for non-biodegrading 5.0 G PAMAM dendrimer types. Urine and faecal excretion of dendrimers with no charge was found to be approximately double that of cationic dendrimers, across 1 week, which suggests that greater numbers of cationic dendrimers were taken up by cells.⁴³ A reduction in fast vascular binding may take place for surface amine group dendrimers when they are conjugated with an anionic capping group, thus concealing surface amine groups. Disposal of the dendrimers from the system then takes place through elimination through the renal and reticuloendothelial system (RES).⁴⁴ This is reported to depend upon anionic group characteristics.⁴⁵ The way acetylated dendrimers and 3 H-labelled 5.0 G PAMAM positive-charge dendrimers were distributed when modelled in DU145 prostate tumour and B16 melanoma displayed more tissue deposits for PAMAM with a positive charge.⁴⁴ While numerous studies investigate dendrimers' pharmacokinetic properties however, there is a need

to systematically explore dendrimer fates *in vivo* to confirm the usefulness of this type of drug carrier.⁴⁵

1.3. Synthesising dendrimers

there are a number of ways to synthesise dendrimers, but synthesis is dominated by two main methods: the divergent and the convergent methods.⁴⁶

1.3.1. Divergent synthesis

Divergent synthesis is the original strategy used to produce the first synthetic dendrimers, developed in 1983 by Tomalia. Divergent synthesis involves slowly combining an original multi-function core with branching units to create another generation, which is repeated as necessary to form the number of generations specified. Joining of a core unit and initial generation or branch is illustrated in Figure 2a. To create the next generation, peripheral functional groups are combined with branching units. Selection of the number of generations is based on calculation of repeat-sequence numbers between the core and surface. This technique is usually applied for dendrimers with many generations. However, divergent synthesis is limited by its production of reactions which are not complete, and by side reactions leading to structural flaws.⁴⁷ In addition, the specified purity level and target functional group numbers cannot always be achieved. This is frequently counteracted by adding excessive numbers of monomer units, which means that the dendrimers must be purified following every stage in the process.⁴⁸

1.3.2. Convergent synthesis

Hawker and Fréchet originally developed convergent synthesis in 1990 as another approach to dendrimer synthesis⁴⁹, in which the process moves from peripheral units to the core). Combination of peripheral molecules creates dendrons or large-scale peripheral molecules

which then join to a multi-functioning core molecule (Figure 2b). Convergent synthesis has the benefit that the dendrimers synthesized show greater homogeneity and purity in comparison with divergent synthesis, being purified through a simpler process and having a lower defect rate. On the other hand, convergent synthesis can be restricted to synthesising low-generation dendrimer types due to the challenge of steric hindrance as larger dendrons react with smaller cores for the high-generation dendrimer⁵⁰.

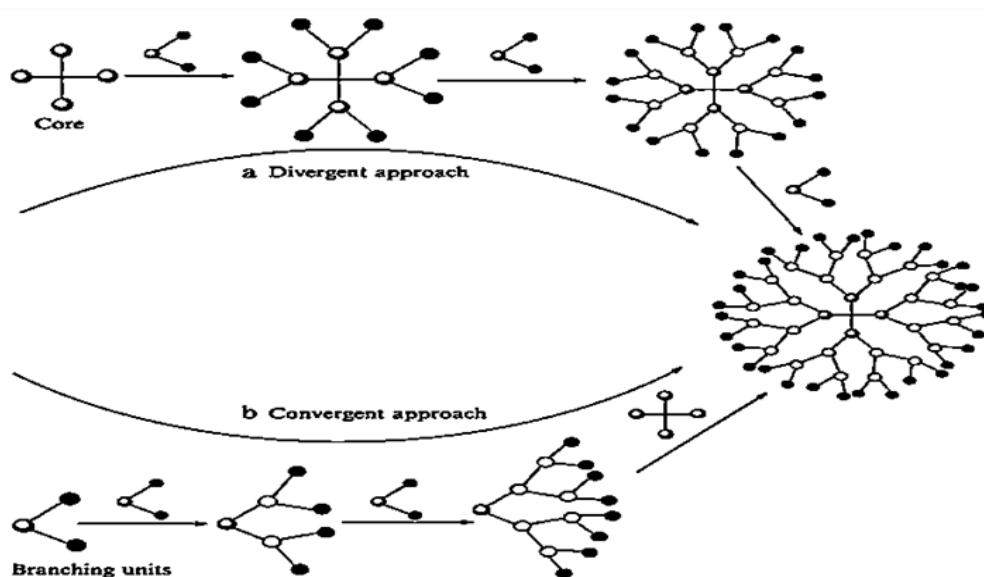


Figure 2 Shows the two main synthetic dendrimers. (a) Divergent synthesis. (b) Convergent synthesis.

1.4. Therapeutic applications for dendrimers

Each structural element which makes up a dendrimer, comprising core, internal branch and surface group components, can be manipulated to give specific properties, such as highly uniform molecules, end-groups with multiple functions and multiple internal spaces, This means that dendrimers are candidates for use in a range of pharmaceutical products with different biomedical or therapeutic aims. Dendrimer application has thus been extensively explored by numerous researchers⁵¹, and the applications identified are briefly described in the subsections which follow.

1.4.1. Dendrimers' therapeutic activities

Development of dendrimers to form topically applied antimicrobials is in progress, investigating the efficacy of polylysine dendrimers to combat herpes simplex virus (HSV).⁵² At present, phase II clinical trials are underway for the effectiveness of this dendrimer in vaginal infections.⁵² The vaginal microbicide SPL7013 Gel (VivaGel[®]) has been put forward by Starpharma Pty Ltd (Melbourne, Australia) for preventing infection with HSV and HIV⁵¹. This drug takes the form of an aqueous gel based on Carbopol, with a dendrimer as its active constituent. The 4-G lysine branched dendrimer contains a core of divalent benzhydryl amine, and capping of peripheral branches using 32 naphthalene disulfonic acid groups: these make the dendrimer hydrophobic and strongly anionic at its periphery⁵³. When VivaGel[®] (Starpharma) was found to be successful, this boosted work to develop further applications for dendrimers. A study by Wang et al (2010). investigated antimicrobial mechanisms in PAMAM dendrimers as modelled in guinea pigs for chorioamnionitis,⁵⁴ to combat ascending uterine infections caused by *Escherichia coli*. The study suggested that antimicrobial effects stemmed from interactions between *E. coli*'s polyanionic lipopolysaccharides and the polycationic dendrimer ⁵⁵. It was subsequently reported for 3.5 G PAMAM dendrimers following

glucosamine glycosylation that they showed anti-inflammatory effects through inhibition of complexed lipopolysaccharide, Toll-like receptor 4 (TLR4) and MD-2, responsible for mediating pro-inflammatory cytokine response⁵⁶. Thus, this property in dendrimers with partial glycosylation may allow them to be investigated for applications in treating inflammatory disease, infections, and malignancy.

1.4.2. Solubilisation

At a molecular level, the majority of drugs are hydrophobic and poorly soluble, thus limiting application and impeding efforts to formulate such drugs for safety, stability, and efficacy. The challenge of solubility has been approached through numerous conventional and innovative techniques. Multiple researchers have investigated the potential of dendrimers to solubilise bioactive agents with a range of therapeutic properties, such as antimicrobial, anticancer, antiviral, antimalarial, and antitubercular and anti-hypertensive agents, as well as non-steroidal anti-inflammatory drugs (NSAIDs).⁵⁷ The mediation of solubilisation through dendrimers depends on a range of characteristics and conditions, such as the size of generations, peripheral groups, internal branching units, the core, dendrimer concentrations, acidity level and temperature. Responsibility for the mediation of solubilisation by dendrimers is attributed to micellar solubilisation, hydrogen bonding, hydrophobic interaction and ionic interaction. Simple modification can be made to dendrimers to enhance make solubilisation more efficient through altering functionality of surface groups, branching units and core, or through surface-engineering using hydrophilic moieties⁵⁸. Research on PAMAM dendrimers with a polypropylene oxide core found that dendrimers exhibit solubilisation efficacy in proportion to concentration and generation.⁵⁹ NSAIDs were investigated in this research, namely Ketoprofen, Diflunisal and Ibuprofen, finding that dendrimers show efficacy in improving solubilisation in this group of drugs⁶⁰. Moreover, dendrimers have been shown to be exceptional carriers for enhancing bioavailability in chemical agents.

1.4.3. Dendrimers in transdermal drug delivery

Recent research has explored dendrimer applications to deliver drugs transdermally, on the basis that: the majority of drugs are poorly water soluble due to hydrophobic moieties limiting the drug's ability to enter biological compartments; and that the majority of designed dendrimers are strongly biocompatible and water soluble.

Efficacy has been shown for dendrimers in delivering drugs transdermally while enhancing their pharmacokinetics³⁰, in studies of dendrimer use with a range of NSAIDs. Jain *et al.* (2008) explored the transdermal delivery capability of 4.0 G PAMAM dendrimers with amino and hydroxyl terminal as well as 4.5 G PAMAM dendrimers, using indomethacin as the drug to be delivered. Pharmacodynamic and pharmacokinetic studies were conducted in vivo using a Wistar rat model, and indomethacin was found at significantly higher concentrations in the blood when it was delivered via PAMAM dendrimers compared with a suspension of the drug only⁶¹. This work was followed by that of Cheng *et al.* (2014) who conjugated diflunisal and ketoprofen with 5.0 G PAMAM dendrimers. Permeation studies were conducted in vitro permeation using the excised skin of rats, and permeation rates were reported to be 3.4 times greater for complexed ketoprofen–dendrimer in comparison to ketoprofen dispersed within saline, while complexed diflunisal and dendrimer led to 3.2 times faster permeation compared to dispersal in saline. Moreover, murine research on anti-nociception effects found reduced writhing between hours one and eight when ketoprofen–dendrimer complex was administered transdermally⁶².

1.4.4. Dendrimers in ocular delivery of bioactive

To treat ocular conditions, bioactive agents must be applied topically. However, intra-ocular drug delivery faces challenges in terms of bioavailability because of compounds being eliminated through tears, as well as excessive fluid being drained through the nasolacrimal duct.⁶³ This means that formulations should be developed which offer solutions to these

challenges, and this goal has become the subject of research interest. Moreover, formulations for ocular application must be non-irritant, non-sensitising, biocompatible, isotonic, biodegradable, and retained well in the eye⁶⁴. Investigations of dendrimer use in delivering bioactive substance to the eye have been made, with Vandamme and Brobeck (2005) finding that PAMAM dendrimers offering carboxyl or hydroxyl end functions increased the ability for the eye to retain pilocarpine. Therefore, the study provides support for the potential for dendrimer-based drug delivery to the eye.⁶⁵

1.4.5. Dendrimers for pulmonary delivery

Previous research assessed the capability of dendrimers to deliver enoxaparin, a heparin with a low molecular weight, through the pulmonary route.⁶⁶ PAMAM dendrimers of 2.0, 2.5 and 3.0 generations were evaluated for facilitating enoxaparin to be absorbed, through indirect estimation via identifying activity for antifactor Xa and analysis of effectiveness for preventing deep vein thrombosis in rodents. The findings showed that cationic 2.0 G and 3.0 G dendrimers gave a 40% increase in Enoxoparin's relative bioavailability, with no negative impacts for mucocilliary transport rates, and no serious lung tissue harm recorded. In contrast, carboxyl end group 2.5 G dendrimers which had a negative charge had no bioavailability effects. Based on this, cationic surface-charged dendrimers have potential to deliver bioactive constituents via the pulmonary route⁶⁷. In addition, a recent review by Mignani *et al.* (2013) has investigated dendrimer drug delivery across different channels, such as transdermal, transmucosal, ocular and oral delivery⁶⁸.

1.4.6. Dendrimers in targeted drug delivery

Present concerns in treating disease include enhancing bioactive agents' effectiveness through delivering them selectively to a precisely targeted region. Thus, a substance's therapeutic index

can be increased, and its side effects reduced. It is possible for dendrimers to be modified in their surface groups and branching units to passively and actively target specific areas. The effectiveness of this technique is especially significant for cancers and disease stemming from parasites, in which clearly defined sites are to be targeted, allowing for the tailoring of dendrimers to carry drugs to these sites.

The flexibility of dendrimers as carriers in this area has been noted as due to their monodispersal, clearly structured architecture, and modifiable surface groups: all characteristics which offer value in delivering bioactive substances. A well-researched instance of this is in dendrimers conjugating with folate for delivery of anticancer bioactive drugs to tumours.⁶⁹ Various cancer cells, including in breast and ovarian cancers, show overexpression of cell-surface folate receptors,⁶⁹ and thus, conjugating folate with dendrimers allows effective targeting of cancer cells to deliver anticancer drugs⁷⁰. One study involved conjugating PAMAM dendrimers and folic acid, before this was coupled to methotrexate, an anticancer agent, and its performance was assessed through confocal microscopy with immunodeficient mouse human carcinoma models, and biodistribution studies. The findings for the latter demonstrated that with dendrimers conjugated with folic acid, the drug was accumulated to triple the level of non-folic acid conjugation after 24 hours. This was supported by findings from confocal microscopy and flow cytometric analysis⁷¹. In Thomas *et al.*'s (2008) study, 5.0 G PAMAM dendrimers with a fluorescein imaging tag were conjugated with antibodies prostate-specific membrane antigen (PSMA) and CD14. Results from confocal microscopy and flow cytometry showed specific binding of the conjugate cells which expressed antigen, and this affinity could be compared to free antibodies, depending on dose and time.⁷² Choi *et al.* (2005) produced PAMAM dendrimers conjugating with FITC for imaging and with folic acid to target tumours cells. They then linked complementary oligonucleotides to achieve cell-

specific binding and internalisation. In this study, dendrimers were demonstrated as a template which can allow conjugation of multiple ligands for multiple functions⁷³.

Dendrimers offer a clearly-defined structure which allows multiple functionalities to be engineered. Jain *et al.* created an effective design for a dual ligand-conjugated dendrimer, in which sialic acid conjugated with a mannosylated dendrimer to target Zidovudine, an anti-HIV drug. The dual-conjugation here efficiently increased biocompatibility and enhanced delivery targeting⁷⁴.

1.5. Hyperbranched polymers

Hyperbranched polymers are complex structures with varying sizes, having three-dimensional shapes, and containing numerous end groups and internal spaces. They are classified as dendritic macromolecules but lack the precise structure of a dendrimer.⁷⁵ Figure 3 provides a visual comparison between the two. These polymers are synthesized using a highly branched design and possess excellent chemical stability, making them effective systems for transporting drugs.⁷⁵

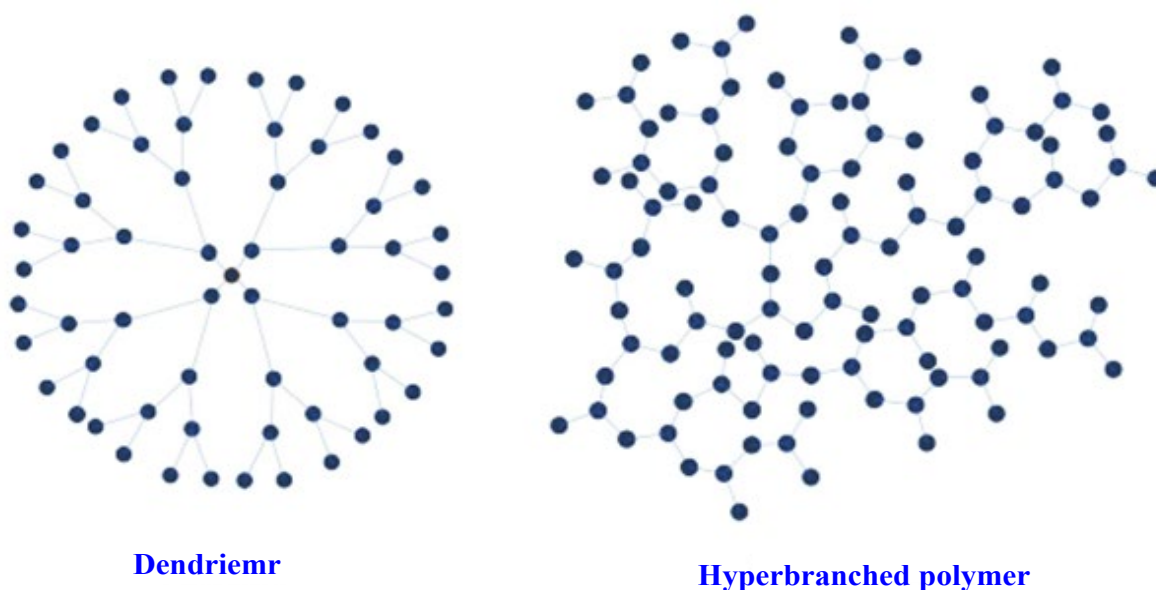


Figure 3: illustrates a diagrammatic depiction of a hyper-branched polymer and a dendrimer.

Typically, HBPs employ both physical encapsulation and covalent binding to encapsulate drugs. Their effectiveness is influenced by their molecular weight as they regulate the cavity and end groups. Kolhe investigated polyglycerol and hyperbranched polyol as potential drug delivery systems. The study found that ester linkages between the two polymers and ibuprofen can create conjugates with a large number of drug molecules. Consequently, both hyperbranched polymers show promising potential for inducing significant therapeutic effects in *in vivo* studies.⁷⁶

Moreover, investigations have revealed that hyperbranched polyglycerol (HPG) can undergo modifications with diverse functional groups. This emphasizes its capacity to successfully bind anticancer medications like docetaxel and cisplatin.^{58 59} HPG is capable of dissolving in water at elevated concentrations without significantly elevating its viscosity, thereby aiding in the improvement of hydrophobic drug solubility in biological fluids⁶⁰. Consequently, research on hyperbranched polymers suggests that they have the potential to serve as efficient carriers for drug delivery, potentially dendrimers.⁷⁶

1.5.1. Synthetic strategies

There are two methods for creating hyperbranched polymers. The first method involves incorporating a single monomer, which can be achieved through step growth or chain growth polymerization. One way to do this is by using an AB_x monomer. The second method involves using two different monomers directly, such as A₂ and B_n, where n is greater than 2. The difference between the AB₂ monomers and the multifunctional A₂ + B₃ monomers is depicted in Figure 4. In the first method, a polymer is formed with a single A-group and multiple B-groups, without any cyclization. In the second method, polymers with multiple A and B functional groups are assembled.

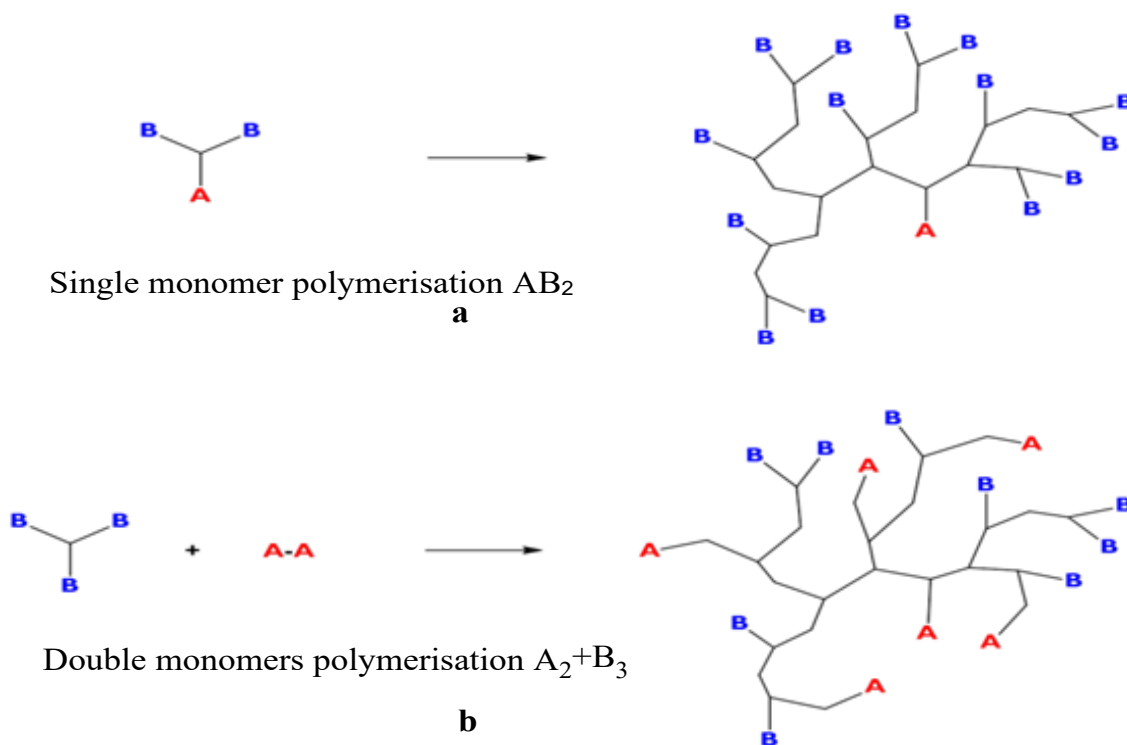


Figure 4: illustrates a diagrammatic depiction of the strategies employed to create hyperbranched polymers, consisting of two different approaches: (a) the polymerization of an AB_2 monomer, and (b) the combination of an A_2 monomer with a B_3 monomer mixture.

The cost-effectiveness of initial monomers plays a significant role in the production of hyperbranched polymers. Utilizing symmetric monomer pairs with functional properties offers advantages over AB_n monomers in terms of their accessibility and versatility. Unlike AB_n monomers, which are not readily available in the market, symmetric monomer pairs such as A_2 and B_n can be easily obtained and synthesized. This provides a flexible foundation for modifying the properties and structures of the polymers. The commercial availability of multifunctional monomers allows for the rapid and cost-effective preparation of hyperbranched polymers without imposing a significant financial burden on the project.

1.5.2. Hyperbranched polymers for drug delivery

(HBPs), like other substances tailored for drug delivery, serve a dual purpose. Firstly, they facilitate drug loading using different methods such as encapsulation or conjugation.⁷⁷ Secondly, they aid in transporting the drug to tumor tissues by leveraging passive targeting

mechanisms, like the significance of adjusting their size or introducing functional groups to extend their circulation duration.⁷⁸

1.5.2.1. Drug loading

Similar to dendrimers, hyperbranched polymer (HBPs) create cavity spaces capable of accommodating various sizes⁷⁹, ranging from compact chemotherapeutic medications like doxorubicin DOX, calprotectin (CPT), cisplatin (CLS), to 5-fluorouracil (5-FU). Wu and colleagues (2018) conducted a study on hyperbranched polyglycerol to assess its capacity for enclosing and transporting guest molecule.⁸⁰

The investigation of drug incorporation into polymer-based drug delivery systems has encompassed several methods involving non-covalent interactions like hydrophobic bonding, hydrogen bonding, ionic attraction, and steric entrapment within a crosslinked framework, as well as the attachment of the drug to the polymer.⁸¹ The essential factor for improving drug stability, achieving high drug loading capacities, and controlling drug delivery lies in the interactions between the drug and the polymer. Since non-covalent drug delivery systems are highly influenced by the physical forces in their surroundings, there is a consideration for attaching the drug covalently to the polymer using linkers that can be adjusted to trigger drug release when the specific conditions at the target site are met. because of the high density of functional groups within HBPs, they offer a means to achieve a substantial drug payload through the attachment of the drug to the end groups of HBPs.⁸²

Kolhe and colleagues (2004) utilized, and attached ibuprofen with fluorescein isothiocyanate (FITC) to the hydroxyl terminal groups of hyperbranched polyglycerols, and N,N'-dicyclohexylcarbodiimide (DCC) used as coupling agent.⁸²

The drugs becomes active when the ester bond is broken by lysosomal enzymes within the cell.⁸³ What's noteworthy is that the drug can also serve as a component of HBPs. Liu and colleagues (2013) have created HBPs containing alternating hydrophobic Di selenide and

hydrophilic phosphate groups.⁸⁴ While Phosphate groups serve as pivotal branching elements, whereas selenium compounds have been documented for their role in cancer treatment, enabling the self-delivery of HBP as an anticancer agent.⁸⁵

1.5.2.2. Passive targeting

Drug delivery targets have been created to enhance how drugs move through the body with the goal of concentrating them in specific areas. nano carriers, encapsulated with the drugs, can move through the bloodstream and tend to gather primarily at the tumor site due to the enhanced permeability and retention effect (EPR). This natural targeting process is encouraged by their extended circulation in the bloodstream and the distinctions between tumour and healthy tissues, like increased blood vessel density and larger gaps between endothelial cells in tumours (up to 1 μm).⁸⁶

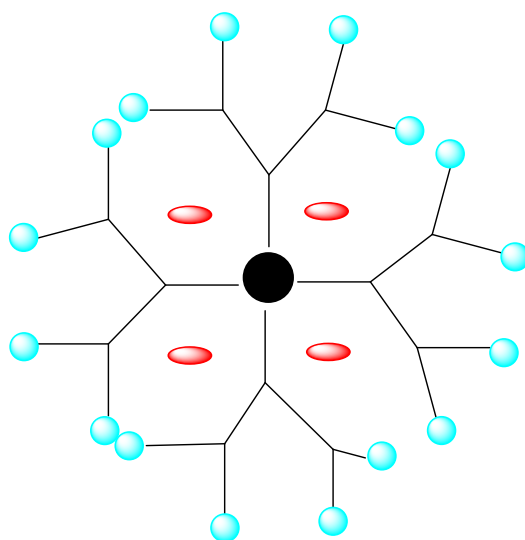
Chapter 2

2. Aims and objectives

Aims and objectives

For several decades, humans have made efforts to develop effective treatments for diseases. One area of focus has been the advancement of drug delivery systems. Scientists have explored various materials, such as nanoparticles and lipids, to deliver drugs. However, the application of these materials is often restricted due to their high toxicity and limitations in drug loading and release efficiency.⁸⁷ To overcome these challenges, polymers offer a promising solution by enhancing biocompatibility and performance. The ability to modify a polymer's composition, structure, and functionality makes them more appealing and adaptable compared to other systems. Dendritic polymers, including dendrimers and hyperbranched polymers, are a relatively recent type of polymers that show potential in enhancing drug delivery properties. Consequently, these novel dendritic polymers could play a crucial role in the future clinical implementation of drug delivery systems.⁸

Since their introduction by Newkome and Tomalia, (1985) dendrimers have garnered significant attention. These structures are precisely defined, uniform in size, and well-organised. Their terminal surfaces possess multiple functionalities, which make them excellent candidates for delivering substances. They can be modified to be soluble in water and can effectively bind drugs that are insoluble in aqueous solutions using their hydrophobic compartments.²⁷ Figure 5 provides an illustration of dendrimers as delivery systems. The interaction between dendrimers and drugs can occur through the encapsulation of drugs within the dendrimer's cavities or by conjugating them with the functional groups on the dendrimer's surface.²⁷ However, the synthesis of dendrimers is challenging, time-consuming, and costly.





-  encapsulation of drug in dendrimer via electrostatic and hydrogen bonding
-  solubilizing group

Figure 5: Depicts a cartoon representation of a dendrimer employed as a carrier for delivering substances.

The stepwise synthesis process of dendrimers is time-consuming and expensive. Consequently, scientists have sought to develop alternative systems that possess similar structural properties to dendrimers but are easier and more cost-effective to synthesize. This endeavour led to the emergence of a novel dendritic system called hyperbranched polymers (HBPs), which can be synthesized through a one-step polymerization process. Although simpler, these methods result in imperfect branching and a less ordered structure.⁷⁸ However, these drawbacks contribute to reduced problems of dense packing and steric hindrance. Overall, these simpler macromolecules have the potential to serve as superior and more affordable alternatives to dendrimers, provided they can efficiently encapsulate and release drug molecules.⁸⁸ This aspect will be a crucial focus of investigation throughout this project and thesis.

In order to determine whether HBPs can be viable alternatives to dendrimers, a comparative analysis is necessary, focusing on similar or identical internal functionalities. To achieve this, an appropriate HBP for comparison with a PAMAM dendrimer should possess identical dendritic units and functional groups. Figure 6 illustrates one such example, featuring a

PAMAM dendrimer alongside a suitable hyperbranched PAMAM (HBPAMAM) with ethylenediamine (EDA) and amide units as repeating components within its interior, and hydroxyl group within its exterior.

One of the primary motivations for utilising a delivery system is to address the issue of poor solubility that many medically active substances exhibit. The limited solubility often acts as a hindrance, preventing the effective utilisation of otherwise beneficial molecules in clinical settings. In this context, it is crucial that any delivery system employed possesses the ability to dissolve in water. This water solubility is essential as it enables the transportation of drugs through the bloodstream and facilitates their targeted delivery to specific sites of action.⁸⁹ Also, the drug delivery system should protect the drug from the body, protect the body from the drug, increase the circulation, slow release and site-specific release.⁹⁰

The proposed research in this thesis primarily focuses on neutral dendritic polymers that are soluble in water. This choice is made due to the potential toxicity associated with the presence of multiple charges on the surface of large globular molecules.

The project will focus on both dendrimers and HBPs, with the main emphasis on comparing their encapsulation, stability, and release properties. Previous studies comparing dendrimers and HBPs have been carried out, but these often involved dendrimers with vastly different structures and internal functionalities to the HBPs. Several factors influence the encapsulation process, such as the size/generation of the dendrimer, its internal composition, and the internal functionalization. In a previous study within our group, we examined PAMAM dendrimers and hyperbranched polyglycerol.⁹¹ The results indicated that the PAMAM dendrimer was able to encapsulate much more drug than the HBP, and we concluded that HBPs were poor drug delivery systems (compared to dendrimers). Although both systems could provide a hydrophobic environment, the connectivity and internal functionality of the dendrimer and HBP were completely different. The PAMAM dendrimer had a wealth of functionality that

could provide additional interactions with the drugs studied. On the other hand, the HBP had no such functionality. For example, Ibuprofen contains a carboxylic acid that can both H-bond to the PAMAM amides or form an acid/base ion pair with the amines. Neither of these interactions were possible for the HBP. As such, the study was flawed and the results meaningless. This study will address this weakness in the original work and aim to compare a dendrimer and HBP with the same connectivity and functionality.⁹²

Our work will initially focus on neutral PAMAM dendrimers, and the encapsulation of several drug molecules.

Encapsulation studies will be carried out using a series of dendrimers of increasing generation and size. OH-ended dendrimers of generations 1.5, 2.5, and 3.5, with 8, 16 and 32 terminal groups will be synthesised. These dendrimers will have molecular weights of 1437 Da, 3272 Da, and 6941 Da, respectively. Our aim is to investigate how the size and concentration of the dendrimers affect their ability to improve solubility and bind hydrophobic drug molecules. To synthesize the OH-ended dendrimers, we will convert ester-terminated dendrimers through a reaction with ethanolamine.

. Our initial objective is to determine any correlation between the size of the dendrimer and the encapsulation of the drug at a fixed dendrimer concentration. This will be followed by a study into the correlation between dendrimer concentration and the maximum levels of drug encapsulation. These studies will be carried out using ibuprofen as the test drug with dendrimer as well as aromatic hyperbranched polymers.

Ibuprofen will be utilised in this research due to its wide availability and extensive use in similar studies.⁹³ It belongs to the propionic acid class of non-steroidal anti-inflammatory drugs and is commonly employed to alleviate pain, reduce fever, and treat inflammation.⁹³ Additionally, this widely used medication is a mildly acidic pharmaceutical compound containing carboxylic groups. These groups can form hydrophobic bonds via hydrogen

bonding with the internal amines (amide groups) of the dendrimers, as well as engage in acid/base interactions with the internal basic amines.

These results using a well-known model/test drug will help inform our future studies using other drug molecules that are poorly soluble and/or require the use of a delivery system (to prevent toxic side effects and/or prevent degradation by the immune system).

Encapsulation free base porphyrins and metal porphyrins in PAMAM dendrimers, and Aromatic hyperbranched PAMAM

We are conducting research to develop new methods for encapsulating free base porphyrins and metal porphyrins, which can be used for photodynamic therapy (PDT). PDT is a validated clinical treatment that involves three components: photosensitizers, light, and oxygen. One challenge with hydrophobic photosensitizers is their poor solubility, which prevents their intravenous injection and limits their medical applications. Although the photosensitizers themselves are not necessarily toxic, they can become activated by specific wavelengths of light, leading to energy transfer to nearby oxygen molecules and causing cell damage⁹⁴. This necessitates complex formulations for effective delivery of hydrophobic photosensitizers.

To address these issues, we will conduct studies on encapsulating porphyrin photosensitizers. Porphyrins can often be hydrophobic, which necessitates use of a delivery system. For our purposes, their encapsulation can be improved by utilising strong metal-ligand coordination through the amine functionality that may be present in the interior of the dendrimers and HBPs. We will investigate the effects of metalation and non-metalation on porphyrin encapsulation efficiency, studying how these secondary interactions influence the process. In a previous study, our group successfully encapsulated simple tetraphenyl porphyrin (TPP) and metal porphyrins (ZnTP) within dendritic molecules, although the drug loadings achieved were extremely low. This limitation was primarily due to the extreme hydrophobicity of TPP and ZnTP, which was

not compatible with our encapsulation process. Further explanation on this topic will be provided later in the thesis.

To enhance the drug loading capacity, we propose using phenolic porphyrins, which possess some degree of water solubility. Also, the phenolic group is acidic and this can potentially form an acid base ion pair with the dendrimers internal amines (Figure 6)

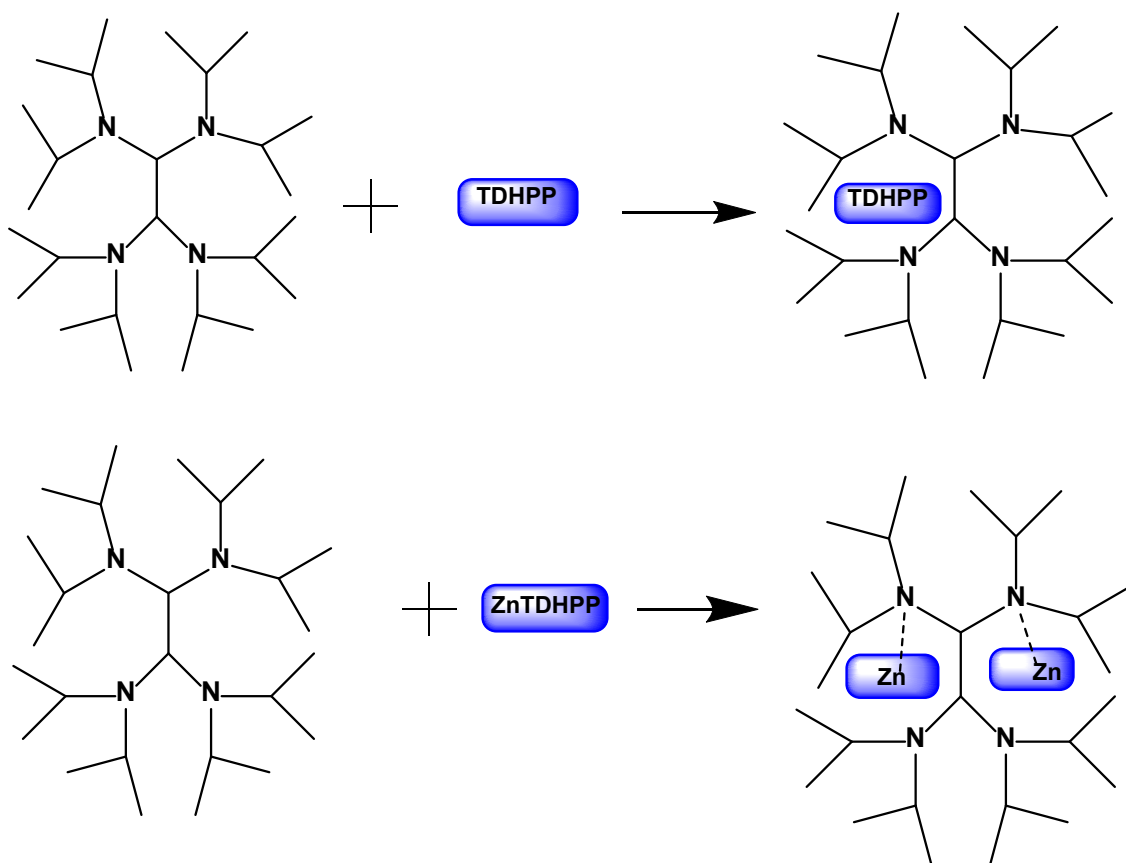


Figure 6: illustrates the integration of free porphyrin and zinc porphyrin molecules into a dendrimer structure through non-covalent interactions.

Specifically, we propose to use tetra-hydroxyphenyl-porphyrin (THPP) as this possesses eight hydroxyl groups, which provide some level of water solubility. THPP is also a recognized and effective photosensitizer in photodynamic therapy (PDT).⁹⁴ Consequently, our objective is to synthesise THPP in both metalated and non-metalated forms and evaluate their encapsulation and release properties within dendrimers, as well as Aromatic hyperbranched polymers (HBPs).

Encapsulation of Anticancer drug called (F73) in water-soluble dendrimers, and Aromatic hyperbranched PAMAM

Building upon the proposed work described above, we will also explore a specific hydrophobic drug that has good anticancer properties, but poor water solubility. As well as evaluating encapsulation, release and stability within a dendrimer and HBP, we also plan to study the in vitro properties of the delivery systems against various cancer cell lines. The specific drug under test is known as F73 (shown in Figure), and was supplied by Professor Chen (Sheffield University). The in vitro work will be carried out in collaboration with Dr Nikki Jordan (Sheffield Hallam University)

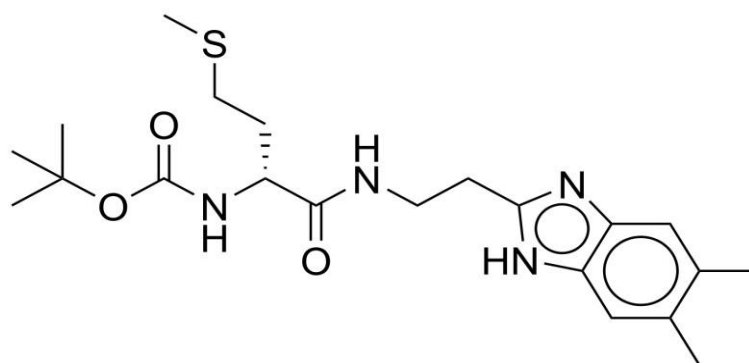


Figure 7: The structure of *tert*-butyl *N*-(1-[(5,6-dimethyl-1*H*-1,3-benzodiazol-2-yl)methyl]carbamoyl)-3-(methylsulfanyl)propyl)carbamate (f73).

The primary purpose of F73 is to inhibit methionine synthase (MetS). Also known as MetS, this enzyme is crucial for metabolizing 5-methyltetrahydrofolate (MeTHF) to regenerate the active form of tetrahydrofolate, which is essential for production of cell glutathione (GSH).⁹⁵ GSH is a nature antioxidant in cells that increase cell survival, So, we need to reduce GSH to kill cancer cells.⁹⁶

Comparing the drugs encapsulation efficacies of a hydroxyl terminated PAMAM dendrimers and an Aromatic HBPAMAM

The final part of this theses has to answer the main question regarding the two delivery systems as set out in the aims. That is, “to determine whether or not the cheaper and more accessible

aromatic hyperbranched polymers could compete with the expensive and complicated dendrimer systems when applied as drug delivery vehicles". To achieve this, we are going to compare the encapsulation, stability, and release properties of a hyperbranched polymer that possessed the same basic functionality as the PAMAM under investigation. Specifically, the study will focused on comparing the Ar-HBPAMAM-OH with the hydroxyl-terminated PAMAM dendrimers.

Finally, the thesis will be laid out, and the results written in different chapters. The first results chapters will describe the synthesis and characterisation of dendrimer. This will be followed by a big chapter describing encapsulation, release, and stability of 3 drugs in it (IBU, Zn-THPP, F73). The third chapter will describe the synthesis and characterisation of Aromatic hyperbranched PAMAM. This will be followed by a big chapter describing encapsulation, release and stability of 3 drugs in it (IBU, Zn-THPP, F73). A final results chapter will consider all 3 drugs together and endeavour to make a comparison between the 2 delivery systems.

Chapter 3

3. Synthesis of PAMAM Dendrimer

3.1. Overview:

The effectiveness of a drug is generally reduced where it cannot reach its intended destination within the body at the correct volume. This may occur due to a drug's poor solubility, due to the aqueous environment of the body, or due to a lack of targeting ability. During the early stages of drug development, researchers may thus initially try to create water-soluble versions of each drug. However, as even minor changes in the drug's structure can significantly impact its performance, scientists often work instead on developing systems that can efficiently deliver drugs without the need to modify their structures in this way.¹ The first line of development for most systems for medical applications utilises conventional drug administration for different conditions across a range of dosage channels, including providing drugs in solution or in suspension, whether in pill, tablet, injection, lotion, paste, cream, ointment, suppository, powder, or fast-release capsule format.⁹⁷ A number of systems have also been developed to incorporate various polymer approaches, and this thesis focuses on the use of highly branched polymers, which offer various advantages over traditional polymer approaches,⁹⁸ and this chapter in particular concentrates on the use of perfectly branched polymers, commonly known as dendrimers.

Dendrimers emerged as promising tools for drug delivery in the pharmaceutical industry during the early 1990s, having been first introduced by Newkome and Tomalia in 1985. These polymers are a set of unique, perfectly branched macromolecules with well-defined structures and numerous terminal groups that, due to their nanostructure and chemical versatility, are attractive candidates for delivering drugs at nanoscale.²

Dendrimers offer several advantages over other polymeric drug delivery systems. Their kinetically stable architecture ensures consistent performance, while their high density and well-defined surface functionalities control solubility in a manner that may be utilised to achieve targeted delivery.⁶⁶ Dendrimers are also monodisperse polymers, thus enhancing the

reliability of pharmacokinetics generally, while suitably functionalised dendrimers have the ability to penetrate cell membranes, allowing for more effective uptake of drug complexes or conjugates.³ Finally, their controllable shapes make these polymers suitable for a wide variety of medical applications due to this ensuring consistent behaviours and predictable interactions with biological systems. In particular, in terms of drug delivery, dendrimers with uniform shapes and sizes offer predictable drug release kinetics and increased targeting efficiency.³

Due to their unique structures, high-generation dendrimers offer large concentrations of functional groups on their outer surfaces; these may be used “as is”, or functionalised further, which makes them useful for both active and passive targeting.⁴ Researchers have previously successfully modified the surface groups of various dendrimers using targeting moieties such as folic acid (FA), peptides, monoclonal antibodies, and sugar groups to achieve both active and passive targeting. Branching units of dendrimers have also been used to achieve targeted drug delivery.² Gupta et al.⁵ conducted a study in which they successfully conjugated folic acid to G5 PPI(poly propylene imine) dendrimers to assess its feasibility for targeted delivery of the anticancer drug doxorubicin, for example: in that case, the FA-conjugated dendrimers exhibited higher uptake in MCF-7 cancer cell lines and significantly reduced toxicity as compared to non-conjugated dendrimers.⁶

The shape of a dendrimer is determined by its specific generation, which influences the three-dimensional structure. When dendrimers are produced at lower generations such as G1 and G2, they are flat or “saucer” shaped; however, as higher generations are achieved, they become spherical and begin to take on a controlled 3D structure, which makes them more suitable for enclosing small host molecules. However, synthesising dendrimers at high generations can be challenging due to the emergence of steric crowding, which can lead to premature termination of the synthesis process.⁷ For dendrimers to be used in drug delivery systems, they must also be soluble in water to allow systemic administration, while for non-covalent encapsulation of

drugs, they must also possess an internal region that can interact with the drug. Most water-soluble dendrimers have hydrophobic regions within their structure, which enables effective encapsulation and solubilisation of hydrophobic drug molecules: this property is particularly beneficial due to the fact that poor drug solubility commonly limits bioavailability, making drug preparation a significant challenge.

Other functionality can also be exploited to enhance encapsulation levels to improve drug solubility, however. For example, dendrimers with internal amide groups can interact with drugs that possess orthogonal hydrogen bonding groups, as exemplified in a study by Duncan et al.⁹, who demonstrated that conjugates of PAMAM dendrimers with Cisplatin, an anticancer drug known for its non-specific toxicity and poor water solubility, exhibited increased solubility in encapsulation, resulting in significant reductions in systemic toxicity. Similarly, a study by Patel et al.⁹ demonstrated that PAMAM dendrimers significantly improved the solubility of poorly water-soluble drugs such as aceclofenac due to interactions between the internal amine groups of the dendrimers and the drug molecules

Yiyun et al.¹¹ documented an increase in the solubility of a poorly soluble non-steroidal anti-inflammatory drug (ketoprofen) when encapsulated within PAMAM-NH₂ dendrimers via several types of interaction, including hydrophobic and hydrogen bonding. Hydrophilic terminal groups can thus be seen to provide solubility to dendrimers. However, care must be taken when selecting the specific terminal group in use. Duncan et al.¹², for example, discovered that PAMAM dendrimers terminated with amines (NH₂) exhibited good levels of cytotoxicity with respect to three cancer cell lines based on compromised cell membranes, damage attributed to the positively charged nature of the amine-terminated PAMAM dendrimer which was directly linked to the generation number, concentration, and incubation time of the dendrimer.⁸ However, these researchers also showed that amine terminated dendrimers were toxic, due to the fact that, in aqueous solution, a number of the terminal amines protonated at

physiological pH, leading to aggregation by means of cooperative charge-charge interactions with negatively charged cells. In contrast, ester-terminated dendrimers were found to be non-toxic but insoluble in water; however, under physiological conditions, these systems undergo rapid hydrolysis to give carboxylic acid terminated dendrimers, which are water soluble.¹³ Another method, originally developed by Newkome et al.¹⁴ was also found to convert PAMAM dendrimers terminated with esters into dendrimers terminated with hydroxyl groups, which are neutral at physiological pH. The current research group thus used this method to generate a number of neutral water soluble PAMAM dendrimers terminated with hydroxymethyl aminomethane (TRIS) or ethanolamine, as appropriate.²

Based on this, one of the objectives for the work described within this segment of the thesis was to examine the ways in which neutral PAMAM dendrimers can enhance drug solubility through a combination of interactions, including hydrophobic, hydrogen bonding, ion pairing, and amine-metal coordination functions.

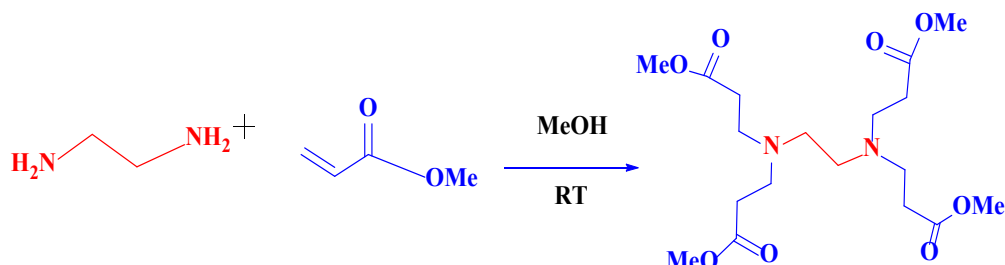
3.2. Synthesis of PAMAM dendrimer

To determine the optimal dendrimer for encapsulation and release studies, the synthesis of neutral OH terminated PAMAM dendrimers of different sizes was investigated. This synthesis was achieved via a series of iterative reactions: Initially, a Michael addition reaction was carried out to form an initial ester-terminated dendrimer; this was followed by an amination reaction to produce amine-terminated dendrimers, and then the final step was the functionalisation of the terminal esters into the required neutral OH groups.

3.2.1. Synthesis of half generation (G0.5) PAMAM dendrimers

To create half-generation dendrimers, two units of methyl acrylate (MA) were introduced for each amine present in either the core ethylenediamine (EDA) or in the dendrimers terminated with amine groups. All half generation dendrimers were thus synthesised by reacting the amine

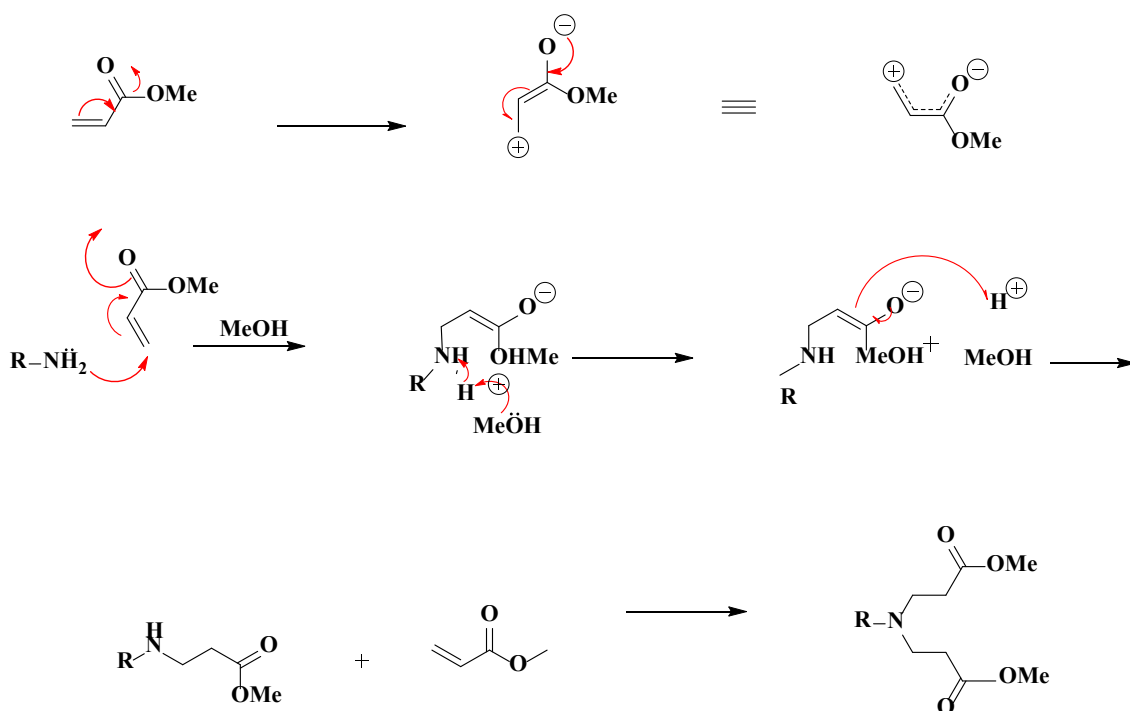
functional group or dendrimers with methyl acrylate in methanol. At the end of the reaction, the solvent and excess reagents were removed using a rotary evaporator; as the reagents and solvents are both volatile, no additional purification steps were necessary. Scheme 2 illustrates the procedure, with a G0.5 **1** dendrimer serving as an illustrative example.



Scheme 2: The synthesis of a half generation (G0.5) PAMAM dendrimer

Larger half generations were synthesised using the same method, though these typically required increased reaction times. To monitor the progress of each reaction and to ensure its completion, small amounts were examined using ¹H NMR; ¹H NMR spectroscopy was also employed to verify the complete removal of all methyl acrylate, as this can detect any remaining alkene signals within the range 4.5 to 6 ppm. All required PAMAM dendrimers were thus obtained: these appeared as pale-yellow liquids for lower generations, progressing to honey-coloured liquids that exhibited higher viscosity as the generations increased.

The mechanism of the Michael addition reaction is illustrated in Scheme 3. Methyl acrylate is an α - β unsaturated carbonyl compound; thus, oxygen's high electronegativity and its conjugation with the double bond leads to the formation of a δ positive charge on the terminal carbon. Consequently, the β carbon becomes electropositive, making it vulnerable to nucleophilic attack by one of the amines of the electron donor-acceptor (EDA).



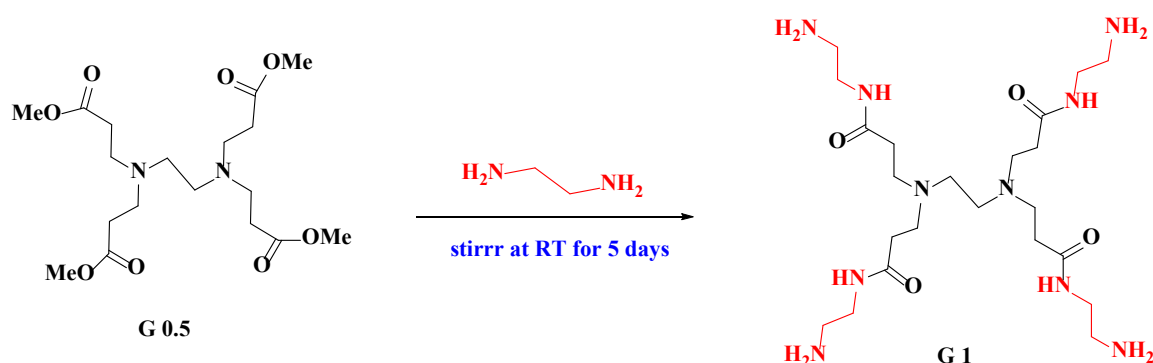
Scheme 3: The Michael addition mechanism for the synthesis of half generation (G0.5) 1 PAMAM dendrimers

3.2.2. Synthesis of complete generation PAMAM dendrimers

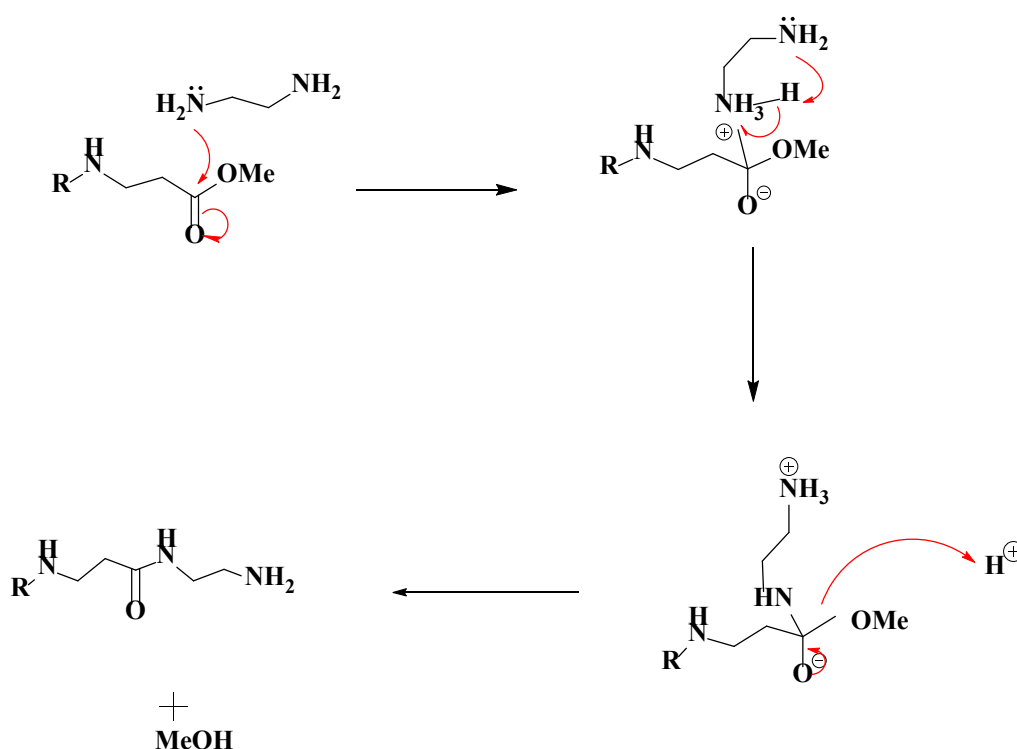
The second step, known as amination, was carried out as illustrated in Scheme 5. Higher generation dendrimers with exponentially increasing numbers of terminal groups were then generated by repeating the Michael addition and amination steps.

The synthesis of full generation PAMAM dendrimers involved the introduction of an excessive amount of ethylenediamine (EDA) to the ester terminated PAMAM dendrimers. This reaction took place in methanol at room temperature. To illustrate the procedure, the G1.0 synthesis is offered as an example in Scheme 4, using the mechanism shown in Scheme 5. In this reaction, the nucleophilic lone pair of nitrogens from the ethylenediamine (EDA) attacks the electropositive carbonyl carbon, resulting in the formation of a tetrahedral intermediate. The secondary amine then undergoes intramolecular deprotonation via a stable cyclic transition state. Subsequently, the carbon double bond reforms and the tetrahedral intermediate releases

the methoxy group, leading to the formation of a carbonyl and the liberation of the product, which deprotonates the ammonium cation to form a molecule of methanol.



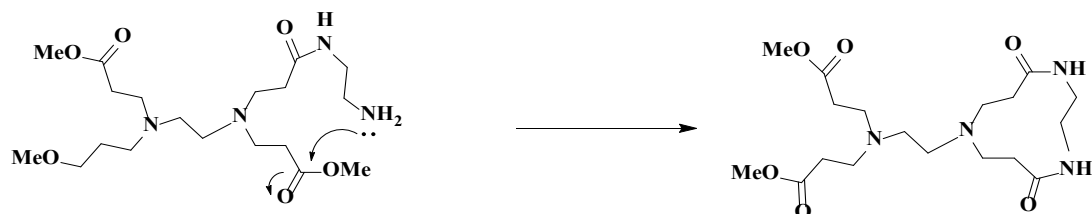
Scheme 4: The synthesis of full generation PAMAM dendrimers



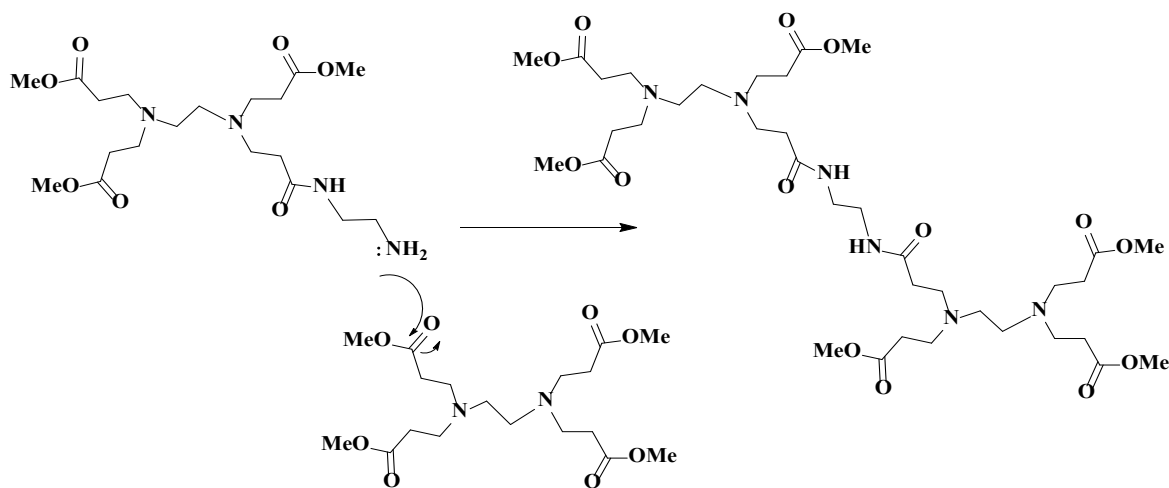
Scheme 5: Amination mechanism for the synthesis of the full generation of dendrimers.

In order to obtain uniform dendrimers without inducing any unwanted reactions, a large quantity of EDA was employed, equivalent to 20 EDA per terminal ester. This excess EDA was required to prevent a number of undesirable side reactions, as illustrated in Scheme 6. The ethylene diamine core also provides a central anchor point for dendrimer growth and

branching, enabling the controlled synthesis of PAMAM dendrimers with precise numbers of generations and functional groups.



Intramolecular reaction(cyclazation)



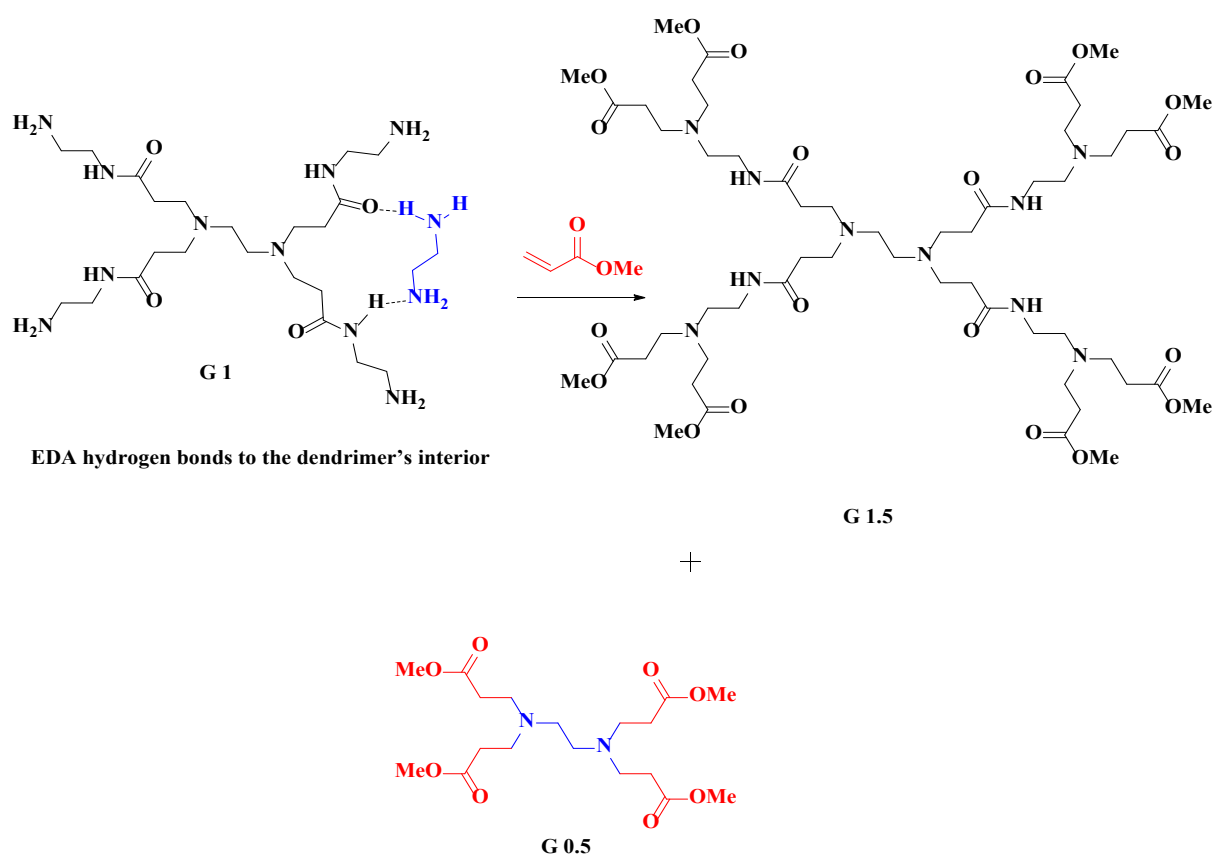
Intermolecular reaction(Dimer formation)

Scheme 6: Potential structural defects resulting from various side reactions during the synthesis of PAMAM dendrimers.

3.3. Purification of PAMAM dendrimers

Purifying half-generation dendrimers is relatively straightforward, involving rotary evaporation and drying under vacuum. However, the purification of amine-terminated PAMAM dendrimers poses a greater challenge. Although an excess of EDA is required, it is essential that all traces are removed after synthesis. If this is not done, then a new G0.5

generation dendrimer will form in the next methyl acrylate (MA) step, generating a polydisperse mixture, as seen in scheme 7.



Scheme 7: The result of incomplete removal of EDA with unwanted products

In the synthesis process for the current work, the majority of excess EDA was removed through rotary evaporation. Nevertheless, a small amount of ethylenediamine was still detected in the ^1H NMR spectrum at 2.7 ppm, as seen in Figure 8. To completely remove the EDA, several washes were thus carried out using a 9:1 azeotropic mixture of toluene and methanol, which was again subsequently subjected to rotary evaporation. This washing process was repeated until no further traces could be seen in the ^1H NMR spectrum. Figure 8 shows the ^1H NMR spectra for the G1.0 dendrimer before and after this purification process.

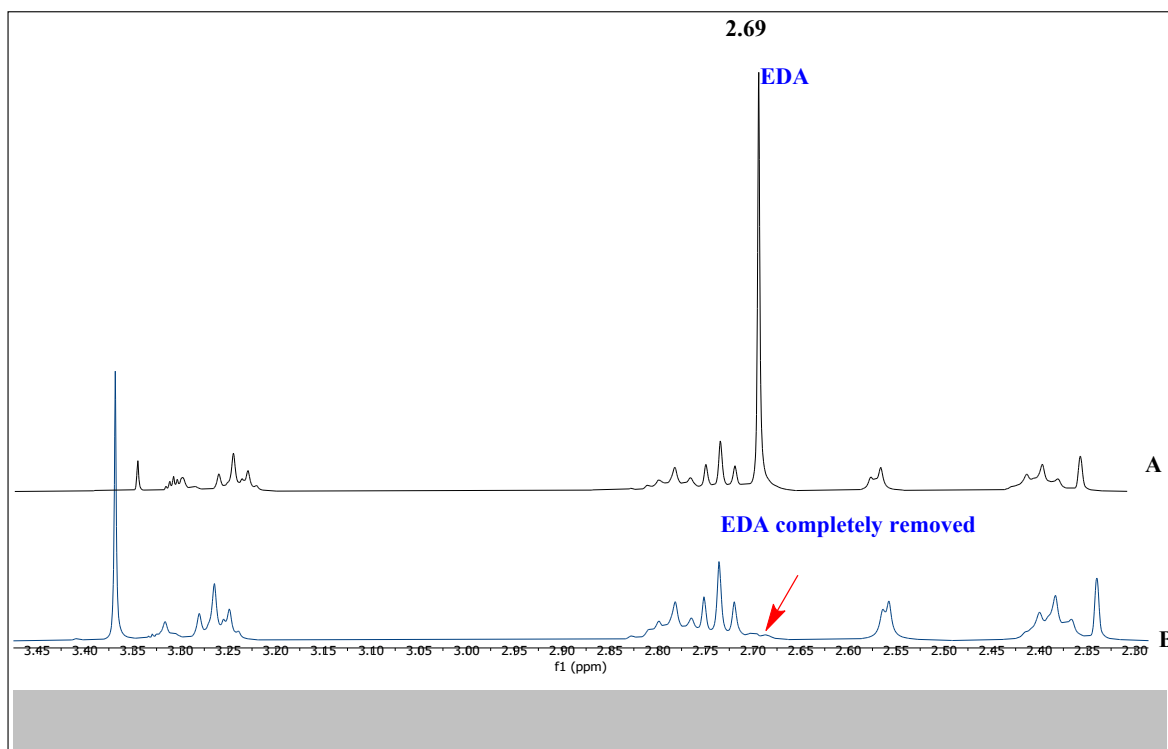


Figure 8: ^1H NMR spectra comparison for the purification process for the G1 PAMAM dendrimer: A. The spectrum captured prior to a toluene: methanol wash. B. A spectrum obtained after multiple toluene: methanol washes.

An azeotropic solvent is required to complete this process due to the robust hydrogen bonds that form between the dendrimer and ethylene diamine (EDA). Typically, methanol tends to displace these hydrogen bonds, yet methanol evaporates faster than EDA, allowing EDA to reattach to the hydrogen bonding sites. Incorporating toluene into the wash results in a higher boiling azeotrope that can outcompete EDA for the H-bonding sites, which is important, as is the EDA is not removed completely, it will react with MA in the next step and act as a fresh starting point for a G 0.5 dendrimer, resulting in the formation of an undesired G 0.5 generation dendrimer, as depicted in Scheme 7. Separating these two dendrimers then becomes extremely challenging due to their similar structural and physical properties: even distinguishing them using ^1H and ^{13}C NMR is difficult, creating a wide distribution of molecular weights in the dendrimers.

3.4. Characterisation of PAMAM dendrimers

There are several ways to analyse PAMAM dendrimers and confirm their structures, though the most effective methods include ^1H and ^{13}C NMR spectroscopy. Half-generation dendrimers display a distinct methoxy peak attributable to the ester groups present at their outermost layer; however, after conversion to the full-generation dendrimer, this methoxy peak is no longer present in the NMR spectra, making this absence indicative of a successful synthesis. To illustrate this, the G 0.5 **1** dendrimer can be considered. The ^1H NMR spectrum of the G 0.5 **1** dendrimer has four distinct proton environments, as depicted in Figure 9. Among these environments, there is a singlet peak observable at 3.69 ppm, which corresponds to the methoxy protons, while two triplet peaks, located at 2.79 ppm and 2.43 ppm, indicate the presence of the two groups of methylene protons within the dendrimer. The core protons (EDA) exhibit a peak at 2.54 ppm.

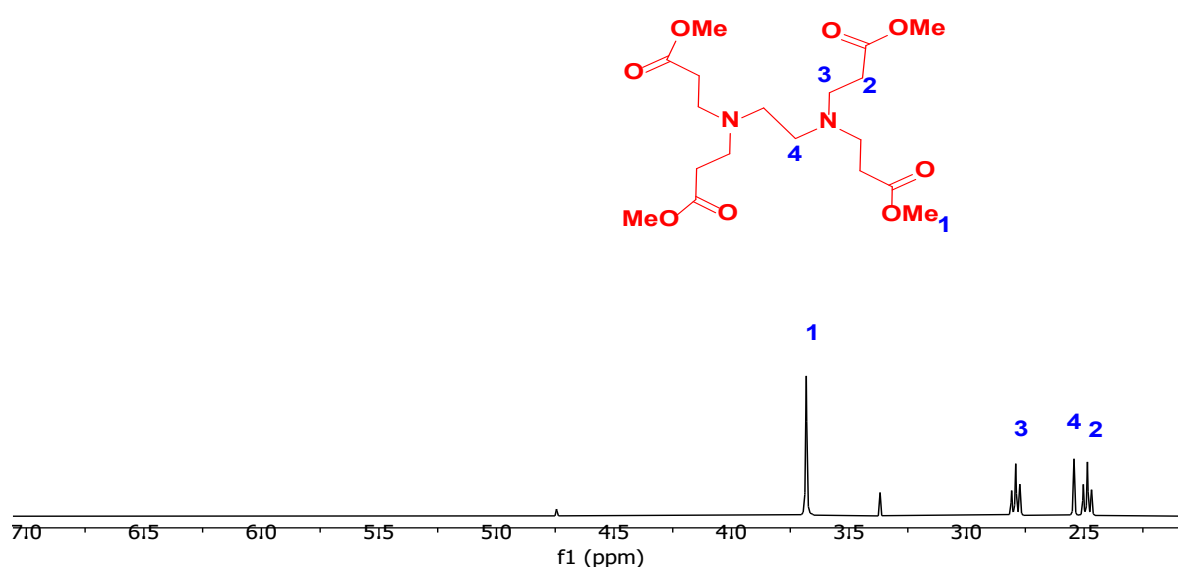


Figure 9: ^1H NMR for G 0.5 PAMAM dendrimer indicating no remaining methyl acrylate (MA) in the alkene region.

The ^{13}C NMR spectra of the dendrimers revealed characteristic chemical shifts for different generations of dendrimers. For example, the G 0.5 **1** spectrum displayed a peak at 173.3 ppm, indicating the presence of an ester carbonyl group, while the G1.0 **2** spectrum showed a peak at 174.3 ppm, indicating the presence of an amide carbonyl group. Higher generation dendrimers also exhibited dual peaks in the carbonyl region, corresponding to carbonyl groups in the exterior and interior environments of the dendrimer structure. The carbonyl region also displayed peaks between 52.4 and 32.2 ppm across all PAMAM dendrimers, indicating the presence of various proton environments.

Mass spectrometry is a valuable technique for analysing dendrimers and identifying any structural defects. This is important, as PAMAM dendrimers can develop structural defects during their synthesis, potentially leading to impurities. Such defects may arise from a retro-Michael reaction, which leads to an asymmetrical structure due to missing arms, though dimer formation and intramolecular cyclization in the amidation step can also contribute to defects. These defects can easily be observed and identified using mass spectroscopy, however.

Electrospray ionization mass spectrometry (ESI-MS) proved to be the best technique to examine smaller generations (G0.5 - G2.0) with molecular weights below 2,500 g mol⁻¹. ESI-MS generates multiple charging phenomena, leading to a greater number of charged molecules in the mass spectra, however, complicating analysis for larger dendrimers. In these cases, matrix-assisted laser desorption ionization (MALDI) was thus deemed best for larger generation dendrimers (G2.5 to G4.5). Table 1 summarises the mass spectrometry data for all dendrimers synthesised.

Dendrimer (G)	Chemical formula	M.W	Terminal Groups
G3.5 7	C ₂₇₀ H ₄₈₀ N ₅₈ O ₉₂	6011	32
G3.0 6	C ₁₄₂ H ₂₈₈ N ₅₈ O ₉₂	3256	16
G2.5 5	C ₁₂₆ H ₂₂₄ N ₂₆ O ₄₄	2804	16
G2.0 4	C ₆₂ H ₁₂₈ N ₂₆ O ₁₂	1429	8
G1.5 3	C ₅₄ H ₉₆ N ₁₀ O ₂₀	1205	8
G1.0 2	C ₂₂ H ₄₈ N ₁₀ O ₄	516	4
G0.5 1	C ₁₈ H ₃₂ N ₂ O ₈	404	4

Table 1: Molecular weights and densities of terminal groups of different PAMAM dendrimer generations.

IR spectroscopy allows for the identification of specific functional groups, offering a valuable and simple technique that can be used to monitor the transformations from half-generation dendrimers to full-generation dendrimers. The half-generation dendrimers exhibit both ester C=O stretching and amide stretching for G 1.5 **3** dendrimers and above, while full-generation dendrimers display only a single amide stretch. The IR data for all dendrimers is given in table2.

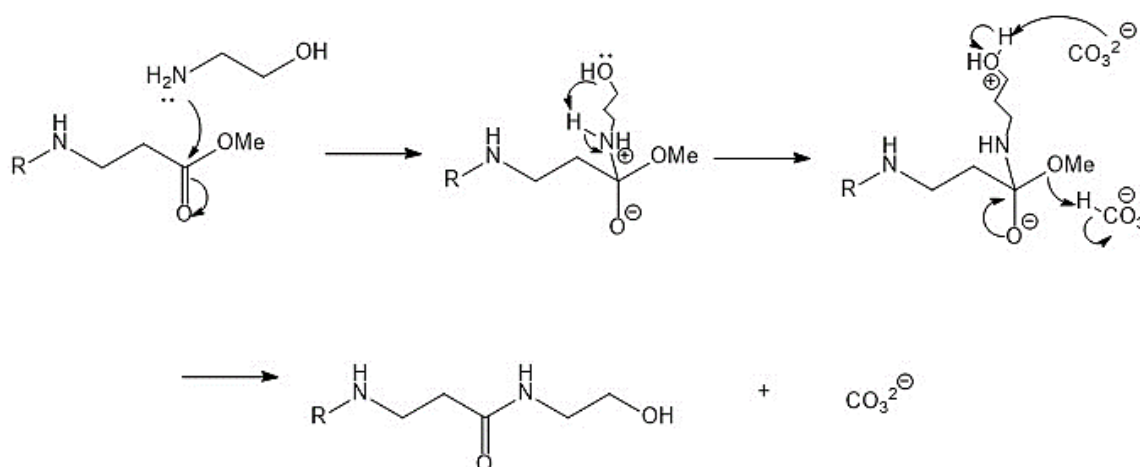
Dendrimer Generation (G)	G 0.5	G 1	G 1.5	G 2	G 2.5	G 3	G 3.5
C=O (ester)	-1731	-	1731	-	1732	-	1732
C=O (amide)	-	1639	1645	1637	1643	1635	1642

Table 2: IR data for PAMAM dendrimers of all generations

The two-step procedure with added purification steps was then used to synthesise a series of half and full generation dendrimers, up to G4.0. The structure of these dendrimers is discussed later in this work.

3.5. Synthesis of hydroxyl-terminated PAMAM dendrimers.

To reduce the toxicity of charged PAMAM-NH₂ dendrimers,⁹⁹ their amine end groups were transformed into neutral hydroxyl groups. As part of this process, a DMSO solution containing half generation PAMAM dendrimers was subjected to treatment with ethanolamine and potassium carbonate. Although this process bears similarities to the EDA reaction, the specific reaction conditions differed from those used in EDA substitution. While in the EDA reactions the terminal amine had sufficient basicity to deprotonate the intermediate by means of a favourable cyclic transition state, with ethanolamine, the terminal group is OH, which is not basic enough. An external base was thus required, as shown in Scheme 8. To eliminate the solid reagents, the crude product was filtered, yielding a thick yellow paste. The product was then dissolved in a small quantity of distilled water and precipitated using acetone, a purification process that was repeated several times to give pure neutral PAMAM-OH dendrimers, offering good yield.



Scheme 8: synthesis of hydroxyl-terminated PAMAM dendrimers by addition ethanolamine

3.6. Characterisation of hydroxyl-terminated PAMAM dendrimers

Similar spectroscopic techniques as employed to characterise the half and full generation dendrimers were used to characterise the terminated PAMAM dendrimers. As previously, the most informative method was found to be ^1H NMR, in which the singlet corresponding to the ester's methoxy protons was no longer observed after reaction with ethanolamine, as shown in Figure 10. Furthermore, a new triplet peak appeared at 3.62 ppm, corresponding to the terminal methylene protons of ethanolamine. These methylene protons also exhibited higher chemical shifts than other methylene groups due to their proximity to the electronegative and deshielding oxygen.

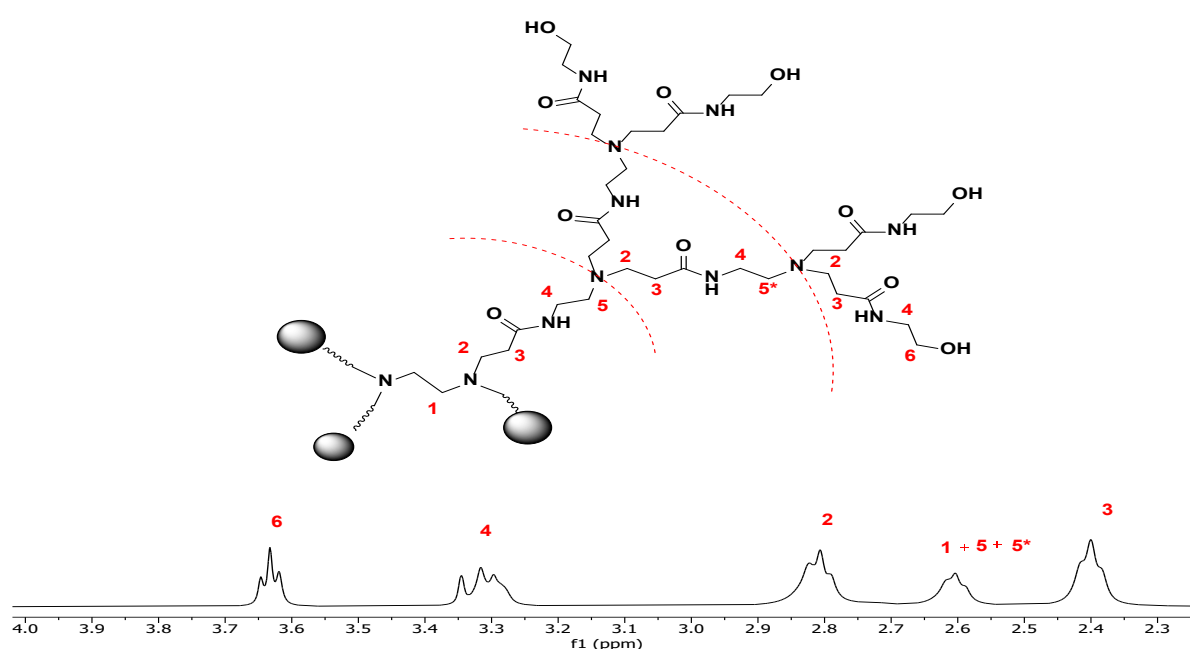


Figure 10: ^1H NMR spectra showing one arm of G3.5-OH 11

The ^{13}C NMR spectrum was expected to show a peak at a relatively high shift, corresponding to the carbon connected to the terminal OH, and this was found to be the case. When comparing the ^{13}C NMR spectrum of ester dendrimers with those of the corresponding neutral dendrimers,

extra peaks around 60 ppm were thus observed, offering good evidence for the expected terminal carbon environments (C-O).

The infrared (IR) spectra further supported the existence of hydroxyl groups at the periphery of the dendrimers, with an obvious broad peak at around 3,300 cm⁻¹. Additionally, an intense peak was visible around 1,650 cm⁻¹, which corresponds to the presence of amide carbonyl groups. The C=O stretch for the initial ester materials was seen at around 1,730 cm⁻¹.

Finally, the neutral dendrimers were analysed using mass spectrometry and the data is summarised in Table 2.

Dendrimer (G)	Chemical formula	M.W	Terminal Groups (OH ending)
G0.5-OH 8	C ₂₂ H ₄₄ N ₆ O ₈	520	4
G1.5-OH 9	C ₆₂ H ₁₂₀ N ₁₈ O ₂₀	1438	8
G2.5-OH 10	C ₁₄₂ H ₂₇₂ N ₄₂ O ₄₄	3273	16
G3.5-OH 11	C ₃₀₂ H ₅₇₆ N ₉₀ O ₉₂	6914	32

Table 2: presents the mass spectrometry results for all PAMAM-OH generations.

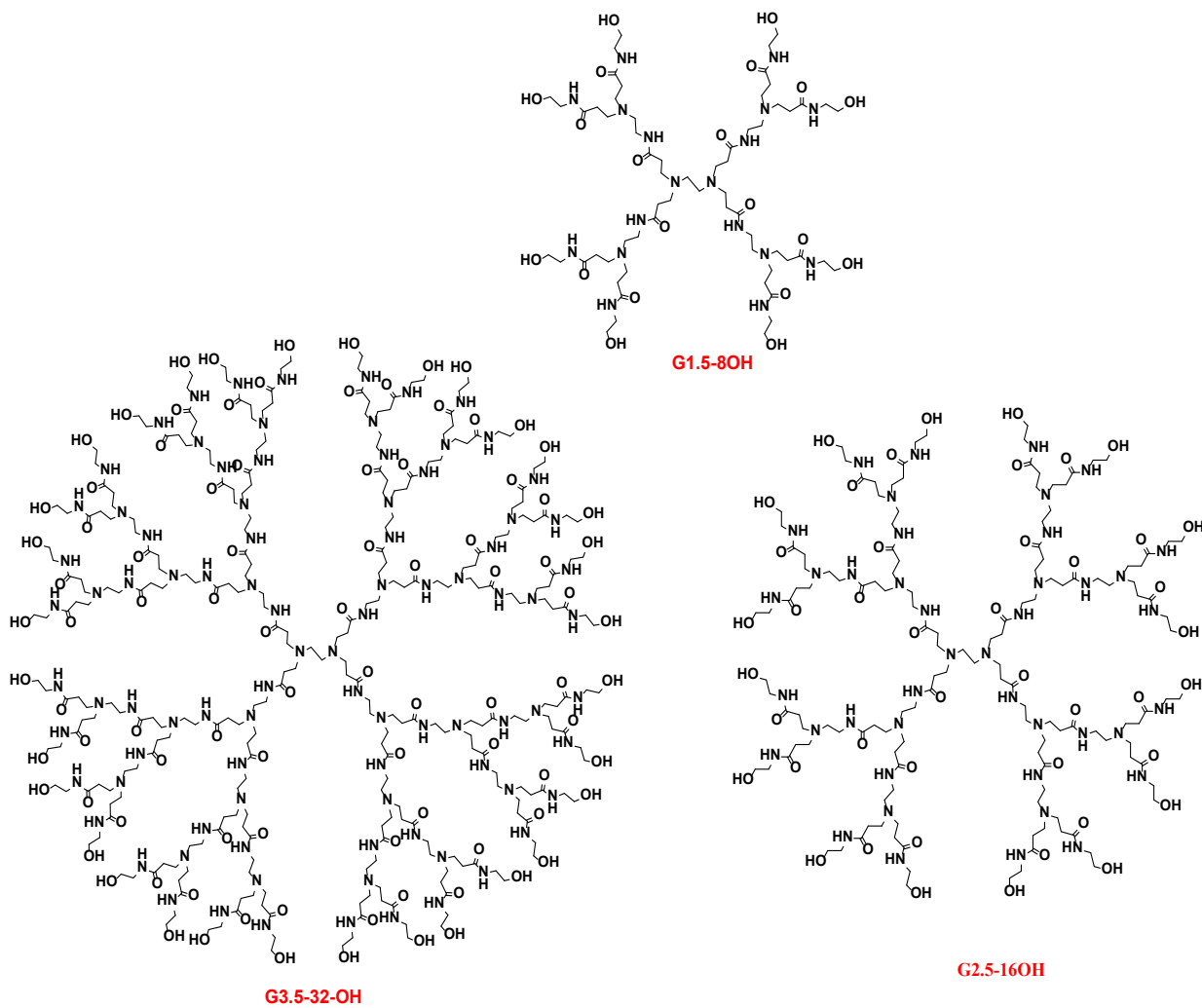


Figure 11: Structure of different generations of neutral PAMAM dendrimers.

Chapter 4

4. Evaluating the drug delivery potential of the hydroxyl terminated PAMAM dendrimers

4.1. Part1: Encapsulation of Ibuprofen in hydroxyl terminated PAMAM dendrimers.

The main objective of this project was to compare the potential of dendrimers and hyperbranched polymers (HBPs) with respect to delivering drugs. In particular, it aimed to investigate whether HBPs could effectively encapsulate and deliver drugs in a similar manner to dendrimers. The initial experiments thus involved dendrimers and a series of drugs that were both readily available and at least partially soluble in water. This facilitated initial assessment of any improvements in solubility achieved by the dendrimer, allowing the development of experiments to determine drug stability within the dendrimer and finally drug release from the dendrimer. Previous research conducted by the Twyman group has indicated that hydrophobic acidic guest molecules can be efficiently encapsulated within dendrimers due to the formation of a simple acid base salt, which provides better interaction than simple hydrophobic effects alone. Additionally, guests with hydrogen bonding groups also showed potential for improved encapsulation. However, the most effective encapsulation occurred with guests possessing both acidic and hydrogen bonding groups, with neutral hydrophobic guests exhibiting lower levels of encapsulation.¹⁰⁰

For the current study, Ibuprofen was selected as the first test drug due to its significant commercial availability and particular molecular structure (figure12). Ibuprofen contains a carboxylic acid group capable of forming salts or hydrogen bonds with dendrimers, as well as being UV-active,¹⁰¹ which facilitated the determination of its solution concentration via a Beer-Lambert plot based on its delta absorbance peak at 273 nm. Due to Ibuprofen's limited ability to dissolve in water, methanol was initially employed as the solvent for the Beer-Lambert analysis, however. The calculated extinction coefficient was thus determined to be $95 \text{ dm}^3 \text{ mol}^{-1} \text{ cm}^{-1}$.

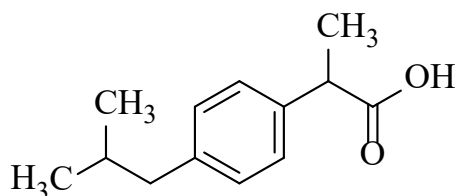


Figure 12: Ibuprofen structure

The first experiment carried out was simple though important, being designed to determine the maximum solubility of Ibuprofen in water (buffer at pH 7.4, 0.01M). This concentration can thus be used in a buffer, which is important, as dendrimers contain a lot of basic amines, and the concentration of buffer must always be higher than the concentration of amine. For future experiments, the dendrimer concentrations were thus the maximum dendrimer concentration of 1E-4M and a maximum generation of 3.5, which contains 30 amines, equating to an amine concentration of 0.003M (30 x 1E-4M).

This experiment also facilitated the development of the procedure for encapsulation to be applied in all experiments involving dendrimer and HBP encapsulation. Ibuprofen was initially dissolved in methanol, with the latter subsequently evaporated. After this, a precise volume of phosphate buffer (pH 7.4, 0.01 M) was introduced into the solution, which was then subject to filtration to remove any excess Ibuprofen. The highest achievable solubility of Ibuprofen through this approach was determined to be 3.5×10^{-3} M. This intrinsic solubility, also referred to as baseline solubility, was then subtracted from all subsequent measurements of dendrimer-boosted solubility.

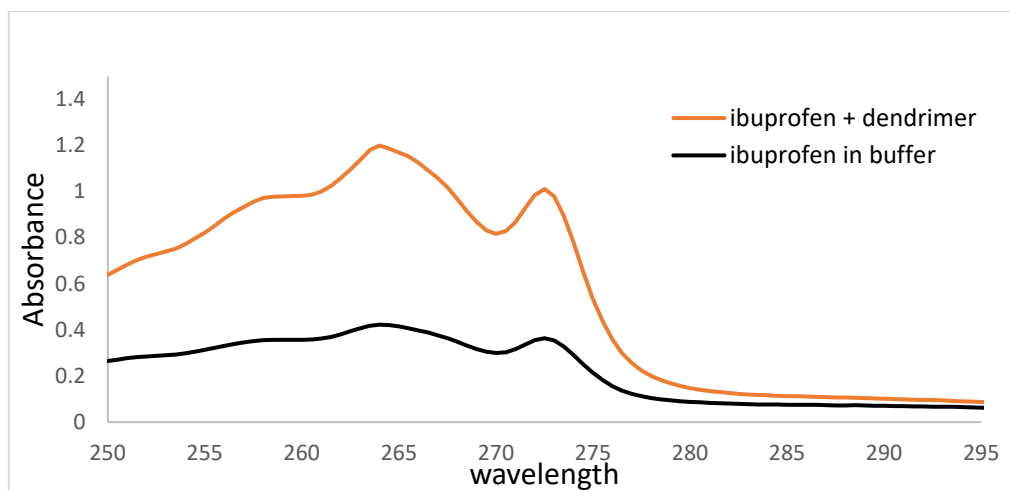


Figure 13: UV spectra of the solubility of free Ibuprofen and a buffer solution of Ibuprofen and PAMAM dendrimer (1×10^{-4} M).

The next step was to determine whether or not dendrimers could increase the solubility of Ibuprofen in water (buffer) and by how much, as seen in figure 14. These experiments examined a range of dendrimers (8OH, 16OH, and 32OH) to determine whether or not there was a size dependent effect on encapsulation and solubility. The dendrimer encapsulation process involved creating a dendrimer and drug complex using the coprecipitate technique, achieved by means of the dissolution of Ibuprofen and dendrimer in methanol. Afterward, the solvent was eliminated by means of a rotary evaporator, yielding a co-precipitate of PAMAM dendrimer and ibuprofen. Following that, a phosphate buffer with a pH of 7.4 and a concentration of 0.01M was introduced before the solutions underwent filtration to eliminate any excess insoluble drug particles. Finally, UV-Vis spectroscopy was employed to assess the concentration of in the resulting soluble complex, which allowed the concentration to be determined using the Beer Lambert analysis. To account for any baseline noise, direct absorption was not used; instead, Δ absorption values were measured within the wavelength range of 265 to 270 nm. All encapsulation experiments were conducted at a dendrimer concentration of 1.00×10^{-4} M with an excess amount of Ibuprofen.

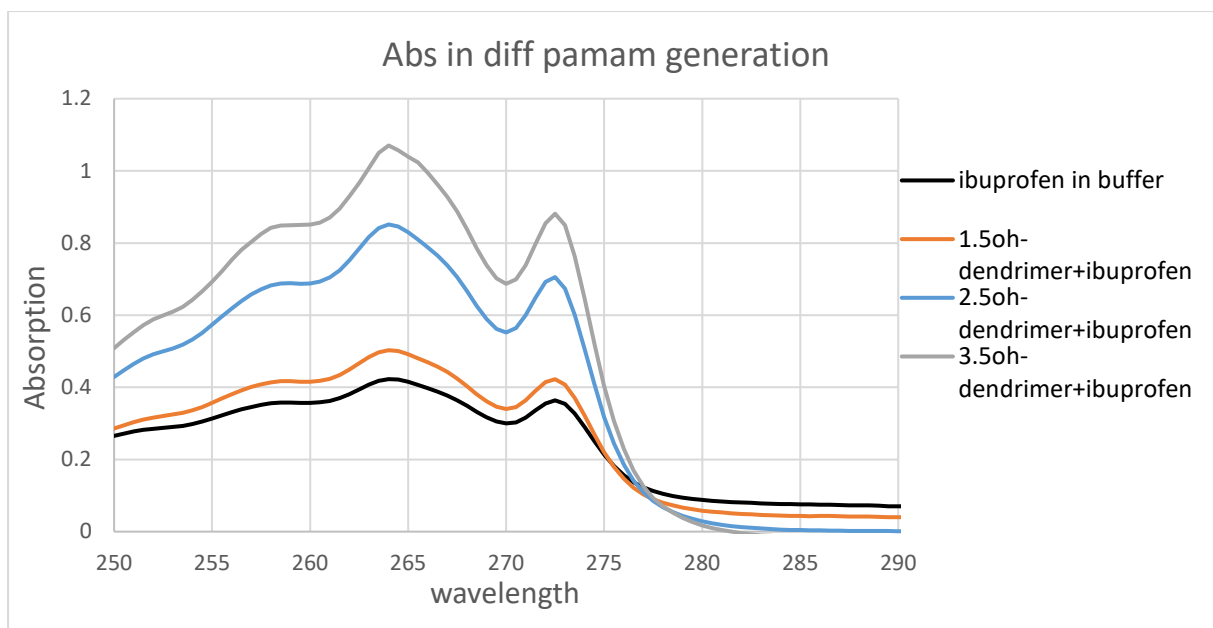


Figure 14: UV spectra for the absorption of Ibuprofen in buffer for different generations of PAMAM dendrimer (1×10^{-4} mol/l).

The total concentration of Ibuprofen in solution was calculated by dividing the delta absorbance by the extinction coefficient of Ibuprofen. The highest concentration of free Ibuprofen observed in the buffer solution had been previously calculated as 1×10^{-3} Mol/L, allowing the concentration of Ibuprofen encapsulated within each dendrimer to be determined by simply deducting 1×10^{-3} Mol/L from the total amount of Ibuprofen in solution. The amount of Ibuprofen encapsulated per mole (loading) was then determined by dividing the Ibuprofen concentration by the dendrimer concentration.

D/G	Δ ABS	ϵ	Total ibuprofen	conc of encapsulated ibuprofen	Loading
G1.5-OH	0.14	94	0.001489362	0.000489362	4
G 2.5-OH	0.27	94	0.00287234	0.00187234	18
G 3.5-OH	0.29	94	0.003510638	0.002510638	20

Table 3: Ibuprofen concentration after encapsulation within different generations of hydroxyl terminated PAMAM dendrimers.

The impact of dendrimer size generation on Ibuprofen solubility was evident from the data obtained as shown in Table 3. Specifically, the G1.5 dendrimer, with just 8OH groups, could only encapsulate four moles of Ibuprofen within its internal voids. In contrast, the G2.5 dendrimers, with 16 OH groups, was able to encapsulate significantly more, with eighteen moles of Ibuprofen encapsulated within dendritic boxes. However, the concentration of Ibuprofen encapsulated in the largest generation G3.5 dendrimers, with 32 OH groups, was only marginally greater than that encapsulated by the G2.5-16 OH dendrimer: when utilising the higher generation G3.5 dendrimers with 32 OH groups, only twenty moles of Ibuprofen were accumulated per mole of dendrimer.

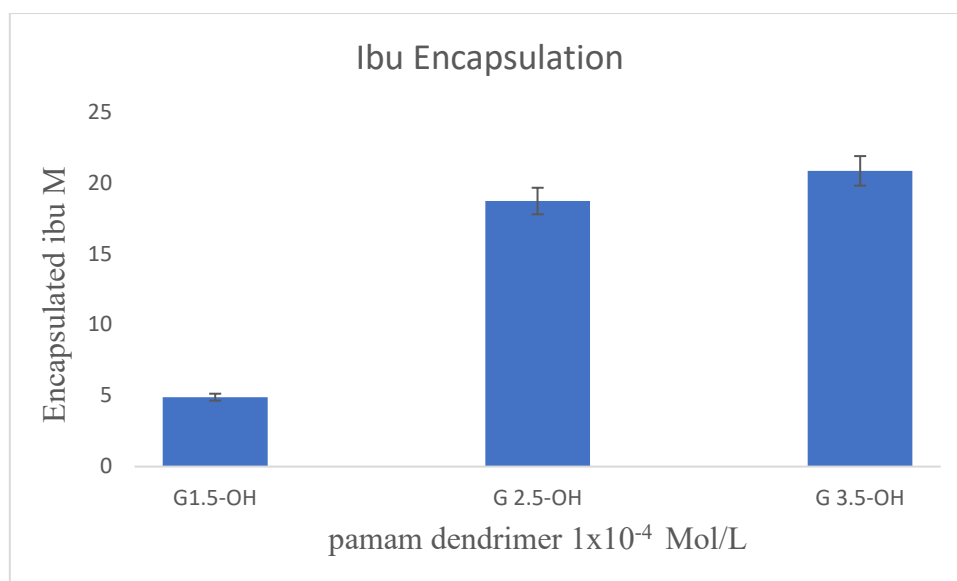


Figure 4: Enhancement in Ibuprofen concentration after encapsulation with different generations of PAMAM dendrimer.

Although there was a large increase in encapsulation between the G1.5-OH and G2.5-OH dendrimers, there was no significant difference between the G2.5-OH dendrimers and G3.5-OH dendrimers as shown in Figure 4. The smaller G1.5-OH dendrimer lacked a well-defined globular structure and does not have a 3-dimensional flat-plate shaped structure. As such, it did not generate or provide a significant number of hydrophobic pockets. On the other hand, the G3.5-OH and G2.5-OH dendrimers took on a globular spherical shape, offering a controlled and well-defined "internal space" that offers a significant hydrophobic environment for the drug. The resulting increase in solubility is significant and provides evidence of the dendrimer's ability to encapsulate Ibuprofen within its hydrophobic cavities. While a larger increase in loading was expected for the higher-generation G3.5-OH dendrimer, the actual increase in loading of ibuprofen for G 3.5-OH dendrimer was only higher by two than that observed for the G 2.5-OH dendrimer. This may be because, although the G3.5 OH dendrimer has a globular well-defined structure, this is accompanied by an increased steric crowding, which generates a reduction of the organised space within the interior and a decrease in binding.

Although hydrophobic interactions probably dominate encapsulation, there are a number of possible secondary interactions that may occur: for example, the acidic components of Ibuprofen can form salts with the tertiary amines of the dendrimer. Furthermore, there are a number of clear hydrogen bonding opportunities possible between Ibuprofen and the internal amide/amine units within the dendrimers. Based on these findings, the G2.5-OH dendrimer was found to be the most suitable generation for encapsulating hydrophobic molecules.

Following investigation into how the size of dendrimers affects their ability to encapsulate substances, with the identification of the G 2.5-OH dendrimer as the optimum host, the next step was to examine the connections between dendrimer concentration and the extent of drug encapsulation. This set of experiments aimed to ascertain how varying concentrations of the G2.5-OH PAMAM dendrimer (1.0E-3, 1.0E-4, 1.0E-5, and 1.0E-6 M), could influence the loading of the drug molecule. In simple terms, it was expected that the level of encapsulation should correlate linearly with the increase in dendrimer concentration such that as the amount of dendrimer was doubled, a doubling of the encapsulation/loading of the Ibuprofen would also occur. However, this proved to be not necessarily the case, requiring further investigation. Drug dendrimer complexes of varying concentration were thus made up using the method described above and the data shown in Table 5.

D conc	Δ ABS	ϵ	Total Ibuprofen Concentration/ E-03	conc of encapsulated Ibuprofen / E-03	Loading/D
0.000001	0.0945	94	1.0	0.005	5.3
0.00001	0.106	94	1.12	0.12	12.7
0.0001	0.27	94	2.87	1.87	18.7
0.001	0.5	94	5.31	4.32	4.3

Table 5: Different Ibuprofen loadings for different concentrations of dendrimer.

The resulting data clearly demonstrates that as the concentration of the dendrimer (G2.5-OH) increases, the solubility of Ibuprofen also increases. However, the increase in Ibuprofen levels does not correlate linearly with the dendrimer concentration, and, in particular, at dendrimer concentrations beyond 1.0E-03 M, there is a noticeable and dramatic decrease in the concentration of Ibuprofen. At concentrations of 1.0E-06 M, 1.0E-05 M, and 1.0E-04 M, there were 5, 12, and 18 equivalents of Ibuprofen encapsulated, respectively. However, only 4 equivalents of Ibuprofen were encapsulated at 1.0E-03 M. This clearly shows that the data does not support the simplistic prediction that drug encapsulation should be linearly related to dendrimer concentration. To refine the data and better determine the precise dendrimer concentration at which Ibuprofen concentration deviates from the expected linear relationship, a series of more finely tuned dendrimer concentrations between 1.0E-3 and 1.0E-4 M were thus investigated. The results are presented in Table 6.

Dendrimer conc	Δ ABS (273-276)	ϵ	Total Ibuprofen /10-3M	Conc of encapsulated Ibuprofen/10-3M	Loading/D
1.00E-04	0.27	94	2.8	1.8	18.7
2.50E-04	0.32	94	3.4	2.4	24
5.00E-04	0.325	94	3.45	2.45	24.5
7.50E-04	0.33	94	3.51	2.51	25

Table 6: Solubility of Ibuprofen in G2.5 -OH dendrimer at concentrations ranging from 1.0E-3 and 1.0E-4 M.

The initial Ibuprofen loading was 18 when the concentration of dendrimer was 1.0E-04M. When the dendrimer concentration increased to 2.5E-04 M, the solubility was thus expected to double to 36 moles per dendrimer. However, only a loading equivalent of 24 Ibuprofens was observed. The deviation from expectations was also worse at higher dendrimer concentrations: for example, when the dendrimer concentration reached 5.0E-04 M, only 18 moles were successfully encapsulated. The data for all concentrations studied is shown in Figure 15.

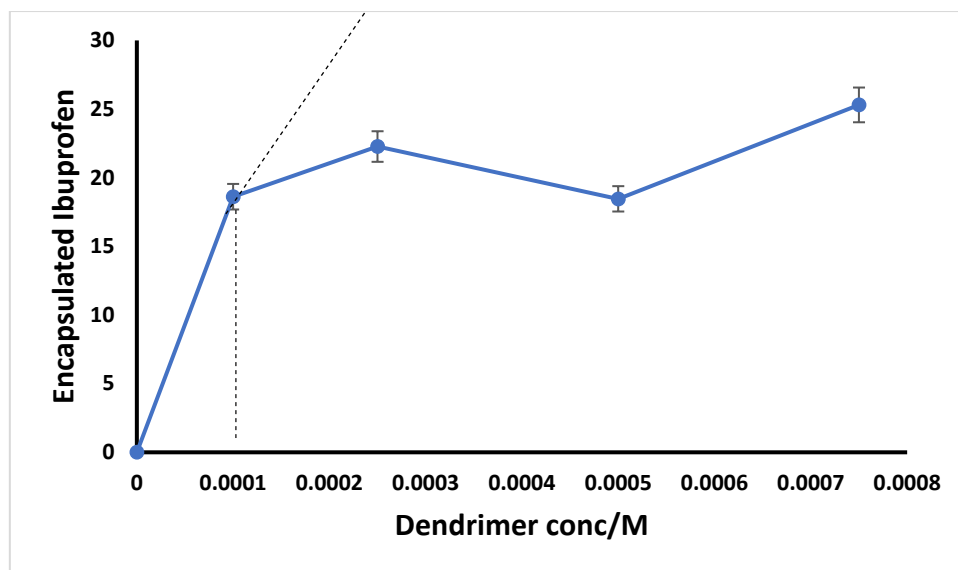


Figure 15: How increases in G2.5OH dendrimer concentrations affect Ibuprofen solubility.

Examining the graph shows that the deviation from linearity occurs at a concentration around 2.5×10^{-4} M of both Ibuprofen and dendrimer. It was thus hypothesised that the dendrimer may aggregate at higher concentrations, where the hydrophobic arms of one dendrimer may interact with the hydrophobic regions of other dendrimers. These interactions may then be reinforced by hydrogen bonding between the arms/branches of neighbouring dendrimers. If this happened, then the amount of free space within each dendrimer would be reduced, with the space taken up by the arms of other dendrimers as they aggregated. Such an aggregation process would necessarily impede the encapsulation of Ibuprofen. To investigate this, Dynamic light scattering (DLS) was utilised to try and observe any large aggregated species, and to measure their size if present. The experiments were carried out at dendrimer concentrations both below and above the point where encapsulation of Ibuprofen began to deviate from the predicted linear response, with DLS measurements taken from the G2.5 16 OH dendrimer at 1×10^{-4} and 2.5×10^{-4} M. The resulting DLS traces are shown in Figure 16.

The DLS data at the lower concentration showed the presence of small molecules with an average diameter of just a few nanometres, consistent with the unimolecular size of a solvated dendrimer. However, at the higher concentration, a broad polydisperse peak was observed, with

an average diameter around 225 nanometres. This clearly supports the presence of large aggregated species, offering good evidence that aggregation is the reason for reduced levels of expected encapsulation at higher concentrations.

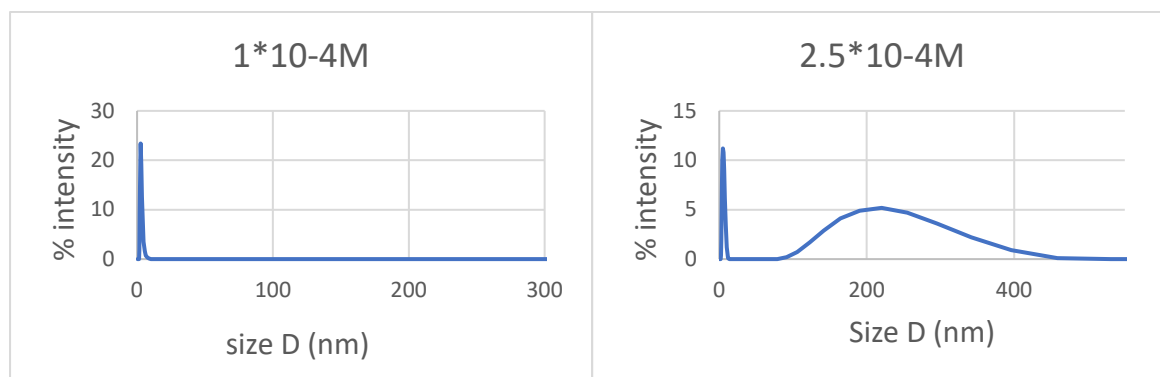


Figure 16: DLS data for G2.5-OH showing (A) dendramer at a concentration of 1.0E-04 M (non-aggregated). (B) dendramer at a concentration of 2.5E-04 M (aggregated).

4.1.1. Stability of Ibuprofen within aqueous dendrimer complexes.

The objective of the study was to investigate the stability of Ibuprofen in dendrimer solutions, including observing any impact from dendrimer size on the stability of the Ibuprofen within the dendrimer solution. All generations of dendrimers were prepared using the co-precipitate technique described previously, then the prepared samples were kept at room temperature at a pH of 7.4 in phosphate buffer for 10 days. Periodically, UV spectra were collected, and the peak at 273 nm was analysed to determine the rate of any degradation. The data for each dendrimer is shown in Tables 7.8,9 and the data for all dendrimers was subsequently plotted in Figure 17.

G1.5-OH at 1X10 ⁻⁴ M			
Time/days	ΔABS	ε	Drug/CONC M
D1	0.14	94	0.001489
D3	0.13		0.001383

D5	0.11		0.00117
D7	0.1		0.001064
D9	0.08		0.000851

Table 7: Stability of Ibuprofen in G1.5-OH.

G2.5-OH at 1×10^{-4} M			
Days	Δ ABS	ϵ	Drug/CONC M
D1	0.27	94	0.002872
D3	0.26		0.002766
D5	0.26		0.002766
D7	0.25		0.00266
D9	0.24		0.002553

Table 8: Stability of Ibuprofen in G2.5-OH.

G3.5-OH at 1×10^{-4} M			
Days	Δ ABS	ϵ	Drug/CONC M
D1	0.29	94	0.003085106
D3	0.27		0.00287234
D5	0.27		0.00287234
D7	0.25		0.002659574
D9	0.24		0.002553191

Table 9: Stability of Ibuprofen in G3.5-OH.

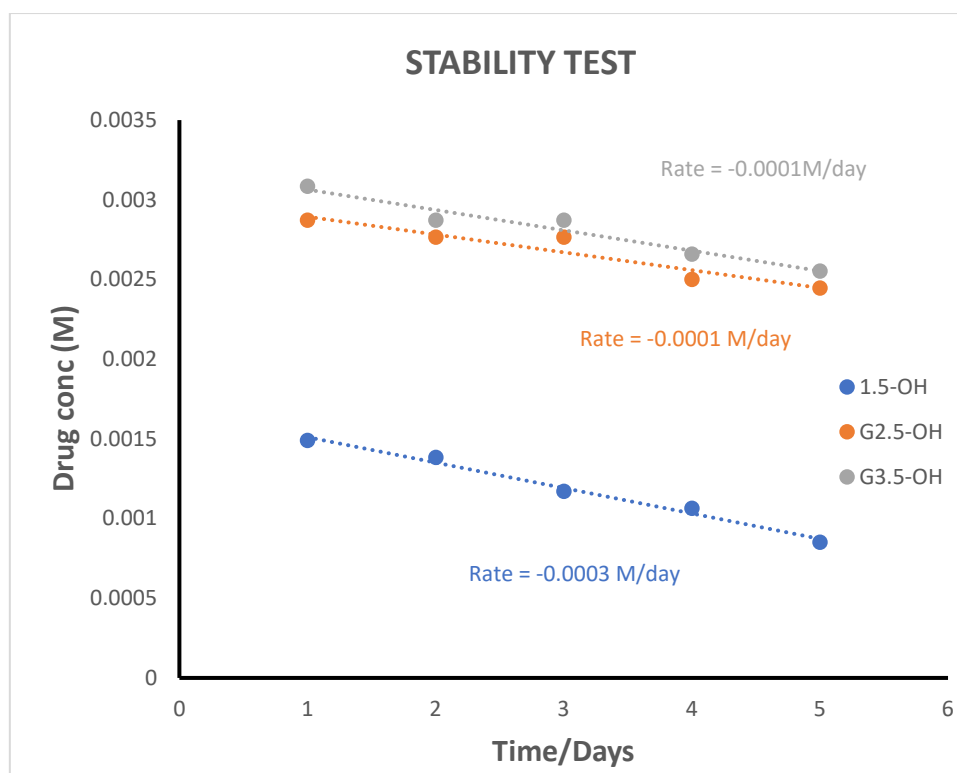


Figure 17: Stability of OH-PAMAM dendrimer-ibuprofen complexes over 10 days.

The results presented above indicate that all drugs exhibited reasonable stability, with G2.5-OH being the drug was the most stable by around 90 %. The stability of Ibuprofen in G2.5-OH can be attributed to the dendrimer's optimised internal structure, which maximises binding by facilitating a significant number of drug/dendrimer interactions, thereby enhancing stability, through protecting the ibuprofen from the external aqueous solution (the degradation pathways are possible, but hydrolysis is the most likely)

4.1.2. Ibuprofen release from G2.5-OH dendrimer.

The encapsulation of a drug can dramatically increase its solubility as well as protecting it from acid in stomach, the body's immune system, and other plasma molecules. However, unless the drug can then be released from the dendrimer, the result will be a poor therapeutic formulation. The stability and encapsulation data for G2.5 PAMAM G2.5-OH confirmed it as the optimum generation for maximum load and stability in initial testing. As a result, G2.5-OH pamam dendrimer was selected for testing to evaluate the release profile for IBU.

An ibuprofen/dendrimer complex of $1 \times 10^{-4} \text{M}$ of dendrimer and 8×10^{-3} ibuprofen was prepared using the methods described previously, and 6 mL of the resulting complex was then placed into osmosis tubing with a molecular weight cut off of 1,000Da. This was then deposited in a beaker containing 200 mL of pH 7.4 phosphate buffer. Samples were removed from the dialysis bag and analysed using UV at time zero, and then periodically every 24 hours for 5 days, based on measuring the absorption of the ibuprofen Soret band at 272 nm. The resulting data is presented in Table 10 and displayed graphically in Figure 18.

Time	$\Delta\text{abs (273-276)}$	CONC E-03	Half life
0	0.8003	8.5	34hr
24	0.507	5.39	
48	0.3219	3.42	
72	0.2305	2.45	
96	0.11	1.17	
120	0	0	
Dendrimer conc $1 \times 10^{-4} \text{M}$			
IBU conc 8.5×10^{-3}			

Table 10: Release of IBU from OH-PAMAM dendrimer over five days.

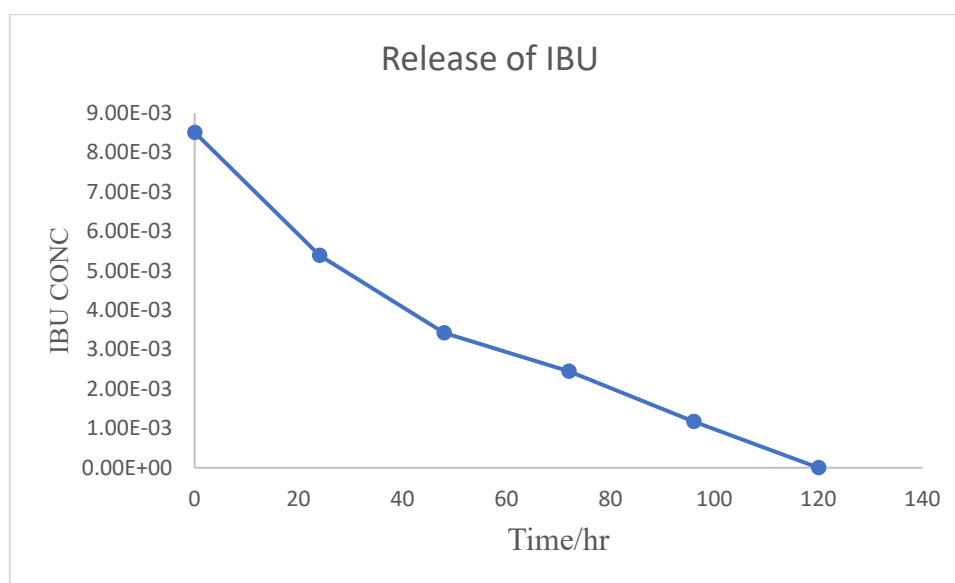


Figure 18: Release of IBU from OH-PAMAM dendrimer over five days

The results clearly demonstrate that Ibuprofen can be released from PAMAM dendrimer, supporting the potential applicability of these systems for drug delivery. Furthermore, the overall release was relatively slow, indicating a reasonably good interaction between dendrimer and the drug, potentially supporting the development of slow-release applications that could provide relief from pain for longer durations, as well as typically requiring less frequent dosing. This might be particularly beneficial for individuals who need pain relief throughout the day or night who prefer not to take multiple doses. Furthermore, the slow release of the medication can potentially lead to fewer spikes in drug concentration, which can help in reducing certain side effects that may otherwise occur with rapid changes in drug levels.

The overall release profile demonstrated two distinct phases, based on the curved nature of the release profile. The first phase is rapid, occurring from $t=0$ to $t=50$ hours. This is then followed by a slower release phase. The experiment began with a saturated solution of Ibuprofen and a fully loaded dendrimer, and thus the overall release occurred in three steps. The first was the release of free Ibuprofen (non-encapsulated) from the saturated solution, which crosses the osmosis membrane relatively rapidly. As this occurs, the concentration of free Ibuprofen in the bulk solution is reduced, making space for more Ibuprofen. During the second step, encapsulated Ibuprofen is thus released from the dendrimer to fill the vacated space in the bulk solution, which is a relatively slower process. This slow release may occur through disruption of the electrostatic and hydrogen bonding interactions that serve to entrap the drug molecules within the dendrimer structure, though the PAMAM dendrimers could also decompose by means of hydrolysis, resulting in drug release. Under physiological conditions, drug release could thus be faster if the interactions became weaker more easily and/or the dendrimer degradation occurred more quickly. The final step is the same as the first, with the newly released Ibuprofen crossing the membrane relatively rapidly.

Overall, the release study was positive, supporting the potential application of dendrimers for drug delivery.

4.2. Part2: Encapsulation of therapeutic porphyrins in hydroxyl terminated PAMAM dendrimers.

Photodynamic therapy is a treatment method that involves using a photosensitive compound of photosensitiser that accumulates in pathological tissues, either locally or throughout the body, before acting to absorb light at a specific wavelength, initiating activation processes that combine with oxygen to selectively eliminate undesirable cells. While PDT can be effective in treating various medical conditions, including certain types of cancer and skin conditions, it does come with some potential risks and considerations, including a high potential impact on healthy tissues.¹⁰¹

Cancer, as a set of diseases without a definitive cure, often requires patients to undergo painful and life-altering treatments based on attempts to eradicate cancerous cells. Surgical removal, chemotherapy, and radiation therapy are commonly employed to treat malignant tumours,^{102 15} while another treatment option, targeted drug therapy, involves administering drugs directly to a tumour to destroy cancer cells.¹⁰² Combining this approach with phototherapy allows the activation of a substance within the tumour, enabling effective cancer treatment. Synthesising porphyrins with optical properties that respond to specific wavelengths of light, such as infrared or near-infrared light, creates ideal candidates for allowing light therapy to penetrate the body; as a corollary, however, patients treated this way must be kept out of the light more generally. There is thus a need for a delivery system that can protect the body from harmful sensitizers while facilitating targeting of the affected area.

Encapsulating porphyrins within nanoparticles can enhance their targeting capabilities enabling them to accumulate within tumours. Furthermore, nanoparticle delivery systems can improve their solubility through encapsulation, effectively dispersing the drug in aqueous environments. Nanoparticle-based drug delivery systems can also protect these drugs from

degradation, enhancing cellular uptake. Porphyrins are also suitable for applications in various diagnostic techniques due to their strong interaction with light.⁹⁴

Porphyrins are a class of tetrapyrrole compounds with planar porphyrin cores surrounded by substituent groups.¹⁰³ They are both essential and abundant in living systems, facilitating various processes, including photosynthesis.⁹⁴ The stable macrocyclic structure of porphyrins allows for complexation with metal atoms.¹⁰⁴ and different derivatives can thus be obtained by substituting groups at specific positions in the pyrrolic molecules. Porphyrins have thus been studied for over a century, based on significant scientific interest in their synthesis, assembly, and applications.¹⁰⁵

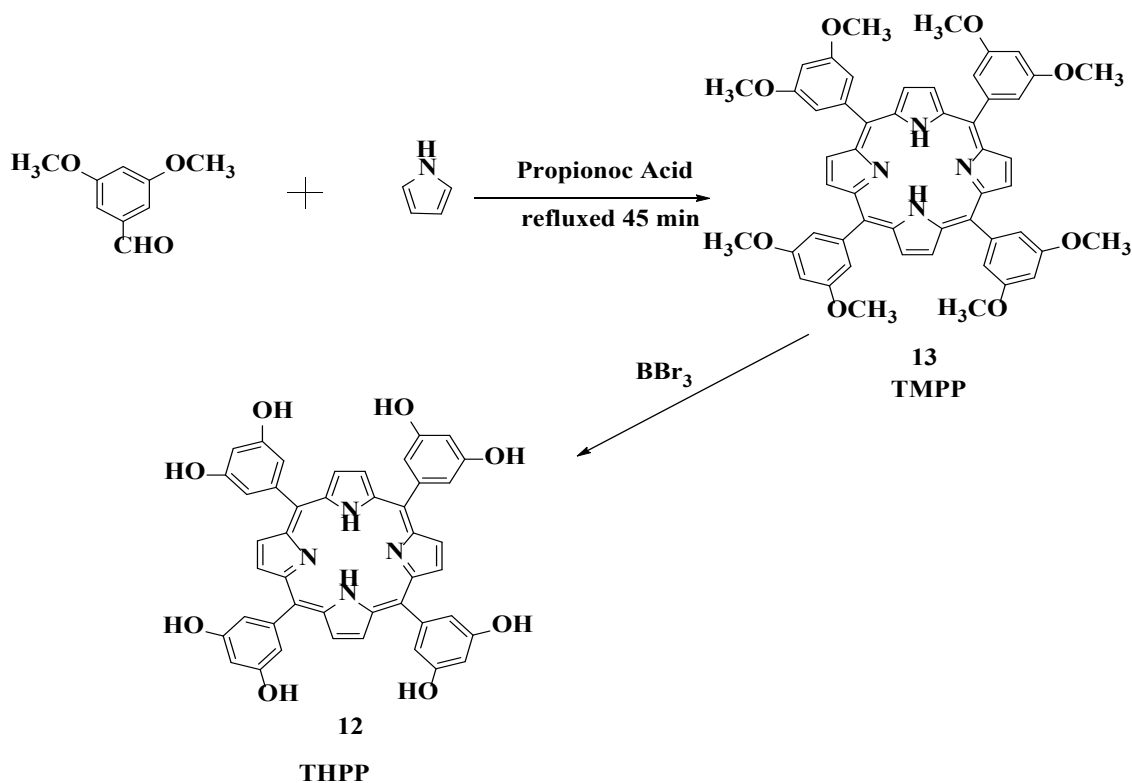
One crucial factor for effective porphyrin-mediated photodynamic therapy is the solubility and delivery of porphyrin derivatives.¹⁰⁶ Porphyrins have a tendency to self-aggregate, forming complex nanostructures.¹⁰⁷ Researchers have found that dendrimers G5 and G4.5, which have 128 surface binding sites, can act as templates to organise the assembly of porphyrins on their periphery. This occurs primarily through electrostatic interactions with the surface amine or carboxyl groups on the PAMAM dendrimers, though the process is influenced by the solution's pH value and the specific functionalization of porphyrins.¹⁰⁸ The self-assembled porphyrin dendrimers are then large enough to accumulate in tumours, making them effective PDT agents. Typically, porphyrins are produced by reacting pyrrole with a selected aldehyde in stoichiometric proportions. The resulting compounds are UV-active, and their absorption as seen in spectroscopy ranges from 400 to 600 nm, depending on how the porphyrin is substituted.¹⁰⁹

One of the aims for this part of the thesis is to determine whether or not metalated porphyrins increase the effectiveness of encapsulation through coordination to the internal amino groups of the dendrimer. Previous studies have examined the use of Tetraphenyl porphyrin (TPP), and Zn - Tetraphenyl porphyrin(Zn-TPP); however, encapsulation efficiency was extremely low

for both at less than one porphyrin per 10 dendrimers. This low loading was attributed to the complete insolubility of TPP and Zn TPP during the coprecipitation/encapsulation process, which suggests that the porphyrins possess some degree of methanol solubility.¹¹⁰ To address the challenge of insolubility, tetra hydroxyphenyl porphyrins (THPP and Zn THPP), which feature hydroxyl groups intended to improve their solubility in methanol were recommended, particularly tetrakis (3, 5-dihydroxyphenyl)-porphyrin (THPP).

4.2.1. Syntheses of Tetrakis (3, 5-dihydroxyphenyl)-porphyrin (THPP)

The synthesis of THPP 12 was a two-step process, as illustrated in Scheme 9. The reaction was initially conducted for 45 minutes under reflux conditions in propionic acid by combining 3,5-methoxybenzaldehyde and pyrrole. The solution was then allowed to cool to room temperature, at which point a precipitate of tetrakis (3,5-dimethoxyphenyl)-porphyrin (TMPP) formed. This was gathered using vacuum filtration and then washed with cold methanol until the filtrate was colourless.



Scheme 9: Synthesis of Tetrakis (3, 5-dihydroxyphenyl)-porphyrin (THPP).

The successful synthesis of TMPP **13** was established through various analytical techniques, including the observation of distinct spectral features in the UV spectrum, such as the porphyrin Soret band at 420 nm and the four Q-bands at 512 nm, 545 nm, 580 nm, and 686 nm. Additionally, the ^1H NMR spectrum also revealed a large singlet, representing the methoxy protons, at 3.98 ppm, alongside a peak for the porphyrin's nitrogen protons at -2.9 ppm. Mass spectrometric analysis similarly detected a molecular ion peak at 855.

THPP **12** was obtained after removal of the methyl groups from TMPP **13** by means of boron tribromide. This was achieved by dissolving the methoxy porphyrin (TMPP) **13** in anhydrous dichloromethane, with the boron tribromide then added in a dropwise manner. This experiment took place at room temperature in a nitrogen atmosphere, complete with stirring for six hours followed by termination with water. Subsequently, the reaction mixture was neutralised using a sodium hydrogen carbonate solution, and the product was isolated using ethyl acetate. The resulting product exhibited excellent solubility in methanol and dichloromethane while remaining insoluble in water.

The successful synthesis of THPP **12** was confirmed through ^1H NMR spectroscopy. This was evidenced by the absence of the methoxy peak at 3.98 ppm, with an alternate peak appearing at 8.96 ppm, corresponding to the hydrogen atom in the pyrrolic moiety of the porphyrin ring. Furthermore, two peaks were observed at 7.06 ppm and 6.70 ppm, indicating the presence of phenylic protons in the ortho and para positions, respectively, while a distinct signal was detected at 9.72 ppm corresponding to the phenylic hydroxyl (OH) protons. Due to significant shielding inside the porphyrin ring, the inner pyrrolic N-H protons were also observed to resonate at -2.9 ppm.

A strong absorption at 419 nm, corresponding to the Soret band, was similarly observed in the UV spectrum, while four Q bands were observed at 520 nm, 560 nm, 595 nm, and 655 nm. As

shown in figure 19. Mass spectrometry analysis then revealed a peak at 743, and FT-IR analysis revealed a broad peak at $3,420\text{ cm}^{-1}$, further supporting the presence of phenolic OH groups.

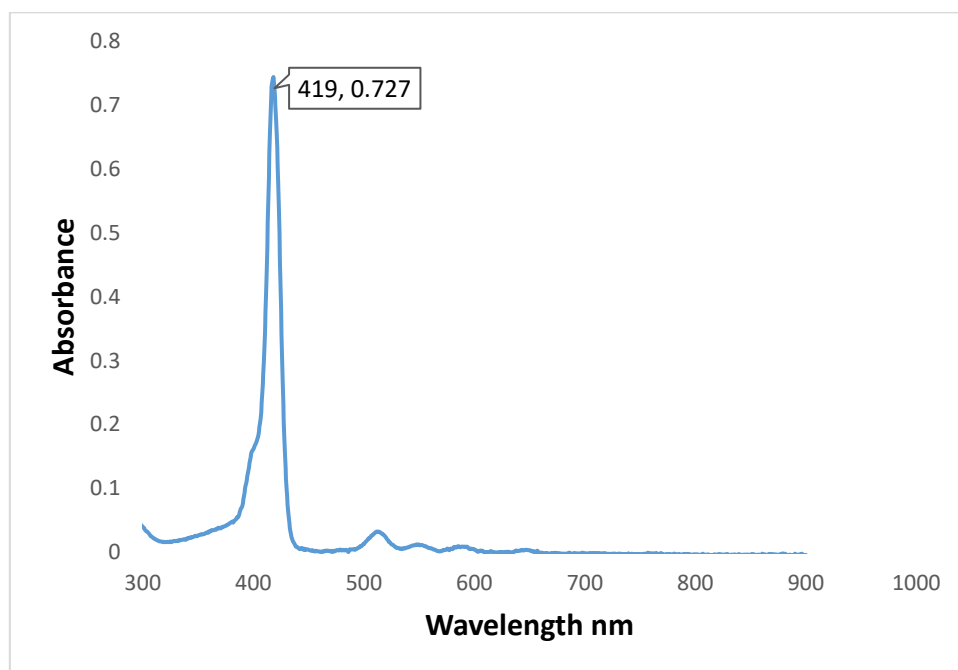


Figure 19: The UV-vis spectrum of THPP in buffer.

4.2.2. Tetrakis (3, 5-dihydroxyphenyl)-porphyrin (THPP) encapsulation within hydroxyl dendrimers

The first encapsulation experiment sought to investigate the encapsulation of non-metalated THPP **12**, a porphyrin that cannot coordinate to internal nitrogens; any encapsulation is thus dominated by simple hydrophobic interactions, supported by the acid base ion pairs between the acidic phenols of the porphyrin and the internal nitrogens within the dendrimer, as shown in Figure 20. To evaluate the encapsulation process and calculate the increased concentration of THPP **12**, any changes in the porphyrin's Soret peak at 418 nm within the UV spectrum were examined, as shown in Figure 20.

Encapsulation efficiency was evaluated across PAMAM-OH, G1.5-OH, G2.5-OH, and G3.5-OH. In all cases, the co-precipitation method was used with a dendrimer concentration of $1.0\text{E}-04\text{ M}$. The concentration of encapsulated THPP **12** was then determined from the extinction coefficient ($9980\text{ dm}^3\text{ mol}^{-1}\text{ cm}^{-1}$), obtained using a Beer-Lambert plot to find the difference

in abs between 419 and 424. Figure 20 shows the UV-vis spectra of THPP **12** encapsulated within the various dendrimers.

Parameter	ϵ	Solubility in buffer
THPP	9980	5×10^{-7}
Characterisation of THPP		

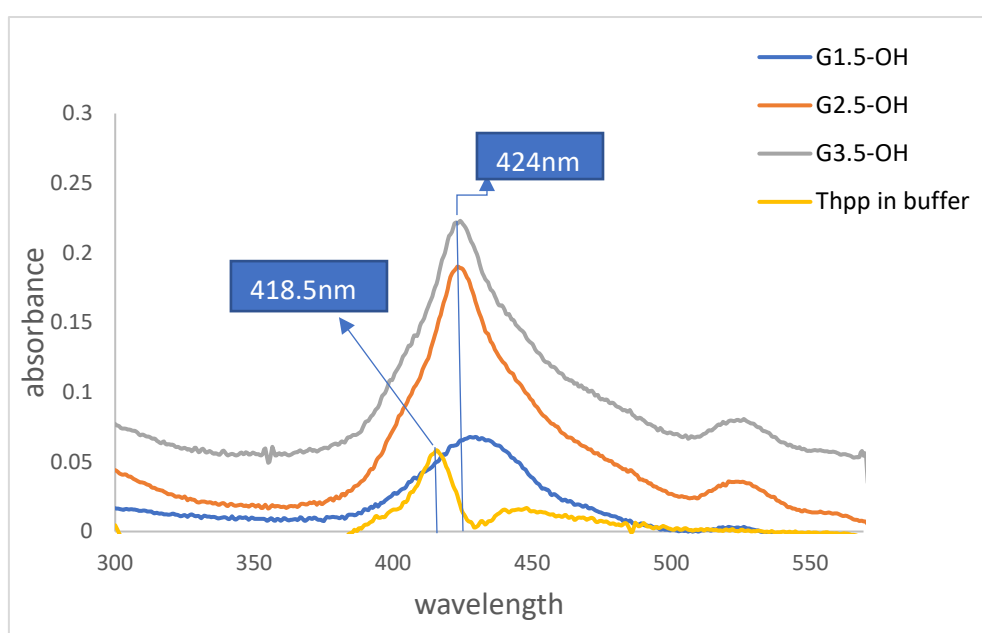


Figure 20: UV absorbance data before and after THPP is encapsulated in different generations of hydroxyl PAMAM dendrimer.

The encapsulated porphyrin spectra exhibit a minor shift towards longer wavelengths.

D/G	Δ ABS (424-427)	Total [THPP 12] E-04 M	Encapsulated [THPP 12] E-04 M	Loading/Dendrimer
G1.5-OH	0.013	0.428	0.477	0.477
G 2.5-OH	0.035	1.30	1.29	1.29
G 3.5-OH	0.039	1.45	1.44	1.44
Maximum free THPP concentration in buffer = 5×10^{-7} M				

Table 11: Encapsulation of tetrakis (3,5-dihydroxyphenyl)-porphyrin (THPP) within PAMAM-OH. Ext. Coefficient of 9,980 $\text{dm}^3 \text{mol}^{-1} \text{cm}^{-1}$ Δ ABS.

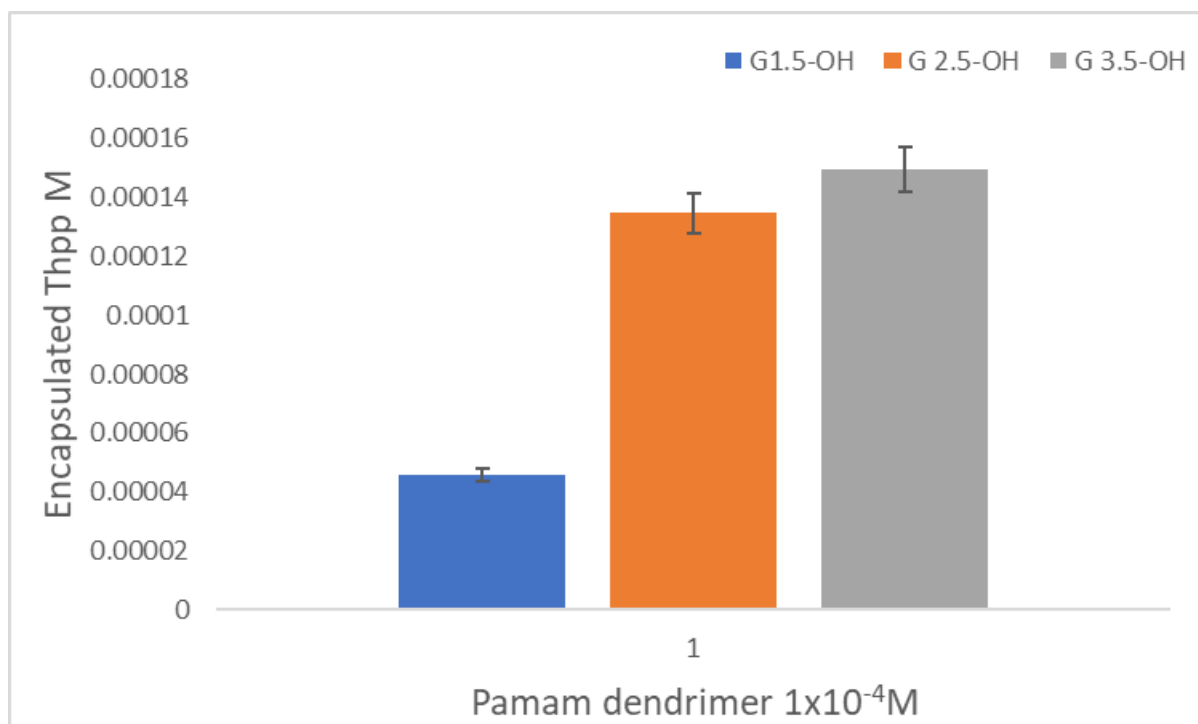


Figure 21: Average concentration increase of THPP within different PAMAM dendrimer generations.

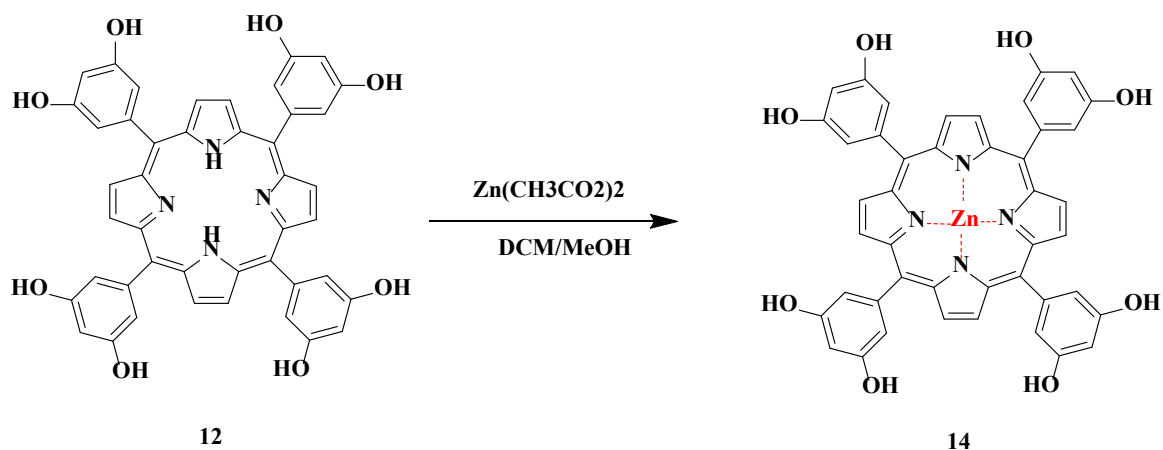
It became evident that the size of the dendrimer influences the solubility of THPP 12, at least up to a point. As shown in Table 11, the G1.5-OH containing eight OH groups was found to incorporate 0.4 M of THPP 12 into the hydrophobic cavity of the dendrimers, while 1.4 M of THPP 12 was encapsulated in G2.5-OH, with the sixteen OH groups. However, only 1.5 M of THPP12 was encapsulated within the dendrimer for the G3.5-OH molecule with 32 OH groups. The smaller G1.5 OH dendrimers' minimal loading could be attributed to its disorganised and open structure. The concentration of encapsulated THPP, though higher for both the G2.5-OH and G3.5-OH dendrimers, showed no significant difference between these two dendrimers. As with Ibuprofen encapsulation, this could be attributed to their more densely packed structures. As well as an increase in absorption, the UV spectra also illustrated a solvatochromic shift. The Soret band of THPP 12 in buffer was 418.5 nm, but this shifted to 424 nm for all dendrimer generations after encapsulation. This suggests that the binding environment within the dendrimers was distinct from that of water, and that the change in shift results from alternative interactions between THPP 12 and the dendrimer. One obvious cause could be an acid/base

interaction between the dendrimer's internal tertiary amines and the phenolic OH groups, which would generate a phenolate anion that could then be stabilised via resonance. If this occurs, the conjugated energy levels of THPP **12** are perturbed in a different manner to the aqueously solvated porphyrin **12**, resulting in a change to the absorption characteristics of THPP **12**.

As well as changing the UV properties of THPP and confirming encapsulation, the acid/base interactions also strengthened the overall binding between the dendrimer and the porphyrin. While the levels of loading were low compared to Ibuprofen, the increase in solubility relative to the free amount of THPP **12**, was significantly greater. For Ibuprofen, the dendrimer doubled the amount in solution, while the amount of THPP **12** in solution was nearly 300 times greater. Although a large increase in the solubility of THPP, the amount loaded was still relatively low. To try and improve loading, we proposed the use of metalated porphyrin, that could provide additional interaction by coordination to the internal amines of the dendrimer.

4.2.3. Synthesis and characterisation of zinc metalated porphyrin (ZnTHPP **14).**

After examining the hydrophobic and electrostatic/acid-base interactions emerging from the encapsulation of THPP **12** within hydrophobic dendrimer cavities, attempts were made to maximise encapsulation by utilising metal coordination. Consequently, THPP **12** was metalated by the addition of zinc acetate in dichloromethane and methanol to give Zn-THPP **14**; this produced a good yield (Scheme 10). The reaction was conducted at ambient temperature for 45 minutes, after which ¹H NMR demonstrated complete metallization of the porphyrin macrocycle cavity, as indicated by a lack of a peak at 2.9 ppm in the internal NH, indicating that the macrocycle vacancy was filled by the zinc. Mass spectrometry then confirmed the insertion of zinc, based on the detection of a molecular ion peak at 806 (MH⁺).



Scheme 10: Synthesis of Zinc Tetrakis (3, 5-dihydroxyphenyl)-porphyrin (ZnTHPP **14**).

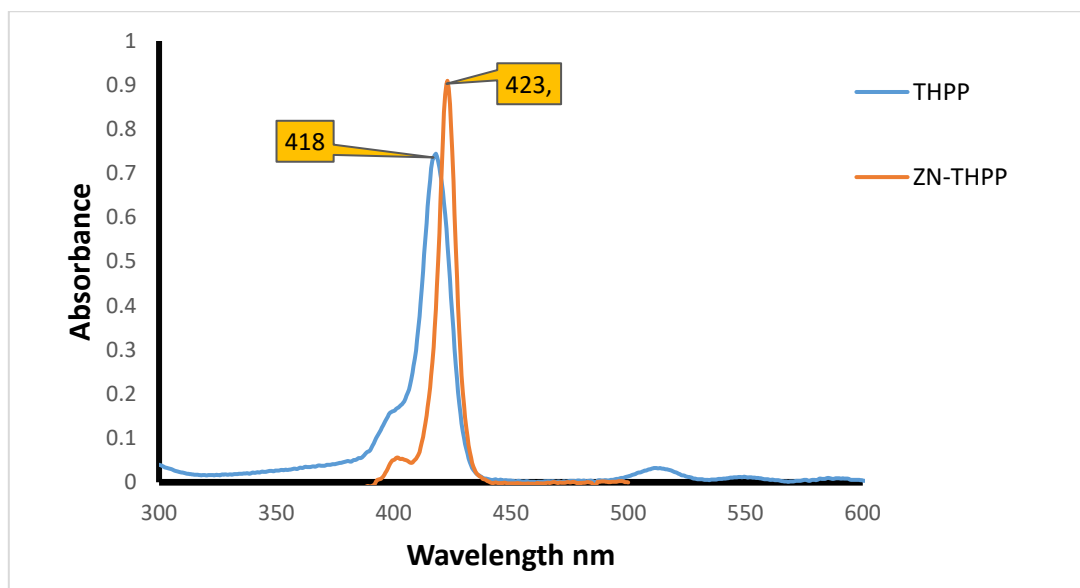


Figure 22: UV-visible spectra of Zn-THPP and THPP dissolved in methanol.

The UV-vis spectrum revealed distinct differences between the bands for free-base and metalated porphyrins. The Zn-THPP **14** Soret band appears at 423 nm, whereas the Soret band for free-base THPP **12** is at 418 nm, (figure 22) potentially due to the coordination complex between the buffer and the zinc metal ions, which can affect the electronic structure of both, resulting in shifts in the UV absorption spectra as compared to the spectra of the individual unchanged components.

Additionally, only two Q bands are observed, at 556 and 593 nm, for the metalated porphyrin **14**, as opposed to the four peaks visible in free base porphyrin.

4.2.4. Zn-THPP **14** coordination with PAMAM dendrimers

Before encapsulation, the delta extinction coefficient for Zn-THPP **14** was determined by means of Beer Lambert analysis in methanol to be $5,854 \text{ dm}^3 \text{ mol}^{-1} \text{ cm}^{-1}$. This was obtained using the difference in absorption between 424 nm and 427 nm.

Using this information, a maximum concentration of $2 \times 10^{-6} \text{ M}$ for the Zn-THPP **14** in phosphate buffer alone (no dendrimer) was calculated. Zn-THPP is more soluble than simple THPP, probably due to the presence of zinc that can provide coordination bonds with various solvent molecules, additional interactions that help solubilize the compound in solution. Zn-THPP **14** was then encapsulated using the same co-precipitation technique used for THPP **12**. To calculate the encapsulated concentration of Zn THPP **14** in the dendrimers, the peak at 423 nm in the UV spectra was monitored, as shown in Figure 23.

Parameter	ϵ	solubility in buffer
Zn-THPP	5854	2×10^{-6}
The Characterisation of Zn-THPP		

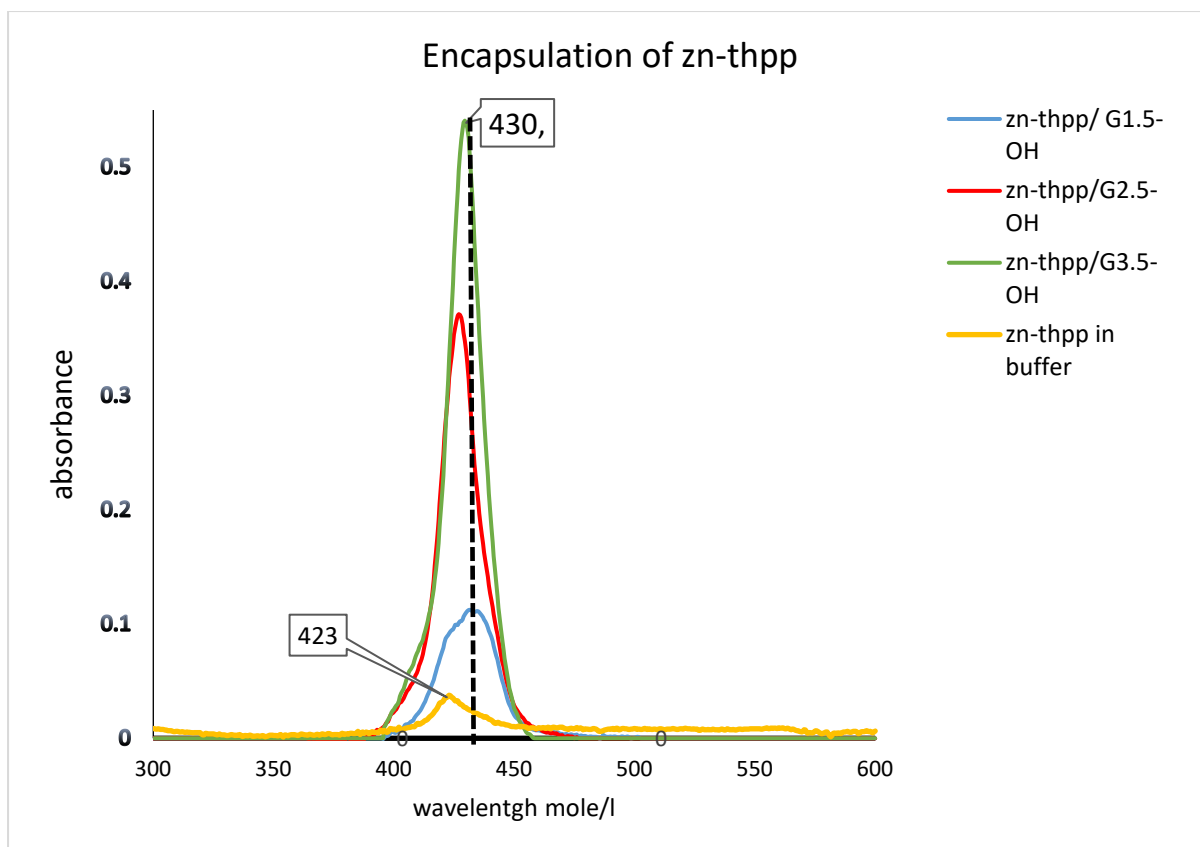


Figure 23: UV-vis spectroscopy displaying Zn-THPP absorbance prior to and following encapsulation.

D/G	Δ ABS	ϵ	Total [Zn-THPP 14] E-04 M	Encapsulated [Zn-THPP 14] E-04 M	Loading/dendri mer
G1.5- OH	0.012	5854. 6	0.758	0.738	0.738
G 2.5- OH	0.028	5854. 6	1.77	1.75	1.75
G 3.5- OH	0.031 4	5854. 6	1.98E	1.96	1.96
Dendrimer concentration is 1×10^{-4}					
Maximum free ZN-THPP concentration in buffer = 2×10^{-6} M					

Table 12: Encapsulation of Zn-THPP in different generations of PAMAM dendrimer.

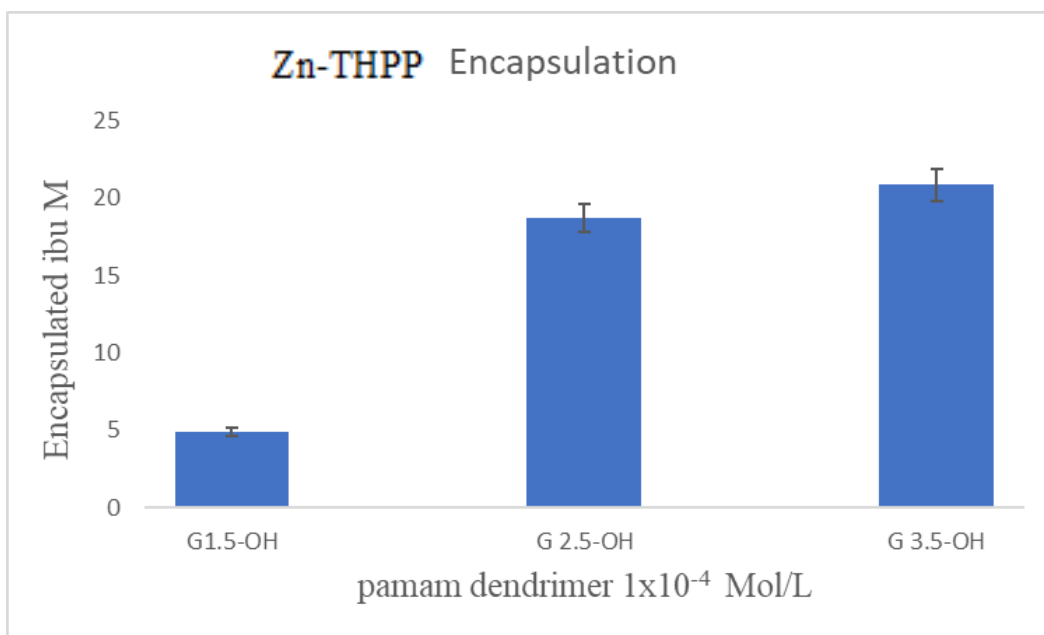


Figure 24: The average concentration of Zn-THPP thus tended to rise as the PAMAM dendrimer generations increase.

The porphyrin-sorted band of Zn-THPP encapsulated in all dendrimers shifted from 423 nm to 430 nm. As the Figure 23 illustrates, in G1.5-OH, two peaks occur, with one at 423 nm and one at a higher value, indicating that some free porphyrin is mixed with the bound porphyrin. This occurs as the encapsulation is very weak. However, while some free porphyrin may occur in the G2.5-OH and 3.5-OH, as the encapsulation is much stronger, only one peak, at 430 nm, can be seen. In comparison to the deprotonation and weak ion pairing observed for THPP **12**, this change reflects the strong coordination between Zn-THPP **14** and the nitrogen within each dendrimer, which further perturbs the delocalised aromatic structure and energy. This coordination also generates increased solubility of Zn-THPP **14** relative to THPP **12**.

As seen previously, solubility/encapsulation is dependent upon the size of the dendrimer. As shown in Table 12, the larger the dendrimer generation, the greater the level of Zn-THPP binding. Both the G2.5-OH and G3.5-OH dendrimers bound slightly more of the metalated porphyrin than the free base porphyrin, to the extent of about 25% in both cases. Interestingly, the G1.5-OH encapsulated nearly 50% more of the metalated porphyrin than it did the free base porphyrin, despite the G1.5-OH dendrimer having a more open structure and only four

accessible tertiary nitrogen's available for coordination. While this was not anticipated, it may be due to the relatively low starting point for the concentration free base porphyrin buffer. Overall, the insertion of zinc resulted in a measurable and large increase in solubility relative to solubility in water alone.

Although increases in solubilities were high for all porphyrins, the loadings were relatively low, with a maximum of nearly two Zn-THPP **14** per dendrimer, seen in the biggest dendrimer tested. In this respect, the results differed from those observed for Ibuprofen, which showed minimal increases in encapsulation and solubility, despite much larger loadings. The reason for this is the very different solubilities of porphyrin and Ibuprofen in water/buffer alone. While Ibuprofen is inherently reasonably soluble, making it harder to increase soluble concentrations even with large loadings, porphyrins are natively almost insoluble in water/buffer alone, such that even low loadings can result in large increases in soluble concentrations.

4.2.5. Stability of ZN-THPP 14 in the dendrimer complexes

The objective of this section of the study was to investigate and confirm the impact of dendrimer size on the stability of Zn-THPP. Porphyrins are photosensitive and can react with light, acting as photosensitisers for PDT. Based on this, the stability experiments were conducted in both the presence and absence of light. All generations of dendrimers were prepared using the co-precipitate technique, and samples were placed in either amber-coloured or glass vials to create dark and light conditions, respectively. These vials were then stored at room temperature in a pH 7.4 phosphate buffer (0.01M) for 10 days, having previously undergone immediate analysis. Periodic assessments were done every three days to observe any signs of precipitation, turbidity, change in consistency, or drug loss: the degradation rate of the drug was indirectly calculated by monitoring the rate of decrease in its concentration. Over the course of 10 days, a total of five data points for the drug in light, and dark condition were examined using UV-vis spectroscopy: essentially, UV spectra were collected and the peak

at 430 nm analysed to determine the rate of any degradation. The plots abs vs time for each dendrimer are shown in Figures 24,25

DARK			
DAYS	G1.5-OH	G2.5-OH	G3.5-OH
D1	8.21576E-05	1.77E-04	1.96E-04
D3	7.58378E-05	1.71E-04	1.90E-04
D5	5.68784E-05	1.64E-04	1.83E-04
D7	4.42387E-05	1.52E-04	1.71E-04
D9	3.15991E-05	1.52E-04	1.64E-04

Table 13: Stability of Zn-THPP in different generations of PAMAM dendrimer in dark storage conditions.

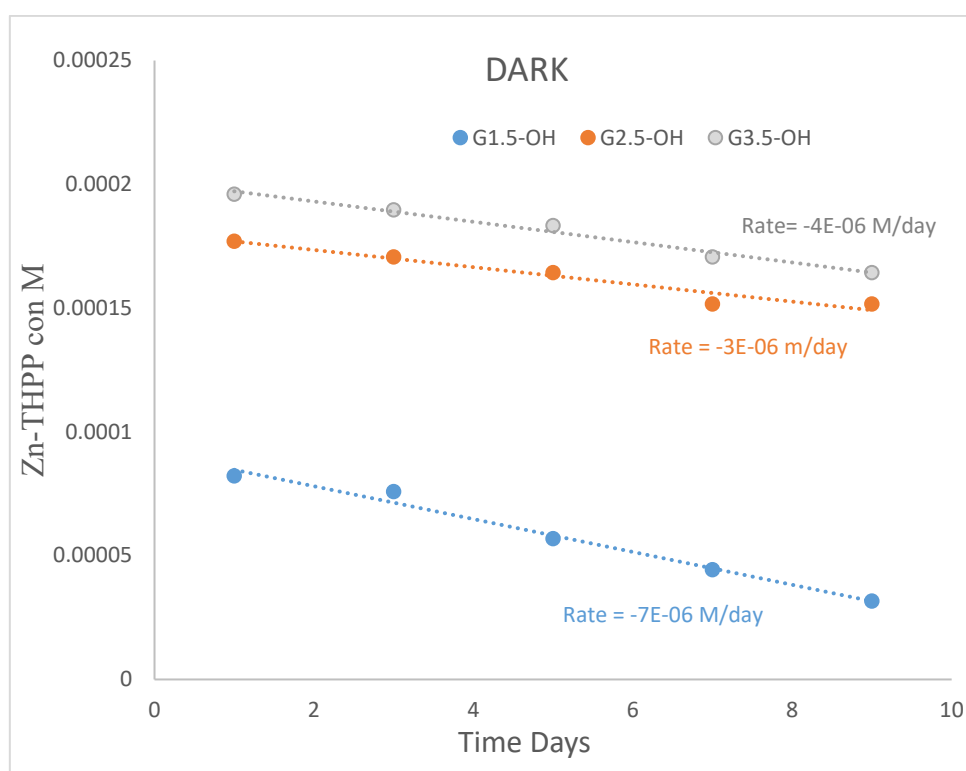


Figure 24: Stability of ZN-THPP in OH-PAMAM dendrimer in dark storage conditions for 10 days.

LIGHT			
DAYS	G1.5-OH E-05	G2.5-OH E-04	G3.5-OH E-04
D1	0.82	1.77	1.96
D3	0.695	1.64	1.83
D5	0.515	1.52	1.71
D7	0.375	1.52	1.58
D9	0.255	1.33	1.52

Table 14: Stability of Zn-THPP in different generations of PAMAM dendrimer in light storage conditions: all data reported at concentrations of 10⁻⁴ M.

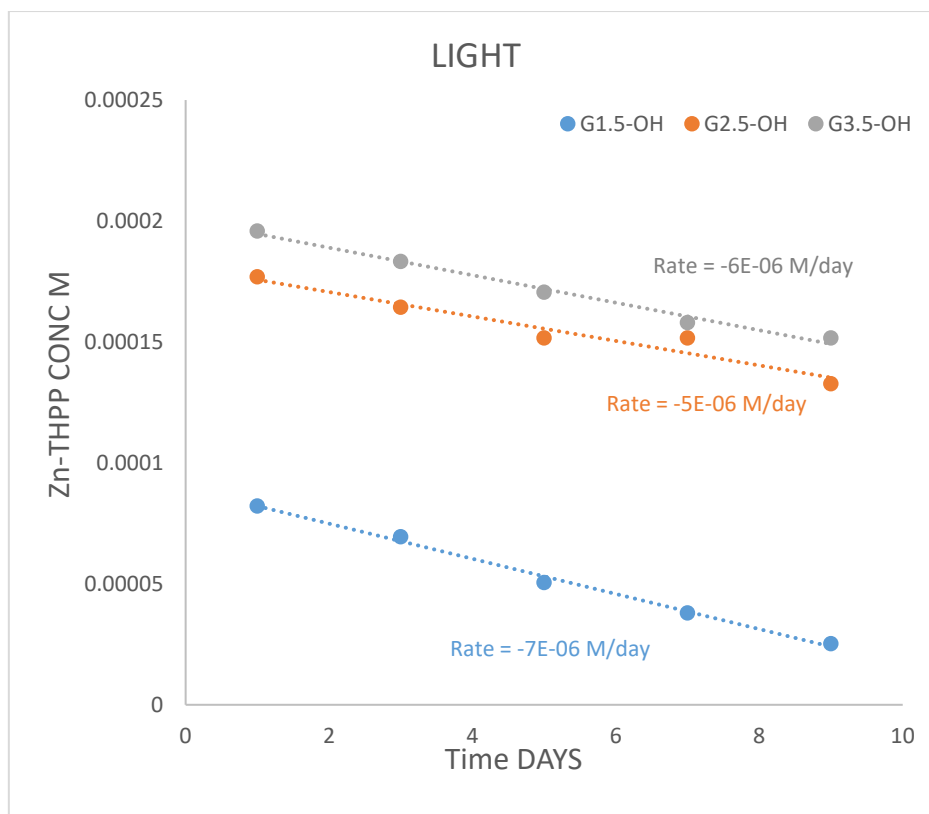


Figure 25: Stability of ZN-THPP in OH-PAMAM dendrimer in light storage conditions for 10 days.

The results presented above indicate that the Zn-THPP **14** exhibit a certain degree of stability in all dendrimers, though ZN-THPP showed better stability in G2.5-OH, by around 90%. The stability of the ZN-THPP in G2.5-OH, can be attributed to the dendrimer’s optimised internal structure; this maximises binding by facilitating a significant number of drug/dendrimer interactions, thereby enhancing stability.

DENDRIMER-Zn-THPP	Rate of degradation in Dark E-06 M/day	Rate of degradation in Light E-06 M/day
Zn-THPP IN G1.5-OH	7.2	7.6
Zn-THPP IN G2.5-OH	3.81	4.53
Zn-THPP IN G3.5-OH	4.51	4.92

Table: Rate of degradation of Zn-THPP from the dendrimer in dark and light conditions.

The results showed that stability was better after dark storage than in light storage, with all generations demonstrating better stability in the dark. The reason for this is porphyrins undergo

photodegradation, in which exposure to light leads to the destruction of the porphyrin structure and properties. Photodegradation is triggered when the energy from light activates porphyrin, triggering chemical reactions that lead to the formation of reactive species that can break down more easily; however, porphyrins can also be sensitive to photooxidation, where exposure to light causes oxygen molecules to react with the porphyrin to form free radicals. These free radicals can then further initiate additional chain reactions, resulting in damage to the porphyrin structure.⁹⁴

4.2.6. Zn-THPP 14 release from G2.5-OH dendrimer.

As previously, PAMAM G2.5-OH was selected as the optimum generation for maximum drug loading and stability, facilitating study of the release of An-THPP. The Zn-THPP/dendrimer complex was prepared with $1 \times 10^{-4} \text{M}$ of dendrimer and 8×10^{-4} of Zn-THPP, then 6 mL of the complex was placed into osmosis tubing with a molecular weight cut-off of 1,000. This was then deposited in a beaker containing 200 mL of pH 7.4 phosphate buffer, and samples were removed from the dialysis bag and analysed using UV at $t=0$ and then periodically every 24 hours for five days by means of measuring absorption of the Zn-Thpp Soret band at 429 nm. The resulting data is presented in Table 15 and displayed graphically in Figure 26.

Time(hr)	$\Delta\text{abs (430-433)}$	CONC E-04	Release rate/day
0	0.24	7.79	0.25
24	0.072	2.34	
48	0.0123	0.4	
72	0.0032	0.1	
96	0	0	
Dendrimer Conc $1 \times 10^{-4} \text{M}$			
Zn-THPP Conc 7.8×10^{-4}			

Table 15: Release of Zn-THPP from OH-PAMAM dendrimer over five days.

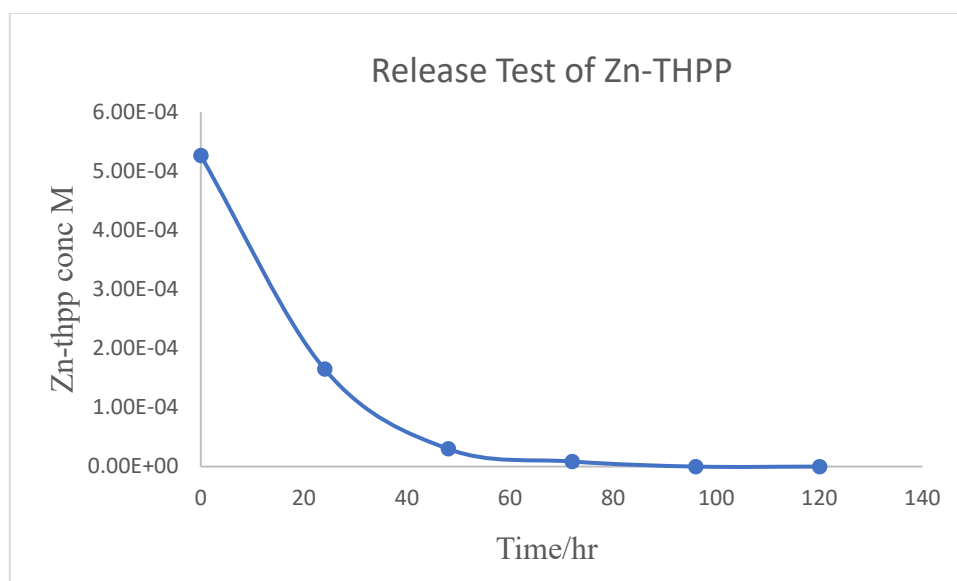


Figure 26: Release of Zn-THPP from OH-PAMAM dendrimer over five days.

The results clearly demonstrate that Zn-THPP **14** can be released from the PAMAM dendrimer. Furthermore, this release is slow, overall, which is positive in terms of potential PDT treatment, as slow release will enable the Zn-THPP complex to circulate around the body multiple times, creating a build-up within tumours without releasing the harmful Zn-THPP photosensitizer throughout the body. This could reduce the harmful side effects often associated with PDT. This slow release may be driven by disruption of the coordination and the electrostatic and hydrogen bonding interactions that serve to entrap the drug molecules within the dendrimer structure. It is, however, also possible that the PAMAM dendrimers can hydrolyse slowly under the conditions tested, with hydrolysis occurring much more rapidly under physiological conditions, led by biochemical enzymatic degradation.¹¹¹ Further tests are, however, required to establish whether this is in fact the case.

The overall release profile occurs over two distinct phases, as demonstrated by the curved nature of the release profile (Figure 26). The first phase is rapid, occurring from $t=0$ to $t=24$ hours. This is then followed by a period of slower release. The experiment begins with a saturated solution of Zn-THPP and a fully “loaded” dendrimer, and the overall release thus occurs in three steps, however. The first step is the release of free Zn-THPP (non-encapsulated)

from the saturated solution, which crosses the osmosis membrane relatively rapidly. When this occurs, the concentration of “free” Zn-THPP in the bulk solution is reduced, creating space for more Zn-THPP. During the second step, the encapsulated Zn-THPP is thus released from the dendrimer to fill the vacated space in the bulk solution, which is a relatively slower process. This slow release is triggered by disruption of the electrostatic and hydrogen bonding interactions that serve to entrap the drug molecules within the dendrimer structure. It is also possible that the PAMAM dendrimers could decompose through hydrolysis, resulting in drug release. Under physiological conditions, drug release may thus be faster where interactions are weaker and dendrimer degradation occurs more quickly. The final step is the same as the first, as the newly released Zn-THPP crosses the membrane relatively rapidly.

Overall, the study of drug release was positive, supporting the potential application of dendrimers for drug delivery.

4.3. Part3: Encapsulation of anticancer drug F37 in hydroxyl terminated PAMAM dendrimers.

Previous investigation and comparison of the encapsulation capacities of various polymers were done using Ibuprofen. Building upon these findings, the objective in this part of the current work was to explore similar effects in an anticancer drug with a more intricate structure. To facilitate this research, Professor Chen's group graciously supplied a quantity of an anti-cancer drug known as F73, whose structure is shown in Figure 27.

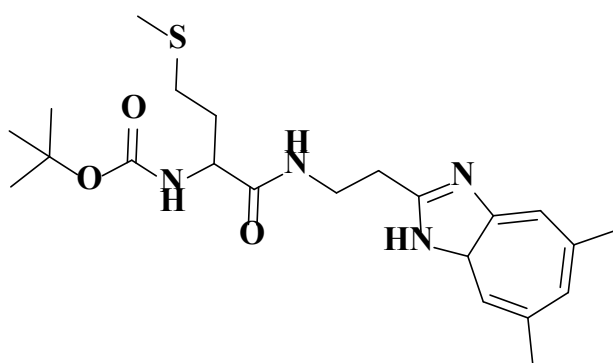


Figure 27: Structure of *tert*-butyl *N*-(1-[[[(5,6-dimethyl-1*H*-1,3-benzodiazol-2yl)methyl]carbamoyl]-3-(methylsulfanyl)propyl)carbamate (f73).

The full name for F73 is *tert*-butyl *N*-(1-[[[(5,6-dimethyl-1*H*-1,3-benzodiazol-2yl)methyl]carbamoyl]-3-(methylsulfanyl)propyl)carbamate. As the name suggests, F73 consists of three main parts: a *t*-Butyloxy carbonyl group on the left, which serves as an amino protecting group; a central methionine component; and a dimethyl benzimidazole ethylamine group, all of which are connected by peptide bonds. Although F73 was developed as a treatment for dementia, it was poorly active in many ranges. However, in tests against cancer cells, it showed good activity alongside IC50 in the nm range. Its mode of action is as a methionine synthase (MetS) inhibitor. This enzyme plays a vital role in the metabolic conversion of 5-methyltetrahydrofolate (MeTHF), thus restoring the active state of tetrahydrofolate. Inhibiting MetS therefore interferes with DNA and RNA synthesis, justifying the use of F73 in cancer therapy.

F73, as with many other anticancer medications, is relatively hydrophobic, and the challenge with all hydrophobic drugs is how to effectively deliver these to cancer cells. To address this issue, the use of both dendrimers and HBPs to encapsulate hydrophobic F73 were assessed. Another reason for selecting F73 was the availability of testing for the activity of the drug delivery system using various cancer cell lines. This allowed a full and complete comparison of the encapsulation, release, delivery, and other activity of the dendrimer and HBP systems, allowing full consideration of the main question of this thesis “are HBPs as good as dendrimers with respect to drug delivery

4.3.1. Encapsulation of anticancer drugs in neutral PAMAM-OH dendrimers

As with Ibuprofen, the initial objective was to determine the maximum amount of drug that could be encapsulated within the various polymer-based systems. In contrast to Ibuprofen, which is readily available, F73 is a scarce and expensive compound, making directly adding an excess of F73 during encapsulation not feasible. To overcome this obstacle, the method for drug encapsulation was modified to initial encapsulation with a 1:1 molar ratio of drug to polymer, based on the predetermined polymer quantity. Subsequently, the drug amount was increased to twice that in the previous group at each step. This process continued until solid formations in the solution indicated that the polymer could no longer accommodate additional levels of the drug, an incremental approach that ensured prevented waste of F73.

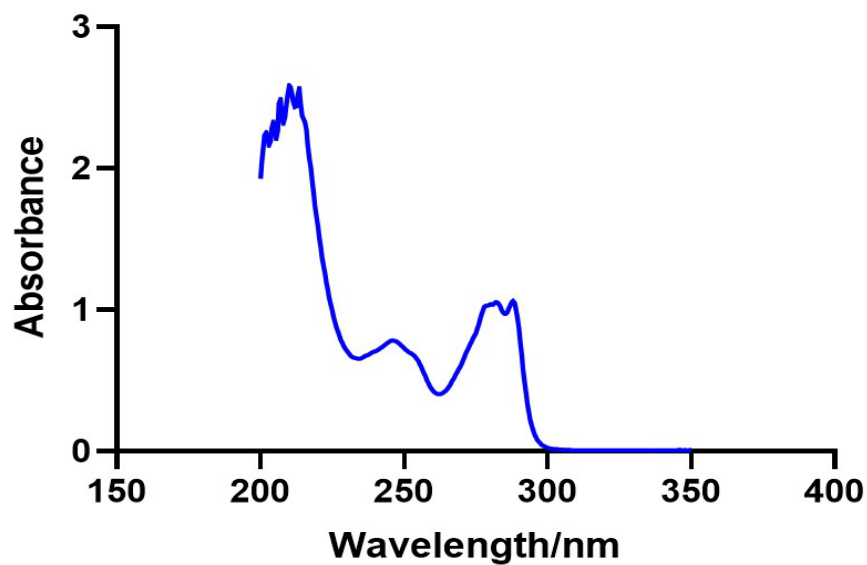


Figure 28: The absorbance of F73 in a phosphate buffer.

Drug	ϵ	Maximum solubility in buffer
F73	5880	0.00035

To further evaluate the effectiveness of the encapsulation technique utilising neutral hydroxyl PAMAM dendrimers, several different generations of those dendrimers, namely G1.5-8OH, G2.5-16OH, and G3.5-32OH were examined. The encapsulation process for each involved using PAMAM dendrimers at a concentration of 1×10^{-4} M to encapsulate excess volumes of anticancer drug F73.

D/G	{Total F73} M E-04	[Encapsulated F37] M E-04	Loading/dendrimer
G1.5-OH	5.4	2.7	2.7
G 2.5-OH	8.5	5	5.0
G 3.5-OH	6	2.9	2.9
Dendrimer conc 1X10 ⁻⁴ M			
Maximum free F73 concentration in buffer = 3.5E-04 M			

Table 16: Encapsulation of F73 in different generation of hydroxyl PAMAM dendrimers.

The data is similar to that obtained for Ibuprofen: notably, both G1.5-OH and G2.5-OH exhibited higher F73 loading than the larger G3.5-OH dendrimer, which may be attributed to the larger cavities present in high-generation polymers (G2.5 to G3.5) that allow for increased drug loading. However, G3.5 steric crowding eventually reduces the amount of internal space and resulting level of encapsulation possible, while the increase in encapsulation of F37 seen between G1.5 and G2.5 was not good as that observed for Ibuprofen: encapsulation of Ibuprofen increased by 14-fold between G1.5 and G2.5, while the equivalent figure was only 2.5-fold for F73 (as shown in Table 16). This difference is most likely a consequence of the higher molecular weight of F73, a supposition supported by the larger drop off in F73 encapsulation between G2.5 and G3.5 as compared to Ibuprofen. Other factors, such as levels of hydrophobicity and number/strength of secondary interactions, may also limit encapsulation levels, however.

4.3.2. Stability Study for F73-Polymer Complexes in PAMAM dendrimer

Following examination of F73 encapsulation, the drug stability in the polymer was evaluated in a similar manner to that previously described for Ibuprofen. The primary method of doing this was to extract a small portion of the top layer from the encapsulated solution each day to

measure its absorbance, which also facilitated monitoring of the drug concentration to assess any decreases over time.

DAYS	G1.5-OH E-04	G2.5-OH E-04	G3.5-OH E-04
1	2.70	5	3
3	2.50	5	2.80
5	1.90	4.8	2.70
7	1.70	4.7	2.50
9	1.40	4.6	2.40

Table 17: Stability of F73 in OH-PAMAM dendrimer for 10 days.

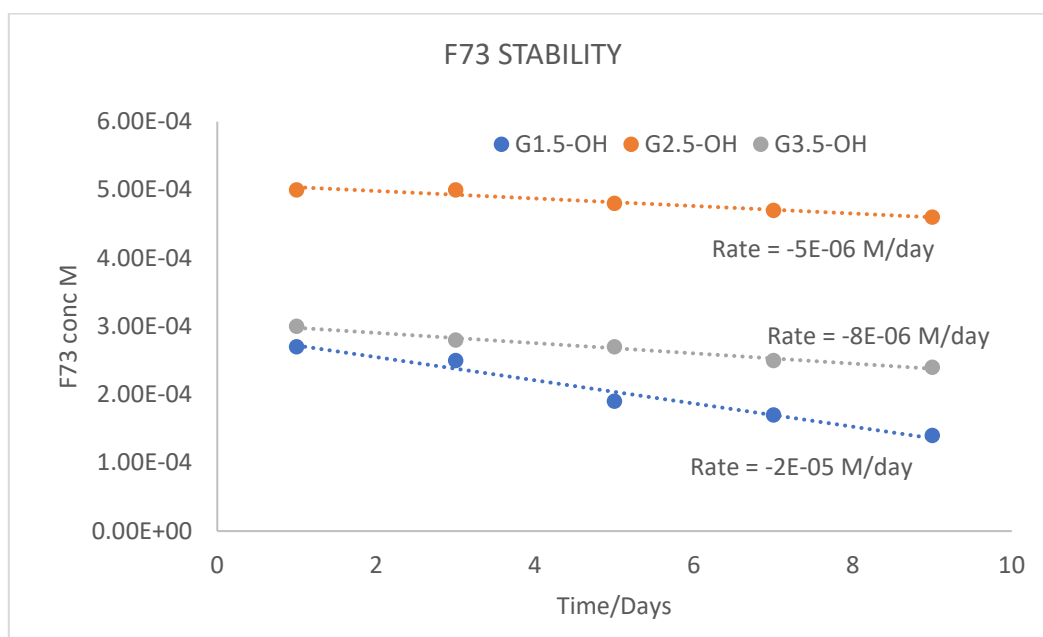


Figure 29: Stability of F73 in OH-PAMAM dendrimer for 10 days.

The figure 29 shows that, for most systems, the level of encapsulation does not drop over time. However, a notable reduction in F73 concentration/absorption for the G1.5-OH dendrimer, cementing a trend that suggests that higher-generation dendrimer-drug complexes tend to provide better stability for the drug; this could be attributed to the larger and more intricate structures present in these higher-generation dendrimers, while G1.5 possesses a flatter structure, which reduces the hydrophobic environment, making it more susceptible to hydrolysis.

4.3.3. F73 release from G2.5-OH dendrimer.

PAMAM G2.5-OH as the optimum generation for maximum load and stability. As a result, we chose to investigate the release of F73 from this dendrimer. The F73/dendrimer complex was prepared using $1 \times 10^{-4} \text{M}$ of dendrimer and 1.9×10^{-4} of F73; 6 mL of the complex was then placed into osmosis tubing with a molecular weight cutoff of 1,000. This was then deposited in a beaker containing 200 mL of pH 7.4 phosphate buffer. Samples were removed from the dialysis bag and analysed using UV at $t=0$, then periodically every 24 hours for five days based on the absorption of the F73 Soret band at 282 nm. The resulting data is presented in Table 18 and displayed graphically in Figure 30.

Time(hr)	abs	CONC E-04M	Half Life
0	1.11	1.89	20hrs
24	0.7	1.19	
48	0.33	0.56	
72	0	0	
Dendrimer conc $1 \times 10^{-4} \text{M}$			
F73 conc 1.9×10^{-4}			

Table 18. Release of F73 from OH-PAMAM dendrimer over 5 days.

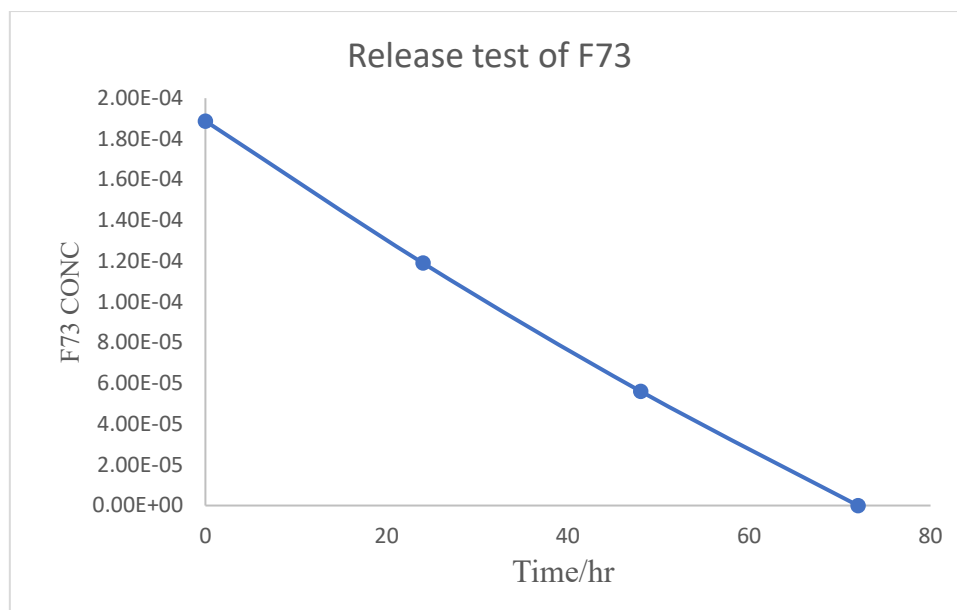


Figure 30. Release of F73 from OH-PAMAM dendrimer over 5 days.

The results clearly demonstrate that F73 is released from the PAMAM dendrimer rapidly, as confirmed by the linear graph; the decrease in the concentration of the drug was also constant, suggesting that the F73 is released from the dendrimer and into the bulk solvent as soon as the F73 that is free in solution crosses the membrane. This means that the F73 release from the dendrimer is much more rapid than rate of F73 transport across the membrane. This rapid release from the dendrimer suggests that any F73 dendrimer interactions must be relatively weak relative to those of Ibuprofen and Zn-THPP, making it clear that, while the dendrimer can enhance the solubility of F73, it may not be a useful or effective drug carrier for F73.

4.4. Discussion:

Three PAMAM dendrimers functionalised with hydroxyl groups were synthesised and examined for their capacity to encapsulate different hydrophobic drugs at concentrations of 1.0×10^{-4} M. Among these dendrimers, the G2.5-OH exhibited the most favourable generation size for drug molecule encapsulation. To explore the impact of dendrimer concentration on drug encapsulation, an encapsulation study was then conducted using this optimal G 2.5-OH dendrimer. It was initially expected that the level of encapsulation would be linearly related to the concentration of dendrimer; however, this proved to not be the case, and a deviation from linearity was observed at higher concentrations of dendrimer. This was postulated to be due to aggregation, where the arms of one dendrimer H-bond to the arms of another, limiting the amount of free space and the number of available dendrimer-drug interactions within the dendrimer's interior. This was confirmed by dynamic light scattering (DLS), which indicated the presence of large aggregated species, with a hydrodynamic radius of 250 nm, at a dendrimer concentration of 2.5×10^{-4} M. Subsequent stability studies on the resulting drug-dendrimer complexes revealed that the G2.5-OH PAMAM dendrimer was able to stabilise the drug complex 90% better than the G 1.5-OH and G 3.5-OH dendrimers, as this dendrimer has an optimised internal structure that can maximise binding through increasing the number of drug/dendrimer interactions, which also helps explain the encapsulation ability of the G 2.5-OH dendrimer.

A release study was also done that showed slow release for both Ibuprofen, and Zn-THPP, as confirmed by the curved line seen on the relevant graphs, and the decrease in the concentration of the drugs not being constant. On the other hand, for F73, the release was rapid, as confirmed by the linear graph, while the decrease in the concentration of the drug was constant.

Chapter 5

5. Synthesis and characterisation of aromatic hyperbranched polymers

5.1. Overview

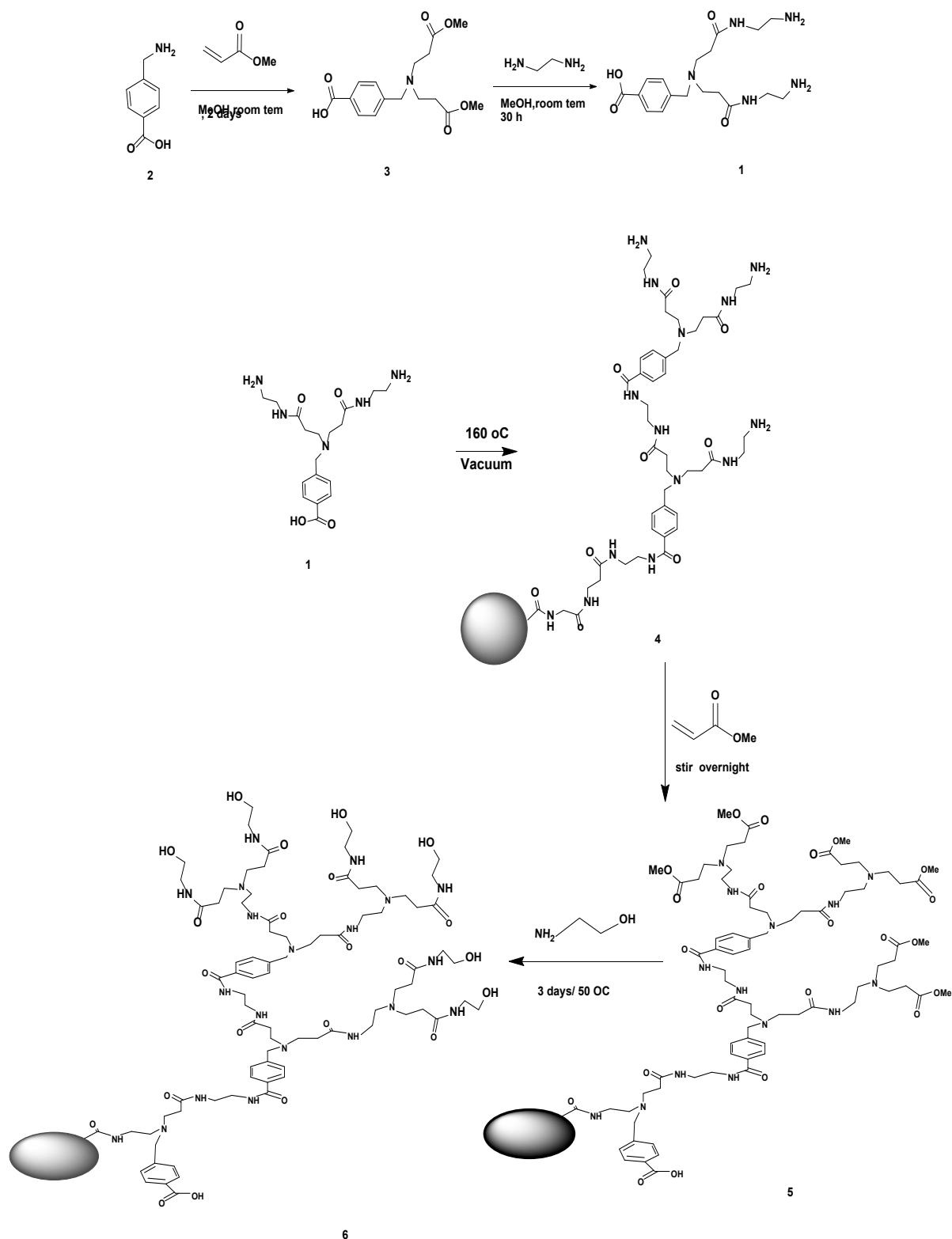
Researchers have become increasingly interested in hyperbranched polymers as drug delivery systems due to their structural similarity to dendrimers.^{79 112} Hyperbranched polymers have a notable advantage over dendrimers in terms of their synthesis, however, as this can be achieved in a single step.¹¹³ As with dendrimers, the structural properties of hyperbranched polymers make them ideally suited for drug delivery: they possess a relatively well-controlled internal structure that can be generated to include a number of functional groups that can be used to interact and encapsulate drug species.¹¹³ In addition, they have a large number of terminal groups that may be used to attach a large number of targeted ligands.⁹

Extensive research has thus been conducted on hyperbranched polymers, including initial comparisons with dendrimers.¹¹⁴ Based on these, it has been suggested that HBPs may be able to offer similar levels of drug delivery efficacy as dendrimers at significantly less effort and cost in terms of synthesis and purification.¹¹⁵ A number of comparison studies have thus been conducted;¹¹⁵ however, none of this work has been carried out using a like-for-like comparison with respect to the specific HBP and dendrimers studied. This is an issue, as the repeat unit's functionality and connectivity play significant roles in terms of encapsulation ability. In the previous study, a PAMAM dendrimer was compared with a hyperbranched polyglycerol; that work determined that the PAMAM dendrimer was significantly better at encapsulation.¹¹⁶ However, while the PAMAM dendrimer was built up from a repeat unit possessing amide and amine units, which could interact with the drug studied (Ibuprofen) by means of both H-bonding and simple acid/base interactions, the hyperbranched polyglycerol does not possess any functionality to help it interact with the drug. As such, it is unsurprising that the PAMAM dendrimer outperformed the HBP¹¹⁶.

In the current work, an AR-HBPAMAM-OH has thus been selected for comparison due to the presence of aromatic rings in its structure that may confer increased thermal and chemical

resistance. This characteristic makes this HBPAMAMs ideal for applications requiring materials that can withstand harsh conditions, while AR-HBP's unique properties make it attractive for various additional purposes. In terms of drug delivery, these Ar-HBPAMAM-OH can be functionalised with different groups to carry therapeutic agents to specific targets in the body, providing a controlled and sustained release of drugs.¹¹⁷ Additionally, Ar-HBPAMAM-OH biocompatibility MAY allows for safe general use, while modifying the surface with targeting moieties can allow it to be directed to specific cells or tissues, increasing drug delivery precision. The functionalisation of aromatic HB-PAMAMs, which allows for controlled drug release, makes them promising candidates in terms of both general pharmaceuticals and targeted medical treatments; based on this, drug delivery systems can be tailored to release medications at specific rates and in targeted locations, enhancing treatment effectiveness and reducing side effects.¹¹⁸

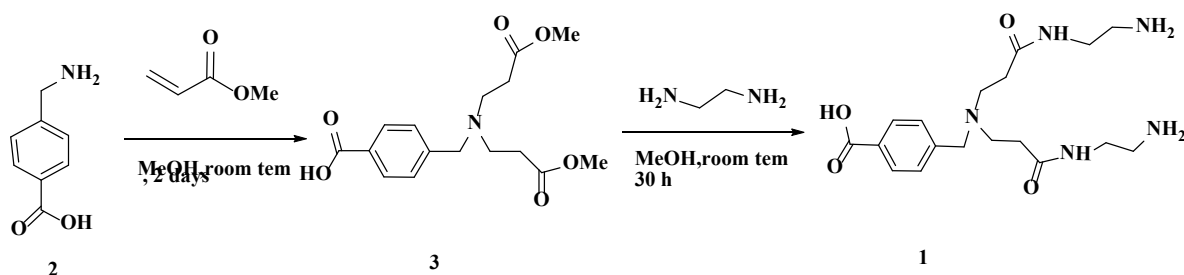
The main aim of this study was to synthesise a hyperbranched polymer with the same functionality and connectivity as an OH-terminated PAMAM dendrimer in order to make a fairer comparison between HBPs and dendrimers in order to definitively answer the question “are dendrimers better drug delivery systems than HBPs?” This required the identification and synthesis of an HBP with similar structure and connectivity to an OH terminated PAMAM dendrimer. The target hyperbranched polymer and its proposed synthesis were thus developed as shown in Scheme 11 below.



Scheme 11: Proposed Synthesis of Ar-HBPAMAM-OH.

To create the intended monomer, the process began with 4-aminomethyl benzoic acid. A step-by-step series of reactions involving Michael addition and amination was then undertaken.

5.2. Synthesis of Ar-HBPAMAM-OH (intermediate 3 and Monomer 1)



Scheme 12: Synthesis of monomer 1 via intermediate 3.

In order to synthesis the PAMAM hyperbranched polymer, a suitable monomer had to be identified. In this case, the aromatic amino acid **1**, which possesses two amines, and a single carboxylic acid was selected (the AB2 monomer).

To produce AB2 monomer **1**, intermediate **3** was required; this was synthesised from aromatic amino acid **2** using the same Michael addition reaction as described for the dendrimers. The reaction involved adding methyl acrylate (MA) to a solution containing 4-aminomethyl benzoic acid **2** and triethylamine, though to help dissolve the 4-aminomethyl benzoic acid **2**, potassium carbonate was introduced to the reaction mixture. The mixture was then stirred for two days at room temperature to ensure reaction completion. The diester intermediate **3** was obtained, and this offered good yield and high purity after filtration and rotary evaporation of the volatile reagents and solvents. For the synthesis of the AB2 monomer **1**, a similar amination step was utilised as for the dendrimers, with an excess of ethylene diamine (EDA) added to intermediate **3** to minimise the intramolecular and intermolecular side reactions.

5.3. Characterisation of intermediate 3, and AB2 monomer 1.

The characterisation methods employed for the HBPs were identical to those used for the dendrimers. For the first intermediate diester **3**, the signals for the distinctive ester peaks for

the methoxy protons and carbonyl carbon were sought at 3.62 ppm and 76.7 ppm, respectively in the ^1H NMR and ^{13}C NMR spectra. After amination to produce the AB2 monomer **1**, however, these peaks were absent from the ^1H and ^{13}C NMR spectra, with all esters being transformed into amides. The changes in the ^1H NMR spectra between **3** and **1** can clearly be seen in Figures 31 and 32. The absence of the distinctive peaks in particular provides good evidence for the changed structure of AB2 monomer **1**.

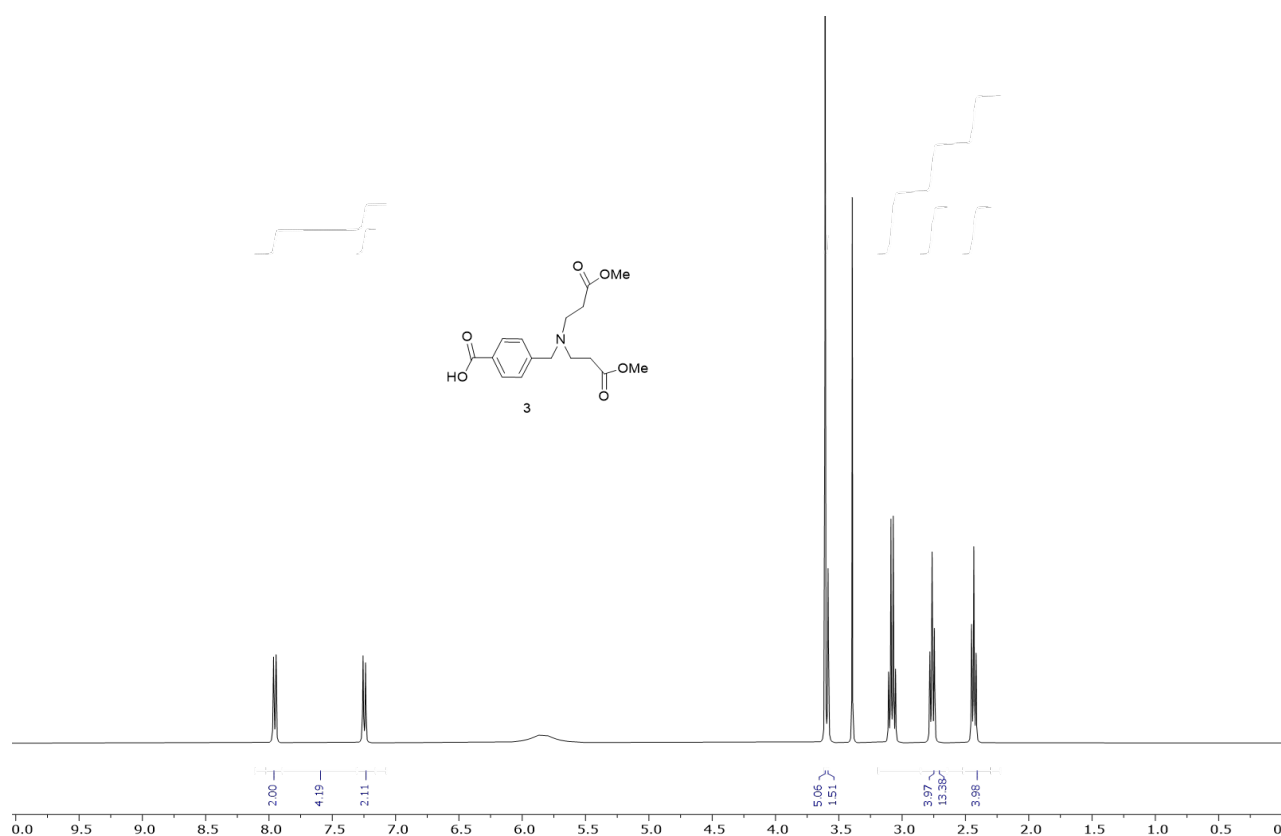


Figure 31: ^1H NMR spectrum for intermediate **3**.

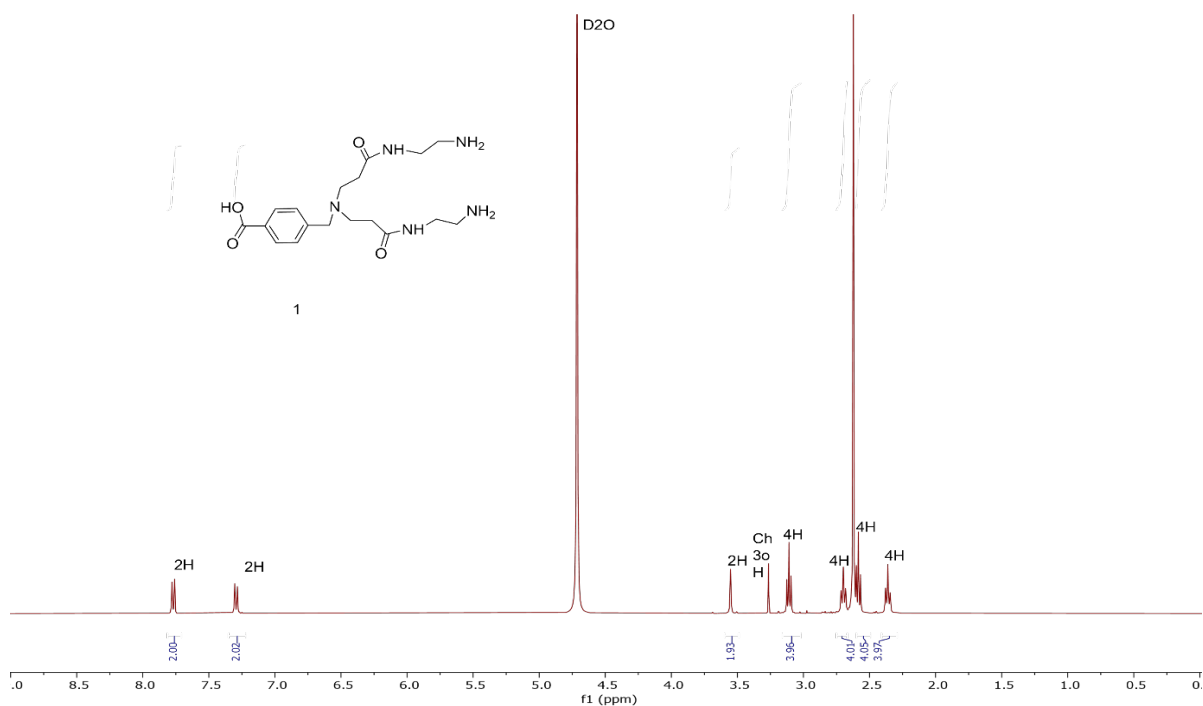
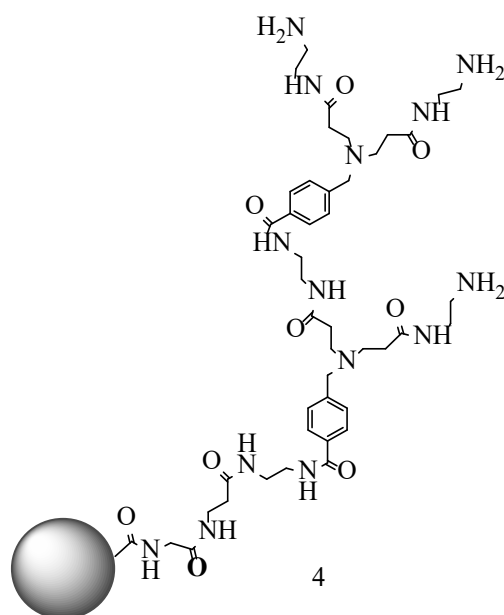


Figure 32: ^1H NMR spectrum for Monomer **1**.

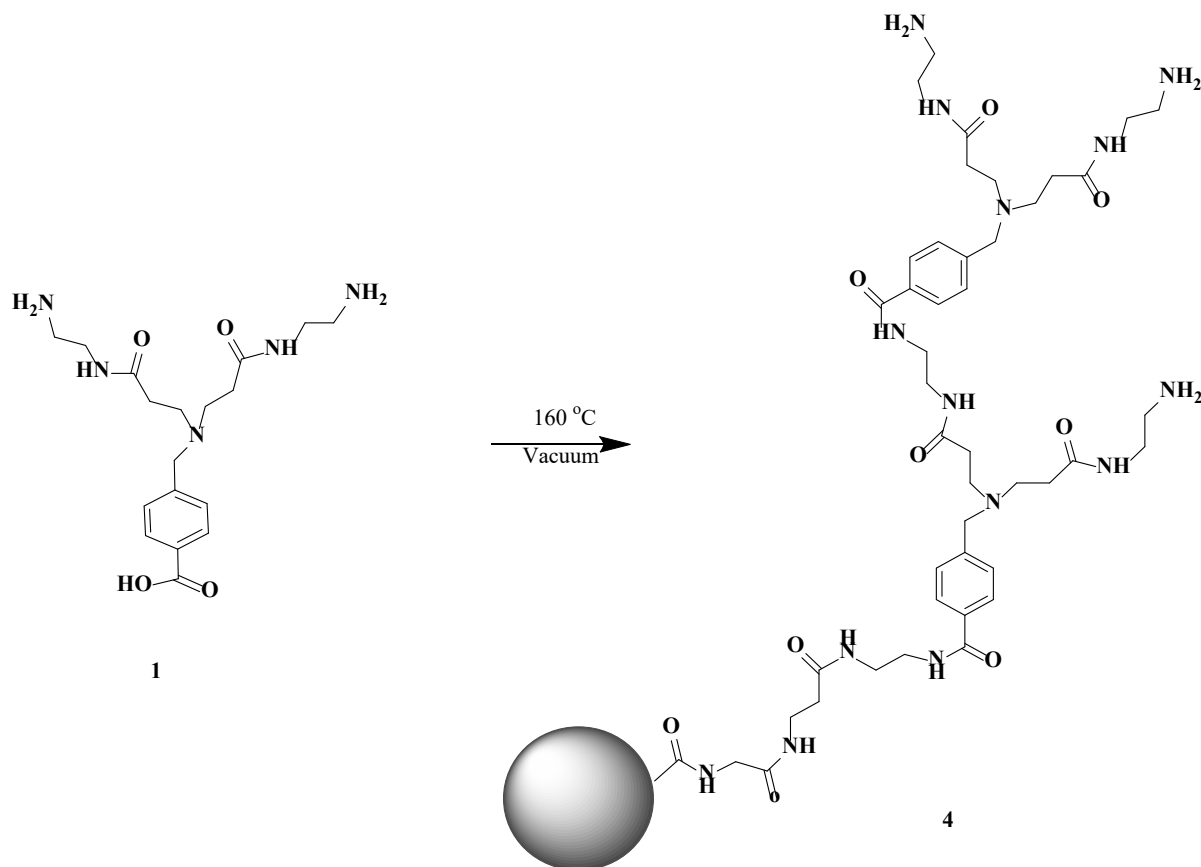
IR spectroscopy was employed to monitor changes in the polymer's functional groups. Intermediate **3** exhibited a characteristic ester $\text{C}=\text{O}$ stretching peak at $1,731\text{ cm}^{-1}$. However, the IR spectrum of the AB2 monomer **1** displayed a carbonyl stretching vibration at $1,640\text{ cm}^{-1}$, with the carbonyl ester peak at $1,731\text{ cm}^{-1}$ no longer apparent. These changes provide good evidence for the presence of AB2 monomer **1**.

The mass spectra intermediate **3** and AB2 monomer **1** had molecular ion peaks at 324 m/z and 380 m/z , respectively. Overall, the spectral data thus clearly confirmed the synthesis of intermediate **3** and AB2 monomer **1**.

5.4. Synthesis of Ar-HBPAMAM-OH (Hyperbranched polymer 4)



The polymer was synthesised via a simple step-growth polycondensation polymerisation of the AB₂ monomer 1. Polymerisation was carried out by heating the AB₂ monomer 1 at 165 °C for 30 hours. This reaction generates water, which acts to hydrolyse any product, however, thus generating the starting materials. To avoid this and to drive the reaction towards completion, the experiment flask was kept under vacuum for the duration of the polymerisation. At the conclusion of the process, a solid material with a glassy texture and a honey-like colour was obtained, which corresponded to the expected hyperbranched polymer 4.



5.5. Characterisation of Ar-HBPAMAM-OH (Hyperbranched polymer4)

Full characterisation of the HBP proved challenging due to its polydispersity. The ^1H NMR spectrum showed peaks in the aromatic and aliphatic regions; however, these were broad and overlapped each other, there was a range of multiplets between 7.85 and 7.30 ppm, which indicated the presence of aromatic hydrogens. The remaining peaks appeared as broad multiplets between 4.35 and 1.71 ppm, corresponding with the aliphatic hydrogens on the HBP. Although somewhat difficult to interpret, the peaks were in the correct position and of an appropriate size to be consistent with those predicted for the Ar-HBPAMAM..

To gain further insight, a ^{13}C NMR spectra was acquired. A peak at 174 ppm confirmed the presence of a C=O environment, while two other peaks at approximately 134.0 ppm and 122.5

ppm were consistent with the presence of an aromatic unit. Additionally, a number of peaks between 46 and 37 ppm provided evidence of C-N and C-C environments.

IR spectroscopy identified the functional groups present in the HBP; however, it could not provide conclusive evidence regarding polymerisation. The IR spectrum of the HBP displayed a characteristic amide stretch at $1,635\text{ cm}^{-1}$, while no observable ester carbonyl stretches occurred, suggesting an absence of ester groups in the polymer. The mass spectrum showed a pattern consistent with a polydisperse polymer, based on the number of peaks of increasing mass and decreasing intensity. Gel permeation chromatography (GPC) provided better data, generating a weight averaged molecular weight (M_w) of 2500 and a number averaged molecular weight (M_n) of 1,500. Taking this data alongside the spectroscopic data, we were confident that the Ar-HBPAMAM shown in Figure 32 was achieved. In order to proceed with the chosen experiments, however, it was necessary to convert the terminal amines of the HBP into hydroxyl group.

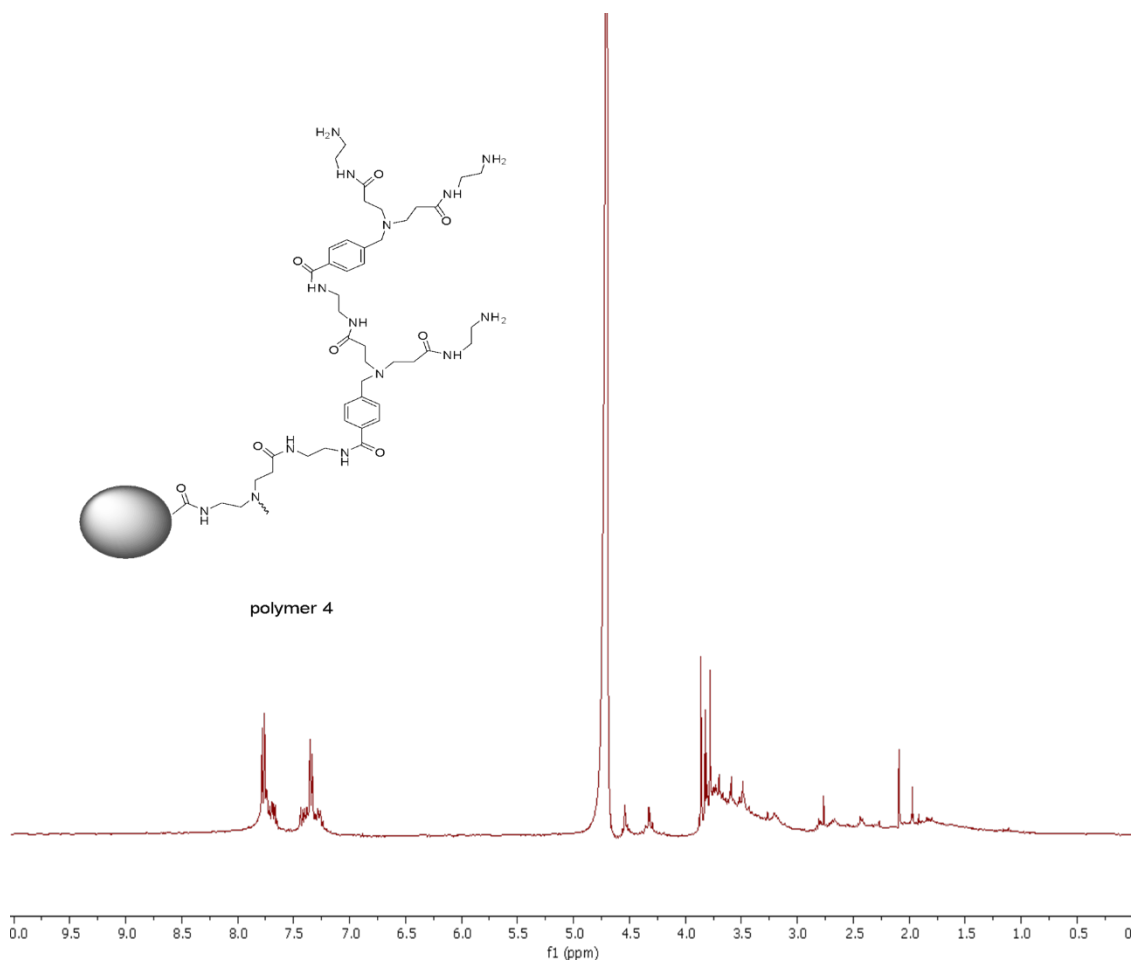


Figure 32: ^1H NMR spectrum of a hyperbranched polymer 4 with MeOD as the solvent.

5.6. Synthesis and characterisation of hydroxyl-terminated aromatic hyper-branched polymers

In order to make appropriate comparisons between dendrimers and HBP in terms of functionality, the terminal amines must be transformed into hydroxyl groups. To achieve this, it was necessary to convert the terminal amines into esters, and then react the product with ethanolamine as previously described for the dendrimer. Esterification was achieved by reacting the Ar-HBPAMAM-OH 4 with MA in methanol. After removal of the volatile reagents and solvent via rotary evaporation, the crude ester-terminated hyperbranched polymer was then dissolved in DMSO and reacted with ethanolamine and potassium carbonate, with that reaction stirred at 50 °C for three days.

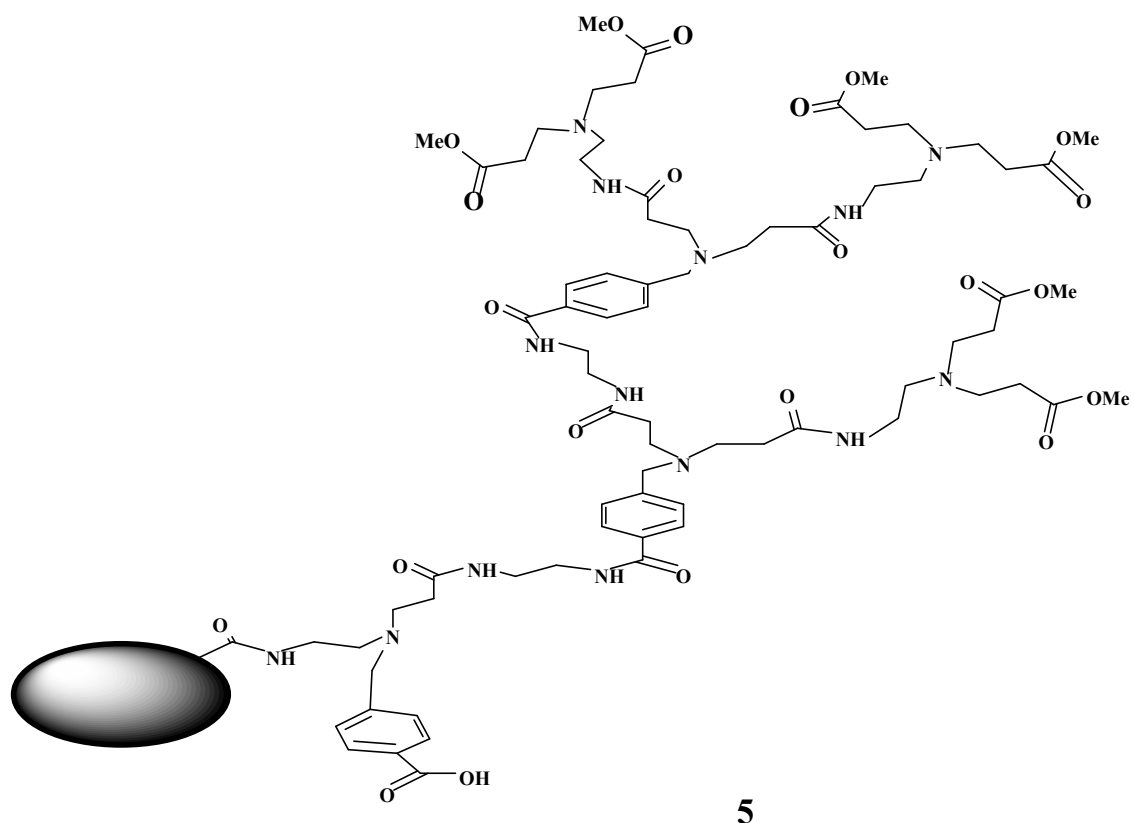


Figure 33: Intermediate ester terminated hyper branched polymer.

The ^1H NMR spectrum showed broad peaks in the aromatic and aliphatic regions, as shown in Figure 34 consistent with the polymer. However, we also observed Multiple peaks ranging from 1.9 to 3.9 ppm in the HBP-OMe spectrum corresponded to methyl acrylate addition. The ^{13}C NMR spectrum also showed a peak at just over 50 ppm related to the carbon attached to oxygen by a single bond (O-CH₃), while the IR spectrum of the HBP-OMe showed a peak at 1,751 ppm related to the carbonyl group of an ester functional group of Ar-HBP-OMe

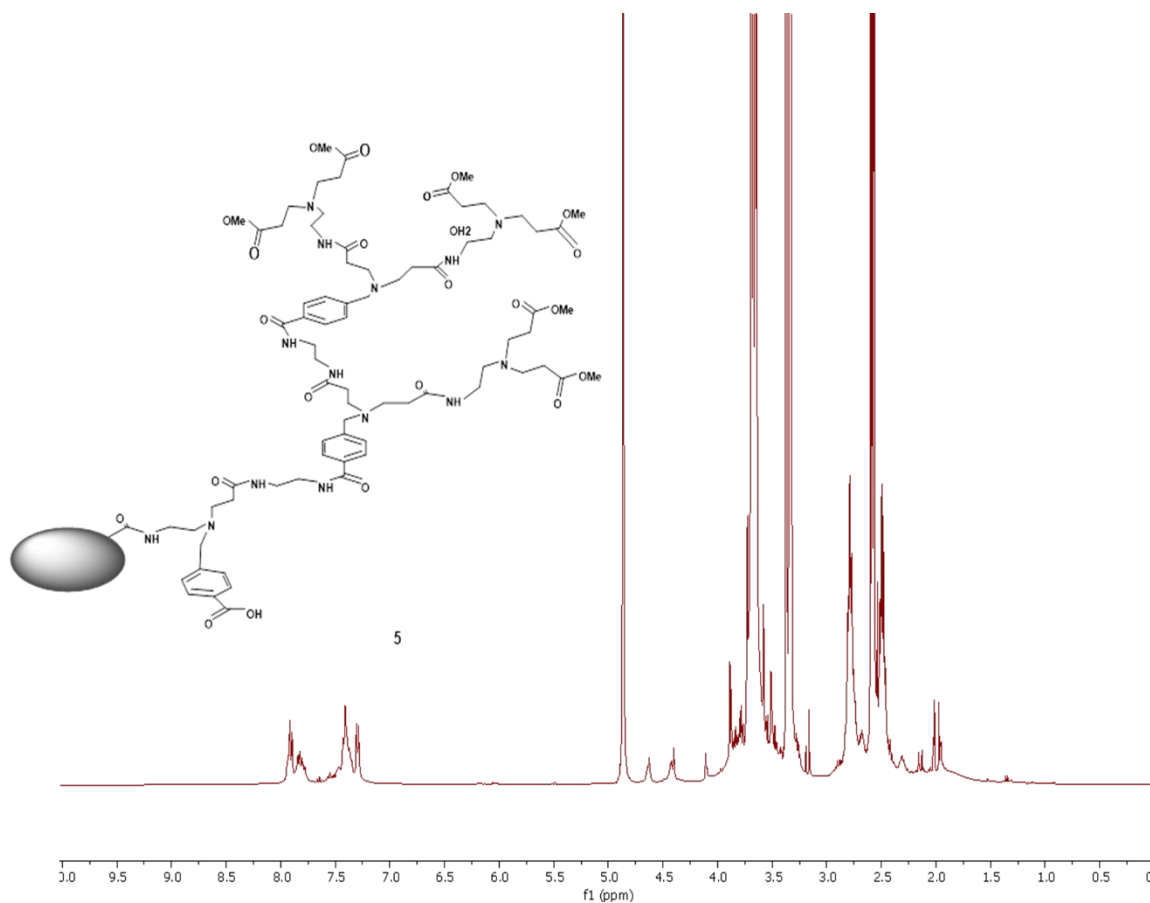
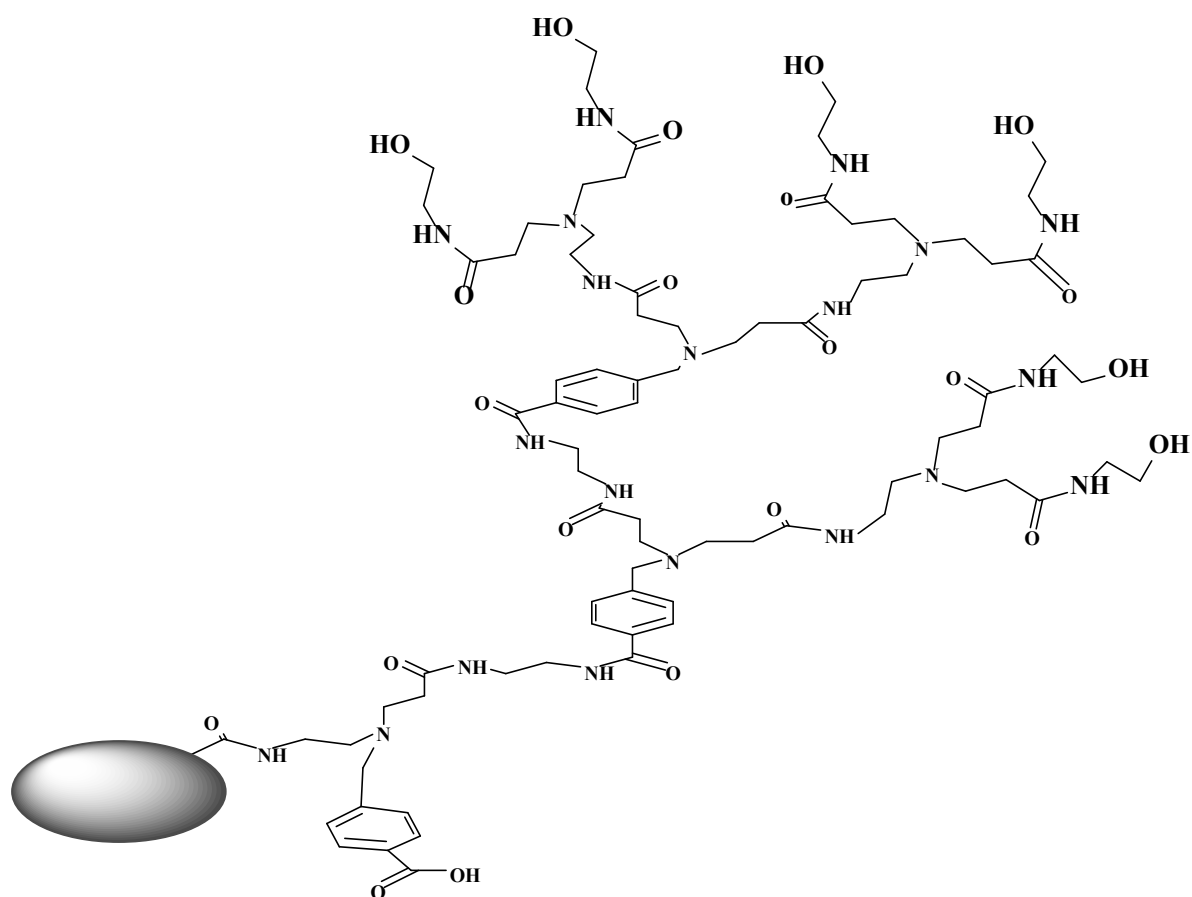


Figure 34: ^1H NMR spectrum ester terminated hyper branched polymer with MeOD as the solvent.

In the final step of the synthesis, the Ar-HBPAMAM-OH, ester-terminated hyperbranched polymer was dissolved in DMSO and reacted with ethanolamine and potassium carbonate. The reaction was then stirred at 50 °C for three days. Purification was done, through washing by acetone many times, to get a sticky brown solid.



6

Figure 35: Hydroxy ester-terminated hyper branched polymer.

The ^1H NMR spectrum showed multiple peaks ranging from 4.27 to 4.10 ppm in the HBP-OH spectrum, as shown in figure 36, indicating the presence of additional proton environments originating from the ethanolamine carbon backbone. The ^{13}C NMR spectrum of HBP-OH also exhibited a peak at approximately 64 ppm, suggesting the presence of carbons adjacent to the alcohol oxygen, with further peaks in the C-N region.

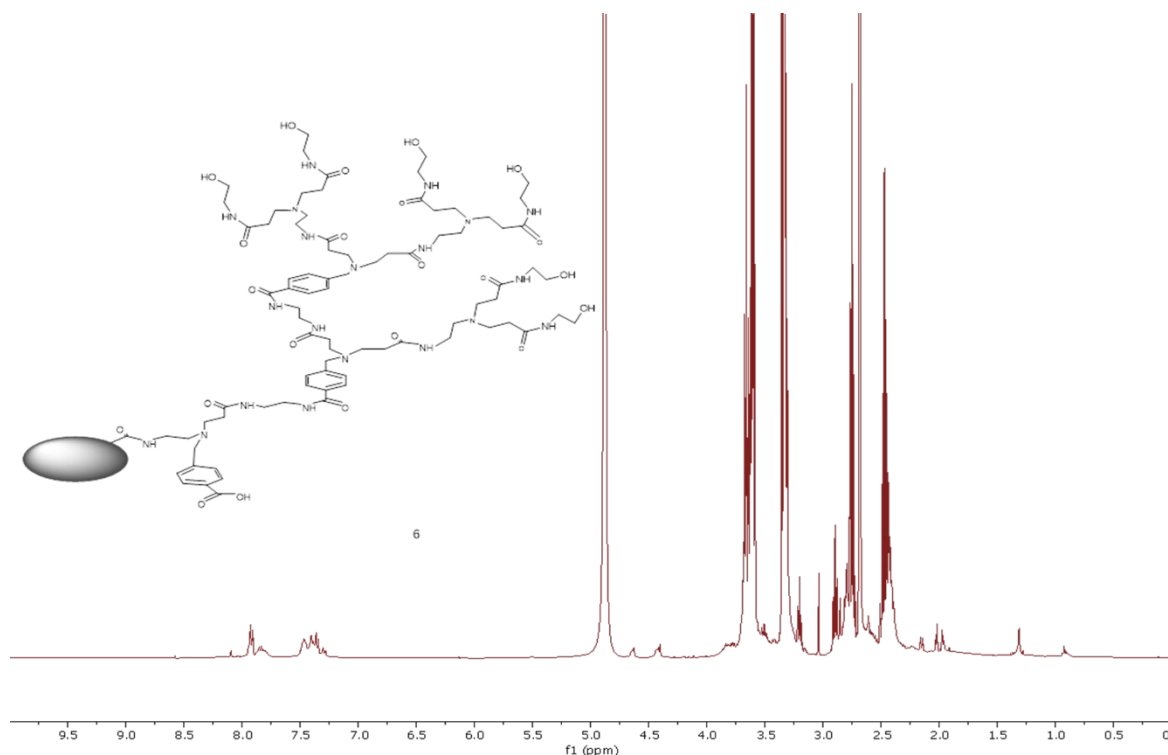


Figure 36: ^1H NMR spectrum hydroxyl terminated hyper branched polymer with MeOD as the solvent.

Comparing the ^1H NMR spectra of HBP-OMe and HBP-OH highlights distinct peaks for HBP-OMe that are not present in HBP-OH, and vice versa. Moreover, the multiple peaks ranging from 4.27 to 4.10 ppm in the HBP-OH spectrum indicate the presence of additional proton environments originating from its ethanolamine carbon backbone. The ^{13}C NMR spectrum of HBP-OH exhibits a peak at approximately 64 ppm, suggesting the presence of carbons adjacent to the alcohol oxygen, which are not present in HBP-OMe. Furthermore, HBP-OMe demonstrates a peak at just over 50 ppm, which is related to carbon attached to oxygen by a single bond (O-CH₃). However, HBP-OH displays more peaks in the C-N region than HBP-OMe, which correlates to the formation of new amide bonds in the former.

Chapter 6

6. Chapter: Evaluating the drug delivery potential of the Aromatic hyperbranched PAMAM (Ar-HBPAMAM-OH).

6.1. Part1: Encapsulation of Ibuprofen in Aromatic hyperbranched PAMAM.

This study sought to investigate whether HBPs can effectively encapsulate and deliver drugs in a similar manner to dendrimers. The initial approach thus involved quantifying the concentration of drugs in a given solution both with and without the presence of HBPs. By using drugs at least partially soluble in water, any improvements in solubility achieved by the hyperbranched polymer could be assessed, permitting judgement of their effectiveness. Previous research conducted by the Twyman group has indicated that acidic guest molecules can be efficiently encapsulated due to their pH-dependent binding, while guests with hydrogen bonding groups also show good potential for encapsulation. However, the most effective encapsulation occurs with guests possessing both acidic and hydrogen bonding groups.¹¹⁹ In contrast, neutral hydrophobic guests exhibit lower levels of encapsulation. In this particular study, Ibuprofen was selected as the drug under investigation due to its wide availability in the commercial market and its particular molecular structure. Ibuprofen contains an acid group capable of forming salts or hydrogen bonds with dendrimers as well as being UV-active, which facilitates the determination of solution concentration via a Beer-Lambert plot, based on its absorbance peak at 273 nm. Ibuprofen has poor solubility in water, however, so methanol was initially used as a solvent.

As an accurate molecular weight of Ar-HBPAMAM-OH was not available, two different methods were used to calculate and corroborate concentrations. The first was a conventional molar concentration, while the second utilised a mass/volume commonly used by polymer chemists. This ensures that the same number of monomer units are in solutions, allowing for comparison of properties between all molecular weights. Accuracy with this method requires the polymers to have identical repeat units, which is not quite the case in our system.

Nevertheless, the structures are similar enough for a qualitative comparison to be made that will help to inform judgement on the validity of the results obtained using traditional molarity method (we are going to write about mass/volume method in the comparison chapter). Using these methods, Ar-HBPAMAM_OH concentrations equivalent to those used for the dendrimer experiments were developed equal to 1×10^{-4} M. In the first step, the extinction coefficient was found to be $95 \text{ dm}^3 \text{ mol}^{-1} \text{ cm}^{-1}$, and for this and all subsequent concentration determinations, the change in absorption between 274 and 276 nm was used to compensate for potential baseline drift (ΔAbs).

The maximum solubility of Ibuprofen in buffer was found to be 1×10^{-4} M. This value was thus used to more accurately determine the values of encapsulated Ibuprofen. The data shown in the Table 19 below is that developed using conventional molar concentration, which clearly shows that substantial amounts of IBU can be encapsulated within the polymer. The second method, which uses mass/volume, is discussed in more detail in chapter 7.

Concentration of HBP	ΔABS	Total [IBU] M	Encapsulated [IBU] M	Loading/HBP
0.0001M	0.25	2.66E-03	1.66E-03	16.5
Free Ibuprofen conc 1×10^{-4} M				

Table 19: Encapsulation of Ibuprofen in Ar-HBPAMAM-OH using the conventional molar concentration method, equivalent to 0.0001.

This maximum solubility experiment clearly demonstrated that Ar-HBPAMAM_OH can encapsulate a relatively large amount of Ibuprofen. The maximum concentration/solubility of Ibuprofen increased from 0.001 M in the bulk mix to 0.0026 M in the Ar-HBPAMAM_OH, at concentration of 0.0001 M or 0.25mg/mL. Subtracting the maximum concentration in bulk, thus gives the encapsulated concentration of Ibuprofen, which equals 0.0016 M. At a polymer concentration of 0.001M, this equates to a loading of 16.5 Ibuprofen equivalents per Ar-HBPAMAM_OH. This high level of encapsulation is most likely due to the hydrophobic

environment created by the Ar-HBPAMAM_OH in conjunction with the internal amines, which interact with the carboxylic functional group on the Ibuprofen.¹²⁰ The resulting secondary interactions include both H-bonding and acid/base ion pairing.

A further experiment was thus designed to investigate what happens when the concentration of polymer is increased, and whether or not a corresponding linear increase in Ibuprofen encapsulation was observed. This allowed investigation of whether aggregation might occur as with the dendrimers, signified by a drop in concentration. The experiment used following concentrations of Ar-HBPAMAM_OH of 0.24, 0.25, 0.26, 0.27, and 0.28 mg/mL (equivalent to molar concentrations of 0.90E-4, 1E-4, 2E-4, and 3E-4). The results are shown in Table 20 and Figure 37.

Ar-HBPAMAM-OH CONC	MG/M L	Δ ABS	{Total Ibuprofen}M E-03	{Encapsulated Ibuprofen}M E-04	Loading/HBP
0.9E-04	0.225	0.17	1.81	8	8
1E-04	0.25	0.25	2.66	16.6	16
2E-04	0.5	0.28	2.98	19.8	20
3E-04	0.75	0.31	3.30	23	23.00

Table 20: The effect of Ar-HBPAMAM-OH concentration on Ibuprofen-loading.

A total of 16 M Ibuprofen was solubilised and encapsulated by encapsulation when the Ar-HBP-OH concentration was 1.0E-04M. When the polymer concentration doubled to 2.00E-04 M, the solubility was expected to double. However, only 20 M of Ibuprofen were solubilised by encapsulation rather than the 32 M expected. The situation worsened at a polymer concentration of 3.00E-04: at this concentration, the expected number of solubilised Ibuprofen moles was 48; however, only 23 M were actually solubilised by encapsulation, the reason is probably due to the same issues as determined for the dendrimers based systems where aggregation driven by intermolecular H-bonding of the polymer arms.¹²¹ Which limit the

amount of internal space for Ibuprofen encapsulation and reduces the number of interactions possible for the Ibuprofen, which reduces the number of Ibuprofen moles that can be accommodated within the Ar-HBPAMAM_OH overall.

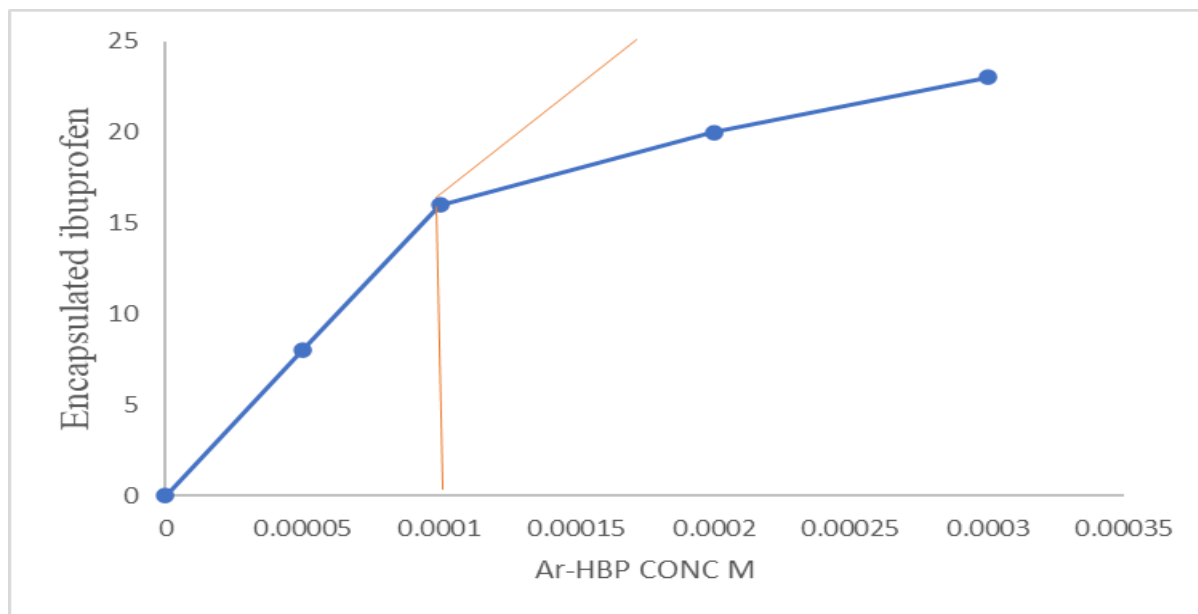


Figure 37: The effect of Ar-HBPAMAM-OH concentration on Ibuprofen loading.

6.1.1. Stability of encapsulated Ibuprofen in Ar-HBPAMAM_OH

The objective of this section was to investigate the impact of Ar-HBPAMAM_OH on the stability of Ibuprofen complexes. The co-precipitate method was used to prepare the AR-HBP–drug complexes (1E-4 M), and the samples were stored at room temperature for 10 days in a phosphate buffer at pH 7.4. Samples were analysed initially and then checked every three days for any precipitation, turbidity, change in consistency, or increase in drug loss. The degradation rate of drug was indirectly determined by measuring the rate at which its concentration decreased. A total of five data points were analysed during the 10-day period using UV-vis spectroscopy. To determine Ibuprofen stability within the complex, the absorbance at 273 nm was monitored over time, as the aim of the study was to determine the stability over time. The resulting data is presented in Table 21 and displayed graphically in Figure 38.

ARHBP- IBUPROFEN COMPLEX			
Days	Δ ABS	ϵ	Ibuprofen Conc M
D1	0.25	94	0.003085106
D3	0.25		0.00287234
D5	0.24		0.00287234
D7	0.23		0.002659574
D9	0.23		0.002553191
Ar-HBPAMAM-OH CONC 1×10^{-4} M			

Table21: Stability of IBU in Ar-HBPAMAM_OH.

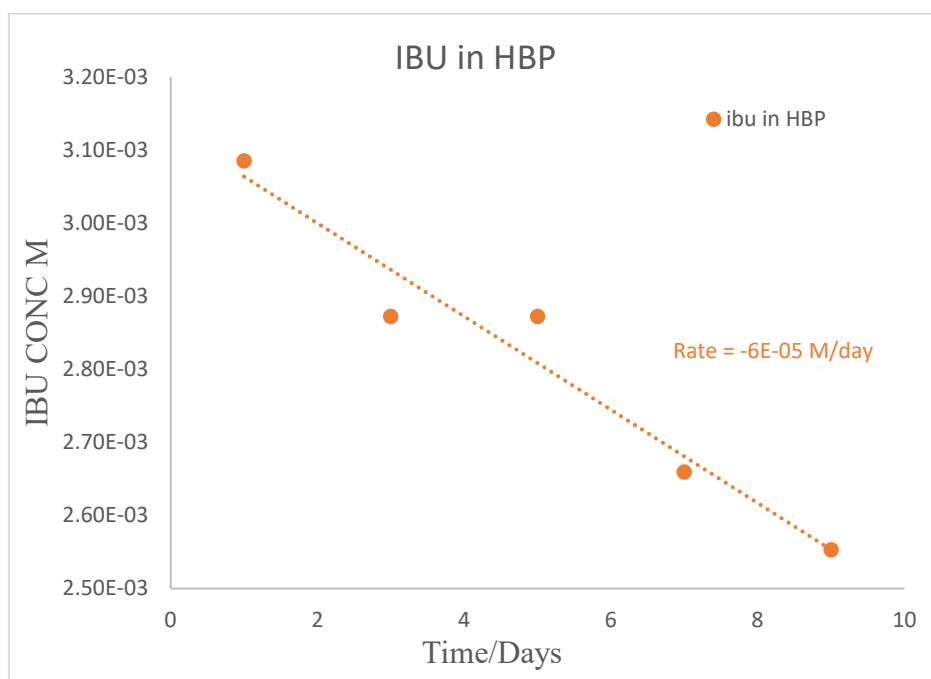


Figure 38: Stability of IBU in Ar-HBPAMAM_OH.

These results show that the ibuprofen was stable over time, as shown in Table21, and Figure 38, which may be attributed to several factors. Aromatic hyperbranched PAMAM dendrimers possess highly branched and compact structures with defined cores and multiple layers of branching. which maximises binding by facilitating a significant number of drug/HBP interactions, thereby enhancing stability, through protecting the drug from the external aqueous solution (the degradation pathways are possible, but hydrolysis is the most likely).

6.1.2. Ibuprofen release from Ar-HBP.

An Ibu/Ar-HBPAMAM-OH complex of $1 \times 10^{-4} \text{M}$ of Ar-HBPAMAM-OH and 8×10^{-3} of IBU was prepared, and 6 mL of the complex was placed into osmosis tubing with a molecular weight cut off of 1,000. This was then deposited in a beaker containing 200 mL of pH 7.4 phosphate buffer. Samples were removed from the dialysis bag and analysed using UV at $t=0$ and then periodically every 24 hours for five days, with the absorption of the IBU Soret band at 272 nm being measured. The resulting data is presented in Table 22 and displayed graphically in Figure 39.

Time (hr)	$\Delta\text{abs (273-276)}$	CONC M	Half life
0	0.8003	8.05E-03	35hr
24	0.507	4.90E-03	
48	0.3219	3.09E-03	
72	0.2305	1.91E-03	
96	0.11	9.57E-04	
120	0	0.00E+00	
Ar-HBPAMAM-OH conc $1 \times 10^{-4} \text{M}$			
IBU conc 8×10^{-3}			

Table 22: Release of IBU from Ar-HBPAMAM_OH over 120hrs.

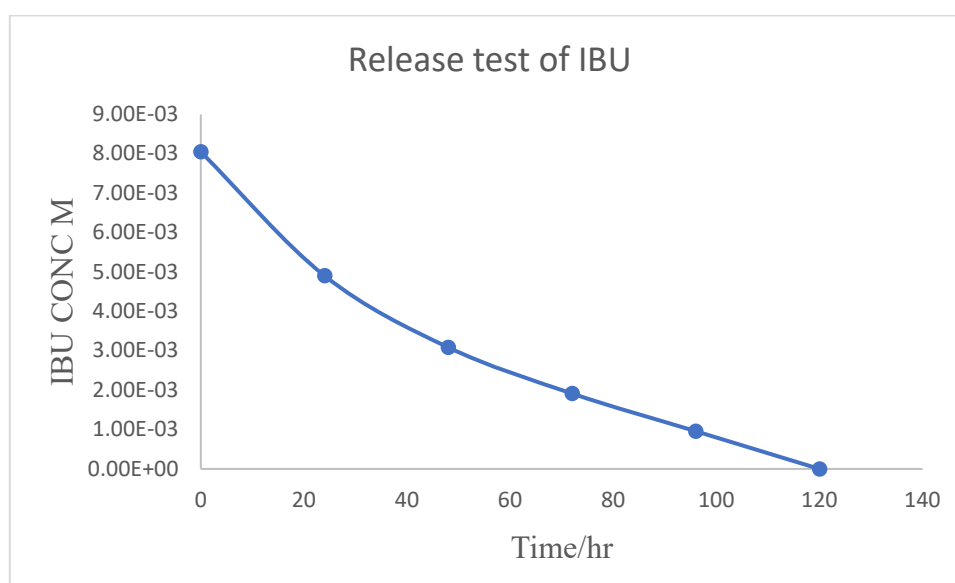


Figure 39: Release of IBU from Ar-HBPAMAM_OH over 5 days

The results show that Ibuprofen can be released from the Ar-HBP, which clearly demonstrates the potential applicability of this system for drug delivery. Furthermore, the overall release is relatively slow, which implies reasonably good interaction between the dendrimer and the drug, which is a positive result in terms of providing relief from pain for longer durations, thus supporting less frequent dosing. This can be particularly beneficial for individuals who need pain relief throughout the day or night without wishing to take multiple doses. This slow release may occur due to the Ar-HBPAMAM-OH dendrimers' complex three-dimensional structures with numerous branches and terminal groups, which can create a dense network that hinders the diffusion of drug molecules out of the dendrimer matrix.¹²² Compatibility between the drug and the Ar-HBPAMAM-OH also affects the release rate.

The overall release profile demonstrates two distinct phases, as illustrated by the curved nature of the release profile. The first phase is very rapid, and this occurs between $t=0$ and $t=50$ hours. This is followed by a slower release phase. The experiment begins with a saturated solution of Ibuprofen and a fully loaded Ar-HBP. The overall release then occurs in three steps. The first step is the release of free Ibuprofen (non-encapsulated) from the saturated solution, which crosses the osmosis membrane relatively rapidly. When this occurs, the concentration of "free" Ibuprofen in the bulk solution reduces, creating space for more Ibuprofen. During the second step, encapsulated Ibuprofen is thus released from the dendrimer to fill the vacated space in the bulk solution, which is a relatively slower process. Such slow release may occur through disruption of the electrostatic and hydrogen bonding interactions that serve to entrap the drug molecules within the dendrimer structure;¹²² however, Ar-HBPAMAM-OH could also decompose through hydrolysis, resulting in drug release. Under physiological conditions, drug release may thus be faster if the interactions were weaker and/or Ar-HBPAMAM-OH degradation occurs more quickly. The final step is the same as the first, with the newly released Ibuprofen crossing the membrane relatively rapidly.

Overall, the release study offered positive results that supported the potential application of Ar-HBPAMAM-OH to drug delivery.

6.2. Part2: Encapsulation of Zn-THPP14 in aromatic hyperbranched PAMAM.

The Zn-THPP14 used in this work was synthesised and characterised as described in Chapter 4, and encapsulation was carried out using the co-precipitate method. The extinction coefficient of Zn-THPP14 in methanol was obtained using a Beer Lambert plot (ϵ Zn-THPP = 5854.6 dm³ mol⁻¹ cm⁻¹), and the maximum concentration of Zn THPP14 in the phosphate buffer was 1.2E-6 mol dm⁻³. It has been previously determined that high concentrations of polymer are susceptible to aggregation. In this work, experiments were thus conducted at concentrations both below and above the aggregation limit to ensure and confirm that the concentration previously determined (1X10⁻⁴ M) offers the best encapsulation.

As noted previously, two concentration methods were used, molar concentration and mass/volume concentration, (which are discussed in more detail in the chapter7. Using these methods), HBP concentrations equivalent to those used for the dendrimer experiments were developed, generating concentrations of Ar-HBP-OH equal to 1x10⁻⁴ M, based on an expectation that Ar-HBPAMAM_OH would be able to increase the concentrations of Zn-THPP14, due to the secondary interactions via of Zn with internal tertiary amines within the Ar-HBPAMAM_OH. The relevant data is shown in Table 23.

Concentration of HBP	Δ ABS	Total [Zn-THPP 14] $\times 10^{-4}$ M	Encapsulated [Zn-THPP 14] $\times 10^{-4}$ M	Loading/HBP
0.0001M	0.023	1.45	1.43	1.43
Maximum free ZN-THPP concentration in buffer = 2X10 ⁻⁶ M				

Table 23: Encapsulation of Zn-THPP14 In Ar-HBPAMAM-OH based on conventional molar concentration methods (equivalent to 0.0001 M).

The concentration of Zn-THPP14 was increased to 1.435×10^{-4} M according to conventional molar concentrations, and this behaved as expected, potentially due to the presence of internal amines. However, a secondary interaction with the tertiary amines inside the Ar-HBPAMAM-OH may also have contributed to this. Aromatic hyperbranched polymers can interact with aromatic drugs through various mechanisms: these include π - π stacking interactions, hydrophobic interactions, and electrostatic interactions.¹²³ Stacking interactions occur between the π -electron clouds of aromatic rings, resulting in the generation of attractive forces; such π - π stacking can enhance the encapsulation efficiency of aromatic drugs and stabilise their molecular conformations within the polymer matrix.¹²⁴ A further experiment was thus designed to investigate the effects where the concentration of polymer was increased, with a particular interest in determining whether a corresponding linear increase in Zn-THPP concentration would be seen, or whether aggregation would occur as with the dendrimers, causing a drop in concentration to be observed. That experiment utilised concentrations of Ar-HBPAMAM_OH at 0.24, 0.25, 0.26, 0.27, and 0.28 mg/mL (equivalent to molar concentrations of 0.90×10^{-4} , 1.00×10^{-4} , 2.00×10^{-4} , and 3.00×10^{-4}). The results are shown in Table 24:

Ar-HBP	Δ ABS	ϵ	Total [Zn-THPP14]	Encapsulated [Zn-THPP14]	Loading M
9.00×10^{-5}	0.014	5854.6	8.85×10^{-5}	8.65×10^{-5}	0.86
1.00×10^{-4}	0.023	5854.6	1.45×10^{-4}	1.43×10^{-4}	1.43
2.00×10^{-4}	0.022	5854.6	1.39×10^{-4}	1.37×10^{-4}	1.37
3.00×10^{-4}	0.018	5854.6	1.14×10^{-4}	1.21×10^{-4}	1.12

Table 24: Encapsulation Zn-THPP IN different concentrations of Ar-HBPAMAM_OH.

Zn-THPP14 loading was found to be 1.4 moles when the Ar-HBPAMAM_OH concentration was 1.0×10^{-4} M; thus, when the Ar-HBPAMAM_OH concentration was 2×10^{-4} M, the solubility was expected to double, giving 2.8 moles per Ar-HBPAMAM_OH. However, in practice, this concentration was only able to load 1.37 moles. Finally, at a concentration of 3×10^{-4} , higher solubility was expected; in practice, however, only 1.12 moles were encapsulated, suggesting

the presence of aggregation. This aggregation may have been caused by hydrophobic interactions, as Ar-HBPAMAM_OH possesses various hydrophobic aromatic groups,¹²³ which can exhibit strong hydrophobic interactions with each other at high concentrations. These interactions promote aggregation and reduce the availability of individual HBP to encapsulate guest molecules.^{121 125}

6.2.1. Stability of Zn-THPP in Ar-HBPAMAM_OH complexes.

The objective of this section was to investigate and confirm the stability of Zn-THPP in Ar-HBPAMAM_OH. Samples were placed in amber-coloured and colourless glass vials to create dark and light conditions, respectively, with all vials then stored at room temperature in a pH 7.4 phosphate buffer for 10 days. The samples underwent initial analysis and subsequent periodic assessments every three days for any signs of precipitation, turbidity, consistency changes, or drug loss. The degradation rate of the drug was indirectly calculated by monitoring the rate of decrease in its concentration. Over the course of 10 days, a total of five data points were thus examined in dark, and light condition as shown in Tables 25 and 26 using UV-vis spectroscopy in which UV spectra were collected and the peak at 429 nm analysed to determine the rate of any degradations.

DARK	
DAYS	AR-HBP Conc
1	0.000143
3	0.000132
5	0.00013
7	0.000128
9	0.000126

Table 25: Stability of Zn-THPP in Ar-HBPAMAM-OH in dark conditions.

LIGHT	
DAYS	AR-HBP
1	0.000143
3	0.000131
5	0.00028
7	0.00024
9	0.0002

Table 26: Stability of Zn-THPP in Ar-HBPAMAM-OH in light conditions.

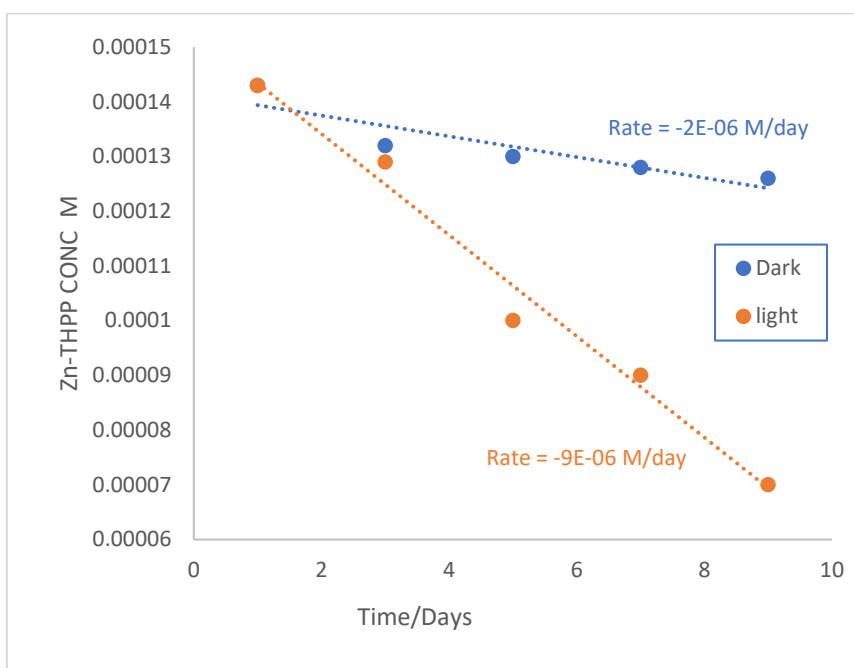


Figure 40: Stability of Zn-THPP in Ar-HBPAMAM_OH in dark and light conditions for 10 days.

The results presented above indicate that Ar-HBPAMAM-OH is close to 90% stable in dark conditions, which can be attributed to several factors. In particular, in terms of structural rigidity, aromatic hyperbranched PAMAM dendrimers possess highly branched and compact structures with defined cores and multiple layers of branching. This structural rigidity helps in maintaining the stability of the drug and prevents it from undergoing conformational changes or collapsing in many cases. However, the stability in light storage conditions was not good as

in dark storage conditions, as drug tends to undergo photodegradation when exposure to light leads to the disruption of the drug structure and properties.¹²⁶

6.2.2. Zn-THPP release from Ar-HBPAMAM-OH

A Zn-THPP/Ar-HBPAMAM-OH complex of $1 \times 10^{-4} \text{M}$ of the Ar-HBPAMAM_OH and 5×10^{-4} of Zn-THPP was prepared, and 6 mL of the complex was placed into osmosis tubing with a molecular weight cut-off of 1,000. This was then deposited in a beaker containing 200 mL of pH 7.4 phosphate buffer. Samples were removed from the dialysis bag and analysed using UV at $t=0$ and then periodically every 24 hours for five days to measure the absorption of the IBU Soret band at 429 nm. The resulting data is presented in Table 27 and displayed graphically in Figure 41.

Time (hr)	$\Delta\text{abs (430-433)}$	Conc.	Half life
0	0.22	5.26E-04	24hrs
24	0.069	1.65E-04	
48	0.0125	2.99E-05	
72	0.0036	8.61E-06	
96	0	0.00E+00	
120	0	0.00E+00	
Ar-HBPAMAM-OH conc. $1 \times 10^{-4} \text{M}$			
Zn-THPP conc. $5.3 \times 10^{-4} \text{M}$			

Table 27: Release of Zn-THPP from Ar-HBPAMAM-OH over 5 days.

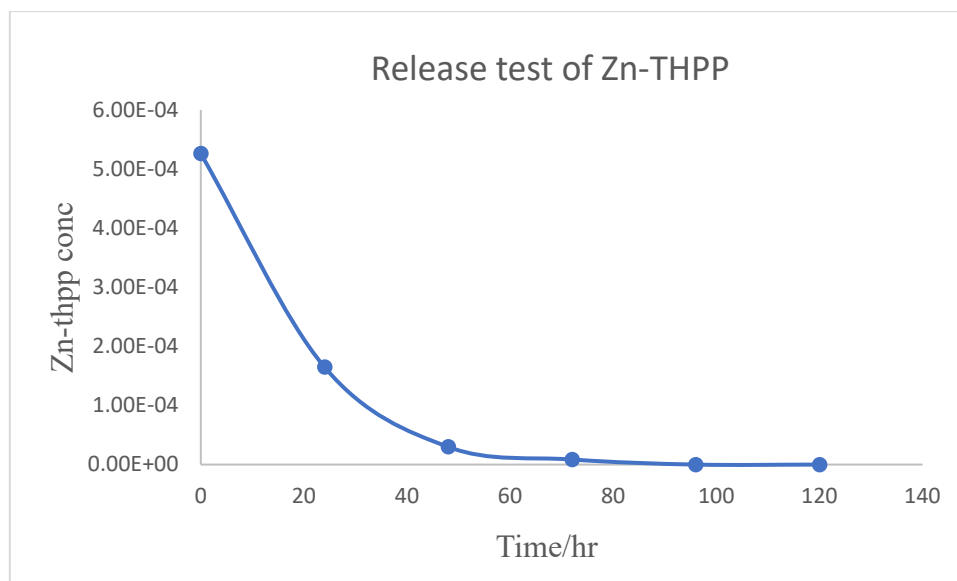


Figure 41: Release of Zn-THPP from Ar-HBPAMAM-OH over 5 days.

The results clearly demonstrate that Zn-THPP can be released from Ar-HBPAMAM_OH relatively slowly. While the decrease in the concentration of the drug was not constant. This release profile indicates a good level of interaction between Ar-HBPAMAM_OH, and the drug, supporting its use in potential PDT treatment, as slow release should enable the Zn-THPP complex to circulate around the body multiple times, thus generating a build-up within tumours. This means that harmful Zn-THPP photosensitizers will not be released and distributed throughout the body, thus reducing the harmful side effects often associated with PDT. This slow release may be attributable to disruption of the coordination and the electrostatic and hydrogen bonding interactions that serve to entrap drug molecules within the Ar-HBPAMAM-OH structure.¹²⁷

6.3. Part3: Encapsulation of anticancer F73 in aromatic hyperbranched PAMAM.

As with Ibuprofen testing, the initial objective was to determine the maximum amount of drug that could be encapsulated within the polymer-based systems. In contrast to Ibuprofen, which is readily available, however, F73 is a scarce and expensive compound. Consequently, directly adding an excess of F73 during encapsulation was not feasible. To overcome this obstacle, the method for drug encapsulation was appropriately modified by initiating encapsulation using a 1:1 molar ratio of drug to polymer, based on predetermined polymer quantity. Subsequently, the drug amount was increased to twice that used in the previous group in each iteration, resulting in a 2 to 1 mole ratio of drug to Ar-HBPAMAM_OH in the second group. This process continued until solid formations in the solution indicated that the polymer could no longer accommodate any additional drug. This incremental approach ensured that no F73 was wasted.

Drug	ϵ	maximum solubility in buffer
F73	5880	0.00035

As an accurate molecular weight for Ar-HBPAMAM-OH is not known, two different methods were used to calculate concentration. The first was the conventional molar concentration method, while the second was a mass/volume method (will be mentioned in comparison chapter) commonly used by polymer chemists (that ensures that the same number of monomer units are in each solution to allow for a comparison of properties between varying molecular weights. Accuracy in such cases does require the polymers to have identical repeat units, however, which was not the case for the current systems. Nevertheless, the structures were deemed similar enough for a qualitative comparison to be made to inform assessment of the validity of the results obtained using molarity. Using the conventional molar method, Ar-

HBPAMAM-OH concentrations equivalent to those used for the dendrimer experiments were accessed, with concentrations of Ar-HBPAMAM-OH equal to 1×10^{-4} M thus used. In the first step, the extinction coefficient was found to be $5,880 \text{ dm}^3 \text{ mol}^{-1} \text{ cm}^{-1}$

Concentration of HBP	Total [F73] mM	Encapsulated [F37] mM	Loading/dendrimer
0.0001M	0.75	0.4	4
Maximum free F73 concentration in buffer = 3.5×10^{-4} M			

Table 28: Encapsulation of F73 in Ar-HBPAMAM-OH using the conventional molar concentration method.

It is clear that Ar-HBPAMAM-OH can encapsulate F37 and improve its solubility. As with dendrimers, the aromatic Ar-HBPAMAM-OH forms multiple non-covalent interactions with F73, including hydrogen bonding, and Van der Waals forces. The polymer concentrations were thus enhanced to 7×10^{-4} M and the loading was 4 mol/dendrimer based on conventional molar concentration methods using the estimated molecular weight from GPC. This high level of encapsulation was attributed to the hydrophobic environment created by the Ar-HBPAMAM_OH alongside the presence of internal amines.

6.3.1. Stability of F73 in Ar-HBPAMAM_OH.

Following the F73 encapsulation study, the drug stability in polymer was assessed in each case. This testing was carried out as previously described for Ibuprofen, with the primary objective of extracting a small portion of the top layer from the encapsulated solution each day to measure ongoing absorbance. This process also allowed monitoring of the drug concentration and any decreases over time.

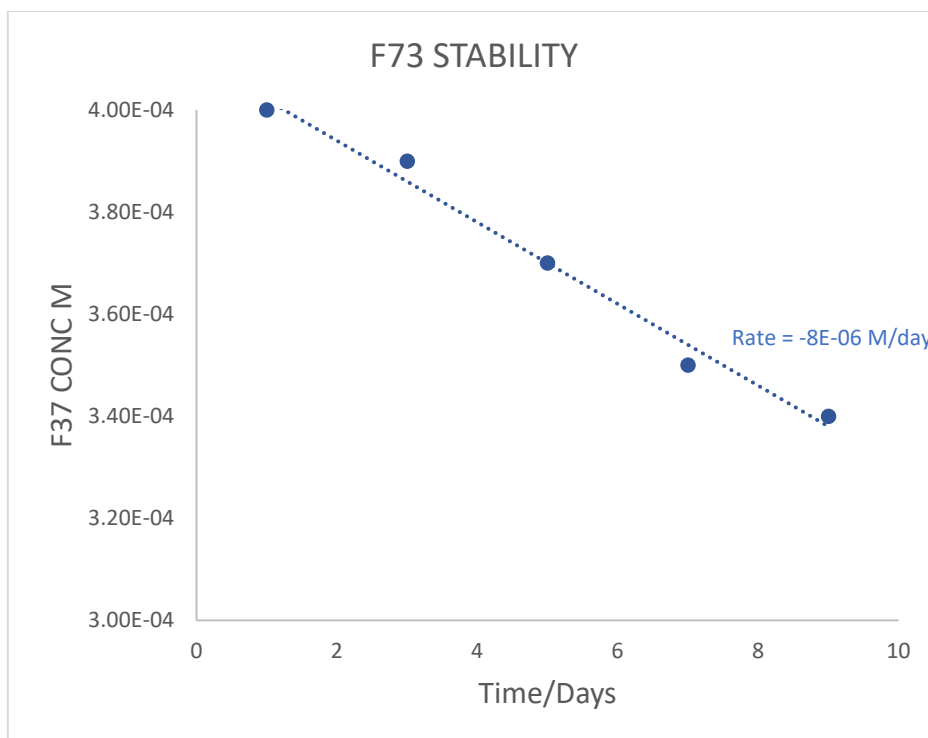


Figure 42: Stability of F73 in Ar-HBPAMAM-OH.

The relevant figure 42 shows that F73 demonstrates good stability, implying that the irregular structure of the Ar-HBPAMAM_OH probably provides a reasonably compact and controlled internal structure that is capable of forming significant hydrophobic pockets.

6.3.2. F73 release from Ar-HBPAMAM-OH.

An F73/Ar-HBPAMAM-OH complex of 1×10^{-4} M of Ar-HBPAMAM_OH and 1.8×10^{-4} of F73 was prepared, and 6 mL of the complex was placed into osmosis tubing with a molecular weight cut-off of 1,000. This was then deposited in a beaker containing 200 mL of pH 7.4 phosphate buffer. Samples were removed from the dialysis bag and analysed using UV at $t=0$, then periodically every 24 hours for five days, with the absorption of the IBU Soret band at 282 nm measured in this manner. The resulting data is presented in Table 29 and displayed graphically in Figure 43.

Time (hr)	Abs	Conc M	Half life
0	1.05	1.79E-04	20hrs
24	0.63	1.07E-04	
48	0.31	5.27E-05	
72	0	0.00E+00	
96	0	0.00E+00	
120	0	0.00E+00	
Ar-HBPAMAM-OH conc $1 \times 10^{-4} \text{M}$			
F73 conc 1.9×10^{-4}			

Table 29: Release of F73 from Ar-HBPAMAM-OH over 5 days.

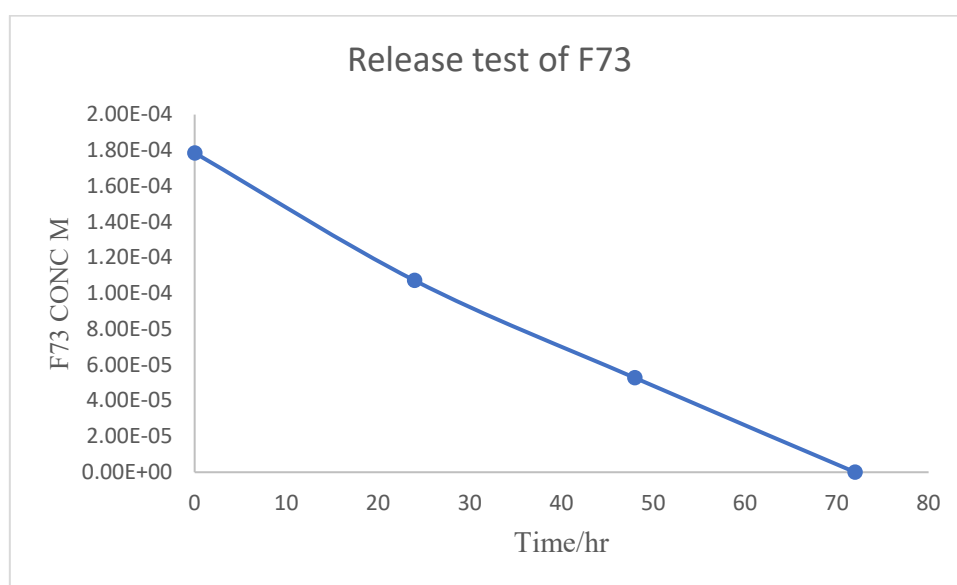


Figure 43: Release of F73 from Ar-HBPAMAM-OH over 5 days.

The results clearly demonstrate that F73 is released from the Ar-HBPAMAM_OH in a rapid manner, as confirmed by the linear nature of the graph, which also shows that the decrease in the concentration of the drug is constant. The F73 is released from the Ar-HBPAMAM_OH into the bulk solvent as soon as any F73 that is free in solution crosses the membrane, which makes F73 release from the Ar-HBPAMAM_OH much more rapid than its rate of transport

across the membrane. This rapid release from the Ar-HBPAMAM-OH suggests that any F73-Ar-HBPAMAM-OH interactions are relatively weak as compared to those of Ibuprofen and Zn-THPP. Thus, while Ar-HBPAMAM_OH can enhance the solubility of F73, it may not be a useful or effective drug carrier for F73.

6.4. Discussion:

Aromatic hyperbranched PAMAM with hydroxyl groups were synthesised and examined with respect to their capacity to encapsulate small hydrophobic drug molecules at concentrations of 1.0E-04 M.

The drugs were found to be well encapsulated, and their solubility was clearly enhanced. The high level of encapsulation was attributed to the hydrophobic environment created by the Ar-HBPAMAM_OH in conjunction with the internal amines. The initial expectation was that the level of encapsulation would be linearly related to the concentration of Ar-HBPAMAM_OH. However, this was found to not be the case, and a significant deviation from linearity was observed at higher concentrations of Ar-HBPAMAM_OH. It was thus postulated that this was due to aggregation limiting the amount of free space available.¹²⁸ Stability and release testing was done for a range of drugs encapsulated in Ar-HBPAMAM_OH, all of which were found to be stable over time, a stability that may be attributed to several factors.

These include structural rigidity, as aromatic hyperbranched PAMAM dendrimers possess highly branched and compact structures with defined cores and multiple layers of branching. Based on the release test, all drugs were readily released from the Ar-HBPAMAM_OH, with the results for Ibuprofen and Zn-THPP clearly demonstrating that both drugs are released slowly from Ar-HBPAMAM_OH. This is an important result, as it clearly demonstrates the potential applicability of this system for drug delivery. However, the release test for F73 demonstrated rapid release from Ar-HBPAMAM_OH, suggesting that any F73-Ar-HBPAMAM-OH interactions are relatively weak as compared to those of Ibuprofen and Zn-THPP. This suggests that while Ar-HBPAMAM_OH can enhance the solubility of F73, it may not be the most useful or effective drug carrier for F73.

Chapter 7

7. Comparisons of macromolecules used for drug delivery.

7.1. Comparing drug encapsulation efficacies of hydroxyl terminated PAMAM dendrimers and aromatic HB-PAMAM

The aim of this brief chapter is to compare the results and decide which of the two delivery systems is best. This assessment will not simply consider which is technically better (i.e., highest levels of encapsulation, but will also consider other factors, such as cost, time, ease of synthesis and any restrictions based on potential therapeutic use. The aim is to consider the systems generically, that is, to compare HBPs as a group with dendrimers as a group. The aim was never to identify which of the two “specific” systems were best (i.e., the PAMAM dendrimers or PAMAM HBPs). Nevertheless, to make a fair comparison, we must consider systems built up using the same functionality. The individual synthesis and properties of two such systems (with PAMAM connectivity) were discussed in the previous chapters. However, in order to compare these systems, we need to consider how we calculate the concentration of the two systems. While there is no problem using molarity for the PAMAM dendrimers, where we know the molecular weight, it is not so easy to determine molarity for the polydisperse Ar-HBPAMAM-OH. The polydisperse nature of the HBP makes it impossible to determine a unique and accurate molecular weight. At best, we can only calculate an average molecular weight using Gel Permeation Chromatography (GPC).¹²⁹ Unfortunately, this method introduces more uncertainty, as it relies on the “size” of linear polymers to calibrate the system, and the size of these linear calibrants is much larger than spherical molecules with equivalent molecular weights.¹²⁹ As such, GPC always underestimates the molecular weight of HBPs due to their globular structures. However, aqueous GPC did estimate an average molecular weight of 2500. Therefore, if we use this as the molecular weight for our Ar-HBPAMAM-OH, we can compare its drug delivery properties with the G2.5-OH PAMAM dendrimer, using molarity as the unit of concentration.

Due to the uncertainty surrounding the precise molecular weight of polydisperse systems, polymer chemists use the mass/volume method as a unit of concentration. This method ensures that the same number of monomer units are in a solution regardless of its molecular weight and allows for a comparison of properties between all molecular weights. However, it does require the polymers to have identical repeat units, which is not the case for the PAMAM dendrimer and Ar-HBPAMAM-OH systems under consideration in this work. Fortunately, their structures are similar enough for a qualitative comparison to be made that can inform and support the validity of the results obtained using molar concentrations. Therefore, in order to make a qualitative comparison between the two systems, we propose to study the various drug delivery properties using both methods for determining concentration - molarity and mass/volume. To do this we will need to use a known molar concentration and a corresponding mass/volume concentration, to use as a baseline for all systems. As mentioned above, we can only determine the exact molarity for the dendrimer, as it is monodispersed and has a unique and known molecular weight. For the experiments described herein, all concentrations (molarity and mass/volume) would be determined and compared using a baseline dendrimer concentration of 1×10^{-4} M, which equates to a mass/volume concentration of 0.75mg/ml.

7.1.1. Encapsulation data for the hydroxyl terminated dendrimer and Ar-HBPAMAM-OH.

based on conventional molar concentrations are shown in Table 30 and compared graphically in Figure 44

	Dendrimer	HBP
IBU	1.80E-03	1.60E-03
Zn-THPP	1.70E-04	1.43E-04
F37	5.00E-04	4.00E-04
Molar conc 1×10^{-4}		

Table 30: Encapsulation different drugs in hydroxyl terminated dendrimer and Ar-HBPAMAM-OH as measured through conventional molar concentration.

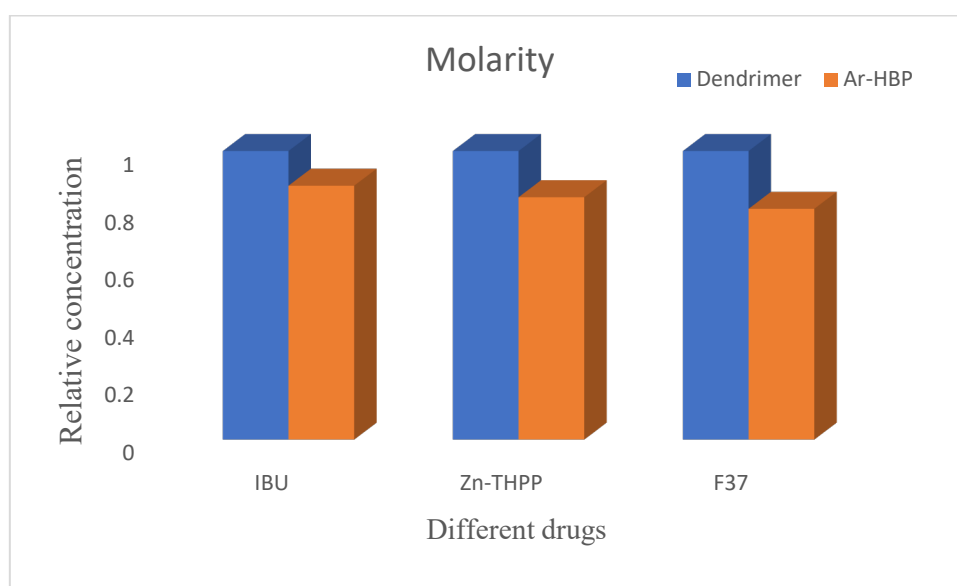


Figure 44: Encapsulation in hydroxyl terminated dendrimer and Ar-HBPAMAM-OH as measured through conventional molar concentration.

The data based on molar concentrations, and showed in this graph as relative concentration, due to the difference in the solubility between the three drugs. The results shows that the differences in encapsulation ability between the dendrimer and the Ar-HBPAMAM-OH are not significant for any of the drugs studied. In this respect, it is clear that the Ar-HBPAMAM-OH performs as well as the more complicated dendrimer-based system, suggesting that the

much simpler and more accessible Ar-HBPs may offer wider access to efficient drug delivery systems. The resulting data is presented in Table 30 and displayed graphically in Figure 44.

7.1.2. Encapsulation data for the hydroxyl terminated dendrimer and Ar-HBPAMAM-OH

based on mass/vol concentration equivalent to 0.0001 M are shown in Table 31 and compared graphically in Figure 45.

	Dendrimer	HBP
IBU	1.80E-03	9.00E-04
Zn-THPP	1.70E-04	1.12E-04
F37	5.00E-04	1.60E-04
Mass/volume		

Table 31: Encapsulation study of hydroxyl terminated dendrimer and Ar-HBPAMAM-OH at mass/vol concentration equivalent to 0.0001.

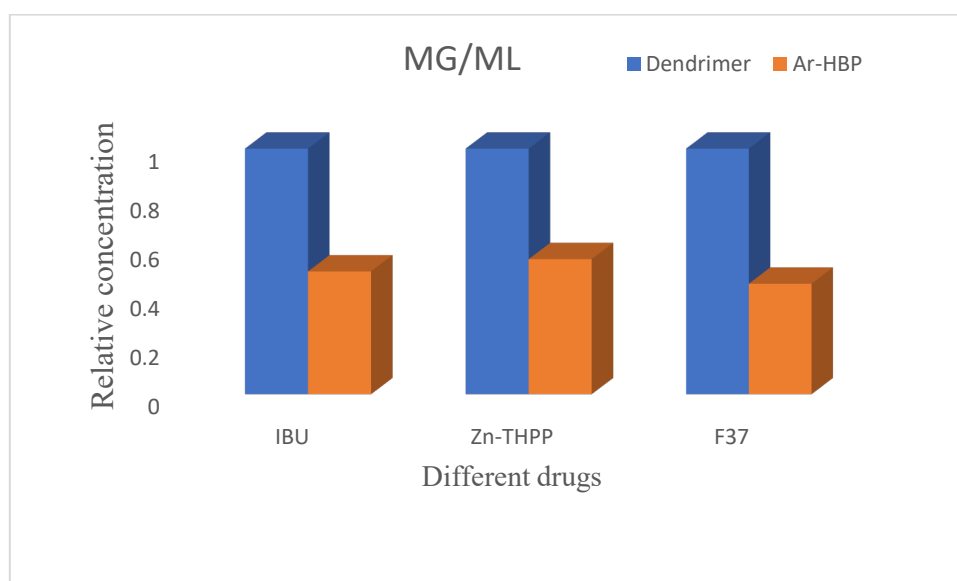
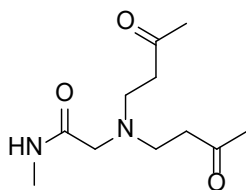


Figure 45: Encapsulation study of hydroxyl terminated dendrimer and Ar-HBPAMAM-OH at mass/vol concentration equivalent to 0.0001.

Comparing encapsulation ability using the mass/vol method for concentration, a large difference in the encapsulation ability for all drugs emerges between the dendrimer and the Ar-HBPAMAM-OH polymers, based on Ar-HBPAMAM-OH having a lower capacity for loading

than the dendrimer-based system. One reason for this may be due to the fact that the number of repeat units in solution in Ar-HBPAMAM-OH is not the same as in the dendrimer solution, being affected by differences in the structure of the Ar-HBPAMAM-OH repeat unit as compared to that of the dendrimer. Specifically, the Ar-HBPAMAM-OH unit has an aromatic group between each monomer and repeat unit, which adds molecular weight and thus reduces the number of monomers and repeat units in the solution. The structures of the two repeat units are shown in Figure 146, which illustrates that the Ar-HBPAMAM-OH repeat unit has a molecular weight of 259, whilst the PAMAM has a molecular weight of only 183, around 30% lower than the Ar-HBPAMAM-OH. As such, for the same mass of delivery system, the Ar-HBPAMAM-OH only offers 70% of repeat units offered by the PAMAM dendrimer, leading to fewer Ar-HBPAMAM-OH in solution. Consequently, the amount of encapsulation for the Ar-HBPAMAM-OH solution is likely to be lower, as seen in the current case. The resulting data is presented in Figure 46.

PAMAM monomer



Ar-HPP monomer

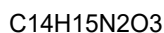
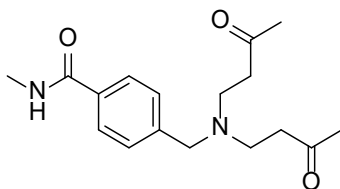


Figure 46: Two single monomers, dendrimer and Ar-HBPAMAM-OH.

7.1.3. Comparing the stability of different drugs within dendrimer and Ar-HBPAMAM-OH

The objective of the study was to investigate and compare stability of IBU, ZnTHPP, and F73 in dendrimer, and Ar-HBPAMAM-OH. All mixes were prepared using the co-precipitate technique, and prepared samples were kept at room temperature in a pH 7.4 phosphate buffer for 10 days. Periodically, UV spectra were collected, with all peaks analysed to determine the rate of any degradation. The degradation rate of each drug was also indirectly calculated by monitoring the rate of decrease in concentration. Over the course of 10 days, a total of five data points were thus examined using UV-vis spectroscopy for each complex. The resulting data is presented in Table 32 and displayed graphically in Figures 47 to 50.

Days	IBU in dendrimer	IBU in HBP	ZnTHPP in dendrimer	ZnTHPP in HBP	F73 in dendrimer	F73 IN HBP
1	2.87E-03	3.09E-03	1.77E-04	1.43E-04	5.00E-04	4.00E-04
2	2.77E-03	2.87E-03	1.71E-04	1.32E-04	5.00E-04	3.90E-04
3	2.77E-03	2.87E-03	1.64E-04	1.30E-04	4.80E-04	3.70E-04
4	2.66E-03	2.66E-03	1.52E-04	1.28E-04	4.70E-04	3.50E-04
5	2.55E-03	2.55E-03	1.52E-04	1.26E-04	4.60E-04	3.40E-04

Table 32: Stability test for IBU, Zn-THPP, and F73 in dendrimer and Ar-HBPAMAM-OH polymers.

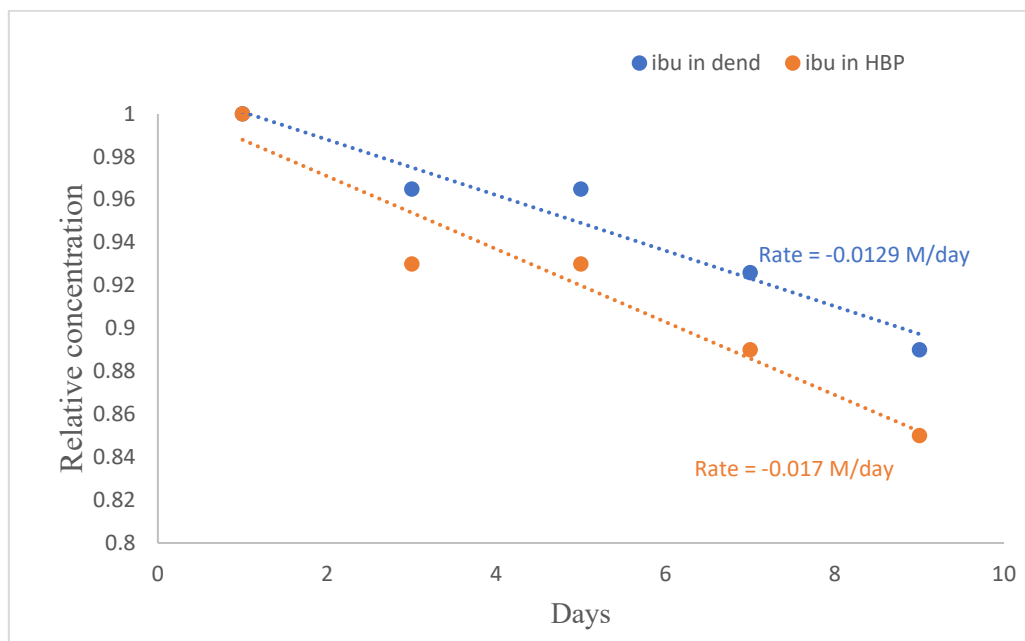


Figure 47: Stability test for IBU in dendrimer and Ar-HBPAMAM-OH polymers.

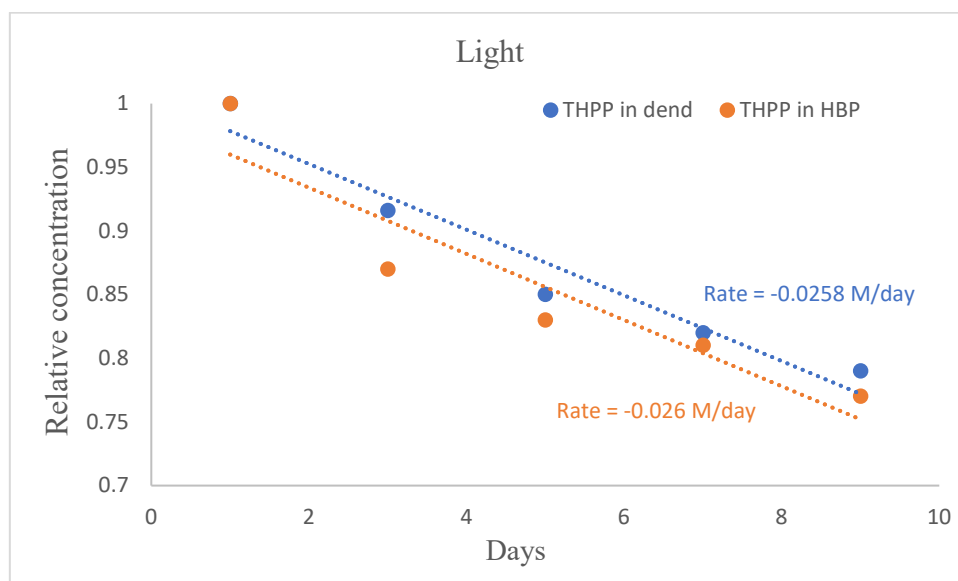


Figure 48: Stability test for Zn-THPP in dendrimer and Ar-HBPAMAM-OH polymers in light conditions.

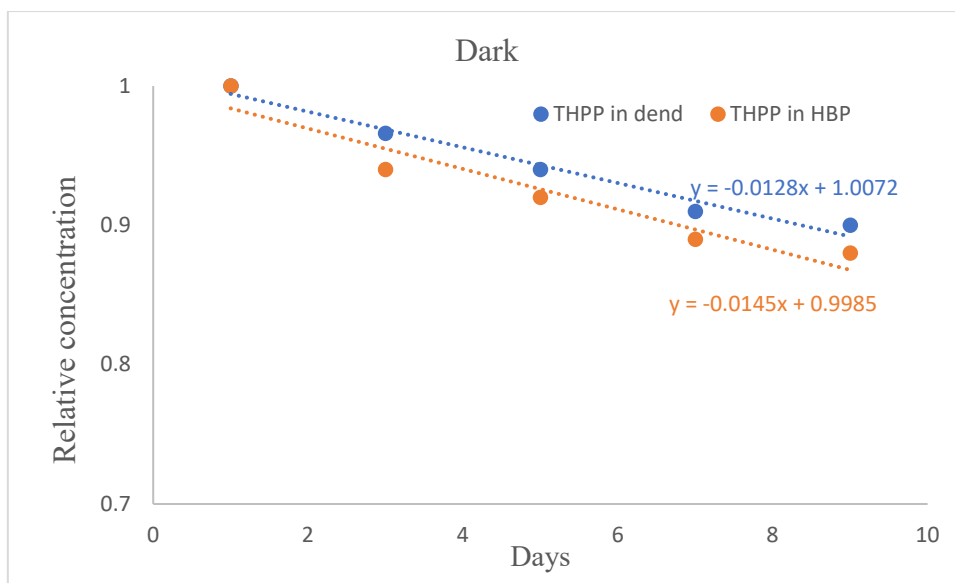


Figure 49: Stability test for Zn-THPP in dendrimer and Ar-HBPAMAM-OH polymers in dark conditions.

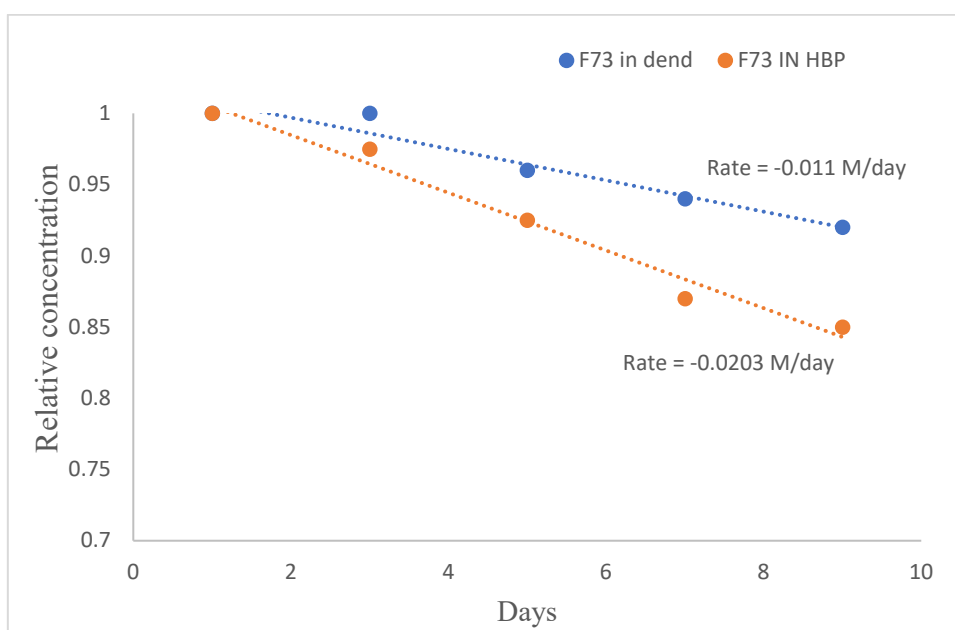


Figure 50: Stability test for F73 in dendrimer and Ar-HBPAMAM-OH polymers.

The results presented above indicate that all drugs almost stable in both polymers (dendrimer and Ar-HBPAMAM-OH) exhibit around 90% stability in G2.5-OH. and a bit decrease in the stability of drugs in Ar-HBPAMAM-OH. Which is not a significant difference between both of them. This stability of drugs in G2.5-OH/drug complexes can be attributed to the dendrimer's optimised internal structure, which maximises binding across a significant number

of drug/dendrimer interactions, thereby enhancing stability. The stability of drugs in Ar-HBPAMAM-OH complex can be similarly attributed to its highly branched and compact structure based on a defined core and multiple layers. This means that the drugs are not degraded by water, with both delivery systems helping preserve drugs in this manner; the results for porphyrin were a little different, however, as porphyrins are photosensitive and may thus be degraded by light. The comparison experiments were thus performed in the dark, with better results, as shown in (Figure 49).

7.1.4. The release of Ibuprofen, Zn-THPP, and F73 from G2.5-OH, and Ar-HBPAMAM-OH systems.

The objective of this study was to investigate the release of Ibuprofen, Zn-THPP, and F73 from G2.5-OH PAMAM dendrimer, and Ar-HBPAMAM-OH to determine which system is faster in terms of such release. Both systems complexes were prepared at $1 \times 10^{-4} \text{M}$, and 6mL of the relevant complex was placed into osmosis tubing with a molecular weight cut-off of 1,000. This was then deposited in a beaker containing 200 mL of pH 7.4 phosphate buffer. Samples were removed from the dialysis bag and analysed using UV at $t=0$ before being periodically re-examined every 24 hours for five days. The resulting data is presented in Table 33 and displayed graphically in Figures 51 to 53.

Time/hr	Dend/Znthpp	ArHBP/Znthpp	Dend/f73	ArHBP/F73	Dend/IBU	ArHBP/F73
0	0.000778955	0.000526136	0.000189	0.0001786	0.008514	0.0080489
24	0.000233686	0.000165015	0.000119	0.0001071	0.005394	0.0049043
48	3.99214E-05	2.98941E-05	5.61E-05	5.272E-05	0.003424	0.0030851
72	1.03861E-05	8.6095E-06	0	0	0.002452	0.0019149
96	0	0	0	0	0.00117	0.0009574
120	0	0	0	0	0	0

Table 33: Release of Zn-THPP, IBU, F73) from PAMAM dendrimer and Ar-HBPAMAM-OH.

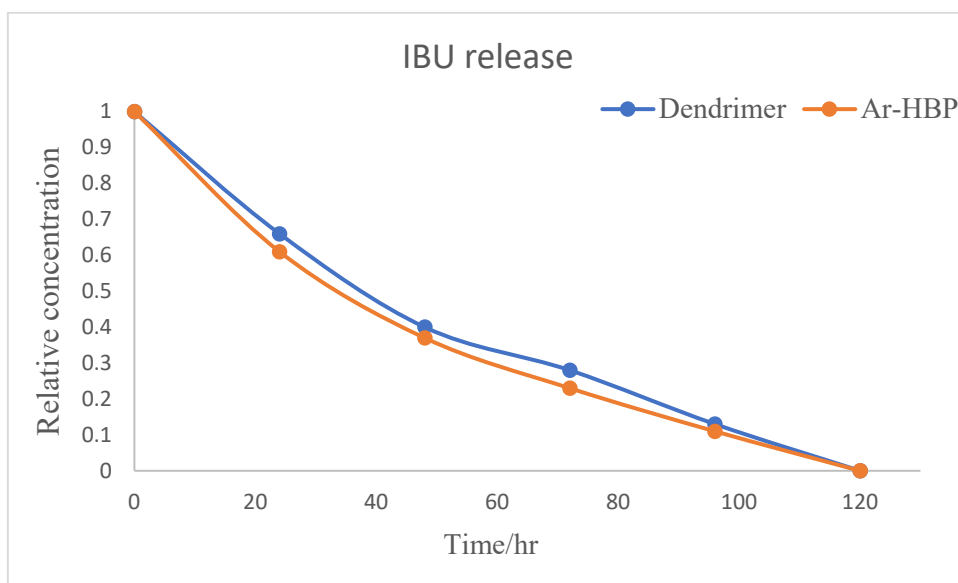


Figure 51: Release of IBU from Dendrimer and Ar-HBPAMAM-OH.

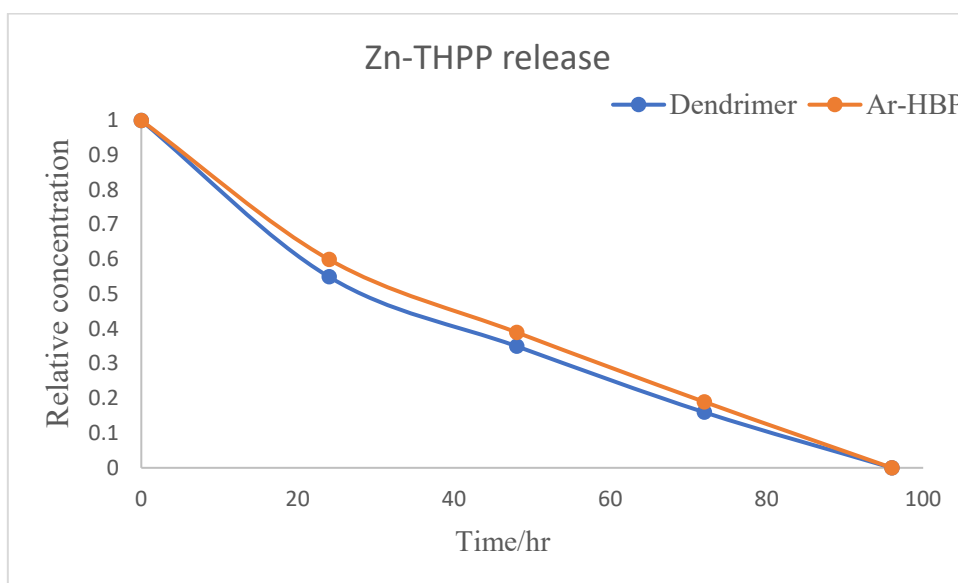


Figure 52: Release of Zn-THPP from Dendrimer and Ar-HBPAMAM-OH.

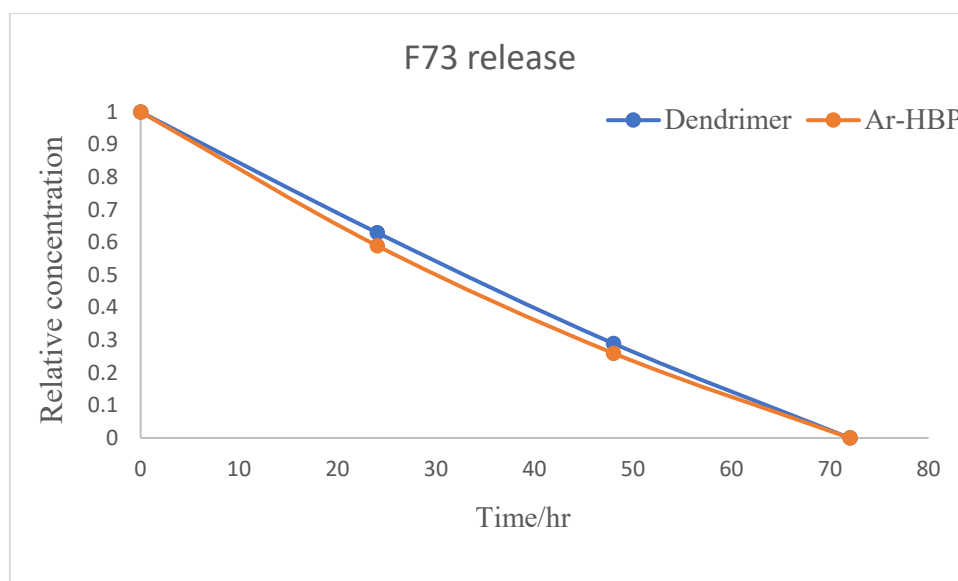


Figure 53: Release of F73 from Dendrimer and Ar-HBPAMAM-OH.

The results clearly demonstrate that all tested drugs are released from G2.5-OH, and Ar-HBPAMAM-OH with the same rate and mechanism, which indicates that any differences in release rate between the dendrimer and the Ar-HBPAMAM-OH are not significant, with the Ar-HBPAMAM-OH thus performing as well as the more complicated dendrimer-based system. Furthermore, this shared release time was slow, which offers potential benefits in terms of enhancing effectiveness while minimising side effects. Slow release ensures that a consistent level of the drug is maintained in the body over an extended period of time, which may be crucial for achieving the optimal therapeutic effect, especially in cases drug concentration must be maintained within a narrow therapeutic window.

Chapter 8

8. Conclusion

In recent times, dendrimers have shown great potential as drug carriers. One of their notable advantages is their ability to encapsulate small molecules within their internal spaces at high generations. This feature allows for active and passive drug targeting, reducing associated side effects.¹³⁰ However, dendritic systems are not without flaws, as discussed earlier, that the synthesis of dendrimers is challenging, time-consuming, and costly.¹³¹

Consequently, both the academic and industrial communities have been exploring alternative macromolecules that can deliver drugs, similar to dendrimers.

A simpler alternative comes in the form of HBPs (Hyperbranched Polymers) due to their effortless and cheap synthesis, which is often achieved in just one pot.⁸² Although HBPs and dendrimers have been compared in the past, previous studies have not conducted direct, like-for-like comparisons and this represents a gap in the literature. Therefore, this project aimed to thoroughly study both branched macromolecules with respect to their size and functionality, and to better understand their capabilities as drug carriers. Ultimately, we wanted to know if hyperbranched polymers were as good as dendrimers when applied as drug delivery vehicles. In this study, we synthesised a range of PAMAM dendrimers, from G0.5 to G3.5, using a series of Michael addition and amination steps. By modifying the terminal groups to hydroxyl groups, we obtained neutral water-soluble PAMAM dendrimers (OH-ended PAMAM dendrimers) with 8OH, 16OH, and 32OH terminal groups. The next objective was an investigation into the ability of these dendrimers to encapsulate Ibuprofen with respect to dendrimer size and any dense packing effects. This would allow us to determine the optimum dendrimer for the remaining studies. We focused on three generations of dendrimers, namely G1.5-OH, G2.5-OH, and G3.5-OH, all tested at a concentration of 1×10^{-4} M. The study revealed that the encapsulation capability of the dendrimers did indeed depend on their size, with G2.5-OH being the most suitable for encapsulating the drug Ibuprofen, achieving a loading of 18.

Although the higher-generation G3.5-OH dendrimer was much larger, it could only encapsulate the same amount of Ibuprofen as the smaller G2.5 OH dendrimer. This was due to the G3.5 OH dendrimer having a more densely packed internal structure.

Further investigation into the effect of dendrimer concentration on the amount of Ibuprofen encapsulation were carried out using the G2.5-OH dendrimer. Experiments were performed at different concentrations, ranging from 1×10^{-3} to 1×10^{-6} M. The results showed that the dendrimer's ability to encapsulate Ibuprofen increased roughly linearly up to a concentration of 1×10^{-4} M, after which the loading remained constant and plateaued. It was proposed that the non-linear relation between dendrimer concentration and drug encapsulation was due to aggregation. This was tested using Dynamic light scattering (DLS), where measurements on the G2.5 OH dendrimer indicated that dendrimers at concentrations above 1×10^{-4} M were significantly larger (200 nm) compared to those recorded below this concentration (5 nm). A similar study using the G3.5-OH at 1×10^{-4} M revealed a similar decrease in encapsulation ability, which was also attributed to dendrimer aggregation. Based on these findings, it was essential to maintain dendrimer concentrations below 1.5×10^{-4} M for future encapsulation experiments, especially when compared to equivalent hydrophobic drug carriers (HBPs).

With respect to determining the drug delivery potential of the dendrimers, we began to investigate the stability of Ibuprofen within the dendrimer complexes. The findings demonstrate that the drug was stable within the G2.5-OH showing the highest level of stability, approximately 100% more stable than the G1.5-OH dendrimer.

the stability of the drug. Essentially, the drug is not degraded or hydrolysed by, or in the presence of the G2.5-OH dendrimer. However, Ibuprofen is less stable in the G1.5-OH dendrimer, due to an open structure that can expose the Ibuprofen to water, and therefore hydrolytic degradation (hydrolysis). The dendrimer may also help (catalyse) the hydrolysis of Ibuprofen.¹³² Furthermore, the results clearly demonstrate that Ibuprofen can be

released from the PAMAM dendrimer. This is an important result, as it clearly demonstrates the potential applicability of these systems for drug delivery. Furthermore, the overall release is relatively slow, which suggests a reasonably good interaction between dendrimer, and the drug.

The next set of experiments focused on a drug that could form metal-ligand complexes allowing us to explore the impact of metal coordination on the encapsulation ability of the dendrimer system. These experiments used a Tetra dihydroxyphenyl porphyrin (THPP), which has been used clinically as a sensitizer for use in photodynamic therapy (PDT). THPP and the zinc metalated form (Zn THPP), were successfully synthesized in three steps, (TMPP, THPP, and Zn-THPP) and all characterized. To assess the encapsulation, we used PAMAM dendrimers (G1.5-OH, G2.5-OH, and G3.5-OH). UV spectroscopy confirmed encapsulation of all the porphyrins, with a noticeable shift in the wavelength of the Soret band. The wavelength of encapsulated THPP was shifted from 418 to 424. And the wavelength of the metalated THPP was shifted from 423 to 430. Which confirm both wavelengths have been shifted after encapsulation.

The encapsulation results showed that the metalated species exhibited significant improvements in encapsulation and solubility. For G2.5-OH, encapsulation increased from 1.29 to 1.75M equivalents for the free base and metalated porphyrins, respectively. For G3.5-OH, the increase was more substantial, rising from 1.44 to 1.96 equivalents for the free base and metalated porphyrins, respectively. The increased encapsulation between the non-metalated and metalated porphyrins was attributed to additional coordination to the terminal OH group.

The study also found that the porphyrin loading was significantly lower than the loading for ibuprofen, and this was due to the larger size of the porphyrin molecule compared to ibuprofen. However, the relative increase in solubility of the porphyrins was substantially higher than that

observed for Ibuprofen. Specifically, solubility doubled for Ibuprofen, but was nearly 300 times higher for the metalated porphyrin.

The stability of the metalated porphyrin within the dendrimer complexes was investigated under both light and dark conditions over a period of ten days. The main objective was to assess how dendrimer size influences the stability of the porphyrin. The dendrimers studied were G1.5-OH, G2.5-OH, and G3.5-OH. During the experiment, The results indicate that all dendrimers exhibit stability, with G2.5-OH being the most stable by around 100%. The results show the stability was better in a dark storage than the light storage, with all generations having better stability in the dark than the light. The reason for that is porphyrins undergo photodegradation, a process in which the exposure to light leads to the degradation of the porphyrin structure and properties.

The release study of the metalated porphyrin within the dendrimer complexes was investigated. The results clearly demonstrate that Zn-THPP **14** can be released from the PAMAM dendrimer. Furthermore, the release is slow, which is good news for any potential PDT treatment. Slow release will enable the Zn-THPP complex to circulate around the body many times, building up within tumours.

Having successfully demonstrated that the OH ended systems could encapsulate ibuprofen, and Zn-THPP with equal levels of efficiency, we wanted to see if the same was true for a different drug. On this occasion, we investigated a research drug called F37, which is an effective anticancer drug. Similar studies to those carried out for Ibuprofen were carried out and the results showed that the F73 exhibited similar improvements in encapsulation and solubility. However, the release studies were very different. In the case of F73, the release profile was linear, which indicates a very fast release from the dendrimer, which was faster than the rate of transport across the membrane. This tells us that the encapsulation was very weak. As such,

the dendrimer is a poor delivery system for F73 and a different, bespoke system would be required for the delivery of F73.

To make a comparison with hyperbranched polymers, an Aromatic HBPAMAM was successfully synthesised. Although the resulting HBPAMAM-NH₂ had been previously synthesised by the Twyman group, it did not possess the required hydroxyl-ended groups. To address this limitation, we synthesised an AR-HBPAMAM with hydroxyl-terminated groups using a post synthetic two step synthesis.

Although we can estimate the average molecular weight of polymers, it is not possible to know it exactly. In fact, due to their polydisperse nature, it is not possible to obtain an exact molecular weight (the polymer is made up of many unique molecules with different sizes/weights). As such the encapsulation of Ibuprofen, Zn-THPP and F73 within the AR-HBPAMAM were carried out using two different methods to determine concentrations: a conventional molar concentration 0.0001M and a mass/volume concentration mg/ml. Although there were differences using the two methods, the encapsulation results were not that different. Nevertheless, we did observe better levels of encapsulation using molar concentration.

The aromatic hyperbranched PAMAM with hydroxyl groups was synthesized and examined for their capacity to encapsulate a small hydrophobic drug at a concentration of 1×10^{-4} M. GPC showed that the Ar-HBPAMAM-OH had an MW of 2500.

The drugs have been well encapsulated, and the solubility of them were clearly enhanced. This high level of encapsulation is due to the hydrophobic environment created by the Ar-HBPAMAM-OH, as well as the internal amines. We initially expected that the level of encapsulation would be linearly related to the concentration of Ar-HBPAMAM-OH. However, this was not the case and a significant deviation from linearity was observed at higher concentrations of Ar-HBPAMAM-OH. We postulated that this was due to aggregation, As such, limiting the amount of free space. The stability, and release test has been done for all

drugs in Ar-HBPAMAM-OH, The drugs were stable over time, this stability is attributed to several factors. Aromatic hyperbranched PAMAM dendrimers possess a highly branched and compact structure with a defined core and multiple layers of branching. And, regarding the release test, the results clearly demonstrate that all drugs can be released from the Ar-HBP. For IBU, and Zn-THPP, the results demonstrated that both drugs could be released slowly from the Ar-HBPAMAM-OH. This is an important result, as it clearly demonstrates the potential applicability of this systems for drug delivery. On the other hand, the release test for F73 demonstrate that release was very fast, suggesting that any F73- Ar-HBPAMAM-OH interactions must be relatively weak (relative to Ibuprofen and Zn-THPP). Therefore, it is clear that the Ar-HBPAMAM-OH can enhance the solubility of F73, but it may not be a useful or effective drug carrier for F73.

The final part of this project attempted to answer the main question regarding the two delivery systems as set out in the aims. That is, “to determine whether or not the cheaper and more accessible hyperbranched polymers could compete with the expensive and complicated dendrimer systems when applied as drug delivery vehicles”. To achieve this, we compared the encapsulation, stability, and release properties of a hyperbranched polymer that possessed the same basic functionality as the PAMAM under investigation. Specifically, the study focused on comparing the Ar-HBPAMAM-OH with the hydroxyl-terminated PAMAM dendrimers. The results indicated that the G2.5/3.5-OH dendrimers were a little better than the Ar-HBPAMAM-OH, but the differences were not significant. For example, the G2.5-OH PAMAM dendrimer and Ar-HBPAMAM-OH could encapsulate and solubilize ibuprofen with maximum concentrations of 2.8E-03 and 1.6E-03, respectively, at concentration 1×10^{-4} for both systems. More significantly, the results using Zn THPP revealed that both systems at concentration 1×10^{-4} were equally proficient at encapsulating the porphyrin.

With respect to stability and release, the results were essentially the same for all drugs tested using both systems, again confirming no real advantage of the dendrimer system over the Ar-HBPAMAM-OH.

In summary, it is evident that HBPs present promising and cost-effective alternatives to dendrimers for drug delivery systems. However, it is important to note that dendrimers have an advantage with their regular and well-balanced mono-dispersed structure, which makes it easier for them to satisfy the requirements of drug approval agencies concerning size, dispersity, and potential clinical application. Conversely, HBPs often exhibit significant polydispersity in terms of molecular weights and structures, making it challenging to obtain the narrowly dispersed materials preferred by drug approval agencies. Consequently, for HBPs to be viable as drug delivery systems, advancements in both their synthesis and purification techniques will be necessary.

Future Work

1- Control experiments.

Whilst writing the thesis I identified some additional control experiments. These would focus on the stability and release experiments (described in the thesis) using just the drug compounds. This may help to fully understand the delivery potential of the dendrimer and HBP systems.

2- Develop a new HBP that does not have the aromatic group within the monomer.

Although the HBP system described in the thesis is similar to the dendrimer, it is not identical (with respect to functionality and connectivity). So, we recommend investigating a method for synthesising a HBP that better resembled the PAMAM dendrimer. This would be followed up with the same encapsulation, stability and release experiments already described in the thesis.

3- Develop and test a dendrimer/HBP delivery system for a lead compound that has a genuine problem with some aspect of its application.

The research conducted thus far has provided valuable insights into the dendrimers and HBP as potential drug delivery vehicles. However, the drugs in question may not necessitate a novel delivery system, except perhaps for the porphyrin compound. With more time, we recommend to identify and collaborate with a researcher to explore lead compounds that truly benefit from a delivery system for therapeutic use. The encapsulation, stability, and release experiments would be the same as those detailed in the thesis.

4- Establish collaborations that would allow us to carry out cell work on the delivery systems (allowing us to compare them with respect to delivery and release).

we would conduct cellular studies to thoroughly assess the dendrimer/HBP drug delivery systems' capabilities, particularly whether the drugs could be effectively released and yield a therapeutic impact on their target cells.

5- Working with our existing collaborators in Medicine, initiate a study using the encapsulated porphyrin systems (described in the thesis) as a new photodynamic system.

TPP (Tetraphenylporphyrin) and THPP (Tetrahydroxyphenylporphyrin) are porphyrin-based compounds utilized as photosensitizers in photodynamic therapy (PDT). While they are effective in clinical settings, the development of a targeted delivery system could enhance their application by enabling site-specific treatment. This would mitigate the need for post-treatment light avoidance, increase therapeutic efficacy, and decrease adverse effects. Our ongoing partnership with Dr. Helen Bryant from Sheffield Medical School will focus on advancing PDT cell research to evaluate the potential toxicity of dendrimer/HBP-based drug delivery systems in both illuminated and non- illuminated environments.

Chapter 9

9. Experimental work

9.1. Chemicals

All chemicals and reagents were acquired from commercial suppliers, predominantly Sigma-Aldrich, and were thus employed as-is without any additional purification. Anhydrous solvents were obtained from the department's Grubbs system.

9.2. NMR Spectroscopy (Nuclear magnetic resonance spectroscopy)

Unless otherwise stated, all NMR spectra were acquired on a Bruker AV3HD-400. The ^1H spectra was acquired at 400 MHz and the ^{13}C at 100 MHz. The NMR FT data was then analysed using Topspin 3.0 NMR software.

9.3. Mass Spectrometry (MS)

Mass spectra were acquired by means of Electrospray Ionisation Mass Spectrometry (ES-MS) using an Agilent 6530 Q-ToF mass spectrometer and by Matrix Assisted Laser Desorption Ionisation Time of Flight (MALDI-TOF) mass spectrometry using either dithranol or dihydroxy benzoic acid matrices on a Bruker III mass spectrometer.

9.4. Ultraviolet-visible spectroscopy (UV-VIS)

The UV/Vis absorption data was measured using an Analytic Jena AG Specord S-600 spectrophotometer, with UV/Vis analysis conducted in Win ASPECT software.

9.5. Gel permeation column (GPC)

A Millipore Waters Lambda-Max 481 LC spectrometer equipped with an LMW/HMW column was utilised to obtain aqueous GPC data. Non-ionised water was employed as the eluent for analysis, while the GPC system was calibrated using polyethylene glycol (PEG) standards for molecular weights ranging from 2,000 to 5,000 Da. The raw data obtained from the GPC analysis was then processed and analysed using dedicated online GPC software.

9.6. Dynamic light scattering (DLS)

The sizes of the resulting polymer particles were analysed using dynamic light scattering (DLS) with a Zetasizer Nano ZS instrument (ZEN 3600) at a temperature of 25 °C. The DLS readings were all taken in triplicate for each measurement.

9.7. pH analysis

The pH of the buffer solution was determined using the UEN pH Meter 3030. Standard buffer solutions of pH 4.0 and pH 10.0 were first used to calibrate the system.

9.8. Fourier Transform Infrared Spectroscopy (FTIR)

The FT-IR samples were analysed using a Perkin-Elmer Paragon 1000 FT-IR spectrophotometer equipped with an integrated Dura Sample IR-II.

9.9. Synthesis of PAMAM dendrimers

9.9.1. General synthesis of half generation PAMAM dendrimers

Methyl acrylate was gradually added dropwise to a solution of amine-terminated PAMAM dendrimer (or EDA) dissolved in MeOH within a round bottomed flask over a period of 30 minutes. The mixture was then held at room temperature for a period sufficient to allow full reaction. The by-products and unreacted reagents were removed using a rotary evaporator at a maximum temperature of 40 °C (to prevent retro-Michael addition). The product was then placed within high vacuum to ensure removal of all by-products.

9.9.2. General synthesis of full generation PAMAM dendrimers

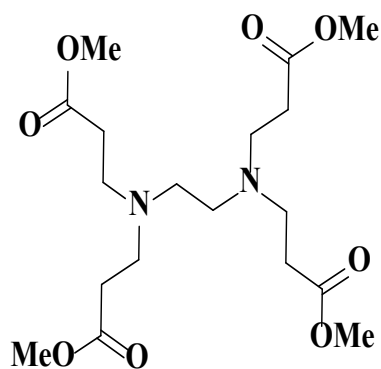
The ester terminated PAMAM dendrimer was dissolved in methanol before ethylenediamine (EDA) was slowly added drop by drop over a 30-minute period. The mixture was then stirred

at room temperature for several days before the solvent and excess reagents were removed using rotary evaporation at 45 °C.

To purify the product, a 9:1 azeotropic mixture of toluene and methanol was added to remove any remaining EDA, a purification step that was repeated multiple times to ensure complete removal of EDA.

9.9.3. Synthesis of G0.5 PAMAM dendrimer (4 OMe terminal groups)

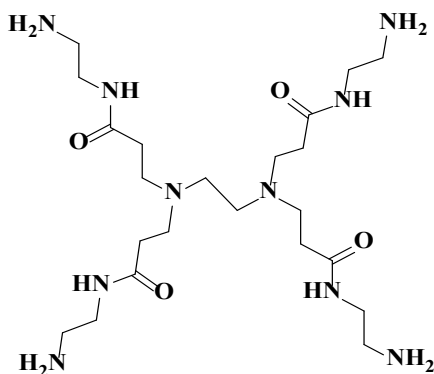
The general method for preparing half generation dendrimers was followed using the following amounts of reactants and solvents: 3.1 grams (0.049 moles) of ethylene diamine (EDA) in 50 mL of MeOH and 25.74 grams (0.294 moles) of methyl acrylate in 30 mL of MeOH. The reaction mixture was stirred overnight at room temperature, offering a yellowish honey-coloured oil with a yield of 24 grams (87% yield).



$^1\text{H NMR}$ (MeOD, 400 MHz): δ 3.67 (s, 12H), 2.75 (t, 8H), 2.53 (s, 4H), 2.47 (t, 8H) $^{13}\text{C NMR}$ (MeOD, 400 MHz) δ 172.8, 50.9, 50.3, 49.2, 47.3, 31.6. FTIR (cm^{-1}), 3285 (amide, NH), 2943 (OCH₃, stretch), 1728 (C=O, ester), 1463 (CH₂, bend), ES-MS, 405 (MH⁺) C₁₈H₃₂N₂O₈ = 404.22.

9.9.4. Synthesis of G1.0 PAMAM dendrimer (4 amine terminal groups)

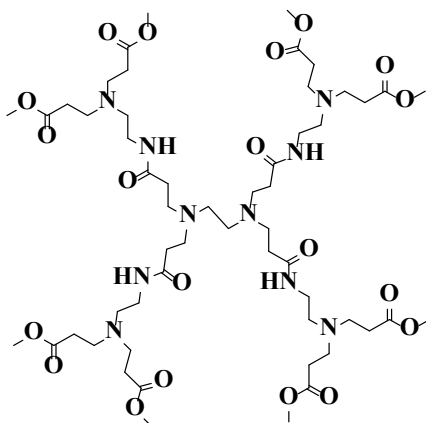
The general method for preparing half generation dendrimers was followed using the following quantities of reactants and solvents: PAMAM dendrimer G0.5 (14.82g, 0.036mol) in 40 mL of MeOH, EDA (43.27g, 0.72 mol) in 50 mL of MeOH The reaction mixture was then stirred at room temperature for 5 days. After purification, the product obtained was a honey-coloured oil (52g, 90% yield).



¹H NMR (MeOD, 400 MHz): δ 3.68 (s, 8H), 3.32-3.26 (m, 16H), 2.80-2.43 (m, 20H) ¹³C NMR (MeOD, 400 MHz) δ 173.2, 49.8, 50.3, 49.4, 47.5 32.9 FTIR (cm⁻¹), 3282 (amide, NH), 2943 (OCH₃, stretch), 1726(C=O, ester), 1461 (CH₂, bend). ES-MS, 516 (MH⁺), Molecular Weight 516.69. Elemental Analysis: C, 51.14; H, 9.36; N, 27.11; O, 12.39 – Chemical Formula: C₂₂H₄₈N₁₀O₄ = 517

9.9.5. Synthesis of G1.5 PAMAM dendrimer

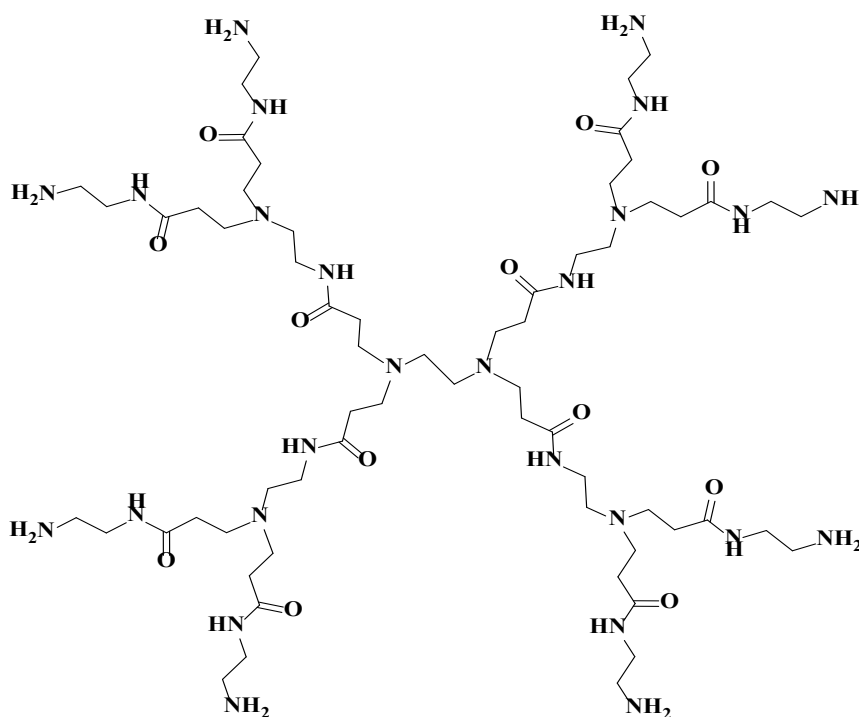
The PAMAM dendrimer featuring four amine terminal groups (G1), which weighed 19.16 g (0.038 mol), was dissolved in 100 mL of methanol inside a 500 mL round bottomed flask. A total of 63.70 g of methyl acrylate (0.74 mol) was then gradually added to the reaction solution, and the mixture was stirred constantly at room temperature for 3 days. Once the reaction was complete, the solvent was concentrated at reduced pressure at 45 °C, and the resulting product was dried to obtain a sticky yellow oil, giving a yield of 55 grams (88% yield).



^1H NMR (MeOD, 400 MHz): δ 3.67 (s, 24H), 3.36 to 3.21 (m, 24H), 2.85 to 2.34 (m, 44H)
 ^{13}C NMR (MeOD, 400 MHz) δ 172.6, 172.1, 51.6, 50.2, 48.7, 48.11, 37.0, 33.3, and 32.1 FTIR (cm^{-1}), 3309 (N-H, stretch), 2951 (C-H, stretch), 2875, 1733, and 1651, (C=O, ester stretch), 1537 (N-H, bend), and 1434 (CH₂, bend).

9.9.6. Synthesis of PAMAM G2.0 PAMAM dendrimer

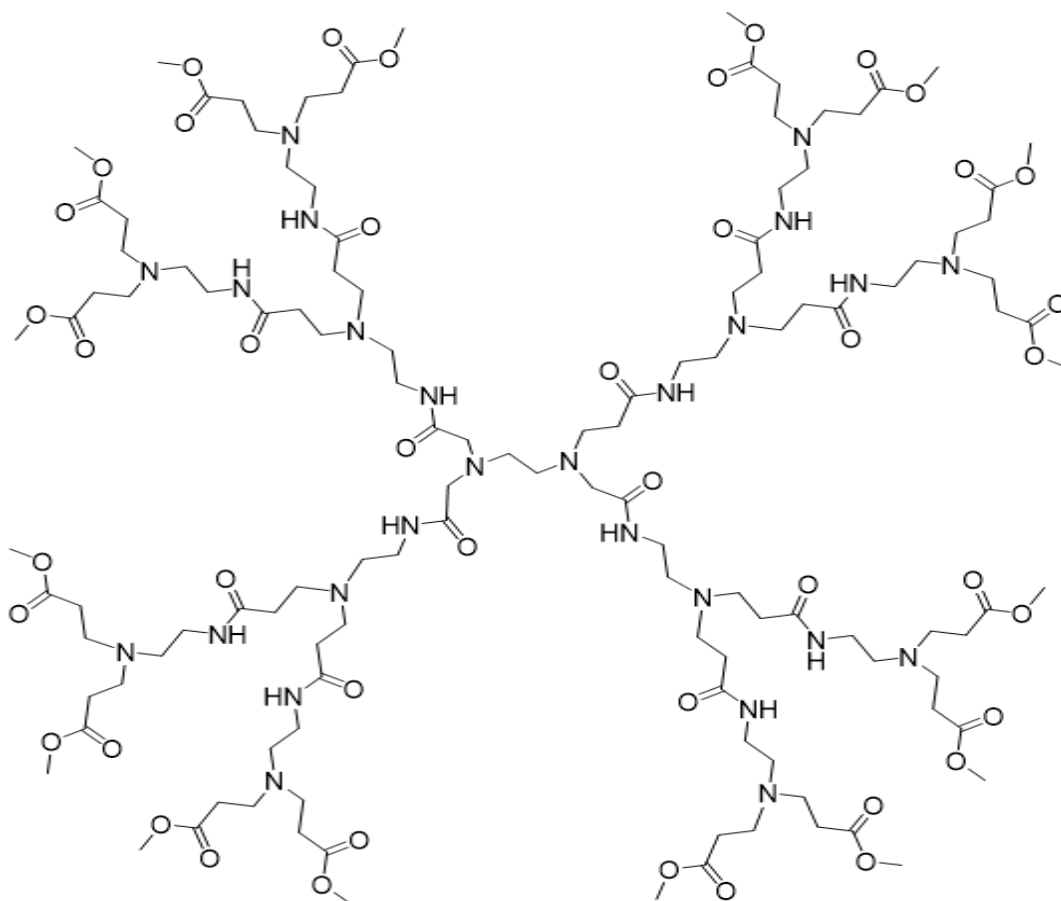
A PAMAM dendrimer with ester-terminated groups (G1.5, 5.5 g, 0.0045 moles) was dissolved in 100 mL of methanol before 9.19 g (0.153 moles) of ethylenediamine (EDA) was gradually added dropwise to the reaction solution over 45 minutes. The reaction mixture was then stirred at room temperature for 5 days. After the reaction was fully complete, a 9:1 mixture of methanol and toluene was used as an azeotropic solution to wash the product and remove any remaining unreacted EDA. This purification process was repeated until all traces of EDA were completely eliminated. The final product, PAMAM dendrimer G2.0, was a honey/brown-coloured thick oil at a weight of 13 g (89% yield).



¹H NMR (MeOD, 400 MHz): δ 4.89 (s, 4H), 3.64 (s, 8H), 3 to 3.39 (m, 24H), 2.25 to 2.87 (m, 76H) ¹³C NMR (MeOD, 400 MHz) δ 173.2, 50.7, 48.3, 46.1, 41.2, 35.9, 32.0, and 31.7 ppm
FTIR (cm⁻¹), 3276 (NH, stretch), 2938 (CH, stretch), 1646(C=O, amide). 1556(NH. bend),
Molecular Weight calculated 1428. (ESI-MS) =1428

9.9.7. Synthesis of PAMAM G 2.5 PAMAM dendrimer

A solution of the mine-terminated product was prepared as discussed in the previous synthesis section (11.5 g, 0.008 mol), and this was dissolved in 150 mL of methanol. To this solution, dropwise addition of methyl acrylate (48.241 g, 0.56 mol) took place under conditions of continuous stirring, with the latter continued at room temperature for three days. Afterward, the solvent (methanol) and excess methyl acrylate were removed by means of a rotary evaporator. The resulting product was then subjected to drying under ultra-high vacuum conditions for 5 hours, yielding a sticky, honey-coloured oil (50 g, 85% yield).

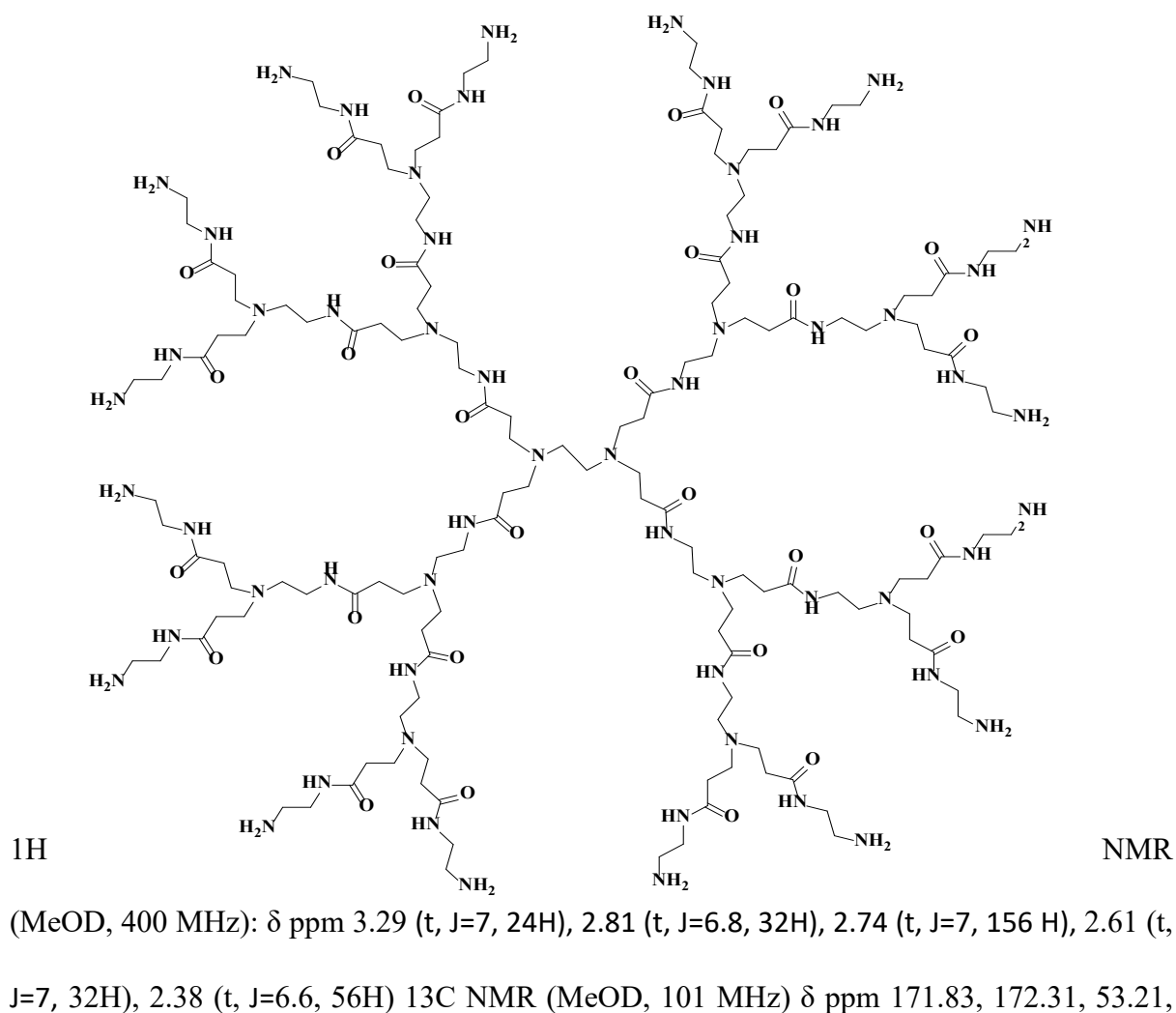


^1H NMR (MeOD, 400 MHz): δ ppm 3.69 (S, 48H), 3.35 to 3.21 (m, 12H), 2.89 to 2.29 (m, 152H). ^{13}C NMR (MeOD, 400 MHz) δ ppm 173.2, 173.3, 52.4, 51.2, 49.1, 48.7, 37.8, 34.1,

32.1. FTIR (cm^{-1}), 3297 (amide N-H, stretch), 2952 (CH, stretch), 2837, 1737 (ester C=O, stretch), 1645 (amide C=O, stretch), 1550 (amide NH, bend), and 1436 (CH_2 , bend). Mass Spectrometry (MALDI-TOF) $m/z = 2805$.

9.9.8. Synthesis of G3.0 PAMAM dendrimer

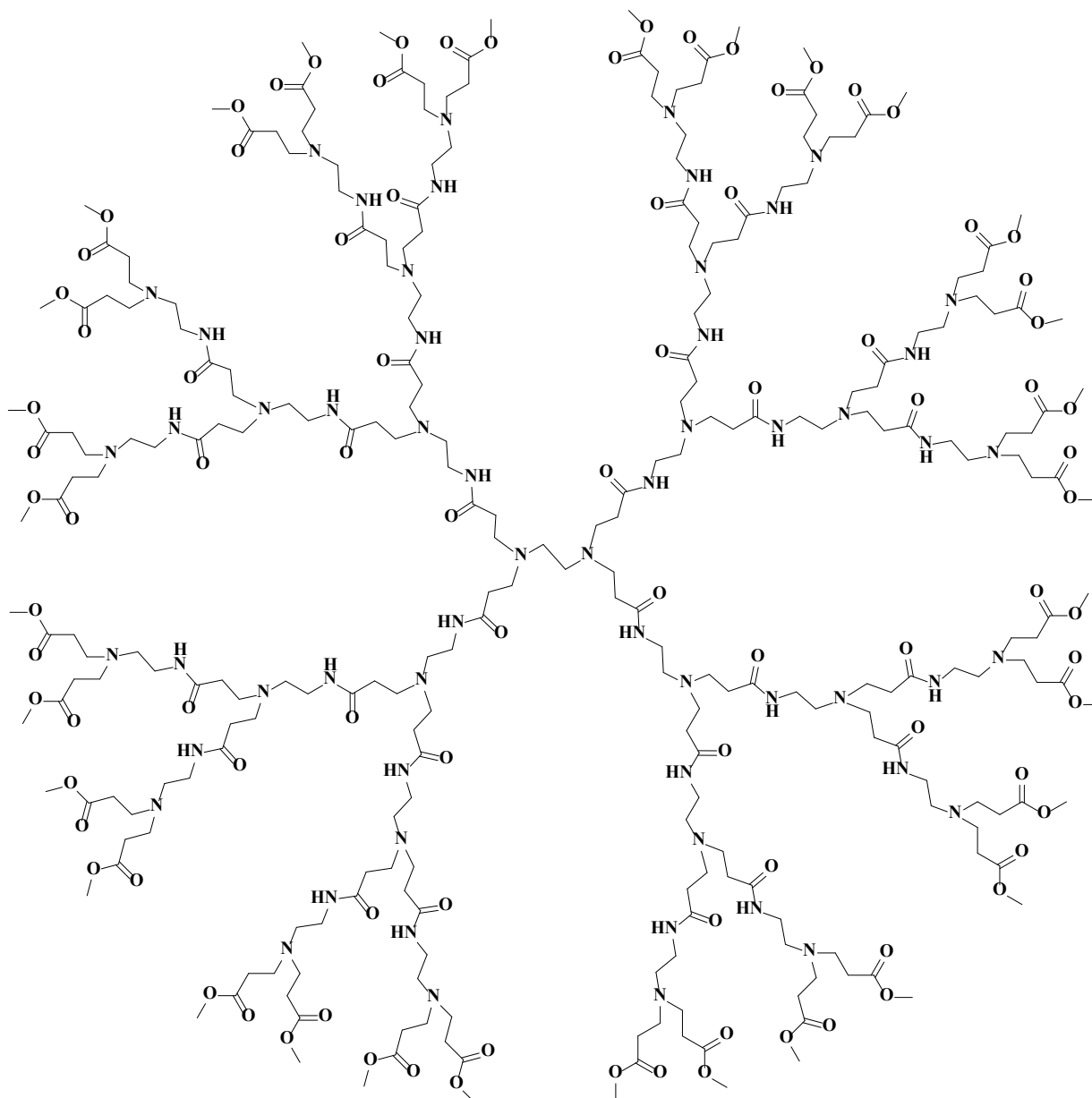
A PAMAM G2.5 product (27 g, 0.0096 mol) was mixed in 100 mL of methanol and then stirred. EDA (38.04 g, 0.633 mol) was added dropwise over a 30 minute period. The mixture was then left to react at room temperature for 5 days. To remove EDA from the crude product, an azeotropic solution of 2.0 L mixture of 9:1 toluene: methanol was also used. This purification process was repeated, with EDA completely eliminated by washing with 100 mL of methanol. The resulting product was then dried, producing a yellow oil with a yield of 43 g (95% yield).



48.69, 46.52, 40.69, 39.89, 37.12, 32.51 FTIR (cm^{-1}), 3289 (NH amide, stretch), 3090 (C-H, stretch), 1636 (C=O) 1569 (N-H amide, bend), 1484 (CH_2 , bend). (MALDI-TOF) $m/z = 3257$

9.9.9. Synthesis of G 3.5 PAMAM dendrimer

A third generation PAMAM G3.0 (32 g, 9.8 mmol) was dissolved in methanol (120 mL) and agitated. Methyl acrylate (127 g, 1.4 mol) was then added slowly over 45 minutes, and the mixture was allowed to react for 5 days. To remove excess methyl acrylate and solvent, the mixture was then subjected to reduced pressure at 4 °C, generating a G3.5 product that resembled a sticky yellow/brown substance to a weight of 90 g (85% yield).



Molecular Weight: 6011.12

$^1\text{H NMR}$ (MeOD, 400 MHz): δ ppm 3.69 (m, 96H), 3.39-3.27 (m, 56H), and 2.9-2.36 (m, 300H)

$^{13}\text{C NMR}$ (MeOD, 101 MHz) δ ppm 174.5, 173.5, 52.7, 52, 51.3, 49.7, 49.0, 37.3, 37.2, 33.4,

and 32.1. FTIR (cm^{-1}), 3298 (N-H amide, stretch), 2953 (C-H, stretch), 2833, 2105, 1734 (C=O,

ester), 1643 (C=O, amide), 1549 (N-H, amide bend), 1439 (CH₂, bend), TOF MS LD+ 6012

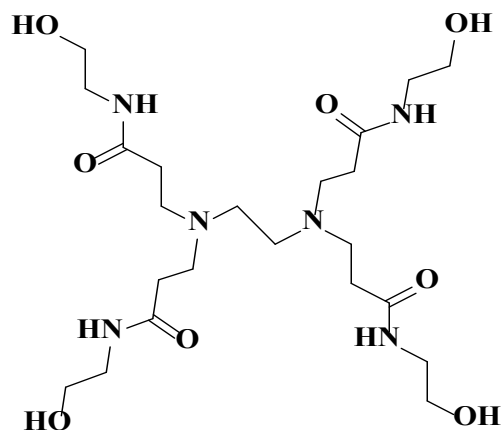
9.10. Synthesis of neutral PAMAM dendrimers

9.10.1. General procedure

As an example, procedure, a half-generation dendrimer was introduced into DMSO in a 250 mL round bottom flask. Subsequently, potassium carbonate and ethanolamine were added dropwise to the mixture. The resulting mixture was stirred and refluxed at 0 °C for 3 days prior to the crude mixture undergoing filtration under reduced pressure to eliminate any potassium carbonate residues. The filtered product was then purified by washing three times in 200 mL of acetone, which caused an oily product to settle at the bottom of the flask. The acetone layer was then carefully removed, and 5 mL of distilled water added to dissolve the product. After the product was allowed to precipitate and settle for 1 hour, the upper layer was poured off. The remaining product was then dried in a vacuum oven, resulting in the formation of PAMAM-OH dendrimer.

9.10.2. Synthesis of G0.5-OH PAMAM dendrimer

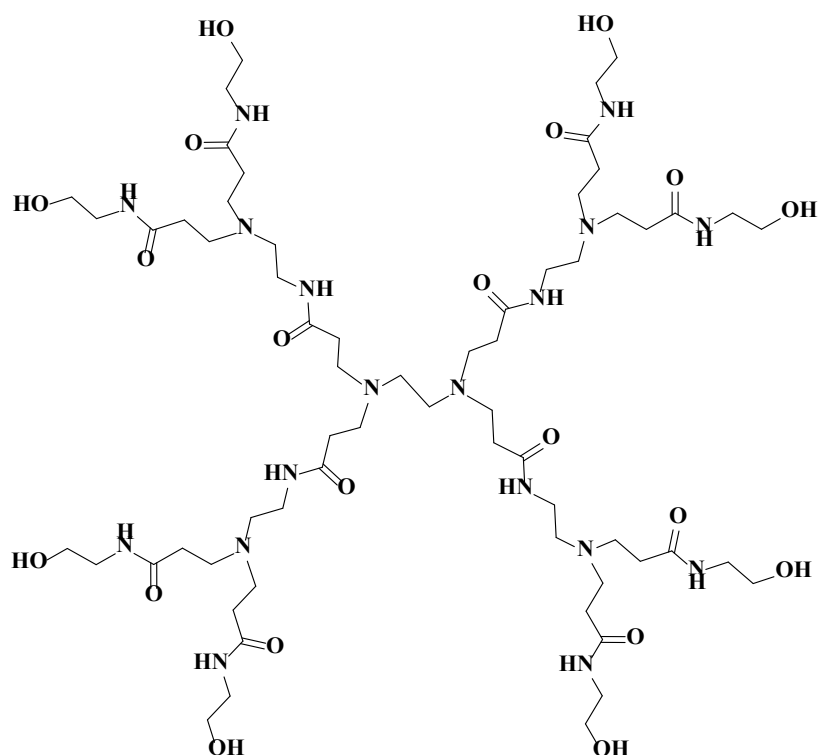
A half-generation PAMAM dendrimer (4.7 g, 0.0031 mol) was dissolved in 10 mL of DMSO, with potassium carbonate (4.25 g, 0.029 mol) and ethanolamine (1.90 g, 0.0312 mol) then added gradually to the solution. The resulting mixture was stirred and heated at 50 °C under reflux for 3 days. The standard purification process was then carried out, yielding a final product, G 0.5-OH, that appeared as a yellow oil after drying; the quantity generated in this manner was 8 g (80% yield).



^1H NMR (D_2O , 400 MHz): δ ppm 3.57 (t, $J=7$, 8H), 3.24(m, 8H), 2.74(m,8H), 2.54(t, $J=6.5$, 4H), 2.37(t, $J=7$, 8H) ^{13}C NMR (D_2O , 400 MHz) δ ppm 175, 173.5, 60,33. FTIR (cm^{-1}), 3295 (N-H stretch), 1653 (C=O), 1560 (N-H), 1445. ES-MS 521

9.10.3. Synthesis of G1.5-OH PAMAM dendrimer

G 1.5 PAMAM dendrimer (4.8 g, 0.0039 mol) was dissolved in 7mL of DMSO. Ethanolamine (1.9g, 0.0312 mol) and potassium carbonate (4.31g, 0.0312mol) were then added gradually subject to continuous stirring. The reaction mixture was then refluxed at 50 °C for 3 days, and the resulting the crude product was subject to purification using the method described earlier in this chapter. Finally, the product was dried under vacuum overnight to give 8 g of G 1.5-OH, a yield of 75%.



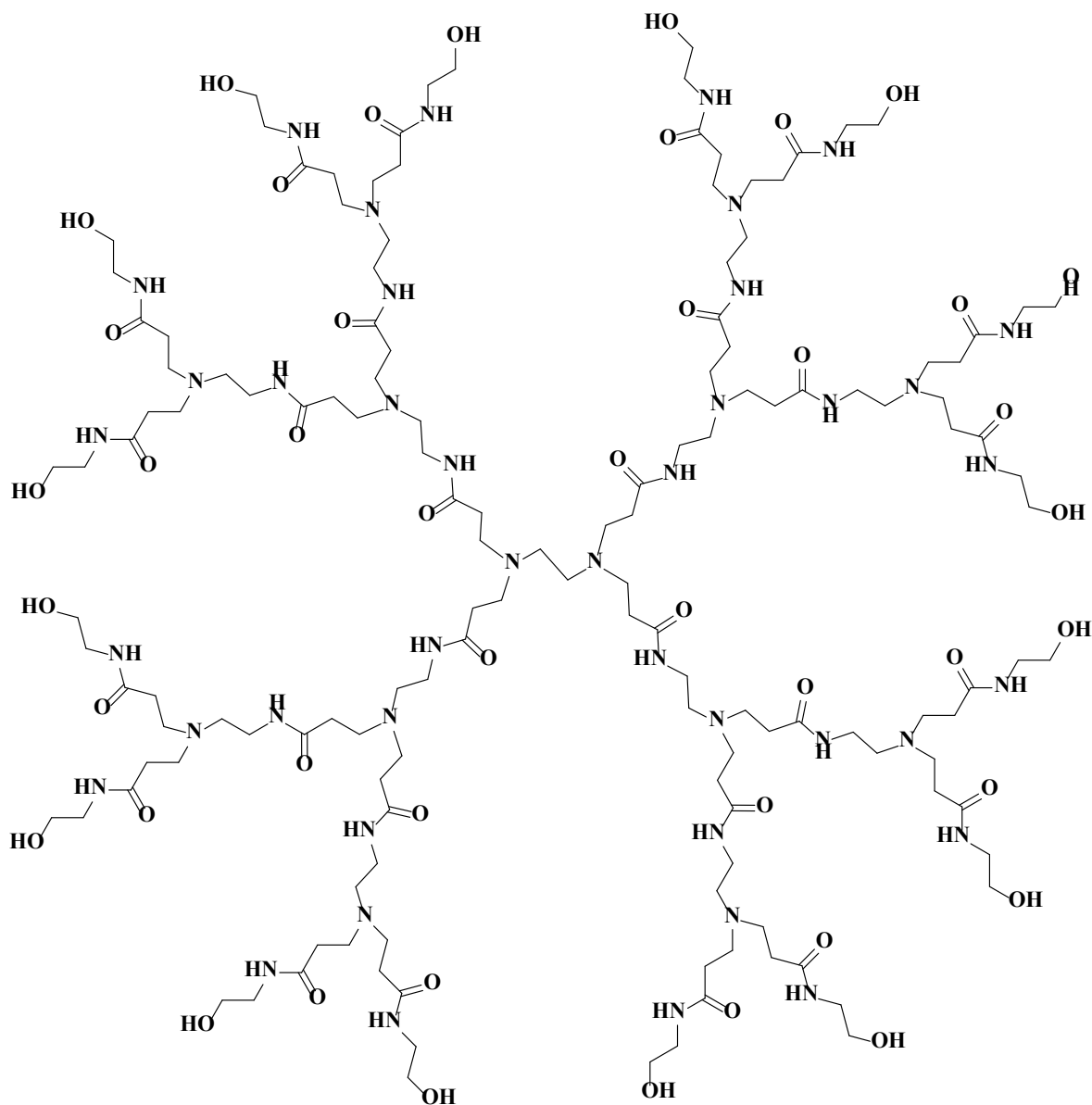
^1H NMR (D_2O , 400 MHz): δ ppm 3.50 (t, $J=6.5$, 16H), 3.17 (m, 24H), 2.68 (m, 24H), 2.49(t, $J=7$, 12H), 2.31 (t, 24H). ^{13}C NMR (D_2O , 400 MHz) δ ppm 1754, 174, 61, 52.0, 50.0, 46.0, 40.5, 36.0, 32.0. FTIR (cm^{-1}), 3295 (N-H, stretch), 3134, 2958, 2847, 1583 (C=O), 1562(N-H),

ES-MS 437

9.10.4. Synthesis of G2.5-OH PAMAM dendrimer

A solution containing 5.3 grams (0.0018 mol) of PAMAM G 2.5 was prepared in 7 mL of DMSO. Ethanolamine (1.75 g, 0.028 mol) and potassium carbonate (3.98 g, 0.028 mol) were then gradually added to this solution, and the resulting mixture was stirred and refluxed at 50 °C

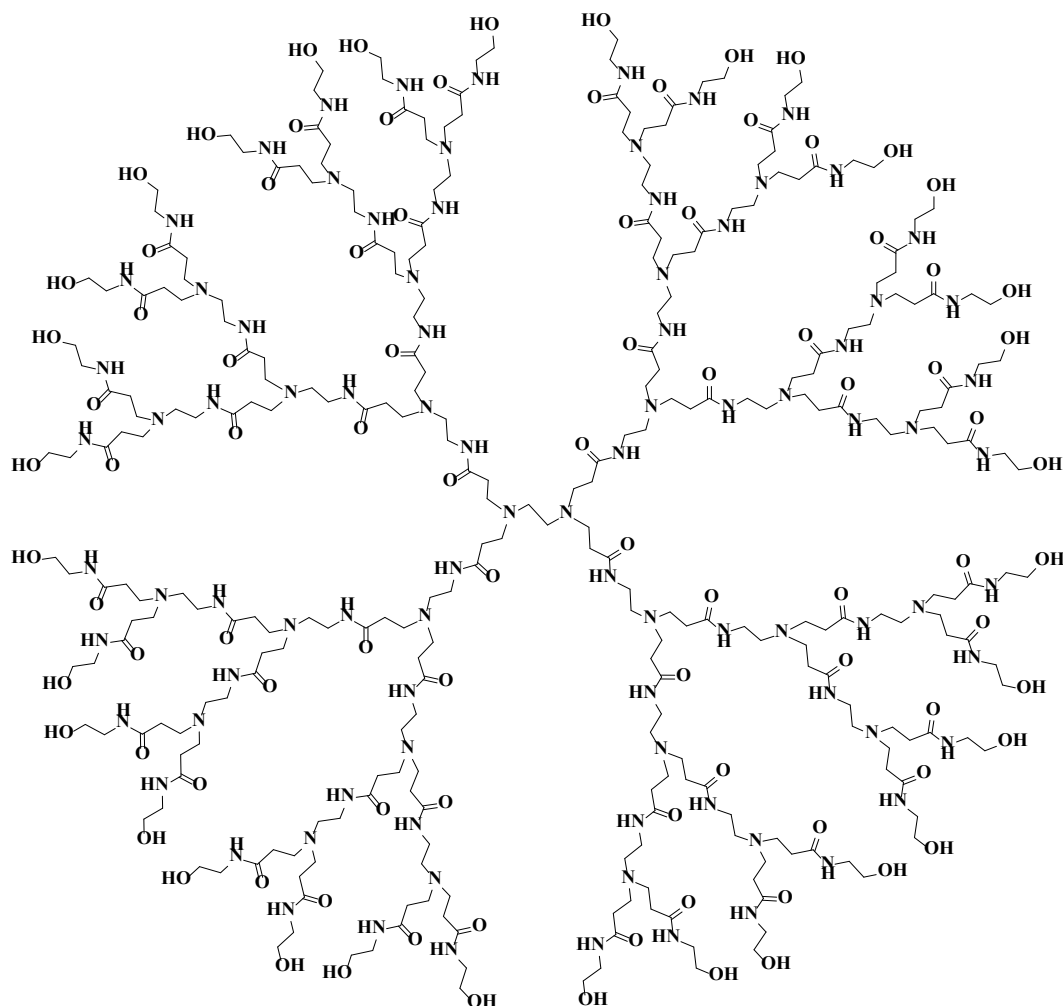
for 72 hours. Subsequently, the mixture underwent the standard purification process, yielding 5.76 g of dendrimer (80% yield).



^1H NMR (D_2O , 400 MHz): δ ppm 3.62 (t, $J=7$, 32H), 3.33 (m, 56H), 2.80 (t, $J=6.8$, 56H), 2.1 (t, $J=7$, 28H), 2.41 (t, $J=7$, 56H) ^{13}C NMR (101 MHz, D_2O) δ 176.2, 175, 52, 48, 42, 38.5, 36, 32.5. FTIR (cm^{-1}), 3420 (N-H, stretch), 2947 (C-H, stretch), 3924, 1640 (C=O), 1549 (N-H, amide bend), 1443 (CH_2 , bend), TOF MS LD+ 3272

9.10.5. Synthesis of G3.5-OH PAMAM dendrimer

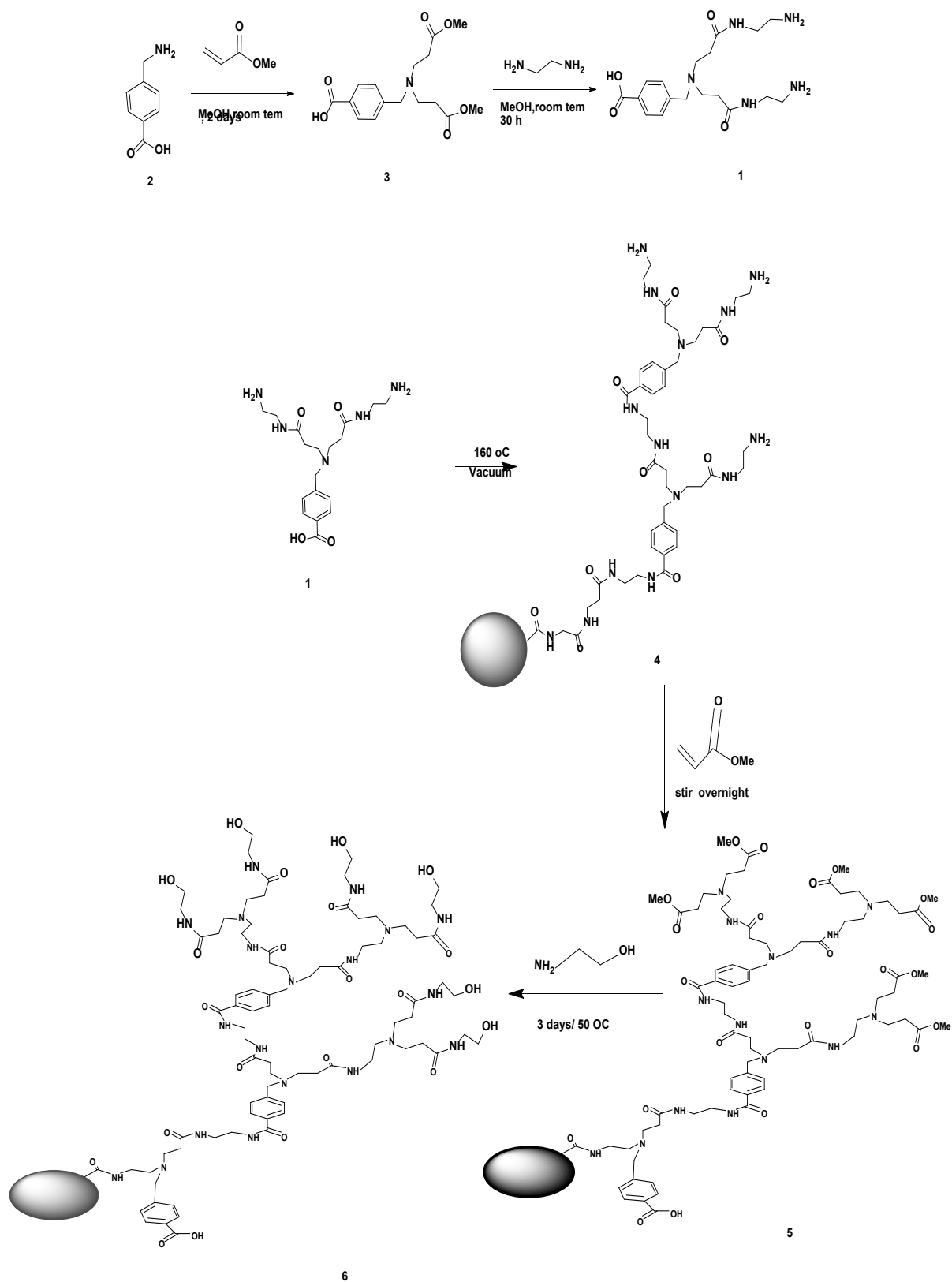
A quantity of 7 mL of DMSO was used to dissolve 2.3 g (0.00038 mol) of G3.5 PAMAM dendrimer in a round bottomed flask. Subsequently, 0.74 g (0.0122 mol) of ethanolamine and 1.68 g (0.0122 mol) of potassium carbonate were introduced into the dendrimer solution. The resulting mixture was then stirred and refluxed at 50 °C for 3 days before the product was purified and dried using a standard procedure to form G3.5-OH. This process offered a yield of 4 g (98%).



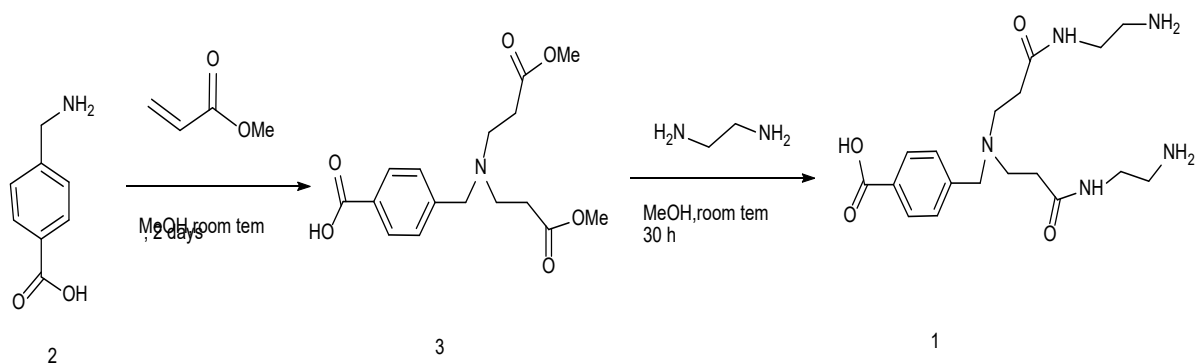
^1H NMR (D_2O , 400 MHz): δ ppm 3.52 (m, 64H), 3.21 (m, 120H), 2.71 (m, 120H), 2.52 (m, 60H), 2.33 (m, 120H) ^{13}C NMR (101 MHz, D_2O) δ 175.5, 174, 58.68, 60, 52.5, 49.5, 47, 41,

37, 33 FTIR (cm^{-1}), 3264 (N-H , stretch), 3071, 2917, 2824, 1639 (C=O, stretch), 1548 (N-H, amide bend), 1437 (CH₂, bend), TOF MS LD+ 6940

9.11. Synthesis of aromatic hyperbranched polymers



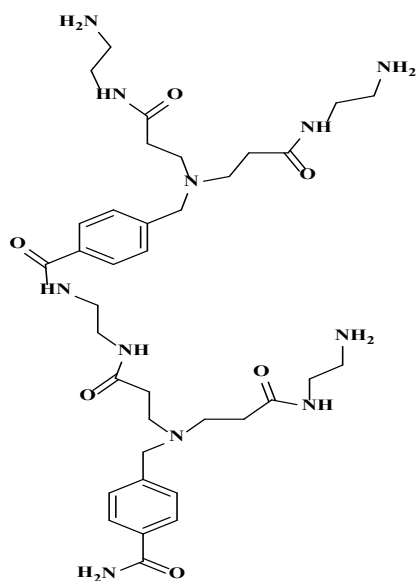
9.11.1. Synthesis AR-HBP (intermediate 3 and monomer 1)



A total of 5 g of MA, equivalent to 0.058 mol, was added to a solution containing 3 g of 4-aminomethyl benzoic acid (0.019 mol) and 3.94 grams of triethylamine (0.039 mol) dissolved in 60 mL of methanol. The resulting mixture was stirred for 5 days before the solution underwent filtration. The filtrate was then subjected to concentration using a rotary evaporator, resulting in the formation of intermediate 3, which demonstrated ester terminations.

Intermediate 3, which weighed 6.11 g, equivalent to 0.0188 mol, was introduced into an abundant quantity of EDA (22.6 g or 0.37 mol) dissolved in 55 millilitres of methanol. The mixture was then agitated for 15 days, facilitating the formation of monomer 1

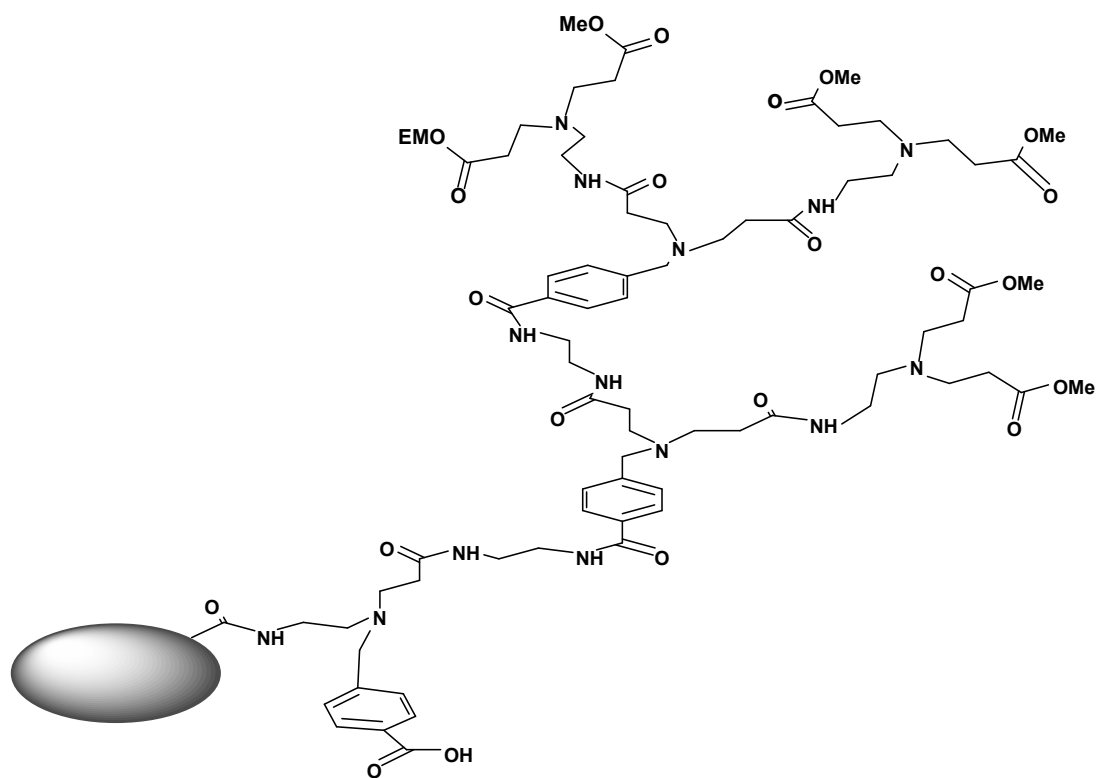
9.11.2. Synthesis of Ar-HBP (hyperbranched polymer 4)



polymer 4

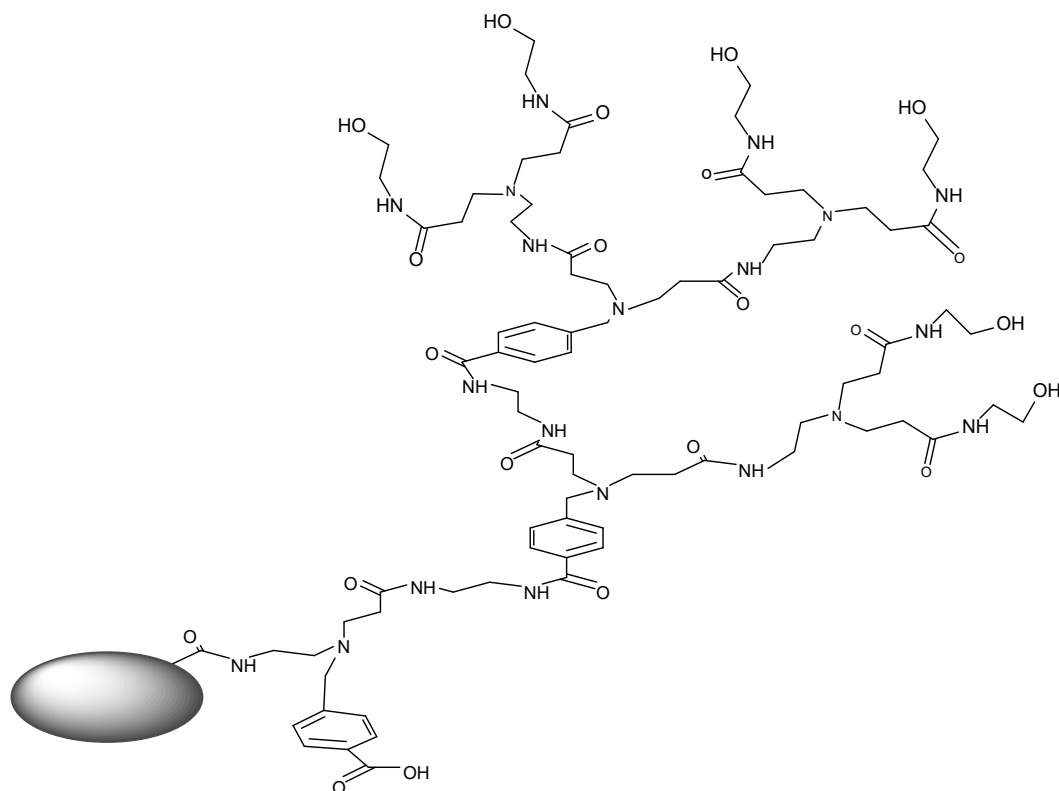
Monomer 1 was subjected to vacuum heating at 165 °C for 48 hours before being allowed to naturally cool to room temperature. The resulting crude product offered a quantitative yield with a dark, honey coloured, glass-like appearance.

9.11.3. Synthesis of an intermediate ester-terminated hyper branched polymer.



A total of 0.5 grams of HBP compound was dissolved in 15 mL of methanol, to which 5 grams of MA (0.058 mol) was introduced. This mixture was then stirred overnight before reaction undergoing purification by being washed six times with 50 mL of methanol. Any remaining solvent was then removed using rotary evaporation, resulting in a sticky brown solid.

9.11.4. Synthesis of a hydroxyl ester-terminated hyper branched polymer.



6

An ester-terminated hyperbranched polymer (1 gram) was dissolved in 5 mL of DMSO, with 1.32 grams (0.0217 moles) of ethanolamine and 3 grams (0.0217 moles) of potassium carbonate then introduced to the solution. The reaction was then kept at reflux temperature (50 °C) for a period of 5 days, after which purification via acetone washing resulted in the formation of a sticky brown solid.

9.12. Solubility and the Beer-Lambert law experiment for Ibuprofen

The solubility of Ibuprofen was assessed by introducing an excess amount of Ibuprofen into a 100 mL conical flask containing 60 mL of phosphate buffer solution at a pH of 7.4. The flask was covered and agitated at a temperature of 25 °C for 30 minutes. The resulting sample was then purified by passing through a 0.45 µm syringe filter. After appropriate dilution, the concentration of Ibuprofen was gauged using UV spectrophotometry. To create a stock solution, 206 mg of Ibuprofen was then dissolved in methanol within a 100 mL volumetric flask: the concentration of this stock solution was determined to be 1×10^{-3} mol/mL. Various standard solutions were subsequently prepared using different known concentrations (0.1, 0.3, 0.4, 0.7, and 1 mM) derived from the stock solution, and the absorbance of Ibuprofen was measured using UV/Vis spectroscopy, with differences in absorption values (Δ absorbance) determined across wavelengths ranging from 273 to 278 nm.

9.13. Phosphate buffer preparation

Sodium phosphate dibasic (1.99 g) and sodium phosphate monobasic (0.29 g) were effectively dissolved in 1.0 L of distilled water. The pH was then carefully set to 7.43 using either HCl or NaOH as appropriate in each case, resulting in the creation of a buffer solution with a concentration of 0.01 M.

9.14. Encapsulation procedures

Preparations of PAMAM dendrimers featuring hydroxyl end groups (G1.5, G2.5, and G3.5) with excess quantities of Ibuprofen were developed using methanol as a solvent. Subsequently, these solutions underwent a 10-minute shaking process before the solvent was eliminated by utilising a rotary evaporator. The resulting dendrimer/ Ibuprofen complexes were then

reconstituted in a 20 mL solution of pH 7.4 phosphate buffer and subsequently filtrated to eliminate any unbound Ibuprofen. Finally, all samples were subjected to analysis using UV-vis spectroscopy.

9.15. Preparation of different generations of hydroxyl terminated PAMAM dendrimers with concentrations of (1×10^{-4} M).

To create a concentrated solution of G1.5-OH at a concentration of 1×10^{-4} M, 13 mg of G1.5-OH was dissolved in 100 mL of methanol. In contrast, the G2.5-OH solution was formulated by dissolving 31 mg of the compound in methanol in a 100 mL volumetric flask, while the G3.5-OH solution was prepared by diluting 69 mg in 100 mL of methanol.

9.16. Preparation of G2.5-OH PAMAM dendrimers with different concentrations (1×10^{-6} , 1×10^{-5} , 1×10^{-4} and 1×10^{-3} M).

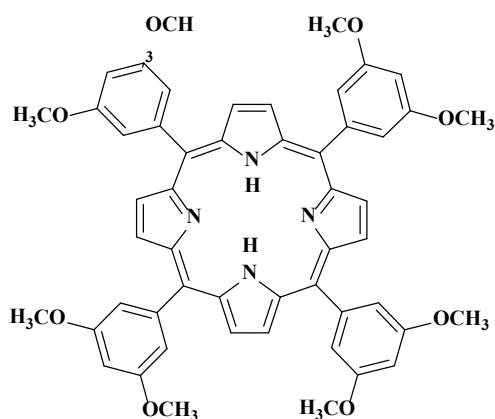
G2.5-OH solutions of varying concentrations were created by dissolving 0.00031 mg, 0.0031 mg, 0.031 mg, and 0.31 mg of the compound in appropriate 100 mL volumetric flasks. This process yielded solutions with concentrations of 1×10^{-6} M, 1×10^{-5} M, 1×10^{-4} M, and 1×10^{-3} M, respectively.

9.17. Preparation of G2.5-OH PAMAM dendrimers with different concentrations (1×10^{-4} , 2.5×10^{-4} , 5×10^{-4} , 7.5×10^{-4} , and 9×10^{-4} M).

Samples of 30 mg, 80 mg, 158 mg, and 238 mg of G3-OH PAMAM dendrimer were individually mixed with methanol in 100 mL volumetric flasks to yield the desired concentrations.

9.18. Synthesis of 5,10,15,20-tetrakis(3, 5-dimethoxyphenyl) porphyrin (TMPP)

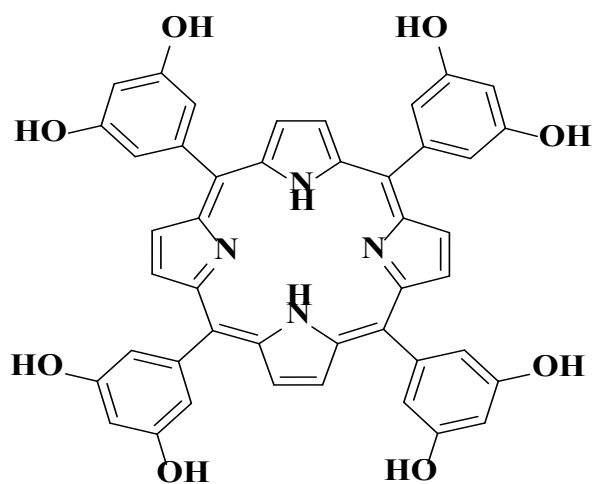
A solution was prepared by combining 6.23 mL (0.09 mol) of freshly distilled pyrrole and 15 g (0.09 mol) of 3,5-dimethoxybenzaldehyde in a round-bottom flask containing 320 mL of propionic acid. This mixture was subjected to reflux at 150 °C for 30 minutes. After the reflux period was complete, the mixture was allowed to cool to room temperature, before being left in this state for 2 hours. The resulting mixture was filtered and subsequently washed thoroughly using propionic acid and methanol. The product obtained from this process was then dried overnight using a vacuum oven, resulting in the formation of purple crystals; the yield was 9 g (60%).



$^1\text{H NMR}$ (400 MHz, CDCl_3): δ 8.89(s, 8H), 7.41(s, 8H), 6.94(s, 4H), 3.96(s, 24H), -2.99 (s, 2H); $^{13}\text{C NMR}$ (400 MHz, CDCl_3): δ 1589, 143, 118.9, 112.9, 102, 25.9; IR: $\nu_{\text{max}}/\text{cm}^{-1}$) 1150 (OMe); UV absorbance (nm)= 420; MH^+ (ESI-MS) = 854.5 (855 gmol^{-1} calculated).

9.19. Synthesis of 5,10,15,20-tetrakis(3, 5-dihydroxy phenyl) porphyrin (THPP)

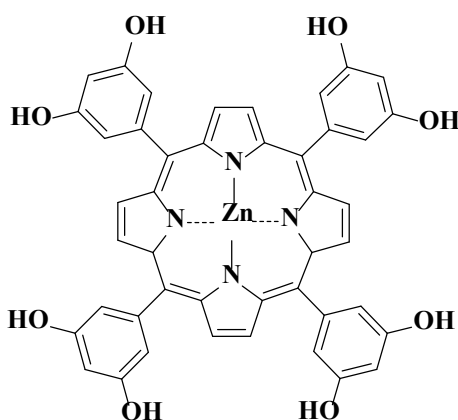
A round-bottom flask with a capacity of 250 mL, equipped with two necks, was filled with 0.5 g (0.00058 mol) of 5,10,15,20-tetrakis(3,5-dimethoxyphenyl) porphyrin and 10 mL of dry dichloromethane. A dropping funnel was then attached to the flask and the entire setup was purged with nitrogen gas. After precise adjustment to the dropping funnel, a solution containing 2 mL of Boron tribromide was slowly introduced to the reaction mixture, which was then gently stirred under a nitrogen atmosphere at room temperature for a 5 hours. Subsequently, the reaction was gradually neutralised by the addition of 5 mL of distilled water before being stirred for an additional 15 minutes.



Yield 1.3 g , 97%; ^1H NMR (400 MHz, CDCl_3) δ 8.90 (d, $J=2.5$, 8H), 7.49 (d, $J=2.5$, 8H), 6.89 (t, $J=2.5$, 4H), 4.89 (s, 8H), -2.87 (s, 2H); ^{13}C NMR (400 MHz, CD_3OD) δ 155, 139.8, 119, 115.5, 99.8, IR (cm^{-1}) 3429 (OH group); UV Absorbance (nm) = 417, MH^+ (ESI-MS) =743 (743 g/mol calculated).

9.20. Synthesis of Zn-THPP (zinc-porphyrin)

A quantity of 0.16g (equivalent to 0.00021mol) of THPP was dissolved in 80 mL of dichloromethane within a round-bottom flask. Separately, an amount of zinc acetate sufficient to create excess was dissolved in 5 mL of methanol. Subsequently, the zinc acetate solution was introduced into the flask containing the THPP solution, and the reaction mixture was then heated to reflux and stirred for a duration of 1 hour at 45 °C. Any remaining unreacted zinc acetate was then separated by filtration under reduced pressure, and the solvent was eliminated by means of a rotary evaporator. The resulting product was subject to purification through recrystallisation: the crystals were then subjected to drying, yielding dark purple Zn-THPP crystals.



^1H NMR (400 MHz, CDCl_3) δ 8.99(d, $J=2.8$, 8H), 7.49(d, $J=2.5$, 8H), 6.92(t, $J=2.5$, 4H), 4.88(s, 8); ^{13}C NMR (400 MHz, DMSO) δ 155.4, 143.2, 119, 112.5, 100. UV Absorbance (nm) 423, mass spec MH^+ (ESI-MS) 808 (808 g/mol calculated).

9.21. Beer-Lambert law for THPP and Zn-THPP

Dissolving 4.5 mg of THPP and 1.9 mg of Zn-THPP in 1L of methanol in a volumetric flask yielded stock solutions with concentrations of 3.2×10^{-6} M and 1.6×10^{-6} M, respectively. A UV spectrophotometer was then employed to gauge the absorbance of these compounds at their characteristic wavelengths, which are 417 nm for THPP and 423 nm for Zn-THPP, using methanol as a reference. Subsequent dilution series were then created at different concentrations to construct an appropriate Beer-Lambert graph.

9.22. THTP and Zn-THTP encapsulation in different generations of PAMAM dendrimer.

All hydroxyl terminated PAMAM dendrimers were maintained at concentrations of 1×10^{-4} M. The solutions of these complexes were created in 10 mL methanol vials, with the dendrimer solutions dissolved using equal amounts of TDHTP or ZnTDHTP in methanol. The methanol was subsequently eliminated using a rotary evaporator (rota-vap), and then a 10 mL solution of phosphate buffer with a pH of 7.4 and a concentration of 0.01 M was introduced to the complex solution before the mixture was filtered. The absorbance of the solutions was then gauged using UV/Vis spectroscopy at wavelengths of 417 nm and 423 nm.

9.23. Stability of drug-dendrimer complexes

Equal concentrations of various PAMAM dendrimer generations (G1.5OH, G2.5OH, and G3.5-OH) were maintained at 1×10^{-4} M. To assess dendrimer stability, surplus Ibuprofen was then introduced in 20 mL of pH 7.4 phosphate buffer, and samples of this mixture were stored at room temperature for up to 10 days under two conditions: darkness and exposure to light.

Subsequently, the degradation of Ibuprofen in the phosphate buffer solutions was quantified by measuring their absorbance values at 273 nm using UV spectrophotometry.

9.24. Zn-THPP 14 release from the G2.5-OH dendrimer and Ar-HBP

A Zn-THPP 14/dendrimer complex of 1×10^{-4} M in both dendrimer and porphyrin was prepared. A sample of 20 mL of the complex was placed into osmosis tubing with a molecular weight cut off of 2,000. This was then deposited in a beaker containing 200 mL of pH 7.4 phosphate buffer. Samples were removed from the dialysis bag and analysed by means of UV at $t=0$, then periodically every 24 hours for five days to measure the absorption of the porphyrin's Soret band at 430 nm.

References

- (1) Wen, H.; Jung, H.; Li, X. Drug Delivery Approaches in Addressing Clinical Pharmacology-Related Issues: Opportunities and Challenges. *AAPS J.* **2015**, *17* (6), 1327–1340. <https://doi.org/10.1208/s12248-015-9814-9>.
- (2) Tibbitt, M. W.; Dahlman, J. E.; Langer, R. Emerging Frontiers in Drug Delivery. *J. Am. Chem. Soc.* **2016**, *138* (3), 704–717. <https://doi.org/10.1021/jacs.5b09974>.
- (3) Pignatello, R.; Matricardi, P. Steering the Clinical Translation of Delivery Systems for Drugs and Health Products. *Pharmaceutics* **2020**, *12* (4). <https://doi.org/10.3390/pharmaceutics12040350>.
- (4) Bock, J.; Burgos-Mira, R. Navigating to the Future: Understanding Common Tasks in a Multi-Campus Environment in the Dramatically Changing Acquisition World. *J. Electron. Resour. Librariansh.* **2010**, *22* (3), 113–123. <https://doi.org/10.1080/1941126X.2010.535737>.
- (5) Kaddurah-Daouk, R.; Kristal, B. S.; Weinshilboum, R. M. Metabolomics: A Global Biochemical Approach to Drug Response and Disease. *Annu. Rev. Pharmacol. Toxicol.* **2008**, *48*, 653–683. <https://doi.org/10.1146/annurev.pharmtox.48.113006.094715>.
- (6) Yiyun, C.; Tongwen, X. Dendrimers as Potential Drug Carriers. Part I. Solubilization of Non-Steroidal Anti-Inflammatory Drugs in the Presence of Polyamidoamine Dendrimers. *Eur. J. Med. Chem.* **2005**, *40* (11), 1188–1192. <https://doi.org/10.1016/j.ejmech.2005.06.010>.
- (7) Yun, Y. H.; Lee, B. K.; Park, K. Controlled Drug Delivery: Historical Perspective for the next Generation. *J. Control. Release* **2015**, *219*, 2–7. <https://doi.org/10.1016/j.jconrel.2015.10.005>.
- (8) Kolhe, P.; Misra, E.; Kannan, R. M.; Kannan, S.; Lieh-Lai, M. Drug Complexation, in

- Vitro Release and Cellular Entry of Dendrimers and Hyperbranched Polymers. *Int. J. Pharm.* **2003**, *259* (1–2), 143–160. [https://doi.org/10.1016/S0378-5173\(03\)00225-4](https://doi.org/10.1016/S0378-5173(03)00225-4).
- (9) Lee, S.; Eom, Y.; Park, J.; Lee, J.; Kim, S. Y. Micro-Hydrogel Particles Consisting of Hyperbranched Polyamidoamine for the Removal of Heavy Metal Ions from Water. *Sci. Rep.* **2017**, *7* (1), 1–9. <https://doi.org/10.1038/s41598-017-10066-x>.
- (10) Zhou, Z.; D’Emanuele, A.; Attwood, D. Solubility Enhancement of Paclitaxel Using a Linear-Dendritic Block Copolymer. *Int. J. Pharm.* **2013**, *452* (1–2), 173–179. <https://doi.org/10.1016/j.ijpharm.2013.04.075>.
- (11) Wang, A. Z.; Langer, R.; Farokhzad, O. C. Nanoparticle Delivery of Cancer Drugs. *Annu. Rev. Med.* **2012**, *63*, 185–198. <https://doi.org/10.1146/annurev-med-040210-162544>.
- (12) Narvekar, M.; Xue, H. Y.; Eoh, J. Y.; Wong, H. L. Nanocarrier for Poorly Water-Soluble Anticancer Drugs - Barriers of Translation and Solutions. *AAPS PharmSciTech* **2014**, *15* (4), 822–833. <https://doi.org/10.1208/s12249-014-0107-x>.
- (13) Elsaesser, A.; Howard, C. V. Toxicology of Nanoparticles. *Adv. Drug Deliv. Rev.* **2012**, *64* (2), 129–137. <https://doi.org/10.1016/j.addr.2011.09.001>.
- (14) Tian, F.; Conde, J.; Bao, C.; Chen, Y.; Curtin, J.; Cui, D. Gold Nanostars for Efficient in Vitro and in Vivo Real-Time SERS Detection and Drug Delivery via Plasmonic-Tunable Raman/FTIR Imaging. *Biomaterials* **2016**, *106*, 87–97. <https://doi.org/10.1016/j.biomaterials.2016.08.014>.
- (15) Logothetidis, S. Nanostructured Materials and Their Applications. *Nanosci. Technol.* **2012**, *59*, 1–23. <https://doi.org/10.1007/978-3-642-22227-6>.
- (16) Elsabahy, M.; Heo, G. S.; Lim, S. M.; Sun, G.; Wooley, K. L. Polymeric Nanostructures for Imaging and Therapy. *Chem. Rev.* **2015**, *115* (19), 10967–11011. <https://doi.org/10.1021/acs.chemrev.5b00135>.

- (17) Sutradhar, K. B.; Amin, M. L. Nanotechnology in Cancer Drug Delivery and Selective Targeting. *ISRN Nanotechnol.* **2014**, *2014*, 1–12. <https://doi.org/10.1155/2014/939378>.
- (18) Wanigasekara, J.; Witharana, C. Applications of Nanotechnology in Drug Delivery and Design - an Insight. *Curr. Trends Biotechnol. Pharm.* **2016**, *10* (1), 78–91.
- (19) Akhtar, N.; Khan, R. A. Liposomal Systems as Viable Drug Delivery Technology for Skin Cancer Sites with an Outlook on Lipid-Based Delivery Vehicles and Diagnostic Imaging Inputs for Skin Conditions'. *Prog. Lipid Res.* **2016**, *64*, 192–230. <https://doi.org/10.1016/j.plipres.2016.08.005>.
- (20) Vila, A.; Sánchez, A.; Tobío, M.; Calvo, P.; Alonso, M. J. Design of Biodegradable Particles for Protein Delivery. *J. Control. Release* **2002**, *78* (1–3), 15–24. [https://doi.org/10.1016/S0168-3659\(01\)00486-2](https://doi.org/10.1016/S0168-3659(01)00486-2).
- (21) Majumder, N.; Das, N. G.; Das, S. K. Polymeric Micelles for Anticancer Drug Delivery. *Ther. Deliv.* **2020**, *11* (10), 613–635. <https://doi.org/10.4155/tde-2020-0008>.
- (22) Abdel-Mottaleb, M. M. A.; Neumann, D.; Lamprecht, A. Lipid Nanocapsules for Dermal Application: A Comparative Study of Lipid-Based versus Polymer-Based Nanocarriers. *Eur. J. Pharm. Biopharm.* **2011**, *79* (1), 36–42. <https://doi.org/10.1016/j.ejpb.2011.04.009>.
- (23) Rinckenauer, A. C.; Schubert, S.; Traeger, A.; Schubert, U. S. The Influence of Polymer Architecture on in Vitro PDNA Transfection. *J. Mater. Chem. B* **2015**, *3* (38), 7477–7493. <https://doi.org/10.1039/c5tb00782h>.
- (24) Cook, A. B.; Perrier, S. Branched and Dendritic Polymer Architectures: Functional Nanomaterials for Therapeutic Delivery. *Adv. Funct. Mater.* **2020**, *30* (2), 1–24. <https://doi.org/10.1002/adfm.201901001>.
- (25) Begines, B.; Ortiz, T.; Pérez-Aranda, M.; Martínez, G.; Merinero, M.; Argüelles-Arias, F.; Alcudia, A. Polymeric Nanoparticles for Drug Delivery: Recent Developments and

- Future Prospects. *Nanomaterials* **2020**, *10* (7), 1–41.
<https://doi.org/10.3390/nano10071403>.
- (26) Landge, D. A.; Shyale, S. S.; Kadam, S. D.; Katare, V. S. Y. S.; Pawar, J. B.
Dendrimer: An Innovative Acceptable Approach in Novel Drug Delivery System.
Pharmacophore **2014**, *5* (1), 24–34.
- (27) Patri, A. K.; Majoros, I. J.; Baker, J. R. Dendritic Polymer Macromolecular Carriers
for Drug Delivery. *Curr. Opin. Chem. Biol.* **2002**, *6* (4), 466–471.
[https://doi.org/10.1016/S1367-5931\(02\)00347-2](https://doi.org/10.1016/S1367-5931(02)00347-2).
- (28) Voskuhl, J.; Kauscher, U.; Gruener, M.; Frisch, H.; Wibbeling, B.; Strassert, C. A.;
Ravoo, B. J. A Soft Supramolecular Carrier with Enhanced Singlet Oxygen
Photosensitizing Properties. *Soft Matter* **2013**, *9* (8), 2453–2457.
<https://doi.org/10.1039/c2sm27353e>.
- (29) *Dendrimer-Based Drug Delivery Systems*; Cheng, Y., Ed.; John Wiley & Sons, Inc.:
Hoboken, NJ, USA, 2012. <https://doi.org/10.1002/9781118275238>.
- (30) Tomalia, D. A.; Fréchet, J. M. J. Discovery of Dendrimers and Dendritic Polymers: A
Brief Historical Perspective*. *J. Polym. Sci. Part A Polym. Chem.* **2002**, *40* (16),
2719–2728. <https://doi.org/10.1002/pola.10301>.
- (31) Jansen, J. F. G. A.; De Brabander-Van Den Berg, E. M. M.; Meijer, E. W.
Encapsulation of Guest Molecules into a Dendritic Box. *Science (80-.)*. **1994**, *266*
(5188), 1226–1229. <https://doi.org/10.1126/science.266.5188.1226>.
- (32) Esfand, R.; Tomalia, D. A. Poly(Amidoamine) (PAMAM) Dendrimers: From
Biomimicry to Drug Delivery and Biomedical Applications. *Drug Discov. Today*
2001, *6* (8), 427–436. [https://doi.org/10.1016/S1359-6446\(01\)01757-3](https://doi.org/10.1016/S1359-6446(01)01757-3).
- (33) Dendrimer : A Novel Polymer for Drug Delivery. **2019**, *1* (2010), 2019.
- (34) Miller, T. M.; Neenan, T. X. Convergent Synthesis of Monodisperse Dendrimers

- Based upon 1,3,5-Trisubstituted Benzenes. *Chem. Mater.* **1990**, 2 (4), 346–349.
<https://doi.org/10.1021/cm00010a006>.
- (35) Tomalia, D. A.; Baker, H.; Dewald, J.; Hall, M.; Kallos, G.; Martin, S.; Roeck, J.; Ryder, J.; Smith, P. A New Class of Polymers: Starburst-Dendritic Macromolecules. *Polym. J.* **2002**, 34 (5 2), 132–147.
- (36) Boas, U.; Christensen, J. B.; Heegaard, P. M. H. Dendrimers: Design, Synthesis and Chemical Properties. *J. Mater. Chem.* **2006**, No. 207890, 3785–3798.
<https://doi.org/10.1039/b611813p>.
- (37) Jevprasesphant, R.; Penny, J.; Jalal, R.; Attwood, D.; McKeown, N. B.; D’Emanuele, A. The Influence of Surface Modification on the Cytotoxicity of PAMAM Dendrimers. *Int. J. Pharm.* **2003**, 252 (1–2), 263–266. [https://doi.org/10.1016/S0378-5173\(02\)00623-3](https://doi.org/10.1016/S0378-5173(02)00623-3).
- (38) Jain, K.; Kesharwani, P.; Gupta, U.; Jain, N. K. Dendrimer Toxicity: Let’s Meet the Challenge. *Int. J. Pharm.* **2010**, 394 (1–2), 122–142.
<https://doi.org/10.1016/j.ijpharm.2010.04.027>.
- (39) Padilla De Jesús, O. L.; Ihre, H. R.; Gagne, L.; Fréchet, J. M. J.; Szoka, F. C. Polyester Dendritic Systems for Drug Delivery Applications: In Vitro and in Vivo Evaluation. *Bioconjug. Chem.* **2002**, 13 (3), 453–461. <https://doi.org/10.1021/bc010103m>.
- (40) Dufès, C.; Uchegbu, I. F.; Schätzlein, A. G. Dendrimers in Gene Delivery. *Adv. Drug Deliv. Rev.* **2005**, 57 (15), 2177–2202. <https://doi.org/10.1016/j.addr.2005.09.017>.
- (41) Kaminskas, L. M.; Boyd, B. J.; Porter, C. J. H. Erratum: Dendrimer Pharmacokinetics: The Effect of Size, Structure and Surface Characteristics on ADME Properties (Nanomedicine (2011) 6:6 (1063-1084)). *Nanomedicine.* 2012, p 168.
<https://doi.org/10.2217/nmm.11.173>.
- (42) Cheng Y, Wang J, Rao T, et al. Laboratory of Functional Membranes, Department of

- Chemistry, University of Science and Technology of China, Hefei, Anhui 230026, China, 2 Hefei National Laboratory for Physical Sciences at Microscale and School of Life Sciences, University of Science & Te. *Front Biosci* **2008**, *13* (4), 1447–1471.
- (43) Boyd, B. J.; Kaminskas, L. M.; Karellas, P.; Krippner, G.; Lessene, R.; Porter, C. J. H. Cationic Poly-L-Lysine Dendrimers: Pharmacokinetics, Biodistribution, and Evidence for Metabolism and Bioresorption after Intravenous Administration to Rats. *Mol. Pharm.* **2006**, *3* (5), 614–627. <https://doi.org/10.1021/mp060032e>.
- (44) Wijagkanalan, W.; Kawakami, S.; Hashida, M. Designing Dendrimers for Drug Delivery and Imaging: Pharmacokinetic Considerations. *Pharm. Res.* **2011**, *28* (7), 1500–1519. <https://doi.org/10.1007/s11095-010-0339-8>.
- (45) Kaminskas, L. M.; Boyd, B. J.; Karellas, P.; Henderson, S. A.; Giannis, M. P.; Krippner, G. Y.; Porter, C. J. H. Impact of Surface Derivatization of Poly-L-Lysine Dendrimers with Anionic Arylsulfonate or Succinate Groups on Intravenous Pharmacokinetics and Disposition. *Mol. Pharm.* **2007**, *4* (6), 949–961. <https://doi.org/10.1021/mp070047s>.
- (46) Abbasi, E.; Aval, S. F.; Akbarzadeh, A.; Milani, M.; Nasrabadi, H. T.; Joo, S. W.; Hanifehpour, Y.; Nejati-Koshki, K.; Pashaei-Asl, R. Dendrimers: Synthesis, Applications, and Properties. *Nanoscale Res. Lett.* **2014**, *9* (1), 1–10. <https://doi.org/10.1186/1556-276X-9-247>.
- (47) Gupta, V.; Nayak, S. K. Dendrimers: A Review on Synthetic Approaches. *J. Appl. Pharm. Sci.* **2015**, *5* (3), 117–122. <https://doi.org/10.7324/JAPS.2015.50321>.
- (48) Gupta, U.; Perumal, O. Chapter 15 - Dendrimers and Its Biomedical Applications; Kumbar, S. G., Laurencin, C. T., Deng, M. B. T.-N. and S. B. P., Eds.; Elsevier: Oxford, 2014; pp 243–257. <https://doi.org/https://doi.org/10.1016/B978-0-12-396983-5.00016-8>.

- (49) Hawker, C. J.; Frechet, J. M. J.; Grubbs, R. B.; Dao, J. Preparation of Hyperbranched and Star Polymers by a “Living”, Self-Condensing Free Radical Polymerization. *J. Am. Chem. Soc.* **1995**, *117* (43), 10763–10764. <https://doi.org/10.1021/ja00148a027>.
- (50) Patra, J. K.; Das, G.; Fraceto, L. F.; Campos, E. V. R.; Rodriguez-Torres, M. del P.; Acosta-Torres, L. S.; Diaz-Torres, L. A.; Grillo, R.; Swamy, M. K.; Sharma, S.; Habtemariam, S.; Shin, H.-S. Nano Based Drug Delivery Systems: Recent Developments and Future Prospects. *J. Nanobiotechnology* **2018**, *16* (1), 71. <https://doi.org/10.1186/s12951-018-0392-8>.
- (51) SVENSON, S.; TOMALIA, D. Dendrimers in Biomedical Applications—Reflections on the Field. *Adv. Drug Deliv. Rev.* **2005**, *57* (15), 2106–2129. <https://doi.org/10.1016/j.addr.2005.09.018>.
- (52) Falanga, A.; Del Genio, V.; Galdiero, S. Peptides and Dendrimers: How to Combat Viral and Bacterial Infections. *Pharmaceutics* **2021**, *13* (1), 1–23. <https://doi.org/10.3390/pharmaceutics13010101>.
- (53) Lindtjørn, B. The Borana Project: A Newly Started Research Project on Nutrition. *Ann. Soc. Belg. Med. Trop. (1920)*. **1990**, *70 Suppl 1*, 42–43.
- (54) Wang, B.; Navath, R. S.; Menjoge, A. R.; Balakrishnan, B.; Bellair, R.; Dai, H.; Romero, R.; Kannan, S.; Kannan, R. M. Inhibition of Bacterial Growth and Intramniotic Infection in a Guinea Pig Model of Chorioamnionitis Using PAMAM Dendrimers. *Int. J. Pharm.* **2010**, *395* (1–2), 298–308. <https://doi.org/10.1016/j.ijpharm.2010.05.030>.
- (55) No Title.
- (56) No Title.
- (57) Thakur, S.; Tekade, R. K.; Kesharwani, P.; Jain, N. K. The Effect of Polyethylene Glycol Spacer Chain Length on the Tumor-Targeting Potential of Folate-Modified PPI

- Dendrimers. *J. Nanoparticle Res.* **2013**, *15* (5), 1625. <https://doi.org/10.1007/s11051-013-1625-2>.
- (58) Yavuz, B.; Pehlivan, S. B.; Unlü, N. Dendrimeric Systems and Their Applications in Ocular Drug Delivery. *ScientificWorldJournal.* **2013**, *2013*, 732340. <https://doi.org/10.1155/2013/732340>.
- (59) Kaur, D.; Jain, K.; Mehra, N. K.; Kesharwani, P.; Jain, N. K. A Review on Comparative Study of PPI and PAMAM Dendrimers. *J. Nanoparticle Res.* **2016**, *18* (6), 1–14. <https://doi.org/10.1007/s11051-016-3423-0>.
- (60) Koç, F. E.; Senel, M. Solubility Enhancement of Non-Steroidal Anti-Inflammatory Drugs (NSAIDs) Using Polypolypropylene Oxide Core PAMAM Dendrimers. *Int. J. Pharm.* **2013**, *451* (1–2), 18–22. <https://doi.org/10.1016/j.ijpharm.2013.04.062>.
- (61) Li, Z.; Tan, S.; Li, S.; Shen, Q.; Wang, K. Cancer Drug Delivery in the Nano Era: An Overview and Perspectives (Review). *Oncol. Rep.* **2017**, *38* (2), 611–624. <https://doi.org/10.3892/or.2017.5718>.
- (62) Cheng, Y.; Man, N.; Xu, T.; Fu, R.; Wang, X.; Wang, X.; Wen, L. Transdermal Delivery of Nonsteroidal Anti-Inflammatory Drugs Mediated by Polyamidoamine (PAMAM) Dendrimers. *J. Pharm. Sci.* **2007**, *96* (3), 595–602. <https://doi.org/10.1002/jps.20745>.
- (63) Suri, R.; Beg, S.; Kohli, K. Target Strategies for Drug Delivery Bypassing Ocular Barriers. *J. Drug Deliv. Sci. Technol.* **2020**, *55* (November 2019), 101389. <https://doi.org/10.1016/j.jddst.2019.101389>.
- (64) Jain, K.; Kesharwani, P.; Gupta, U.; Jain, N. K. A Review of Glycosylated Carriers for Drug Delivery. *Biomaterials* **2012**, *33* (16), 4166–4186. <https://doi.org/10.1016/j.biomaterials.2012.02.033>.
- (65) Vandamme, T. F.; Brobeck, L. Poly(Amidoamine) Dendrimers as Ophthalmic

- Vehicles for Ocular Delivery of Pilocarpine Nitrate and Tropicamide. *J. Control. Release* **2005**, *102* (1), 23–38. <https://doi.org/10.1016/j.jconrel.2004.09.015>.
- (66) Bai, S.; Thomas, C.; Ahsan, F. Dendrimers as a Carrier for Pulmonary Delivery of Enoxaparin, a Low-Molecular Weight Heparin. *J. Pharm. Sci.* **2007**, *96* (8), 2090–2106. <https://doi.org/10.1002/jps.20849>.
- (67) Mansour, H. M.; Rhee, Y.-S.; Wu, X. Nanomedicine in Pulmonary Delivery. *Int. J. Nanomedicine* **2009**, *4*, 299–319. <https://doi.org/10.2147/ijn.s4937>.
- (68) Mignani, S.; El Kazzouli, S.; Bousmina, M.; Majoral, J.-P. Expand Classical Drug Administration Ways by Emerging Routes Using Dendrimer Drug Delivery Systems: A Concise Overview. *Adv. Drug Deliv. Rev.* **2013**, *65* (10), 1316–1330. <https://doi.org/10.1016/j.addr.2013.01.001>.
- (69) Cao, J.; Huang, D.; Peppas, N. A. Advanced Engineered Nanoparticulate Platforms to Address Key Biological Barriers for Delivering Chemotherapeutic Agents to Target Sites. *Adv. Drug Deliv. Rev.* **2020**, *167*, 170–188. <https://doi.org/10.1016/j.addr.2020.06.030>.
- (70) Quintana, A.; Raczka, E.; Piehler, L.; Lee, I.; Myc, A.; Majoros, I.; Patri, A. K.; Thomas, T.; Mulé, J.; Baker, J. R. Design and Function of a Dendrimer-Based Therapeutic Nanodevice Targeted to Tumor Cells through the Folate Receptor. *Pharm. Res.* **2002**, *19* (9), 1310–1316. <https://doi.org/10.1023/a:1020398624602>.
- (71) Kukowska-Latallo, J. F.; Candido, K. A.; Cao, Z.; Nigavekar, S. S.; Majoros, I. J.; Thomas, T. P.; Balogh, L. P.; Khan, M. K.; Baker, J. R. Nanoparticle Targeting of Anticancer Drug Improves Therapeutic Response in Animal Model of Human Epithelial Cancer. *Cancer Res.* **2005**, *65* (12), 5317–5324. <https://doi.org/10.1158/0008-5472.CAN-04-3921>.
- (72) Thomas, T. P.; Patri, A. K.; Myc, A.; Myaing, M. T.; Ye, J. Y.; Norris, T. B.; Baker, J.

- R. In Vitro Targeting of Synthesized Antibody-Conjugated Dendrimer Nanoparticles. *Biomacromolecules* 5 (6), 2269–2274. <https://doi.org/10.1021/bm049704h>.
- (73) Choi, Y.; Thomas, T.; Kotlyar, A.; Islam, M. T.; Baker, J. R. Synthesis and Functional Evaluation of DNA-Assembled Polyamidoamine Dendrimer Clusters for Cancer Cell-Specific Targeting. *Chem. Biol.* **2005**, 12 (1), 35–43. <https://doi.org/10.1016/j.chembiol.2004.10.016>.
- (74) Gajbhiye, V.; Ganesh, N.; Barve, J.; Jain, N. K. Synthesis, Characterization and Targeting Potential of Zidovudine Loaded Sialic Acid Conjugated-Mannosylated Poly(Propyleneimine) Dendrimers. *Eur. J. Pharm. Sci.* **2013**, 48 (4–5), 668–679. <https://doi.org/10.1016/j.ejps.2012.12.027>.
- (75) Wang, D.; Zhao, T.; Zhu, X.; Yan, D.; Wang, W. Bioapplications of Hyperbranched Polymers. *Chem. Soc. Rev.* **2015**, 44 (12), 4023–4071. <https://doi.org/10.1039/c4cs00229f>.
- (76) Daniel, W.; Stiriba, S. E.; Holger, F. Hyperbranched Polyglycerols: From the Controlled Synthesis of Biocompatible Polyether Polyols to Multipurpose Applications. *Acc. Chem. Res.* **2010**, 43 (1), 129–141. <https://doi.org/10.1021/ar900158p>.
- (77) Wang, D.; Jin, Y.; Zhu, X.; Yan, D. Synthesis and Applications of Stimuli-Responsive Hyperbranched Polymers. *Prog. Polym. Sci.* **2017**, 64, 114–153. <https://doi.org/10.1016/j.progpolymsci.2016.09.005>.
- (78) Bal-Öztürk, A.; Tietilu, S. D.; Yücel, O.; Erol, T.; Akgüner, Z. P.; Darıcı, H.; Alarcin, E.; Emik, S. Hyperbranched Polymer-Based Nanoparticle Drug Delivery Platform for the Nucleus-Targeting in Cancer Therapy. *J. Drug Deliv. Sci. Technol.* **2023**, 81 (October 2022). <https://doi.org/10.1016/j.jddst.2023.104195>.
- (79) Irfan, M.; Seiler, M. Encapsulation Using Hyperbranched Polymers: From Research

- and Technologies to Emerging Applications. *Ind. Eng. Chem. Res.* **2010**, *49* (3), 1169–1196. <https://doi.org/10.1021/ie900216r>.
- (80) Wu, H.; Yin, T.; Li, K.; Wang, R.; Chen, Y.; Jing, L. Encapsulation Property of Hyperbranched Polyglycerols as Prospective Drug Delivery Systems. *Polym. Chem.* **2018**, *9* (3), 300–306. <https://doi.org/10.1039/c7py01419h>.
- (81) Ke, X.; Ng, V. W. L.; Ono, R. J.; Chan, J. M. W.; Krishnamurthy, S.; Wang, Y.; Hedrick, J. L.; Yang, Y. Y. Role of Non-Covalent and Covalent Interactions in Cargo Loading Capacity and Stability of Polymeric Micelles. *J. Control. Release* **2014**, *193*, 9–26. <https://doi.org/10.1016/j.jconrel.2014.06.061>.
- (82) Kolhe, P.; Khandare, J.; Pillai, O.; Kannan, S.; Lieh-Lai, M.; Kannan, R. Hyperbranched Polymer-Drug Conjugates with High Drug Payload for Enhanced Cellular Delivery. *Pharm. Res.* **2004**, *21* (12), 2185–2195. <https://doi.org/10.1007/s11095-004-7670-x>.
- (83) Lloyd, J. B. Lysosome Membrane Permeability: Implications for Drug Delivery. *Adv. Drug Deliv. Rev.* **2000**, *41* (2), 189–200. [https://doi.org/10.1016/S0169-409X\(99\)00065-4](https://doi.org/10.1016/S0169-409X(99)00065-4).
- (84) Liu, J.; Pang, Y.; Chen, J.; Huang, P.; Huang, W.; Zhu, X.; Yan, D. Hyperbranched Polydiselenide as a Self Assembling Broad Spectrum Anticancer Agent. *Biomaterials* **2012**, *33* (31), 7765–7774. <https://doi.org/10.1016/j.biomaterials.2012.07.003>.
- (85) Álvarez-Pérez, M.; Ali, W.; Marc, M. A.; Handzlik, J.; Domínguez-Álvarez, E. Selenides and Diselenides: A Review of Their Anticancer and Chemopreventive Activity. *Molecules* **2018**, *23* (3). <https://doi.org/10.3390/molecules23030628>.
- (86) Matsumura, Y.; Maeda, H. A New Concept for Macromolecular Therapeutics in Cancer Chemotherapy: Mechanism of Tumoritropic Accumulation of Proteins and the Antitumor Agent Smancs. *Cancer Res.* **1986**, *46* (8), 6387–6392.

- (87) Zhang, Y.; Chan, H. F.; Leong, K. W. Advanced Materials and Processing for Drug Delivery: The Past and the Future. *Adv. Drug Deliv. Rev.* **2013**, *65* (1), 104–120. <https://doi.org/10.1016/j.addr.2012.10.003>.
- (88) Jhaveri, A. M.; Torchilin, V. P. Multifunctional Polymeric Micelles for Delivery of Drugs and SiRNA. *Front. Pharmacol.* **2014**, *5 APR* (April), 1–26. <https://doi.org/10.3389/fphar.2014.00077>.
- (89) Sawant, R. R.; Jhaveri, A. M.; Torchilin, V. P. Immunomicelles for Advancing Personalized Therapy. *Adv. Drug Deliv. Rev.* **2012**, *64* (13), 1436–1446. <https://doi.org/10.1016/j.addr.2012.08.003>.
- (90) Ranade, V. V. Drug Delivery Systems. 1. Site-Specific Drug Delivery Using Liposomes as Carriers. *J. Clin. Pharmacol.* **1989**, *29* (8), 685–694. <https://doi.org/10.1002/j.1552-4604.1989.tb03403.x>.
- (91) Haag, R. Dendrimers and Hyperbranched Polymers as High-Loading Supports for Organic Synthesis. *Chem. - A Eur. J.* **2001**, *7* (2), 327–335. [https://doi.org/10.1002/1521-3765\(20010119\)7:2<327::AID-CHEM327>3.0.CO;2-M](https://doi.org/10.1002/1521-3765(20010119)7:2<327::AID-CHEM327>3.0.CO;2-M).
- (92) Milhem, O. M.; Myles, C.; McKeown, N. B.; Attwood, D.; D’Emanuele, A. Polyamidoamine Starburst® Dendrimers as Solubility Enhancers. *Int. J. Pharm.* **2000**, *197* (1–2), 239–241. [https://doi.org/10.1016/S0378-5173\(99\)00463-9](https://doi.org/10.1016/S0378-5173(99)00463-9).
- (93) Malam, Y.; Loizidou, M.; Seifalian, A. M. Liposomes and Nanoparticles: Nanosized Vehicles for Drug Delivery in Cancer. *Trends Pharmacol. Sci.* **2009**, *30* (11), 592–599. <https://doi.org/10.1016/j.tips.2009.08.004>.
- (94) Kwiatkowski, S.; Knap, B.; Przystupski, D.; Saczko, J.; Kędzierska, E.; Knap-Czop, K.; Kotlińska, J.; Michel, O.; Kotowski, K.; Kulbacka, J. Photodynamic Therapy – Mechanisms, Photosensitizers and Combinations. *Biomed. Pharmacother.* **2018**, *106* (July), 1098–1107. <https://doi.org/10.1016/j.biopha.2018.07.049>.

- (95) García-Giménez, J. L.; Romá-Mateo, C.; Pérez-Machado, G.; Peiró-Chova, L.; Pallardó, F. V. Role of Glutathione in the Regulation of Epigenetic Mechanisms in Disease. *Free Radic. Biol. Med.* **2017**, *112* (July), 36–48.
<https://doi.org/10.1016/j.freeradbiomed.2017.07.008>.
- (96) Ruffmann, R.; Wendel, A. GSH Rescue by N-Acetylcysteine. *Klin. Wochenschr.* **1991**, *69* (18), 857–862. <https://doi.org/10.1007/BF01649460>.
- (97) Gaillard, P. J.; De Boer, A. G. *2B-TransTM Technology: Targeted Drug Delivery across the Blood-Brain Barrier*; 2008; Vol. 437. https://doi.org/10.1007/978-1-59745-210-6_8.
- (98) Haag, R.; Kratz, F. Polymer Therapeutics: Concepts and Applications. *Angew. Chemie - Int. Ed.* **2006**, *45* (8), 1198–1215. <https://doi.org/10.1002/anie.200502113>.
- (99) Bielawski, K.; Bielawska, A.; Muszyńska, A.; Popławska, B.; Czarnomysy, R. Cytotoxic Activity of G3 PAMAM-NH₂ Dendrimer-Chlorambucil Conjugate in Human Breast Cancer Cells. *Environ. Toxicol. Pharmacol.* **2011**, *32* (3), 364–372.
<https://doi.org/10.1016/j.etap.2011.08.002>.
- (100) Beezer, A. E.; King, A. S. H.; Martin, I. K.; Mitchel, J. C.; Twyman, L. J.; Wain, C. F. Dendrimers as Potential Drug Carriers; Encapsulation of Acidic Hydrophobes within Water Soluble PAMAM Derivatives. *Tetrahedron* **2003**, *59* (22), 3873–3880.
[https://doi.org/10.1016/S0040-4020\(03\)00437-X](https://doi.org/10.1016/S0040-4020(03)00437-X).
- (101) Krakowiak, R.; Frankowski, R.; Mylkie, K.; Kotkowiak, M.; Mlynarczyk, D. T.; Dudkowiak, A.; Stanis, B. J.; Zgoła-Grzeskowiak, A.; Ziegler-Borowska, M.; Goslinski, T. Titanium(IV) Oxide Nanoparticles Functionalized with Various Meso-Porphyrins for Efficient Photocatalytic Degradation of Ibuprofen in UV and Visible Light. *J. Environ. Chem. Eng.* **2022**, *10* (5).
<https://doi.org/10.1016/j.jece.2022.108432>.

- (102) Hopper, C. Photodynamic Therapy: A Clinical Reality in the Treatment of Cancer. *Lancet Oncol.* **2000**, *1* (4), 212–219. [https://doi.org/10.1016/S1470-2045\(00\)00166-2](https://doi.org/10.1016/S1470-2045(00)00166-2).
- (103) Tian, J.; Huang, B.; Nawaz, M. H.; Zhang, W. Recent Advances of Multi-Dimensional Porphyrin-Based Functional Materials in Photodynamic Therapy. *Coord. Chem. Rev.* **2020**, *420*, 213410. <https://doi.org/10.1016/j.ccr.2020.213410>.
- (104) Shao, S.; Rajendiran, V.; Lovell, J. F. Metalloporphyrin Nanoparticles: Coordinating Diverse Theranostic Functions. *Coord. Chem. Rev.* **2019**, *379*, 99–120. <https://doi.org/10.1016/j.ccr.2017.09.002>.
- (105) Paolesse, R.; Nardis, S.; Monti, D.; Stefanelli, M.; Di Natale, C. Porphyrinoids for Chemical Sensor Applications. *Chem. Rev.* **2017**, *117* (4), 2517–2583. <https://doi.org/10.1021/acs.chemrev.6b00361>.
- (106) Kubát, P.; Lang, K.; Janda, P.; Anzenbacher, P. Interaction of Porphyrins with a Dendrimer Template: Self-Aggregation Controlled by PH. *Langmuir* **2005**, *21* (21), 9714–9720. <https://doi.org/10.1021/la051106g>.
- (107) Rotomskis, R.; Augulis, R.; Snitka, V.; Valiokas, R.; Liedberg, B. Hierarchical Structure of TPPS4 J-Aggregates on Substrate Revealed by Atomic Force Microscopy. *J. Phys. Chem. B* **2004**, *108* (9), 2833–2838. <https://doi.org/10.1021/jp036128v>.
- (108) Kubát, P.; Lang, K.; Zelinger, Z. Interaction of Porphyrins with PAMAM Dendrimers in Aqueous Solution. *J. Mol. Liq.* **2007**, *131–132* (SPEC. ISS.), 200–205. <https://doi.org/10.1016/j.molliq.2006.08.038>.
- (109) Al-rawashdeh, N. *Edited by Jamal Uddin*; 2014.
- (110) Aboshnaf, F. The Synthesis and Application of Dendritic Polymer for Photodynamic Therapy. **2018**.
- (111) Bharathi, S.; Wong, P. T.; Desai, A.; Lykhytska, O.; Choe, V.; Kim, H.; Thomas, T. P.; Baker, J. R.; Choi, S. K. Design and Mechanistic Investigation of Oxime-

- Conjugated PAMAM Dendrimers as the Catalytic Scavenger of Reactive Organophosphate. *J. Mater. Chem. B* **2014**, *2* (8), 1068–1078.
<https://doi.org/10.1039/c3tb21267j>.
- (112) Burakowska, E.; Zimmerman, S. C.; Haag, R. Photoresponsive Crosslinked Hyperbranched Polyglycerols as Smart Nanocarriers for Guest Binding and Controlled Release. *Small* **2009**, *5* (19), 2199–2204. <https://doi.org/10.1002/sml.200900465>.
- (113) Zheng, Y.; Li, S.; Weng, Z.; Gao, C. Hyperbranched Polymers: Advances from Synthesis to Applications. *Chem. Soc. Rev.* **2015**, *44* (12), 4091–4130.
<https://doi.org/10.1039/c4cs00528g>.
- (114) Caminade, A. M.; Yan, D.; Smith, D. K. Dendrimers and Hyperbranched Polymers. *Chem. Soc. Rev.* **2015**, *44* (12), 3870–3873. <https://doi.org/10.1039/c5cs90049b>.
- (115) Nie, J.; Wang, Y.; Wang, W. In Vitro and in Vivo Evaluation of Stimuli-Responsive Vesicle from PEGylated Hyperbranched PAMAM-Doxorubicin Conjugate for Gastric Cancer Therapy. *Int. J. Pharm.* **2016**, *509* (1–2), 168–177.
<https://doi.org/10.1016/j.ijpharm.2016.05.021>.
- (116) Steinhilber, D.; Seiffert, S.; Heyman, J. A.; Paulus, F.; Weitz, D. A.; Haag, R. Hyperbranched Polyglycerols on the Nanometer and Micrometer Scale. *Biomaterials* **2011**, *32* (5), 1311–1316. <https://doi.org/10.1016/j.biomaterials.2010.10.010>.
- (117) Bai, L.; Yan, H.; Bai, T.; Feng, Y.; Zhao, Y.; Ji, Y.; Feng, W.; Lu, T.; Nie, Y. High Fluorescent Hyperbranched Polysiloxane Containing β -Cyclodextrin for Cell Imaging and Drug Delivery. *Biomacromolecules* **2019**, *20* (11), 4230–4240.
<https://doi.org/10.1021/acs.biomac.9b01217>.
- (118) Sun, Y.; Jiao, Y.; Wang, Y.; Lu, D.; Yang, W. The Strategy to Improve Gene Transfection Efficiency and Biocompatibility of Hyperbranched PAMAM with the Cooperation of PEGylated Hyperbranched PAMAM. *Int. J. Pharm.* **2014**, *465* (1–2),

- 112–119. <https://doi.org/10.1016/j.ijpharm.2014.02.018>.
- (119) Garric, J.; Léger, J. M.; Huc, I. Encapsulation of Small Polar Guests in Molecular Apple Peels. *Chem. - A Eur. J.* **2007**, *13* (30), 8454–8462.
<https://doi.org/10.1002/chem.200700640>.
- (120) Osman, A. I.; Ayati, A.; Farghali, M.; Krivoshapkin, P.; Tanhaei, B.; Karimi-Maleh, H.; Krivoshapkina, E.; Taheri, P.; Tracey, C.; Al-Fatesh, A.; Ihara, I.; Rooney, D. W.; Sillanpää, M. *Advanced Adsorbents for Ibuprofen Removal from Aquatic Environments: A Review*; Springer International Publishing, 2023.
<https://doi.org/10.1007/s10311-023-01647-6>.
- (121) Gunasekhar, R.; Sathiyathan, P.; Reza, M. S.; Prasad, G.; Prabu, A. A.; Kim, H. Polyvinylidene Fluoride/Aromatic Hyperbranched Polyester of Third-Generation-Based Electrospun Nanofiber as a Self-Powered Triboelectric Nanogenerator for Wearable Energy Harvesting and Health Monitoring Applications. *Polymers (Basel)*. **2023**, *15* (10). <https://doi.org/10.3390/polym15102375>.
- (122) Patel, V.; Rajani, C.; Paul, D.; Borisa, P.; Rajpoot, K.; Youngren-Ortiz, S. R.; Tekade, R. K. *Dendrimers as Novel Drug-Delivery System and Its Applications*; 2019.
<https://doi.org/10.1016/B978-0-12-814487-9.00008-9>.
- (123) Tian, W.; Li, X.; Wang, J. Supramolecular Hyperbranched Polymers. *Chem. Commun.* **2017**, *53* (17), 2531–2542. <https://doi.org/10.1039/c6cc09678f>.
- (124) Higashihara, T.; Segawa, Y.; Sinananwanich, W.; Ueda, M. Synthesis of Hyperbranched Polymers with Controlled Degree of Branching. *Polym. J.* **2012**, *44* (1), 14–29. <https://doi.org/10.1038/pj.2011.99>.
- (125) Yang, H.; Yu, D.; Wang, H.; Xie, Q.; Wu, J.; Wang, J. Aggregation Behavior of Amphiphilic PAMAM-Based Hyperbranched Polymer in the Presence of Conventional Small Molecular Surfactants. *Adv. Chem. Eng. Sci.* **2013**, *03* (03), 11–18.

- <https://doi.org/10.4236/aces.2013.33a1002>.
- (126) Trawiński, J.; Skibiński, R. Studies on Photodegradation Process of Psychotropic Drugs: A Review. *Environ. Sci. Pollut. Res.* **2017**, *24* (2), 1152–1199.
<https://doi.org/10.1007/s11356-016-7727-5>.
- (127) Wang, Y.; Zhao, J.; Dong, Z.; Wang, C.; Meng, H.; Li, Y.; Jin, H. Aggregation-Induced Emission-Active Antibacterial Hydrogel with Self-Indicating Ability for Real-Time Monitoring of Drug Release Process. *Mater. Today Chem.* **2021**, *21*.
<https://doi.org/10.1016/j.mtchem.2021.100537>.
- (128) Gröhn, F.; Bauer, B. J.; Akpalu, Y. A.; Jackson, C. L.; Amis, E. J. Dendrimer Templates for the Formation of Gold Nanoclusters. *Macromolecules* **2000**, *33* (16), 6042–6050. <https://doi.org/10.1021/ma000149v>.
- (129) Kissin, Y. V. Molecular Weight Distributions of Linear Polymers: Detailed Analysis from GPC Data. *J. Polym. Sci. Part A Polym. Chem.* **1995**, *33* (2), 227–237.
<https://doi.org/10.1002/pola.1995.080330205>.
- (130) Danhier, F.; Feron, O.; Pr at, V. To Exploit the Tumor Microenvironment: Passive and Active Tumor Targeting of Nanocarriers for Anti-Cancer Drug Delivery. *J. Control. Release* **2010**, *148* (2), 135–146. <https://doi.org/10.1016/j.jconrel.2010.08.027>.
- (131) Boas, U.; S ontjens, S. H. M.; Jensen, K. J.; Christensen, J. B.; Meijer, E. W. New Dendrimer - Peptide Host - Guest Complexes: Towards Dendrimers as Peptide Carriers. *ChemBioChem* **2002**, *3* (5), 433–439. [https://doi.org/10.1002/1439-7633\(20020503\)3:5<433::AID-CBIC433>3.0.CO;2-0](https://doi.org/10.1002/1439-7633(20020503)3:5<433::AID-CBIC433>3.0.CO;2-0).
- (132) Twyman, L. J.; King, A. S. H.; Martin, I. K. Catalysis inside Dendrimers. *Chem. Soc. Rev.* **2002**, *31* (2), 69–82. <https://doi.org/10.1039/b107812g>.

